BEHAVIOR OF THIN-WALLED, SEGMENTALLY CONSTRUCTED POST-TENSIONED BRIDGE PIERS

APPROVED:

Supervisor: _____
John E. Breen

_____
Ned H. Burns

To my parents, who have been a great inspiration.

ACKNOWLEDGEMENTS

The author would like to take this opportunity to express his gratitude to his supervisor, Dr. John E. Breen, who offered many suggestions and guidance throughout the compilation of this thesis. Special thanks are also due to Dr. Ned H. Burns who acted as the second reader of this thesis. The author also wishes to thank Andrew W. Taylor, who made this project work, for the innumerable hours he put into this project. His patience and advice are greatly appreciated.

The financial assistance of the Texas State Department of Highways and Public Transportation, sponsor of the overall project of which this thesis is a part, was also greatly appreciated. The author would also like to express his gratitude to all of the technical and secretarial personnel at Ferguson Lab who have helped make my stay more pleasant.

Thanks is also due to Blake Brooker and Alfredo Santolamazza whose enthusiasm and hard work seemed to make the experimental work somewhat enjoyable.

Most importantly, deepest gratitude goes to the author's family whose support and encouragement made this thesis possible and to God for allowing such an opportunity.

Randy B. Rowell

Austin, TX
April, 1990

TABLE OF CONTENTS

Chapter Page

Chapter Page

Chapter Page

Chapter Page

LIST OF TABLES

LIST OF FIGURES

Figure | Page

CHAPTER 1

INTRODUCTION

1.1 Background

In recent years, bridge designers have moved toward designing hollow bridge pier sections for tall piers in order to save on materials (1). Although the majority of these piers are monolithically cast in place, it is becoming more common to use segmental construction techniques. In order to speed construction in the field, the segmental piers are often match-cast off-site. At the job site, the pier segments are epoxied together, lightly post-tensioned to hold them in position and then fully post-tensioned for main reinforcement. Although construction time is reduced and better concrete quality is expected, questions arise as to how the strength and stiffness of the precast pier is affected. The study documented in this thesis focuses on those effects.

The trend of designing hollow pier sections has moved towards the design of hollow sections with relatively thin walls. As part of the progression towards the use of very thin-walled sections, the question has arisen as to how thin the walls may become without having problems due to local instability (2,3).

In order to address the preceding question, a comprehensive study was begun in 1987 at the Phil M. Ferguson Structural Engineering Laboratory at the University of Texas. The experimental part of the project was primarily concerned with studying the effect of the unsupported wall length to thickness ratio, X_u/t_f (Fig. 1.1), on the strength and stiffness of the piers. In order to have a good representation of actual

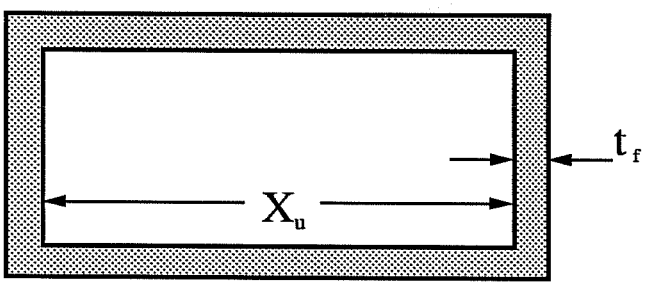

Typical Monolithic Pier Cross-section

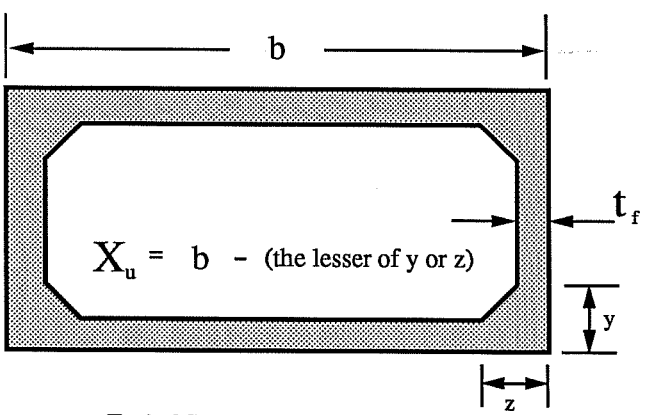

Typical Segmental Pier Cross-Section

$$\frac{X_u}{t_f} = \text{Wall Slenderness Ratio}$$

Figure 1.1 Wall Slenderness Ratio

bridge pier designs, the experimental program included both monolithically and segmentally constructed pier test specimens.

Several notable examples of thin-walled segmental piers include the Neches River Bridge in Jefferson County, Texas, the Oleron Viaduct in France, and the Dauphin Island Bridge off the Alabama coast. Each of these bridges have X_u/t_f ratios ranging from 16 to 19, relatively high values.

Using the data obtained from an experimental study of both monolithic and segmental piers, it was felt that the effects of segmental construction on the behavior of the piers could be evaluated. This thesis will document the relative behavior of the segmental piers and will make recommendations based on the observations and conclusions drawn therefrom.

1.2 Objectives and Scope

The basic thrust of this study was to compare the behavior of segmentally constructed piers with a companion series of monolithically constructed piers in order to determine the effects of segmental construction.

The specific objectives of this study were to:

1) Determine the effect of segmental construction on the strength and stiffness of the hollow reinforced concrete bridge piers.

2) Develop an analytical model which adequately accounts for the observed behavior of the segmental piers.

3) Establish design criteria for segmental piers.

The scope of the study included an experimental program to obtain an understanding of how the monolithic and segmental specimens perform. Experimental data was evaluated to determine the effects of segmental construction. An analytical model was developed to include the effects of segmental construction. Design recommendations and conclusions were drawn from the results.

The specimens were designed on the basis of code specifications and details of existing piers in the United States. The description of the test specimens, materials used, and their construction are presented in Chapter 2. The test setup and procedure are outlined in Chapter 3. Data and observations from the tests are presented in Chapter 4. The analysis of the test results, the basis and findings from the analytical model, and design recommendations are given in Chapter 5. A brief summary and final conclusions are presented in Chapter 6.

1.2.1 Literature Review

Although a comprehensive literature search was made, only a few references to hollow bridge piers were found. Poston (2) investigated the axial load-moment-curvature relationship and

plane section assumption of hollow pier sections by testing four model bridge piers subject to both uniaxial and biaxial bending. Proctor (4,5) conducted a series of tests on hollow reinforced concrete columns to determine their mode of failure. The only reference to tests of segmental pier sections was found in a paper by Jobse (3). Jobse performed a limited number of tests on very high strength concrete thin-walled box sections to determine if design could be governed by the overall buckling of the pier rather than buckling of the individual wall plates.

Several papers concerned with the effects of prestress on columns were reviewed in the development of the analytical model. Nathan (6,7,8) has thoroughly investigated the effect of prestress on the interaction curve for prestressed concrete columns. In addition, Zia (9) investigated the effects of concrete strength, steel percentage, and eccentricity on prestressed column capacity.

1.2.2 Experimental Program

The experimental program included the fabrication and testing to ultimate of seven reduced scale model bridge piers. Of the seven piers, three of the piers were segmentally constructed. The three segmental piers and one of the monolithic piers were post-tensioned. Various X_u/t_f ratios and concrete strengths were utilized in the tests.

By analyzing the results of the tests of the segmental piers and comparing the results with a companion series of monolithic piers, the effect of segmental construction on the strength and stiffness of the piers was investigated.

CHAPTER TWO

TEST DESCRIPTION

2.1 Test Objectives

The investigation to determine the effect of segmental construction on the strength and stiffness of the piers had the following objectives:

1) Investigate the effect of the discontinuity of mild steel at the joint.

2) Determine if the plates act as a unit across the joint, i.e. same as a monolithic joint.

3) Determine the effect of the post-tensioning force and tendons.

2.2 General

A series of seven specimens are directly compared in this study. The specimens are grouped under three categories: monolithic, segmental, and post-tensioned monolithic.

2.2.1 Basis for Models

Current AASHTO (10) and ACI (11) specifications for piers and walls were used to determine the design details for the models. As specified in the ACI Building Code provisions for walls, two curtains of steel were used in every specimen. Several existing designs of post-tensioned piers were also used for obtaining certain details.

2.2.2 Scale Factor

The scale factor used for all of the specimens was one-fifth. This factor was chosen so that the test setup capacity would be adequate for testing a wide range of wall slenderness ratios and to prevent modeling problems caused by using smaller scale factors.

2.2.3 Wall Slenderness Ratios

To insure that the entire range of wall slenderness ratios, X_u/t_f, currently used by designers was investigated, a wide range of ratios was selected for the test specimens. Ratios examined in this study are 8.4, 10, 15.5, 18, 22.3, and 24.7.

2.2.4 Post-tensioning System

The post-tensioning system devised by the Dyckerhoff and Widmann Company was used in this study. The Dywidag system includes threaded bars, threaded nuts, threaded couplers, and bearing plates.

2.3 Monolithic Specimens

These specimens were designed to model the behavior of monolithic, cast-in-place piers. Each specimen has continuous longitudinal reinforcement anchored within the load heads. Specimens 1M and 2M were cast in one lift. In order to make the casting operation less difficult and to more accurately

represent actual construction procedures, Specimen 3M was cast in three lifts of 24 inches. All vertical reinforcement was continuous over the construction joints.

Two basic pier sections were used for all the specimens. Specimen 1M has outside dimensions of 15 by 30 inches. Specimens 2M and 3M have outside dimensions of 20 by 40 inches. Elevations of each section are shown in Figures 2.1 and 2.2. Load heads were used to insure a uniform loading on the piers.

Transverse reinforcement includes hoops which confine the inner and outer curtains of steel from buckling out of plane. To satisfy lateral reinforcement provisions, it was determined that the transverse hoop reinforcement would be spaced at the same width as the wall thickness (Fig. 2.3).

Crossties provide additional confinement to the longitudinal steel (Fig. 2.3). The crossties were arranged to satisfy ACI (11) and AASHTO (10) requirements. The horizontal spacing of the crossties depends on the spacing of the longitudinal reinforcement, while the vertical spacing is governed by the spacing of the transverse reinforcement (Fig. 2.3).

2.3.1 Specimen 1M

The outside dimensions of this specimen are 15 x 30 inches with 2.5 inch walls giving it a wall slenderness ratio of 10. The reinforcement layout is shown in the cross-sectional view of

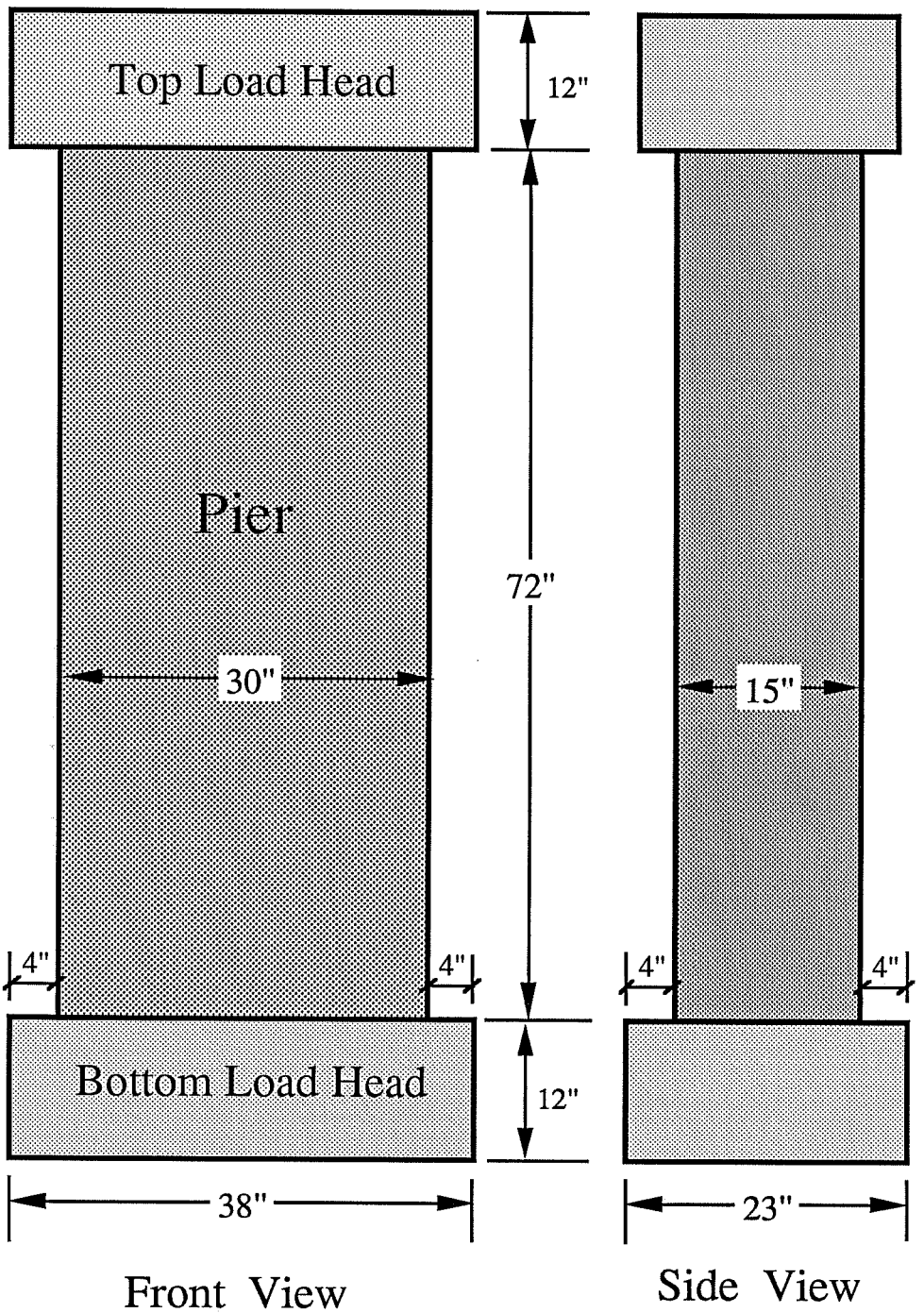

Figure 2.1 Specimen 1M Elevation

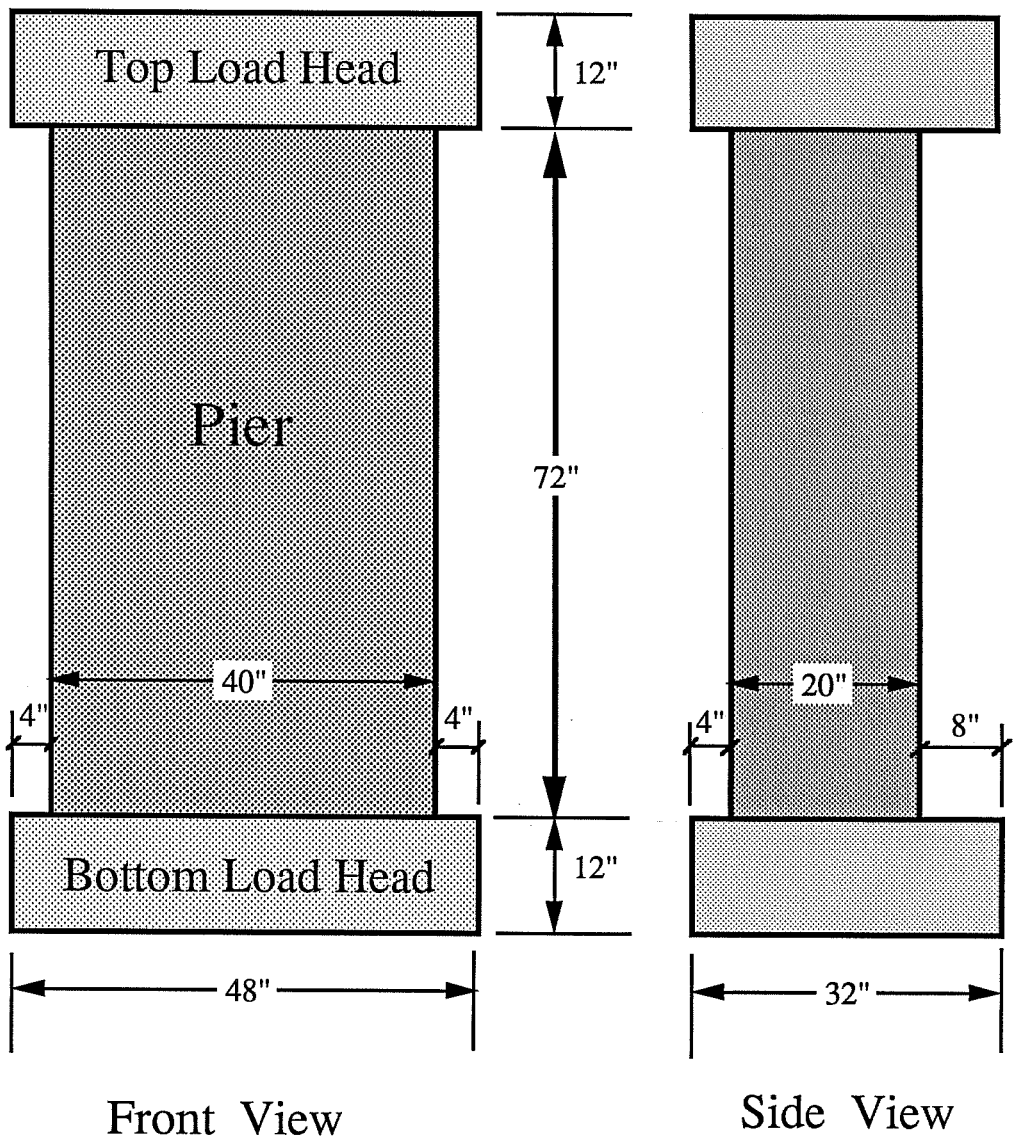

Figure 2.2 Specimens 2M and 3M Elevation

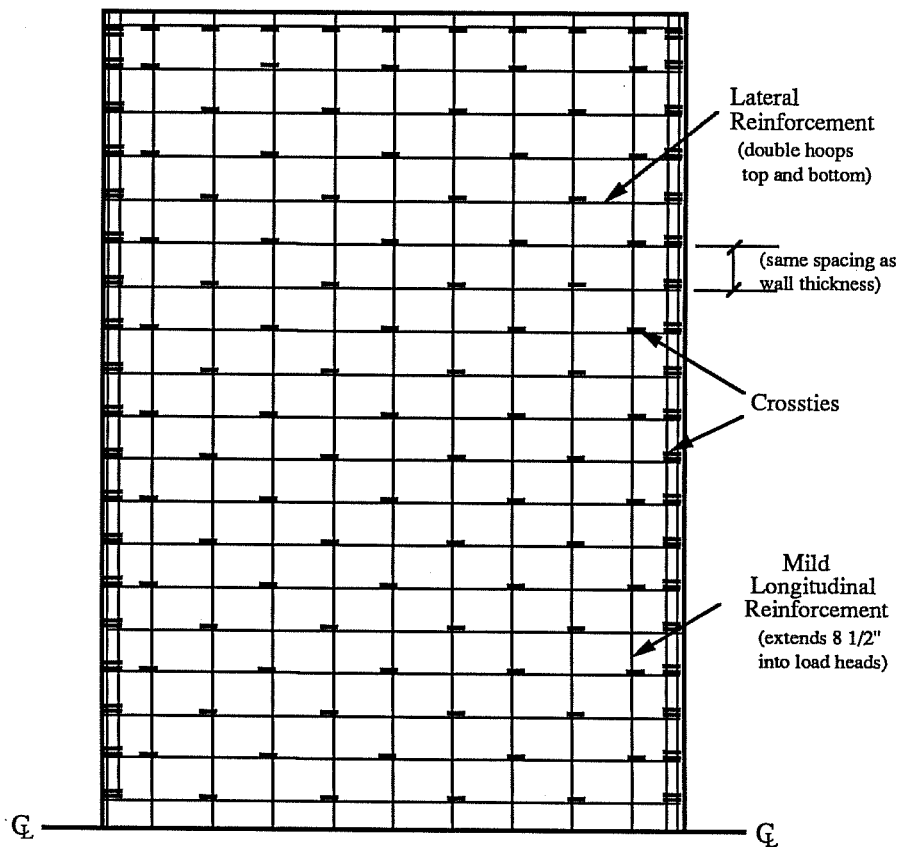

Elevation

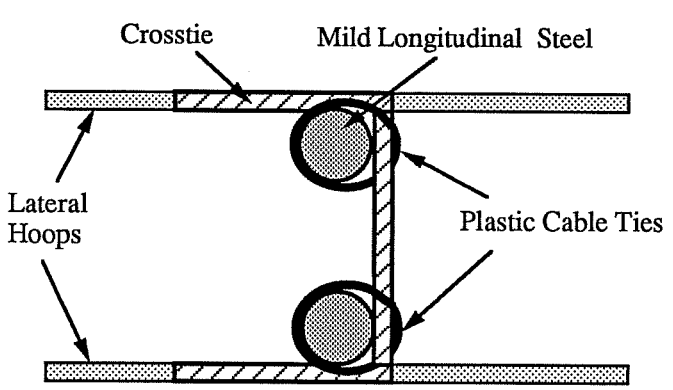

Section

Figure 2.3 Transverse Reinforcement Layout

Figure 2.4. Configurations and dimensions of the transverse reinforcement are shown in Figure 2.5.

After the specimen was tested, measurements were made to determine the actual wall thickness. These measurements are listed in Figure 2.6.

2.3.2 Specimen 2M

The outside dimensions of this specimen were 20 X 40 inches with a 2 inch wall thickness, giving it a wall slenderness ratio of 18. The reinforcement layout is shown in the cross-sectional view of Figure 2.7. In order to meet the desired reinforcement ratio, AASHTO (10) longitudinal reinforcement spacing requirements were slightly exceeded. Transverse reinforcement similar to that of Specimen 1 was used (see Fig. 2.5).

Actual wall thickness measurements are given in Figure 2.6.

2.3.3 Specimen 3M

The outside dimensions of this specimen were 20 X 40 inches with a 1.5 inch wall thickness (Fig. 2.8). The wall slenderness ratio for this section is 24.67, the highest ratio tested. This specimen was cast in three 24 inch lifts. Construction joints were roughened and cleaned prior to placing the next lift.

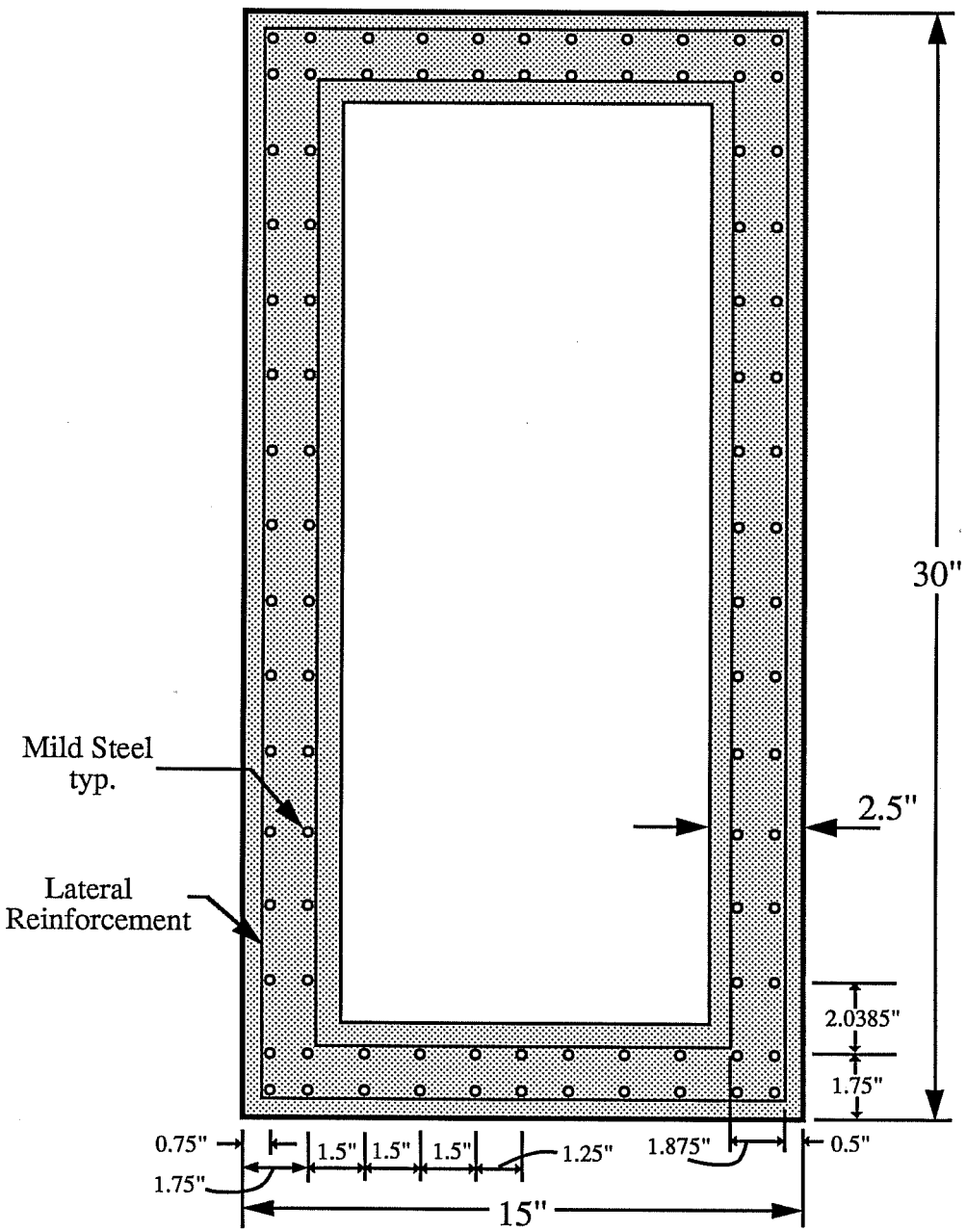

Figure 2.4 Specimen 1M Reinforcement Layout

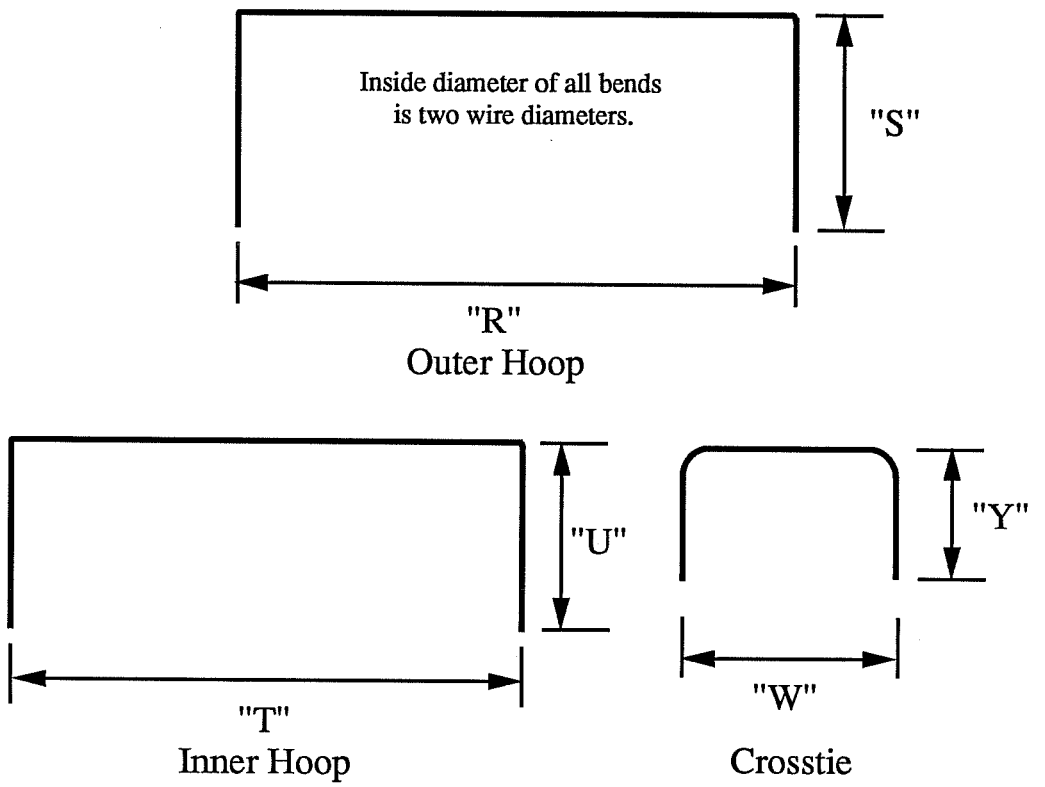

(All dimensions out-to-out)

Specimen	Outer Hoop		Inner Hoop		Crossties	
No.	"R"	"S"	"T"	"U"	"W"	"Y"
1M	28 3/4"	11"	26 1/4"	9 3/4"	1 9/16"	1 3/8"
2M	39 1/4"	13 1/2"	37"	12 1/2"	1 1/4"	1 1/4"
3M	39 5/8"	13 7/8"	37 5/8"	12 7/8"	1 1/4"	1 1/4"
1S	28 3/4"	11"	26 1/4"	9 3/4"	1 9/16"	1 3/8"
2S	39 1/4"	13 1/2"	37"	12 1/2"	1 1/4"	1 1/4"
3S	39 5/8"	13 7/8"	37 5/8"	12 7/8"	1 1/4"	1 1/4"
3PM	39 5/8"	13 7/8"	37 5/8"	12 7/8"	1 1/4"	1 1/4"

Figure 2.5 Lateral Reinforcement Schedule

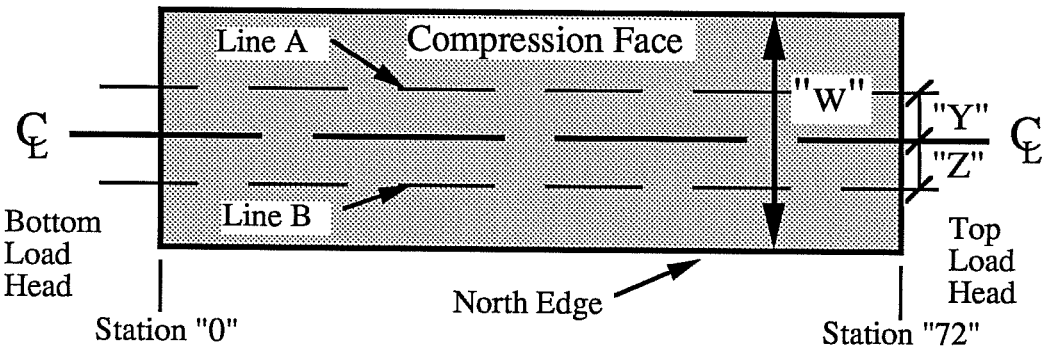

Specimen 1M W = 30" Y = 2" Z = 6"			
Station	Line A	Station	Line B
2	2 5/8"	1	2 5/8"
7	2 19/32"	4	2 9/16"
10	2 19/32"	7	2 9/16"
16	2 9/16"	10	2 9/16"
20	2 9/16"	16	2 9/16"
26	2 9/16"	20	2 9/16"
37	2 17/32"	26	2 9/16"
44	2 9/16"	37	2 17/32"
51	2 1/2"	44	2 9/16"
58	2 9/16"	51	2 1/2"
70	2 15/32"	58	2 17/32"
		70	2 1/2"
Average = 2.554" Standard Deviation = 0.0371"			

Specimen 2M W = 40" Y = 4" Z = 4"		
Station	Line A	Line B
2	2 1/8"	2 5/32"
6	2 3/16"	2 3/16"
12	2 5/32"	2 5/32"
18	2 5/32"	2 3/16"
24	2 3/16"	2 3/16"
30	2 5/32"	2 3/16"
36	2 5/32"	2 5/32"
42	2 1/8"	2 5/32"
48	2 3/32"	2 3/32"
54	2 1/16"	2 1/16"
60	2 1/32"	2 1/32"
64	2 1/32"	n.a.
Average = 2.132" Standard Deviation = 0.0537"		

Specimen 3M W = 40" Y = 2" Z = 6"		
Station	Line A	Line B
2	1 1/2	1 15/32
6	1 1/2	1 1/2
12	1 1/2	1 15/32
23	1 1/2	1 17/32
25	1 9/16	1 17/32
30	1 9/16	1 9/16
36	1 9/16	1 9/16
42	1 5/8	1 5/8
47	1 9/16	1 17/32
49	1 19/32	1 9/16
60	1 5/8	1 19/32
66	1 5/8	1 9/16
Average =1.551 Standard Deviation = 0.0476		

Specimen 3PM W = 40" Y = 2" Z = 7"		
Station	Line A	Line B
2	1 7/16	1 15/32
6	1 15/32	1 1/2
12	1 1/2	1 17/32
23	1 7/16	1 15/32
25	1 9/16	1 9/16
30	1 17/32	1 19/32
36	1 1/2	1 15/32
42	1 15/32	1 15/32
47	1 13/32	1 13/32
54	1 17/32	1 1/2
60	1 15/32	1 15/32
66	******	1 7/16
Average = 1.486 Standard Deviation = 0.0477		

Figure 2.6 Specimens 1M, 2M, 3M, and 3PM Wall Thicknesses

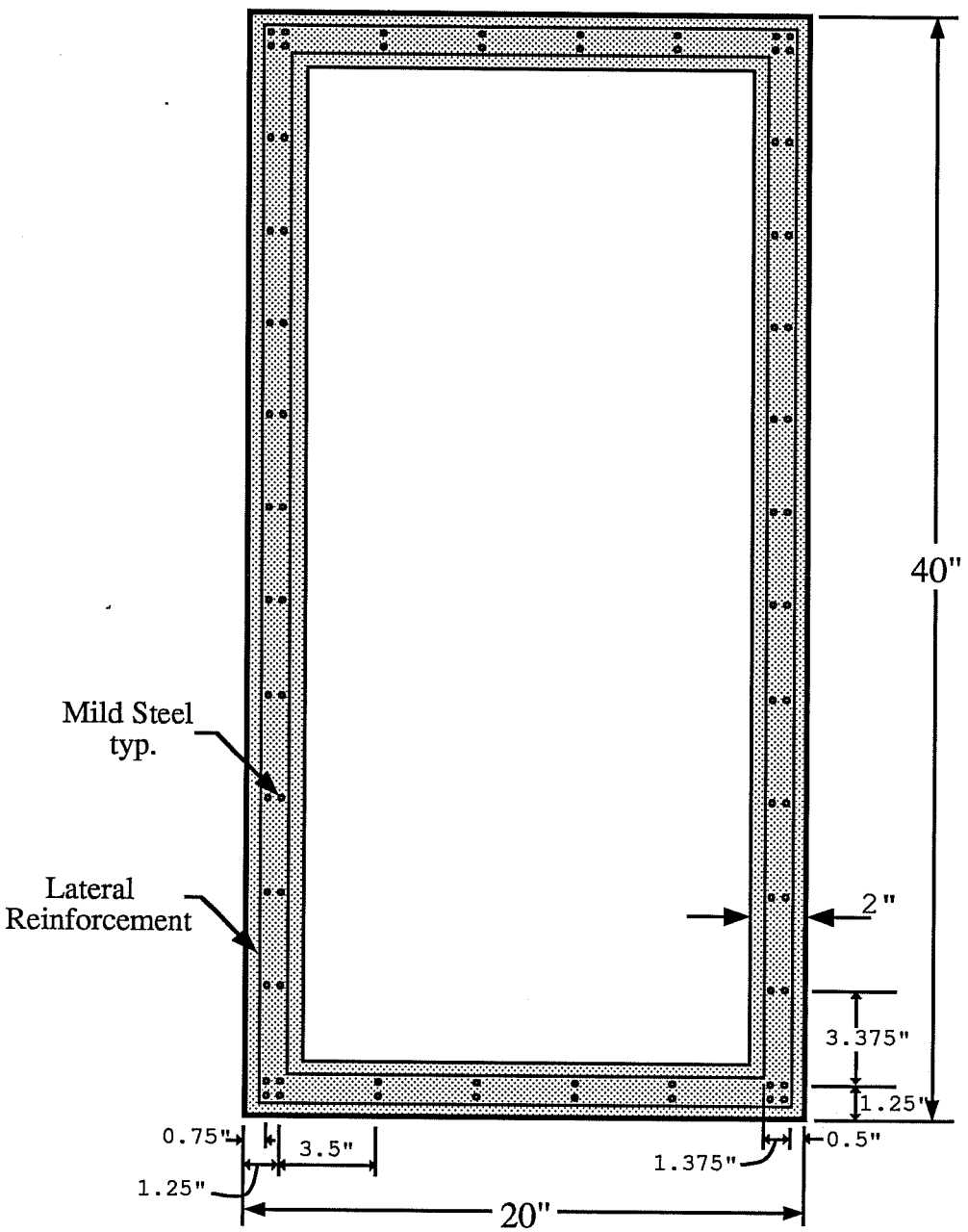

Figure 2.7 Specimen 2M Reinforcement Layout

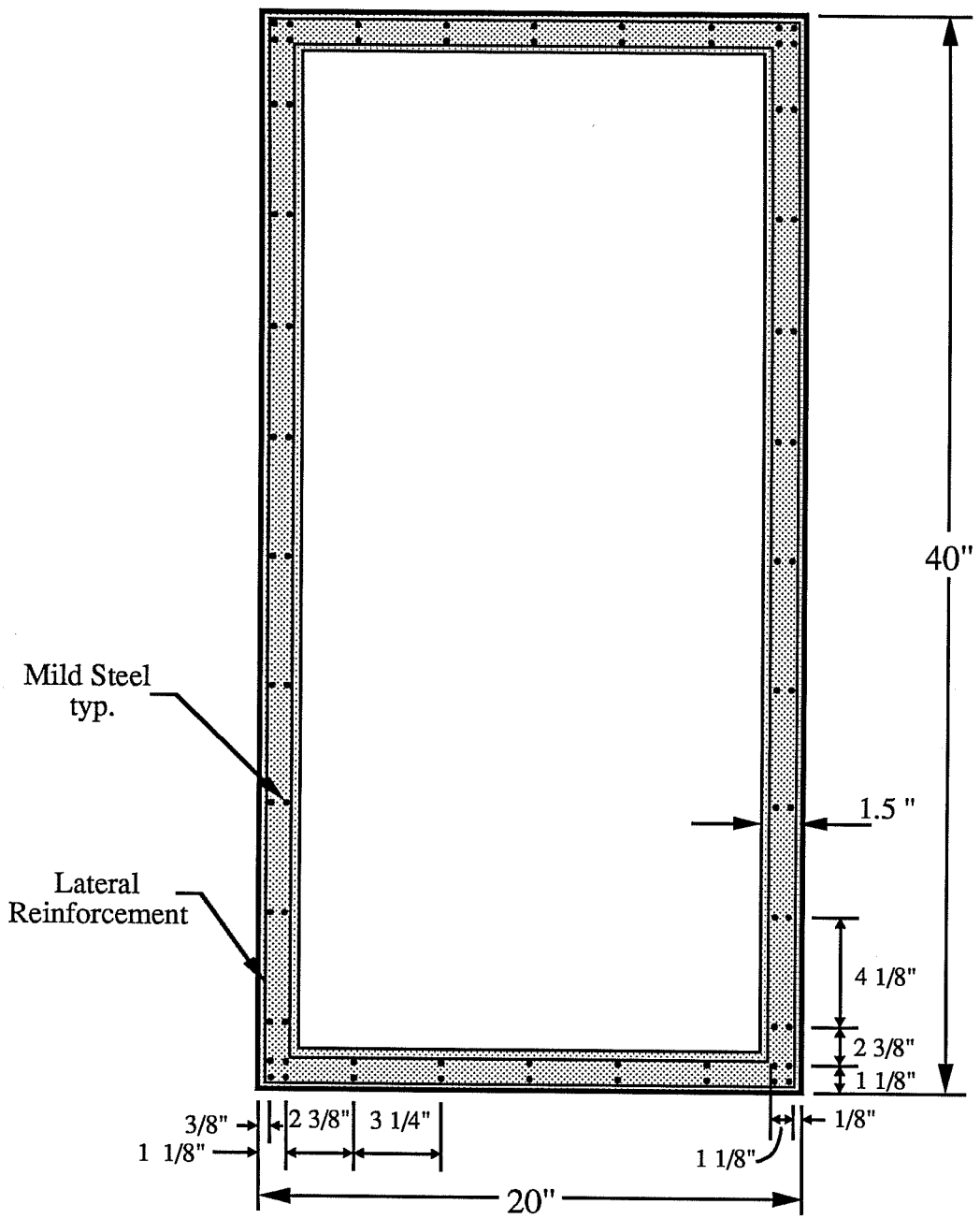

Figure 2.8 Specimen 3M Reinforcement Layout

The reinforcement layout for Specimen 3M is shown in the cross-sectional view of Figure 2.8. As in Specimen 2M, AASHTO (10) longitudinal reinforcement spacing requirements were exceeded. The lateral reinforcement layout is the same as the other specimens, though the dimensions are different (Fig. 2.5). For practical considerations in constructing the 1.5 inch walls, AASHTO (10) and ACI (11) cover requirements were violated.

Actual wall thickness measurements are given in Figure 2.6.

2.4 Segmental Specimens

The purpose of these specimens was to model the behavior of segmentally constructed, precast piers. The three specimens presented here are the segmental equivalents of the monolithic specimens already discussed.

The segmental specimens consists of three 24 inch match-cast segments (Figs. 2.9 and 2.10). The load heads were also match-cast with the pier. Each of the segments has discontinuous, non-prestressed mild longitudinal reinforcement (Fig. 2.11).

The transverse reinforcement spacing in the segmental specimens followed the same rules as for the monolithic specimens. The spacing for a typical segment is shown in Figure 2.12.

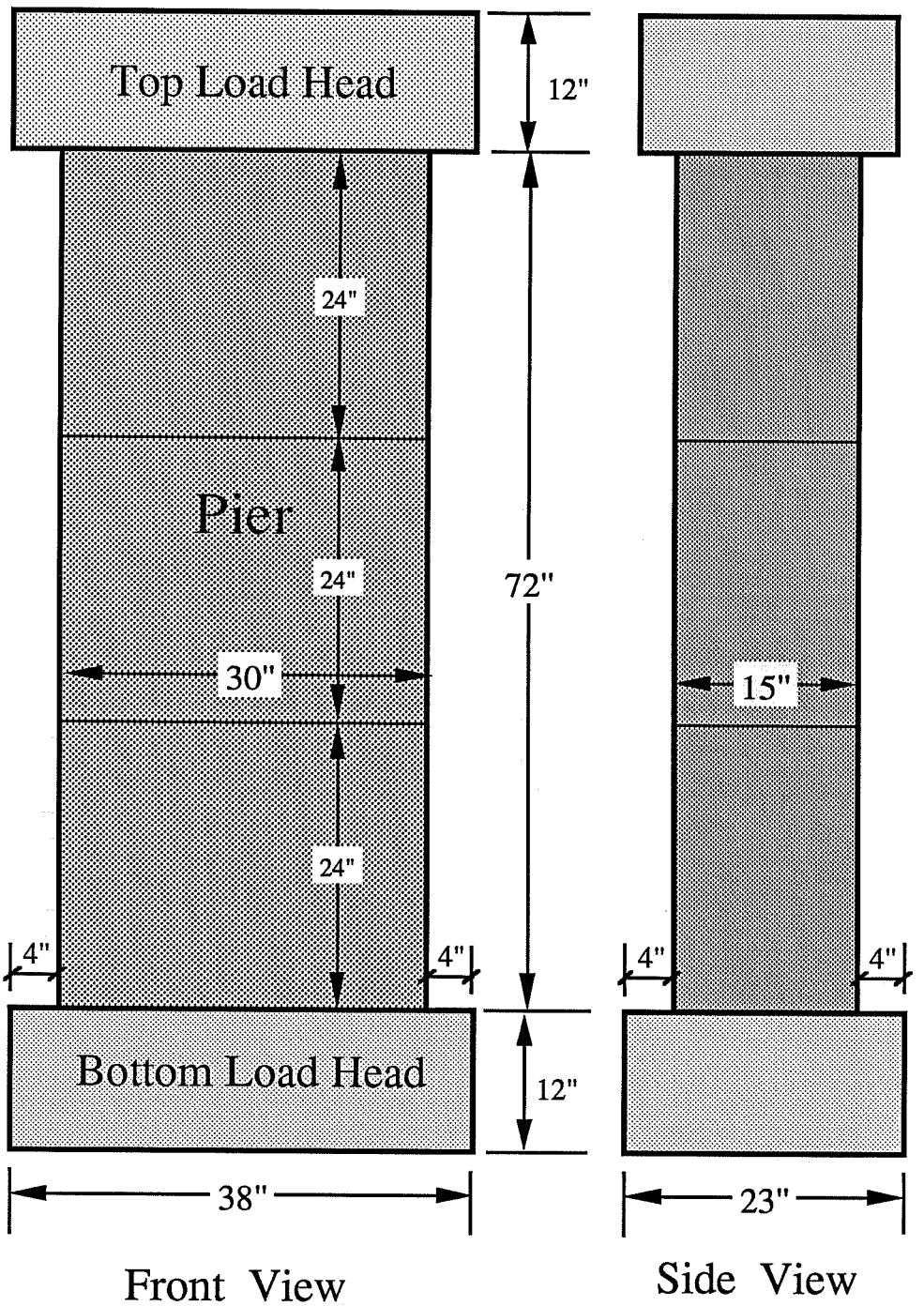

Figure 2.9 Specimen 1S Elevation

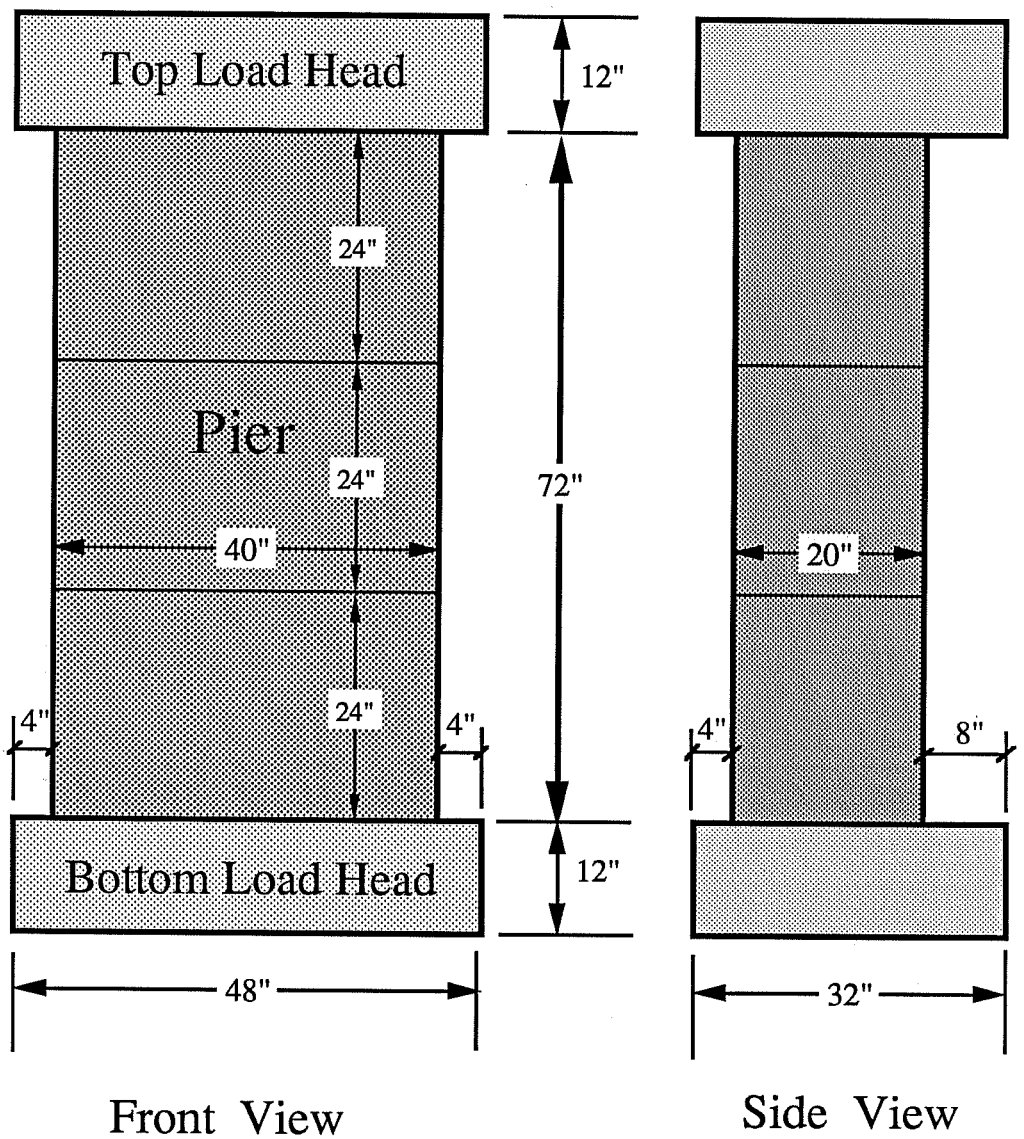

Figure 2.10 Specimens 2S and 3S Elevation

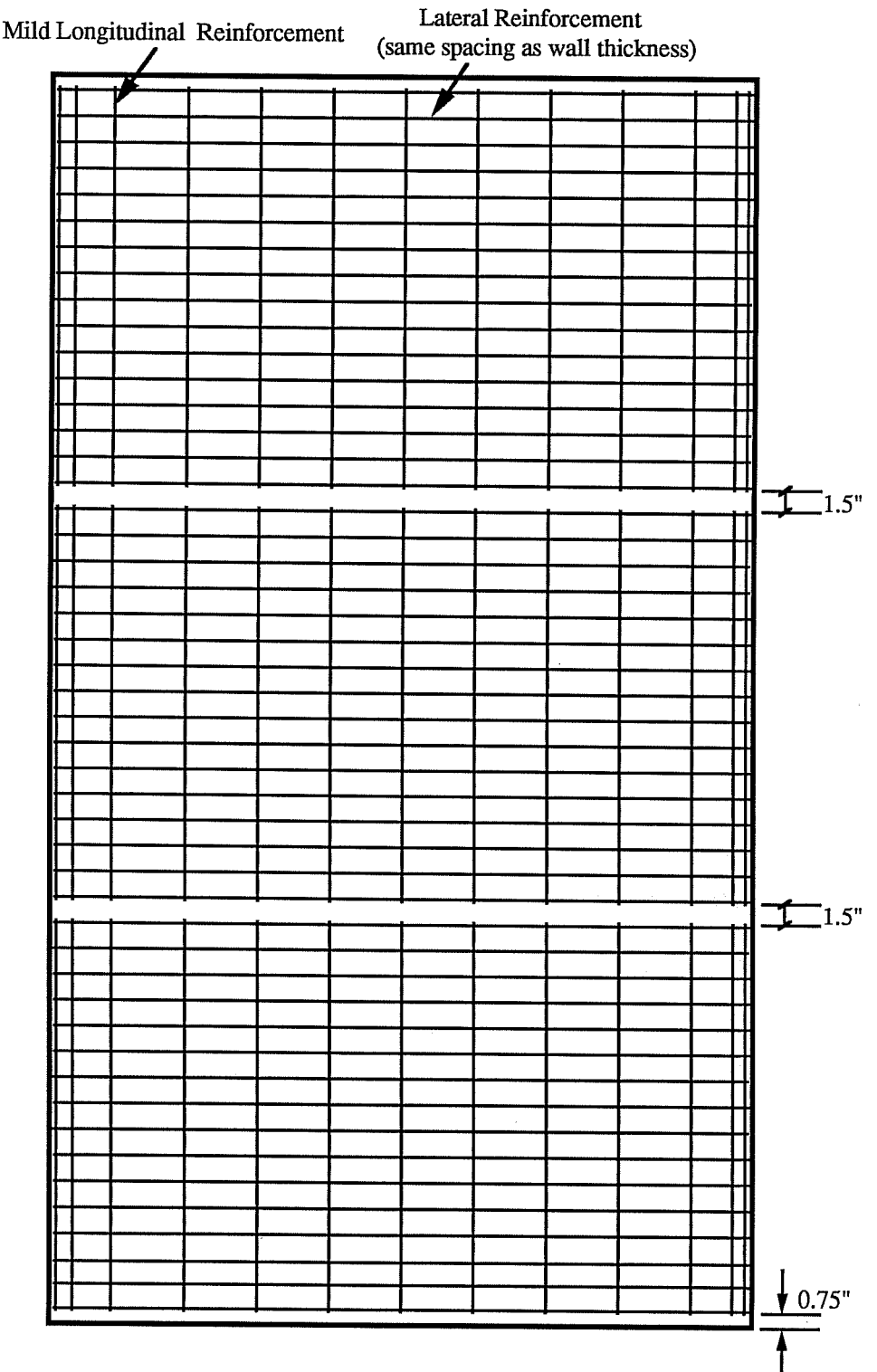

Figure 2.11 Segmental Reinforcement Elevation

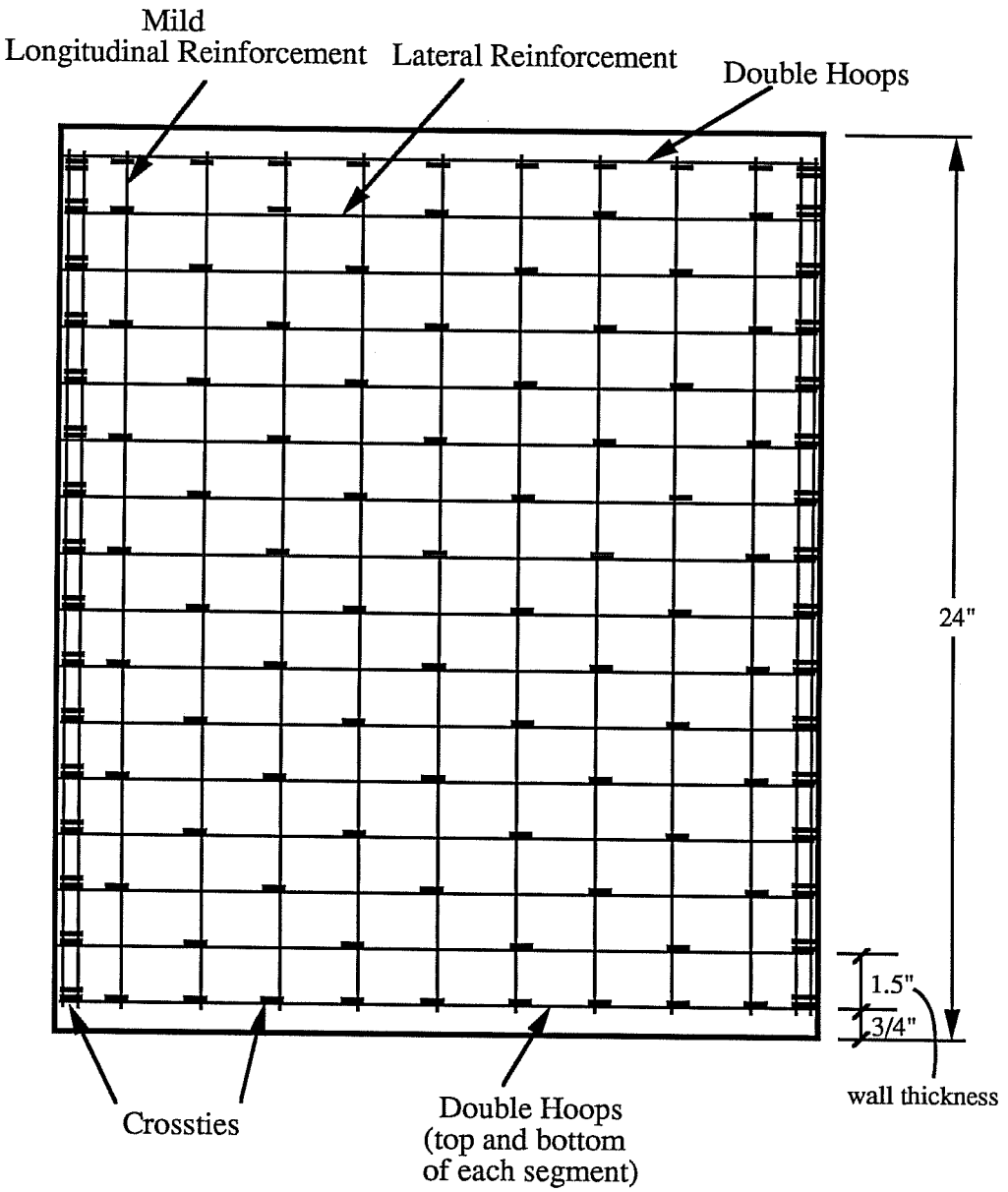

Figure 2.12 Segmental Transverse Reinforcement Layout

2.4.1 Specimen 1S

The outside dimensions of this specimen were 15 X 30 inches with a 2.5 inch wall thickness, identical to those of Specimen 1M. This specimen includes both mild reinforcement and post-tensioned reinforcement. The longitudinal and post-tensioning reinforcement layout is shown in the cross-sectional view of Figure 2.13. The corner bevels reduced the wall slenderness ratio from 10, found in Specimen 1M, to 8.4.

The transverse reinforcement for this specimen was identical to that of Specimen 1M (Fig. 2.5), the only exception being the addition of corner ties to confine the post-tensioning reinforcement as shown in Figure 2.14.

Actual wall thickness measurements were taken after debonding the match-cast segments. These measurements are given in Figure 2.15.

2.4.1.1 Epoxy Joining Procedure

The epoxy was mixed according to specifications and a thin layer was applied to both faces of the match-cast segments to be bonded. Before the epoxy began to set, the segments were joined together by applying enough pressure to create 100 psi contact stress on the pier cross-section. This contact stress was held for approximately 24 hours.

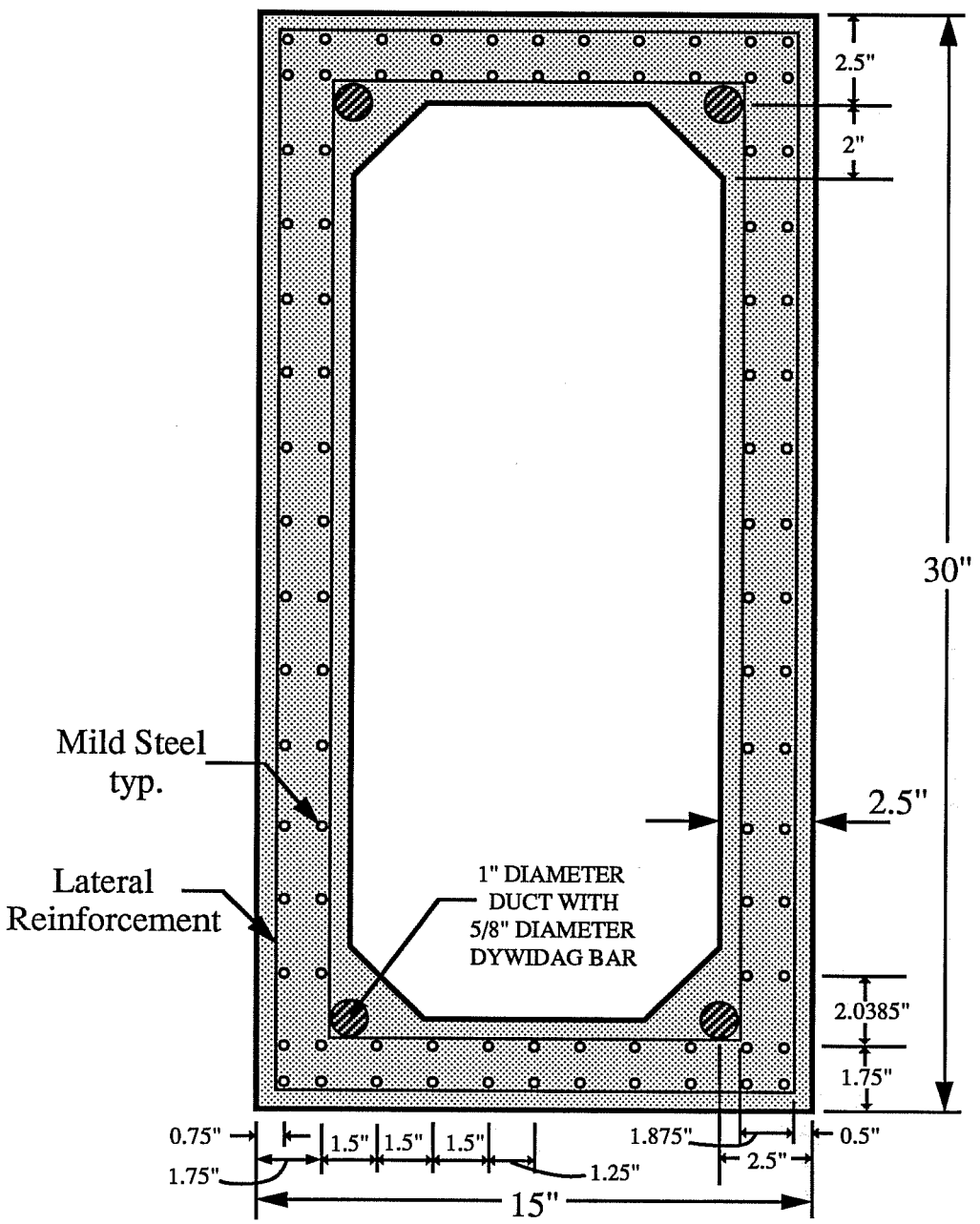

Figure 2.13 Specimen 1S Reinforcement Layout

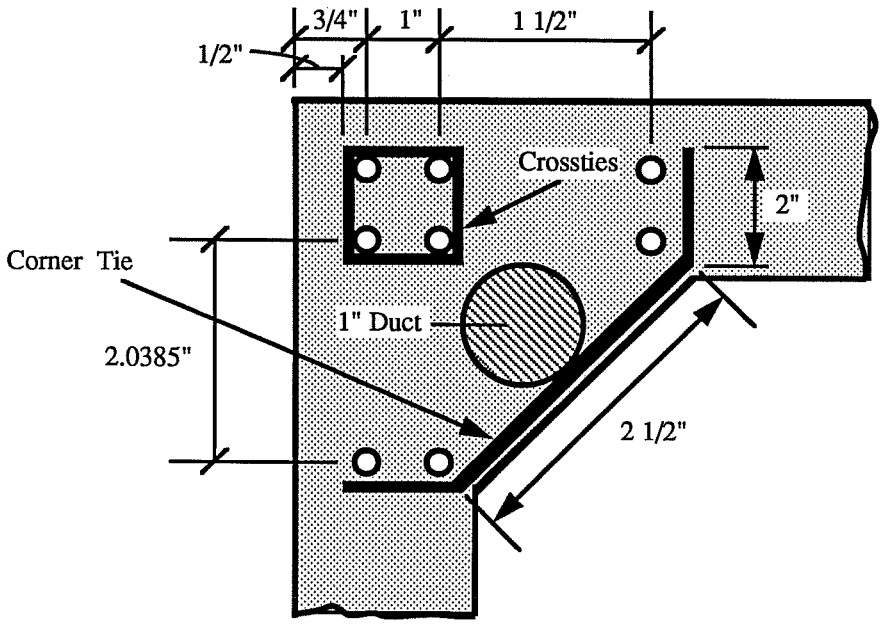

Specimen 1S Corner Detail

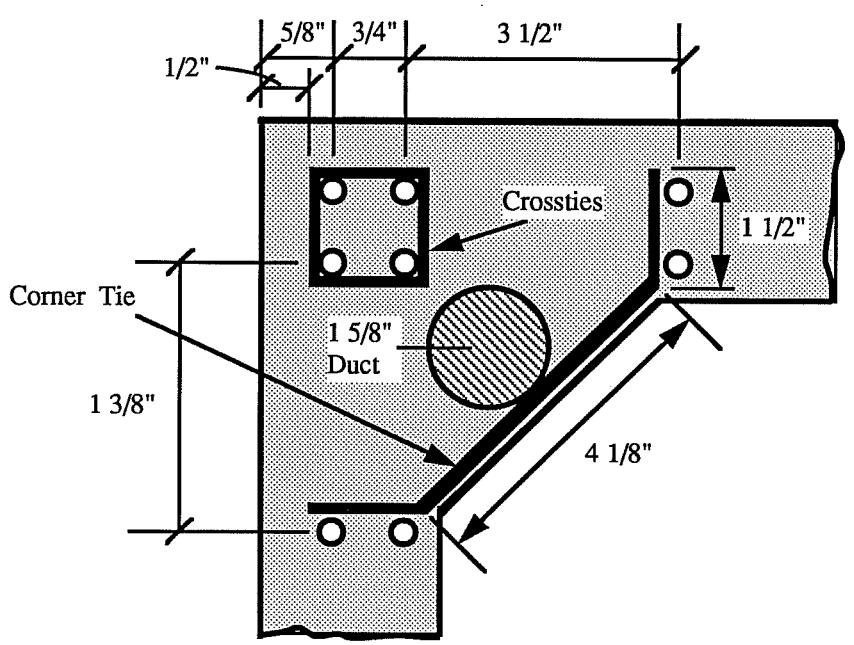

Specimen 2S Corner Detail

Note: Lateral hoop reinforcement is not shown.

Figure 2.14 Corner Details for Specimens 1S and 2S

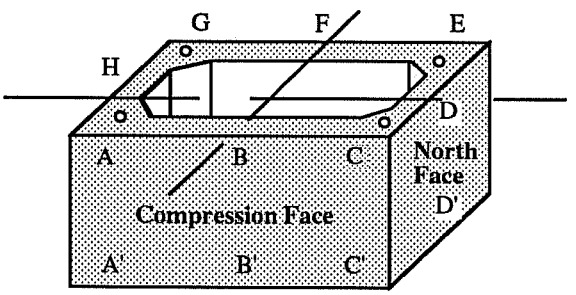

Locations A through H are 1" below top edge.
Locations A' through H' are 1" above bottom edge.
B, D, F, H, B', D', F' and H' are on centerlines of sides.
A, C, E, G, A', C', E', and G' are 1" from bevels.

** Note: All dimensions are in inches.

SPECIMEN 1S

Segment	A/A'	B/B'	C/C'	D/D'	E/E'	F/F'	G/G'	H/H'
Top	2 15/32 2 7/16	2 1/2 2 1/2	2 15/32 2 1/2	2 13/32 2 13/32	2 5/16 2 7/16	2 3/8 2 1/2	2 11/32 2 9/16	2 7/16 2 1/2
Middle	2 9/32 2 3/8	2 13/32 2 17/32	2 3/8 2 17/32	2 7/16 2 1/2	2 11/32 2 9/16	2 7/16 2 15/32	2 15/32 2 15/32	2 1/2 2 1/2
Bottom	2 13/32 2 3/8	2 1/2 2 7/16	2 1/2 2 3/8	2 1/2 2 1/2	2 11/32 2 11/32	2 3/8 2 13/32	2 3/8 2 15/32	2 15/32 2 3/8
Average Stand. Dev.		2.443 0.067		2.458 0.429		2.422 0.074		2.464 0.046

SPECIMEN 2S

Segment	A/A'	B/B'	C/C'	D/D'	E/E'	F/F'	G/G'	H/H'
Top	2 1/8 2 1/16	2 5/32 2 1/16	2 2 1/32	2 1/32 2 3/32	2 1/8 2 1/16	2 3/16 2 1/8	2 3/32 2 3/32	2 3/16 2 1/16
Middle	2 1/32 2 1/8	2 1/16 2 1/8	2 1/16 2 1/16	2 1/16 2 1/16	2 1/32 1 31/32	2 1/32 2	2 1 15/16	2 1 31/32
Bottom	2 1/32 1 7/8	2 3/32 1 15/16	2 1 13/16	1 7/8 1 31/32	1 15/16 2 1/32	1 29/32 2 1/8	1 7/8 2 1/16	1 7/8 1 15/16
Average Stand. Dev.		2.036 0.086		2.016 0.074		2.033 0.083		2.005 0.0995

SPECIMEN 3S

Segment	A/A'	B/B'	C/C'	D/D'	E/E'	F/F'	G/G'	H/H'
Top	1 19/32 1 1/2	1 5/8 1 19/32	1 1/2 1 17/32	1 11/16 1 1/2	1 5/16 1 7/16	1 3/8 1 1/2	1 11/16 1 15/32	1 17/32 1 17/32
Middle	1 13/32 1 1/2	1 17/32 1 5/8	1 17/32 1 19/32	1 11/16 1 1/2	1 13/32 1 15/32	1 15/32 1 17/32	1 13/32 1 17/32	1 7/16 1 7/16
Bottom	1 17/32 1 3/8	1 5/8 1 7/16	1 9/16 1 5/16	1 7/16 1 13/32	1 3/8 1 1/2	1 15/32 1 17/32	1 1/2 1 9/16	1 13/32 1 15/32
Average Stand. Dev.		1.521 0.087		1.536 0.112		1.474 0.082		1.469 0.048

Figure 2.15 Specimens 1S, 2S, and 3S Wall Thicknesses

2.4.1.2 Post-tensioning and Grouting Procedure

After waiting for the required concrete strength to develop, the four post-tensioning tendons were stressed to provide 700 psi contact stress on the pier cross-section. This required stressing each tendon to 35 kips. The tendons were stressed in sequence from one tendon to the tendon on the opposite corner and so forth. Load cells were used to measure the force in each tendon. Hydraulic rams were used to stress the tendons. After stressing all of the tendons, the locking nuts were fastened against the bearing plates until the force on the load cells began to drop.

Each post-tensioning duct was grouted the same day the tendons were post-tensioned. The grout was pumped through each duct until a continuous stream of grout poured out of the outlet on the opposite end of the specimen.

2.4.2 Specimen 2S

As with Specimens 1M and 1S, Specimens 2M and 2S were identical except for their construction method and the addition of the post-tensioned reinforcement. The outside dimensions of this specimen were 20 X 40 inches with a 2.0 inch wall thickness (Fig. 2.16). With the addition of the corner bevels for the post-tensioning reinforcement, the wall slenderness ratio for this specimen was reduced from 18, in Specimen 2M, to 15.5.

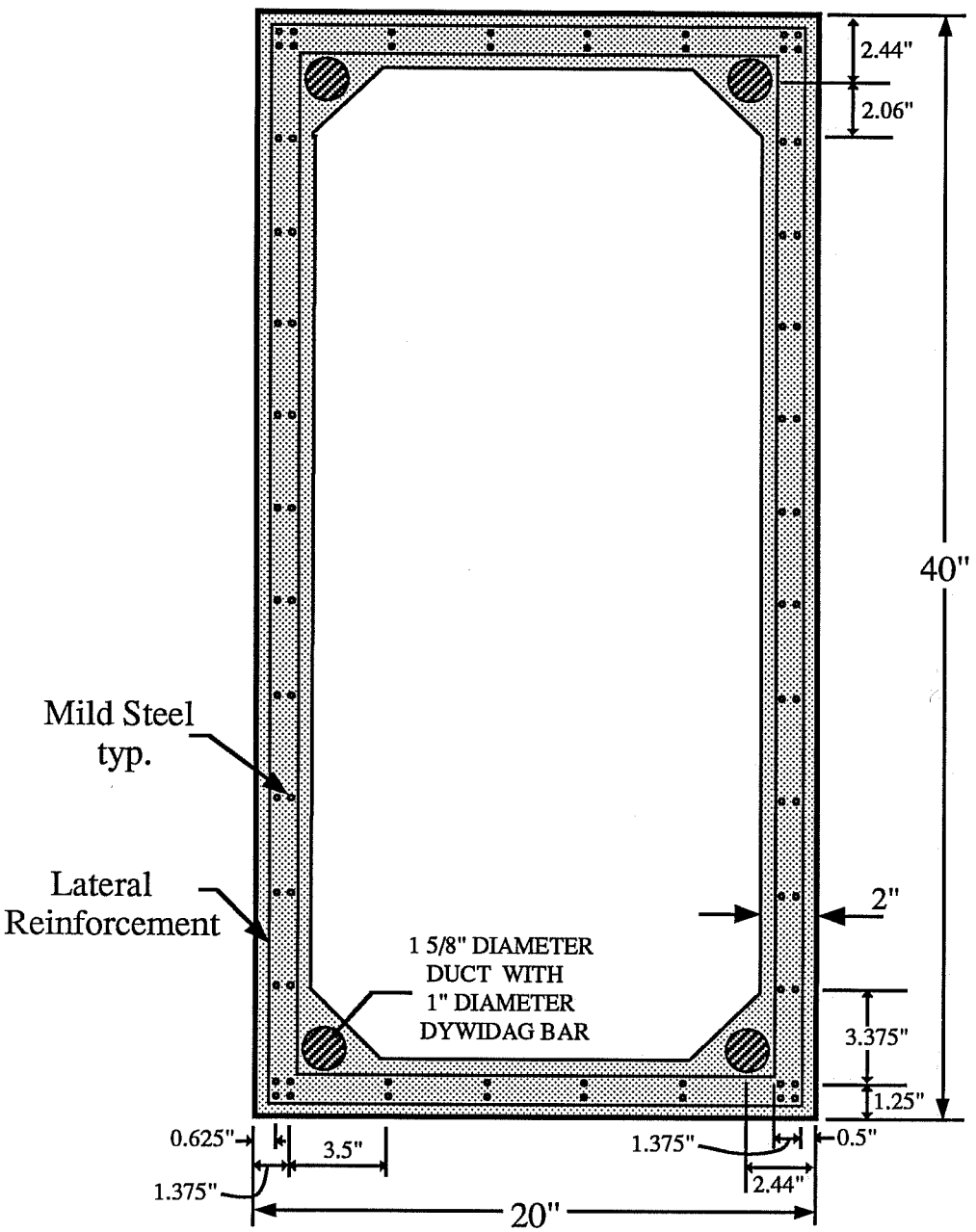

Figure 2.16 Specimen 2S Reinforcement Layout

The reinforcement layout is shown in the cross-sectional view of Figure 2.16. With the exception of the corner ties shown in Figure 2.14, the transverse reinforcement layout and dimensions are identical to that of Specimen 2M (Fig. 2.5).

Wall thickness measurements are shown in Figure 2.15.

2.4.2.1 Epoxy Joining Procedure

Epoxy was applied following the same procedure used for Specimen 1S.

2.4.2.2 Post-tensioning and Grouting Procedure

The four post-tensioning tendons were stressed to provide 750 psi contact pressure on the pier cross-section. The procedure was as follows:

1) extended rams approximately 1/2 inch
2) snugged up nuts on ram piston
3) stressed alternate corners to approximately 3100 psi on four dial gages (42.6 kips per tendon)
4) tightened locking nut until pressure began to drop on gages
5) released pressure on two rams at a time, on opposite corners
6) removed hardware

The post-tensioning ducts were grouted the same day as the tendons were stressed. The same procedure used in the preceding specimen was followed. However, grout leaked into the inside of the specimen from one of the segmental joints of the duct. This

duct was then grouted from both ends though a void near the leaking joint was expected.

2.4.3 Specimen 3S

The outside dimensions of this specimen were 20 X 40 inches with a 1.5 inch wall thickness, identical to those of Specimen 3M. However, the addition of corner bevels reduced the wall slenderness ratio from 24.7 to 22.3.

The reinforcement layout is shown in the cross-sectional view of Figure 2.17. Transverse reinforcement dimensions were identical to that of Specimen 3M (Fig. 2.5). The corner ties can be seen in the corner detail of Figure 2.18.

Wall thickness measurements are found in Figure 2.15.

2.4.3.1 Epoxy Joining Procedure

The same procedure used for Specimens 1S and 2S was followed.

2.4.3.2 Post-tensioning and Grouting Procedure

The four post-tensioning tendons were stressed to provide 750 psi contact pressure on the pier cross-section. The same procedure used for Specimen 2S was followed, the only exception being a change in hydraulic pressure from 3100 psi to 6800 psi. This caused a force of 32.1 kips in each tendon. As in Specimen 2S, one duct leaked and had to be grouted from both ends of the specimen.

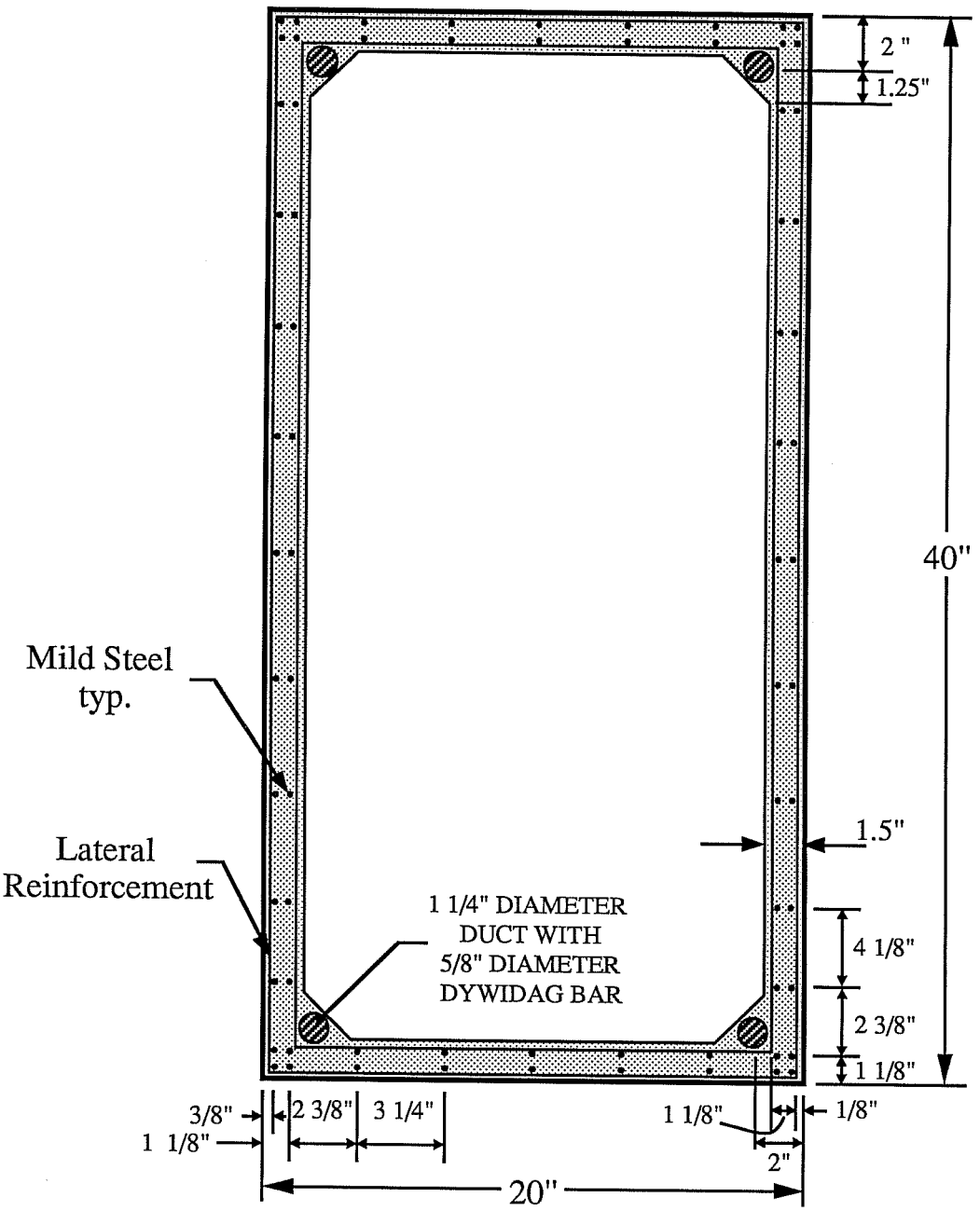

Figure 2.17 Specimens 3S and 3PM Reinforcement Layout

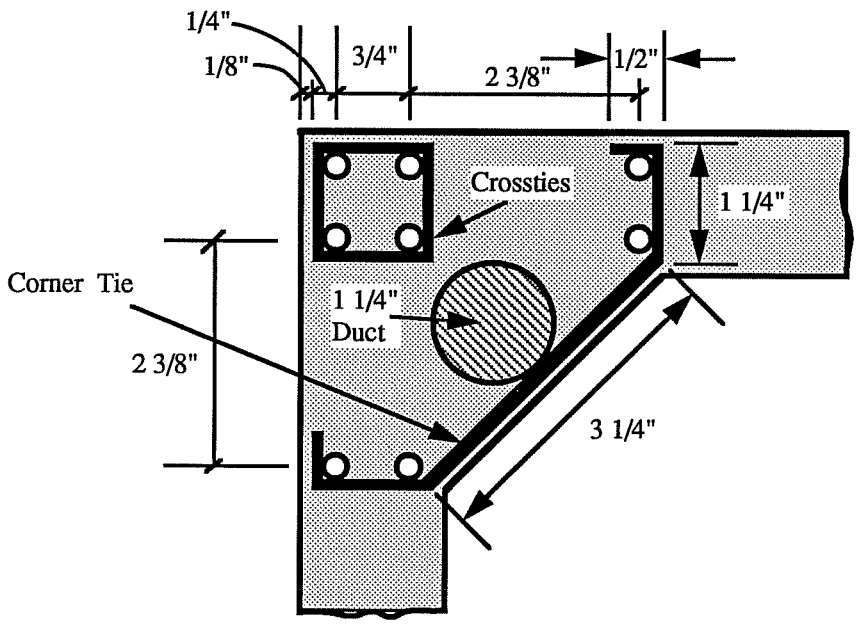

Specimen 3S Corner Detail

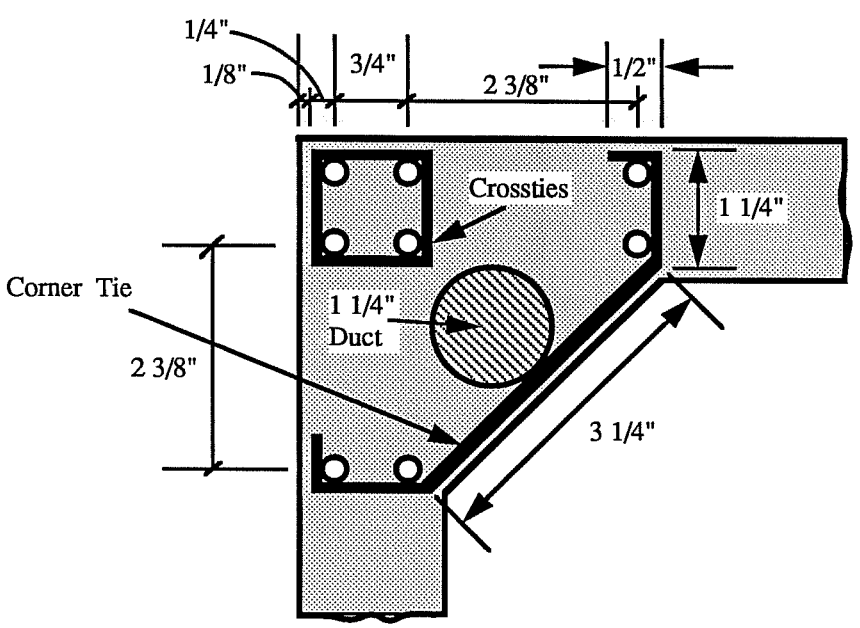

Specimen 3PM Corner Detail

Note: Lateral hoop reinforcement is not shown.

Figure 2.18 Corner Details for Specimens 3S and 3PM

2.5 Post-Tensioned Monolithic Specimen

This specimen was designed in order to help determine how the segmentally, post-tensioned specimens differed from the monolithic specimens. By post-tensioning a monolithic specimen, the effect of the segmental construction was isolated from the effect of the post-tensioned reinforcement.

2.5.1 Specimen 3PM

With outside dimensions of 20 X 40 inches and a 1.5 inch wall thickness, this specimen was almost identical to Specimens 3M and 3S. Like Specimen 3S, this specimen included post-tensioned reinforcement and corner bevels which reduced the wall slenderness ratio to 22.3 (see Fig. 2.17).

Cast in three lifts of 24 inches, construction of this specimen was very similar to that of Specimen 3M, the only differences being the post-tensioning steel and continuous mild longitudinal reinforcement.

The reinforcement layout is shown in the cross-sectional view of Figure 2.17. The lateral reinforcement and corner ties were identical to that of Specimen 3S (see Figs. 2.5 and 2.18).

Wall thickness measurements are listed in Figure 2.6.

2.5.1.1 Post-tensioning and Grouting Procedure

The four post-tensioning tendons were stressed to provide 750 psi contact pressure on the pier cross-section. The same procedure used for Specimen 2S was followed, the only exception

being a change in hydraulic pressure from 3100 psi to 6800 psi. As with Specimen 3S, each tendon had a force of 32.1 kips.

2.6 Materials

2.6.1 Concrete

The concrete used for casting the pier of Specimens 1M and 2M was delivered to the laboratory from a local ready-mix company. This was necessary because the quantity of concrete needed was greater than the quantity that could be produced in one batch at the laboratory. Since smaller quantities were required, the concrete used for casting the remaining specimens was mixed in the laboratory in order to have better control over the mix. Due to the wide range of wall slenderness ratios, the design strength of each mix was varied to meet the limitations of the testing machines. Mix design strengths and batch quantities are found in Table 2.1.

Concrete mix designs for each specimen are given in Table 2.2. The segmental piers required a mix design for each of the three segments. However, except for Specimen 1S, the designs for each segment in a particular pier were identical. Three separate mix designs were required for Specimen 1S because the moisture content of the aggregates changed from one mixing to the next.

Table 2.1 Mix Design Strengths and Batch Quantities

Specimen	Design Strength	Batch Quantity	Comments
1M	5.0 ksi	5.5 CY	monolithic
1S	5.0 ksi	5.0 CF	bot. seg.
1S	5.0 ksi	6.0 CF	other seg.
2M	4.5 ksi	3.0 CY	monolithic
2S	5.0 ksi	6.0 CF	all seg.
3M	7.0 ksi	6.0 CF	all lifts
3S	7.0 ksi	6.0 CF	all seg.
3PM	7.0 ksi	6.0 CF	all lifts

Table 2.2 Concrete Mix Designs

Specimen No.	Cement (lbs)	Water (lbs)	Aggregates (lbs)		Admx. (oz)	
			Coarse	Fine	Reducer	Super-plasticizer
1M	3102.	1540	8938.	8079.	92.40	372
1S Bot.	108.8	48.5	286.6	291.9	0	0
1S Mid.	130.6	74.5	338.2	334.7	0	0
1S Top	130.6	59.4	343.3	350.1	0	0
2M	1554.	791.	5360.	3811.	66.0	200
2S	140.0	71.0	340.0	335.0	0	0
3M Bot.	146.2	62.4	329.9	336.5	0	9.0
3M Mid.	146.2	62.4	329.9	336.5	0	4.5
3M Top	146.2	62.4	329.9	336.5	0	4.5
3S	146.2	62.4	329.9	336.5	0	9.0
3PM	146.2	58.6	331.8	338.4	0	4.0

Type I and II portland cement was used for casting all specimens. The coarse aggregate was pea gravel graded for 3/8 inch maximum diameter. The fine aggregate was normal weight sand. The admixtures were added for workability. Admixtures used included a pozzolith water reducer and superplasticizer.

Following ACI standards (11), a minimum of nine 6 by 12 inch concrete cylinders were made from each mix. They were capped and allowed to cure under the same conditions as the pier specimens. The concrete strength was measured at the time of the pier tests. Cylinder strengths for each specimen are listed in Table 2.3.

2.6.2 Mild Reinforcing Steel

2.6.2.1 Longitudinal Reinforcement

The longitudinal reinforcing steel used in each section were 6 mm diameter bars obtained from Sweden. The actual area of these bars is 0.0475 square inches with a diameter of 0.246 inches. From the results of tension tests with a two-wire strain gage in conjunction with a Measurements Group Model P-350A strain indicator, the yield stress of the 6 mm bars was found to be 75.1 ksi. Other properties found are as follows:

Yield Strain	2590 $\mu\epsilon$
Modulus of Elasticity	28,900 ksi
Ultimate Stress	90.4 ksi
Elongation at Break	9.9 %

Table 2.3 Cylinder Strengths the Day of Test

Specimen	Segment	Avg. Stress (psi)	Age (days)	Cylinders Tested
1M	Center	7862	38	3
	Bot. Load Head	6651	91	3
	Top Load Head	7991	35	4
1S	Bottom	6980	85	5
	Middle	5696	82	8
	Top	6383	75	5
	Bot. Load Head	12,212	118	3
	Top Load Head	12,928	69	3
2M	Center	7705	64	3
	Bot. Load Head	11,670	90	3
	Top Load Head	12,269	41	3
2S	Bottom	5458	39	3
	Middle	5205	36	3
	Top	4837	31	3
	Bot. Load Head	8032	50	3
	Top Load Head	8985	28	3
3M	Bottom	7040	57	3
	Middle	6800	62	3
	Top	6311	64	3
	Bot. Load Head	8018	71	3
	Top Load Head	11083	41	3
3S	Bottom	6916	105	3
	Middle	7101	99	3
	Top	6894	92	3
	Bot. Load Head	7922	115	3
	Top Load Head	7913	86	3
3PM	Bottom	6358	37	3
	Middle	6473	35	3
	Top	6463	30	3
	Bot. Load Head	9572	48	3
	Top Load Head	9546	27	3

2.6.2.2 Transverse Reinforcement

To meet modeling requirements, the transverse reinforcement used was cold drawn 10 gauge wire. The diameter of the 10 gauge wire is approximately 1/5 that of a #5 reinforcing bar. Meeting standard specifications, the diameter of this wire is 0.135 inches with an area of 0.014 square inches. The wire was provided in coils. Representative sections of the coils were cut to length and tension tests were conducted. These tests revealed brittle behavior for this wire. There was no well-defined yield plateau. The wire was then heat treated in order to get properties more representative of reinforcing bar ductility.

The heat treatment consisted of the following steps:

1) Preheating the heat treating oven to 900°F and providing a carbon-rich environment.

2) Placing the coils in the oven for one hour at a temperature of 900°F.

3) Allowing the coils to air cool.

Two separate heats of wire were required to fabricate the specimens. Specimens 1M, 2M and 1S were fabricated from the first heat.

Tension tests were performed on the first heat using an extensometer with an 8 inch gage length. An 8 1/8 inch gage length was used on the second heat. The second heat was

subjected to two heat treatments. The properties of the wire before and after the heat treatment were as follows:

1st Heat

Description	Yield Stress	Ultimate Stress	Elongation at break
cold drawn	89.0 ksi	98.8 ksi	1.9 %
heat treated	77.7 ksi	91.5 ksi	7.5 %

2nd Heat

Description	Yield Stress	Ultimate Stress	Elongation at Break
cold drawn	102.2 ksi	107.1 ksi	1.9 %
heat treat 1	85.7 ksi	99.8 ksi	8.5 %
heat treat 2	89.1 ksi	100.2 ksi	7.5 %

With the exception of the percent elongation at break, the above properties meet the requirements of ASTM A615 which specifies a minimum yield strength of 60 ksi, a minimum ultimate strength of 90 ksi, and 9% elongation at break.

2.6.3 Post-tensioning Steel

The characteristics of the post-tensioning steel were furnished by the Dywidag Company. The 5/8 inch threadbar diameter used in Specimens 1S, 3S, and 3PM has an ultimate stress of 157 ksi with a nominal cross-sectional area of 0.28 square inches. The 1 inch threadbar diameter used in Specimen

2S has an ultimate stress of 150 ksi with a nominal cross-sectional area of 0.85 square inches.

2.6.4 Ducts

Smooth plastic electrical conduit ducts were used for Specimen 1S. Ribbed metal electrical conduits were used for Specimens 2S, 3S, and 3PM. After the concrete had cured, the metal conduit was removed from the duct in order to get a direct bond between the ribbed concrete and the grout.

2.6.5 Epoxy

The two component segmental bridge epoxy specified and supplied by the Texas State Department of Highways and Public Transportation (TSDHPT) was used to bond the segments of Specimens 1S, 2S, and 3S. High-range epoxy number B-75 was utilized to bond the segments of Specimens 1S and 2S. Because of lower temperatures, mid-range epoxy number B-73 was used to bond the segments of Specimen 3S. For both epoxies, the ratio of resin to hardener specified by the manufacturer was 2.5.

After mixing the epoxy, one inch diameter cylinders two inches high were filled with epoxy. Following standard procedures (12), cylinder strengths of the epoxy for each specimen were determined at the time of the specimen test.

Specimen	Cylinder Strengths	Comments
1S	13,536 psi	avg. of 5
2S	12,372 psi	avg. of 3

Because of a quick setting time, epoxy cylinders were not made for Specimen 3S.

2.6.6 Grout

The grout mix design was based on TSDHPT standard specifications. The grout mix used for grouting the post-tensioning ducts of each specimen is as follows:

Cement	Water	Interplast
1 sack	5.5 gal	0.94 lbs

Interplast was used as an expansive admixture. The water/cement ratio of the preceding mix is 0.48, slightly above the 0.45 limit specified by the ACI Code (11) and PTI Manual (13).

The compressive strengths of 2 inch cube grout samples at the time of testing each specimen are listed below.

Specimen No.	Stress (psi)
1S	2347
2S	2196
3S	2814
3PM	2843

2.7 Formwork and Construction

2.7.1 Fabrication of Forms

The outer formwork was constructed so that the pier specimen complete with load heads could be cast entirely within it. Care was taken to insure that the outer formwork was sufficiently stiff to insure close tolerances for casting the

specimens. The outer formwork was cleaned after each specimen was cast and reused.

The inner formwork had to be custom built for each specimen depending on the wall thickness specified. By making the inner form larger or smaller, various wall thicknesses could be obtained.

As illustrated in Figure 2.19, the inner forms were made with a series of collapsible diaphragms so that they could be removed after casting the pier. After construction, the inner forms were wrapped with plastic to insure a smooth finish on the concrete and to keep cement paste and water from leaking into the hollow core.

Plexiglas forms were used as the outer formwork for confining the concrete. Plexiglas was used so that the condition of the concrete could be observed during placement. After shoring the plexiglas forms with wooden wales and sealing them with silicon to prevent leakage of paste, the specimens were ready to cast. Completed forms ready for casting are shown in Figure 2.20.

2.7.2 Fabrication of Cages

Reinforcing cages were fabricated in several different ways, depending on how the specimen was to be cast. For the monolithic specimens, the entire cage was assembled in one piece. Only that part of the cage associated with casting the

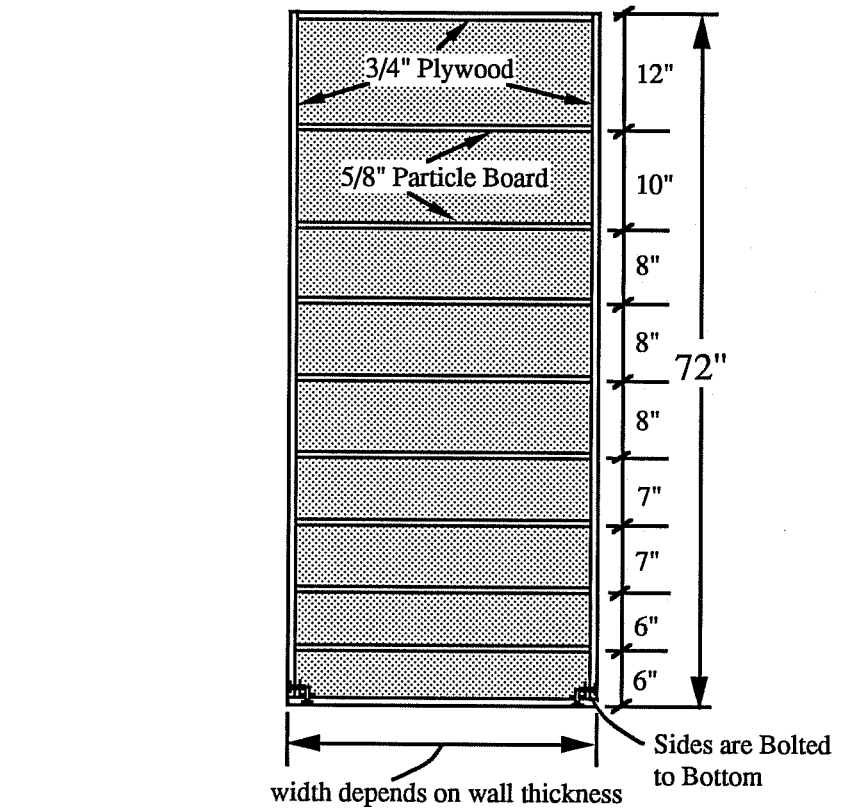

Figure 2.19 Inner Form Construction

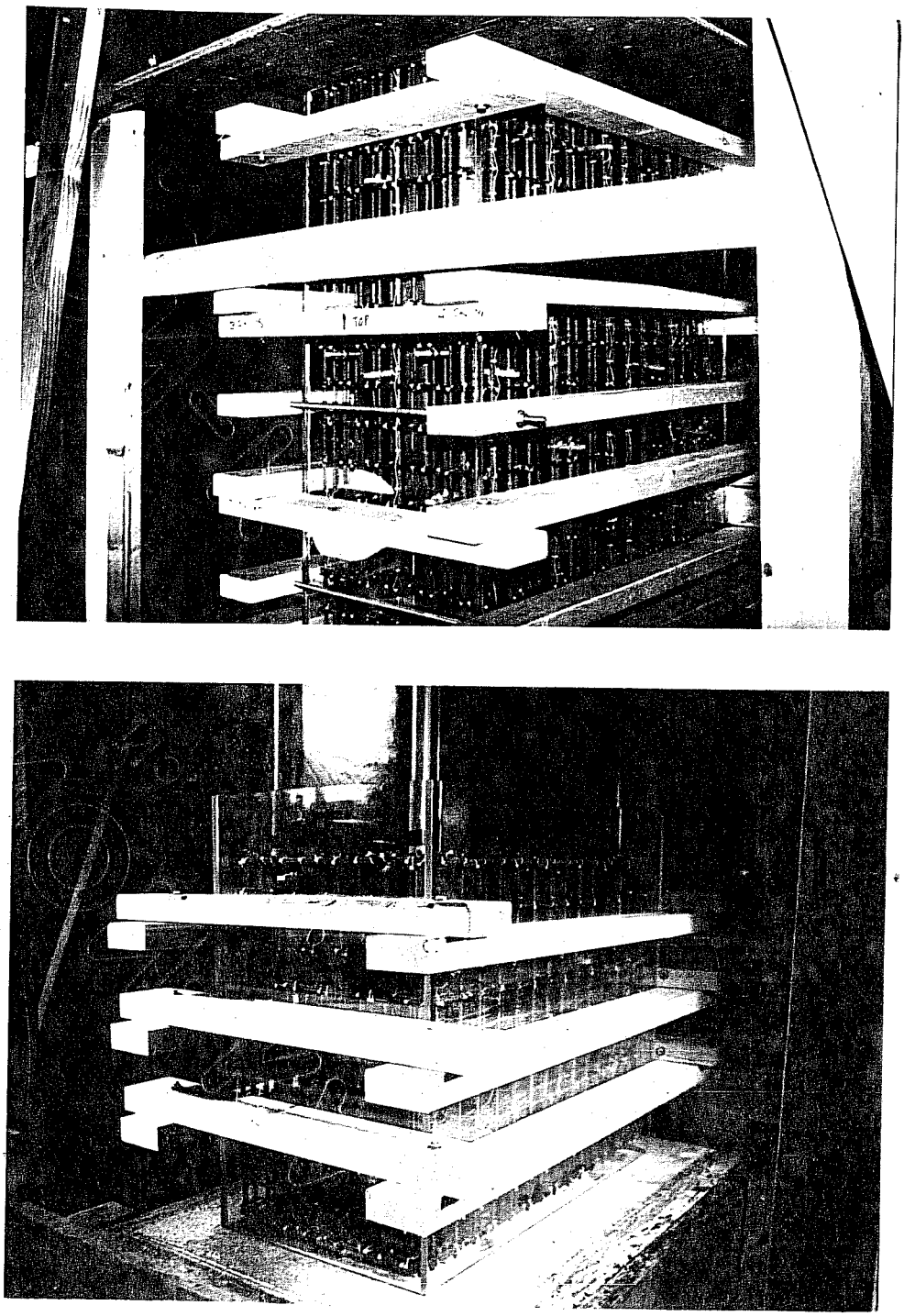

Figure 2.20 Completed Monolithic and Segmental Forms

appropriate segment was fabricated for the segmental specimens. Figure 2.21 illustrates each of the preceding types of cages.

Wooden spacers were used to position the two curtains of steel (Fig. 2.22). Plastic cable ties were used to tie the cages together because of their ease of use and because of the difficulty in getting the wire ties to remain tight around the smooth lateral reinforcement when vibrating the concrete during placement. Figure 2.23 shows a close-up of the cages.

Studs made of 3/8 inch diameter finely threaded rod were inserted through the plexiglas forms into the cages for instrumentation purposes (Fig. 2.22).

2.7.3 Placement of Concrete

To aid the placement of the concrete, careful vibration of the concrete was performed to insure consolidation throughout the length of the specimen. Observation through the plexiglas forms insured a satisfactory cast.

The concrete was allowed to cure for a minimum of 24 hours before removing the forms.

2.7.4 Segmental Construction

To prevent widely varying strengths in each pier segment, each segment was cast as quickly as it was prepared for casting. The time variation between casts of the top and bottom segments ranged from 7 to 13 days.

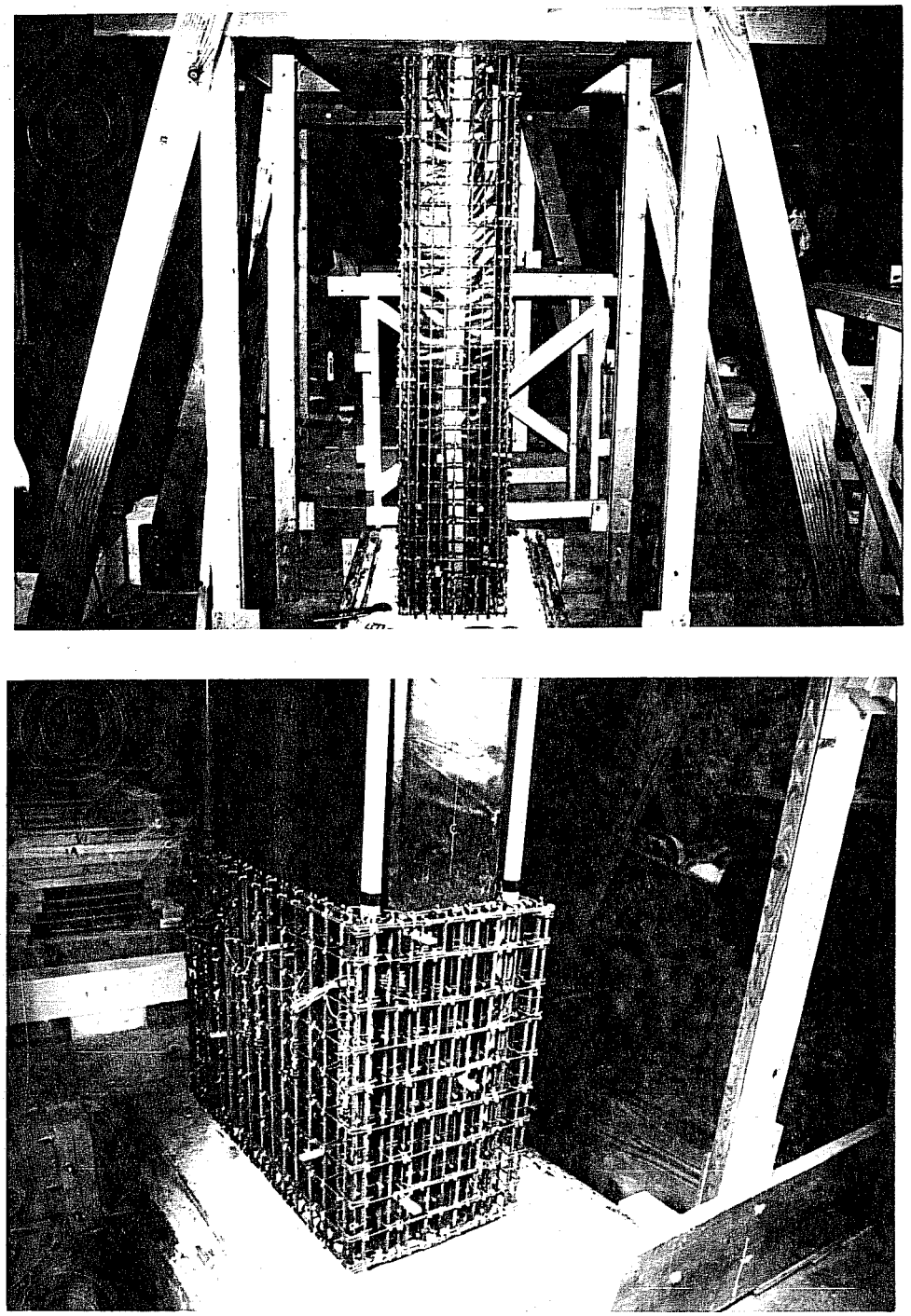

Figure 2.21 Monolithic and Segmental Reinforcement Cages

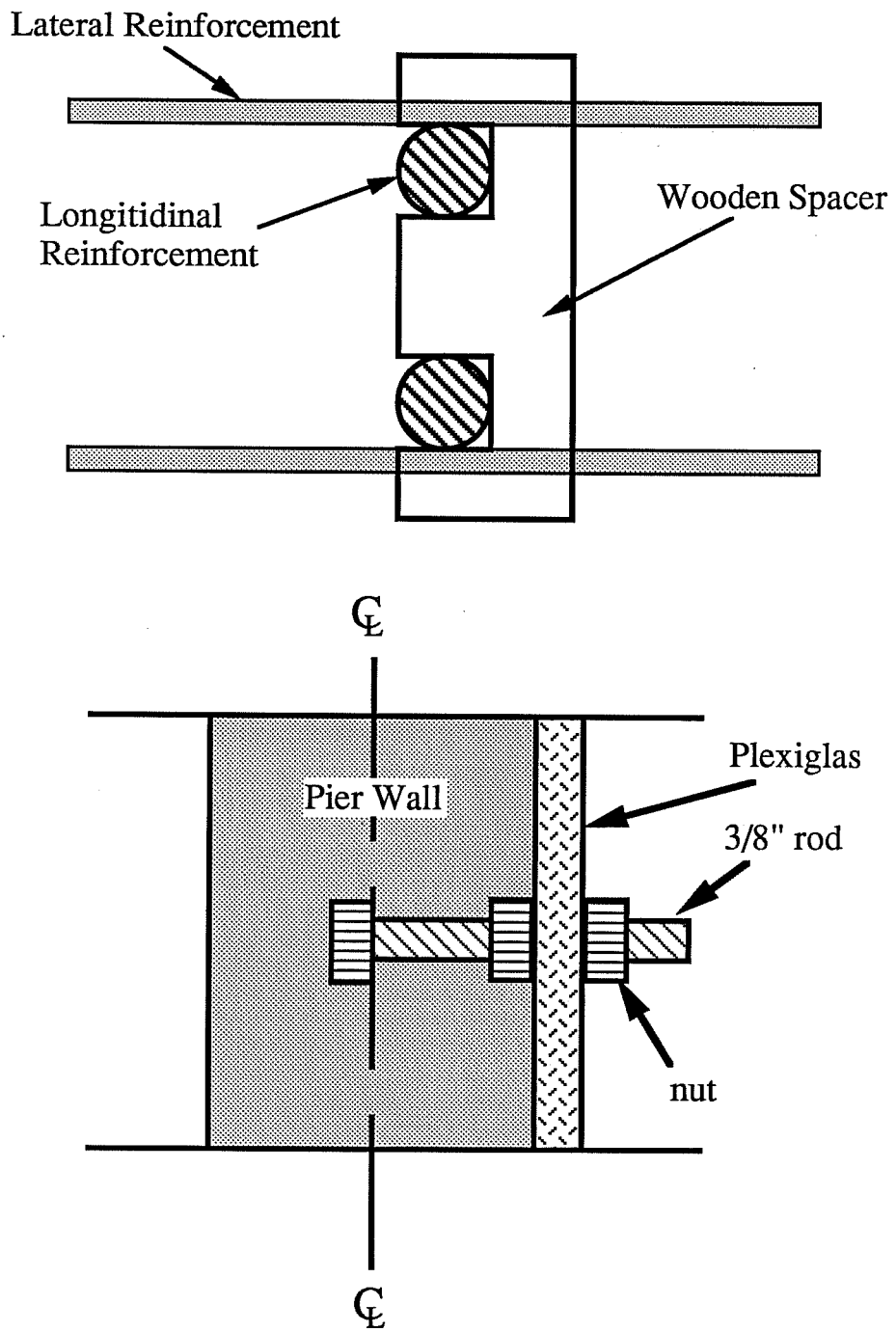

Figure 2.22 Wooden Spacer and Instrument Stud

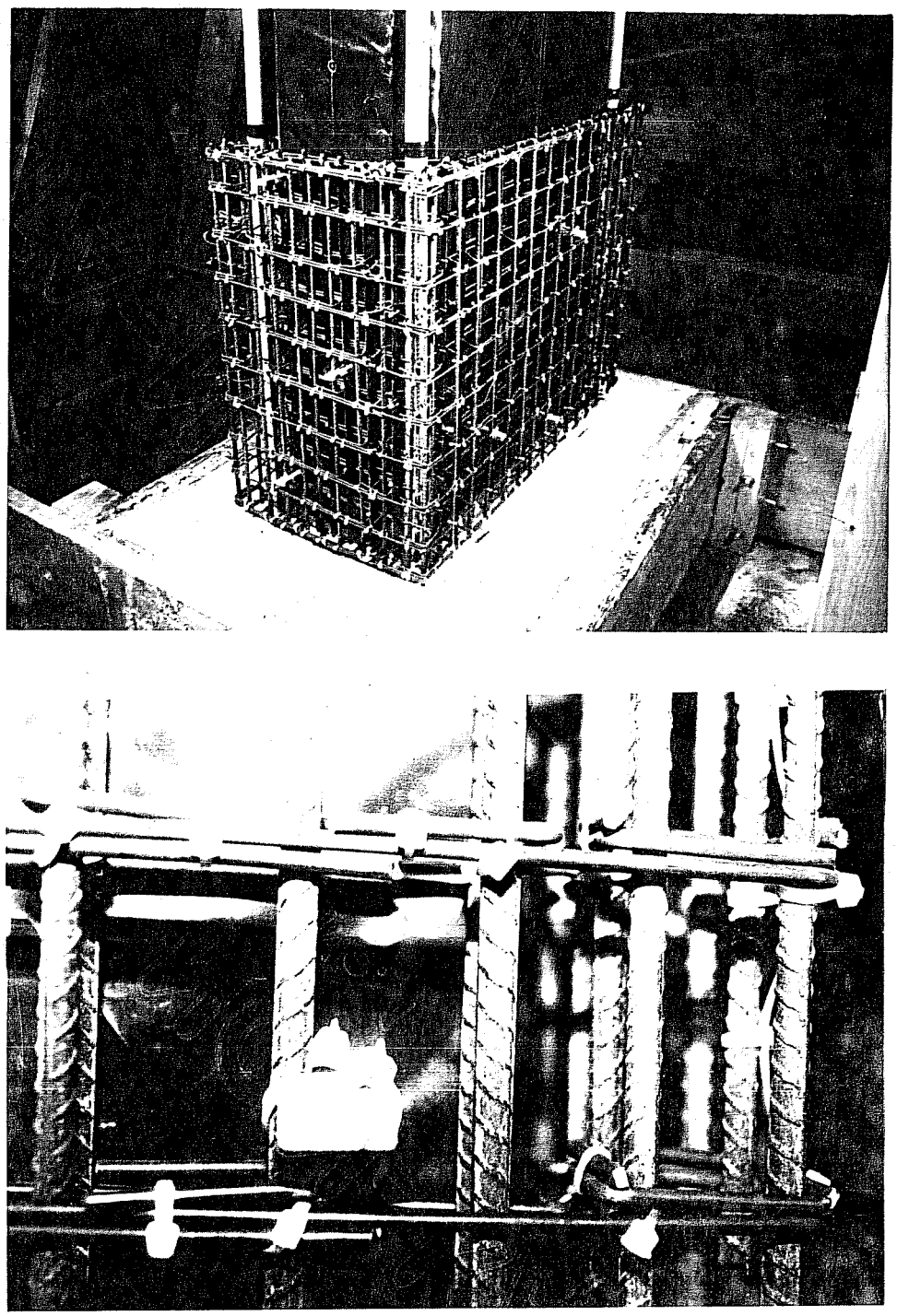

Figure 2.23 Reinforcing Cages

2.7.4.1 Debonding and Alignment

A debonding agent of four parts flax soap and one part talcum powder was applied to the construction joints to prevent the new concrete from bonding to the old. Debonding of the specimens usually occurred several days after the top load head was cast.

Alignment keys were cast into the concrete to aid in the realignment of the segments for epoxying and post-tensioning after their separation.

After debonding the segments, the surfaces to be joined by epoxy were lightly sandblasted to remove the debonding mixture and any loose particles. The segments were then aligned and the post-tensioning tendons inserted before epoxying (Fig. 2.24).

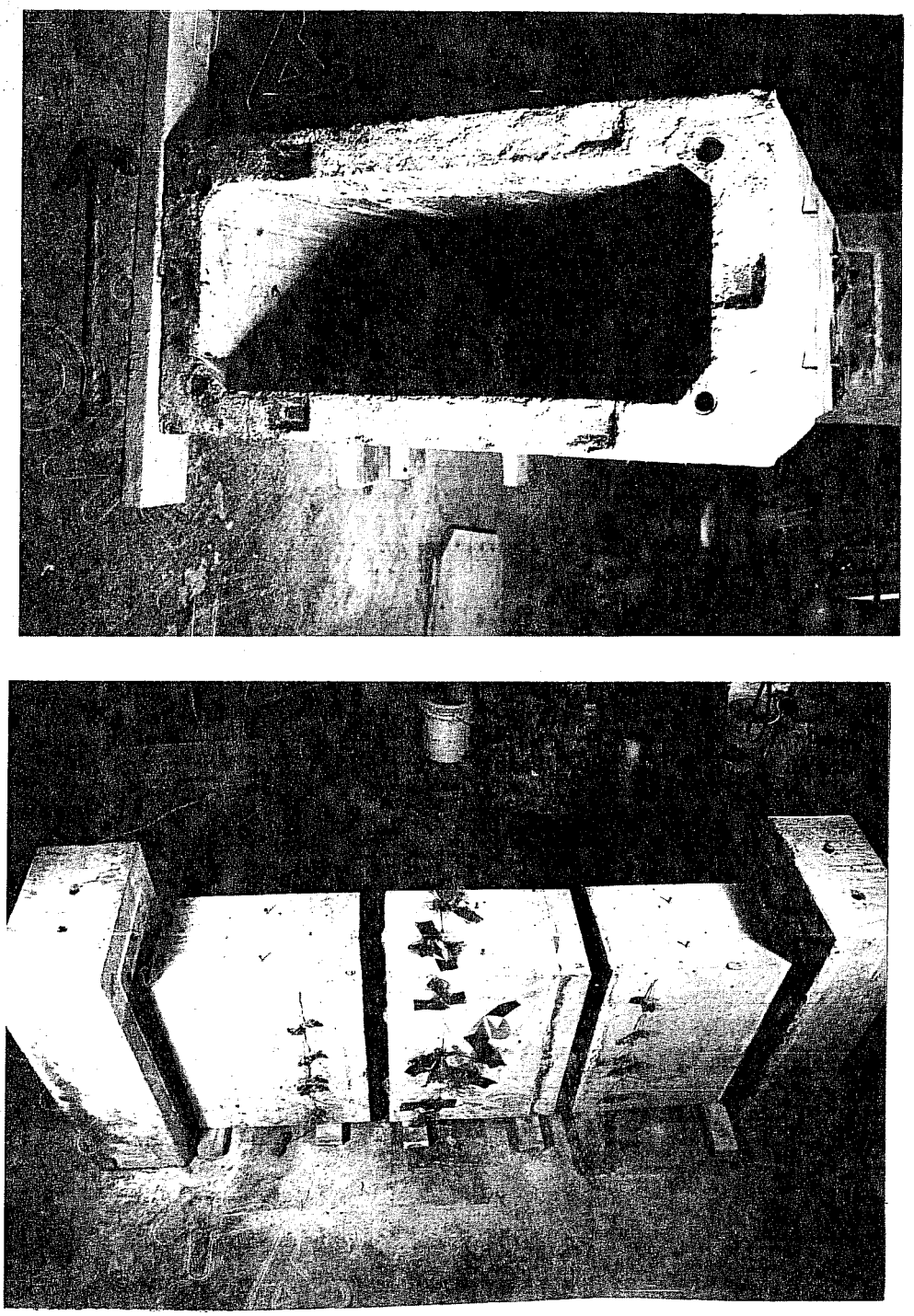

Figure 2.24 Segmental Specimen Ready for Epoxying

CHAPTER 3

TEST SETUP AND PROCEDURES

3.1 Setup

3.1.1 General Layout

Test specimens were loaded eccentrically about the weak axis so compressive failure would occur on the compression face of the specimen (Fig. 3.1) and to account for the minimum eccentricity specified by the codes (10,11).

Two testing machines were used to load the test specimens: A 600 kip capacity testing machine was used to load Specimen 1M (Fig. 3.2a), while a 1200 kip capacity machine was used to load the remaining specimens (Fig. 3.2b).

The 600 kip mechanical machine consisted of a rigid frame with a power driven load head and a fixed base (Fig. 3.3). Specimens were compressed between the machine's load head and base.

The 1200 kip hydraulic machine was made of two concrete bulkheads, one fixed and one movable, connected by eight 1-3/8 inch Dywidag bars (Fig. 3.4). A 1200 kip capacity ram was used to compress the specimen between the bulkheads which placed the Dywidag bars in tension.

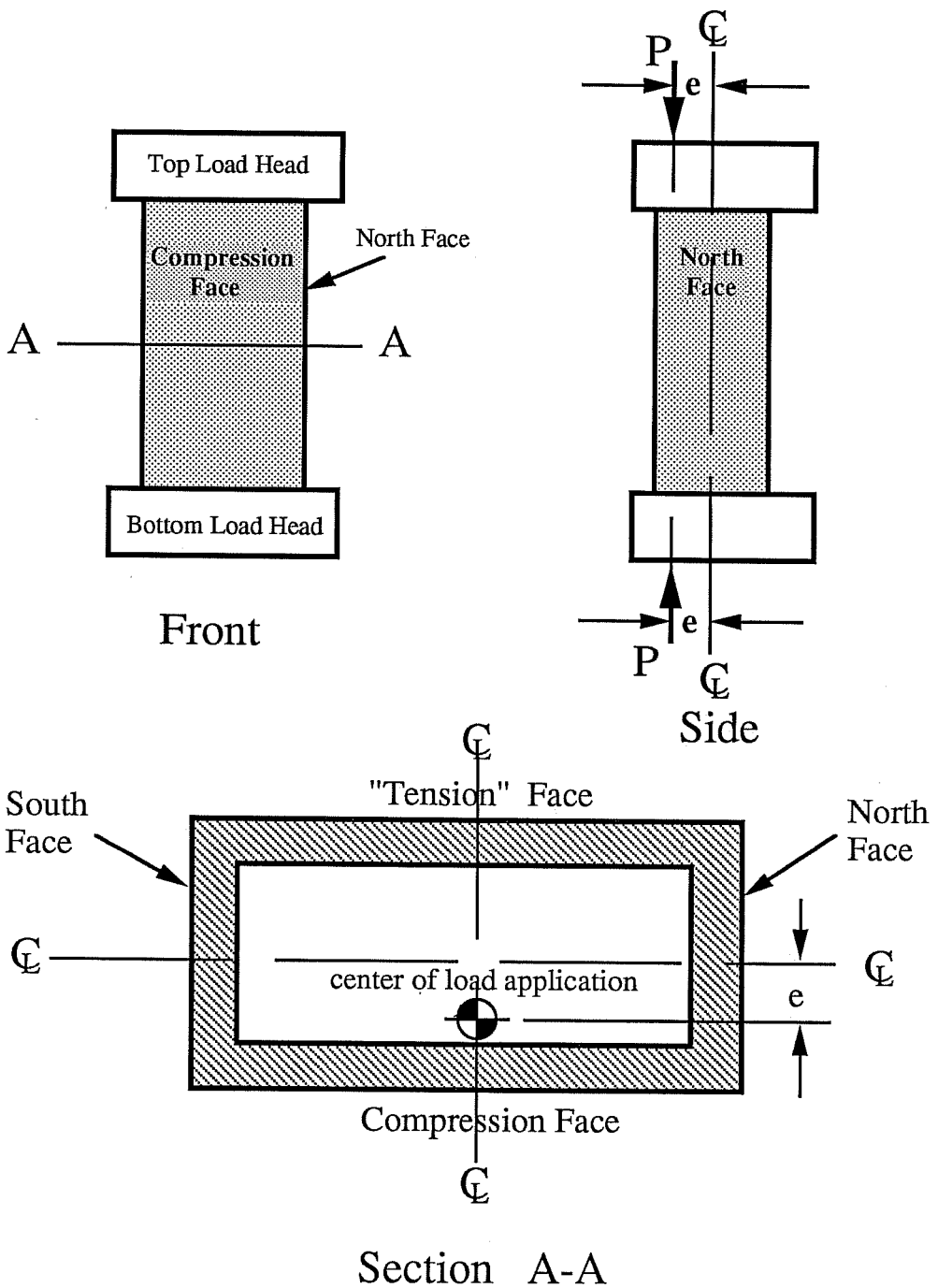

Note: Naming convention in section A-A used throughout thesis.

Figure 3.1 Test Specimen Loading

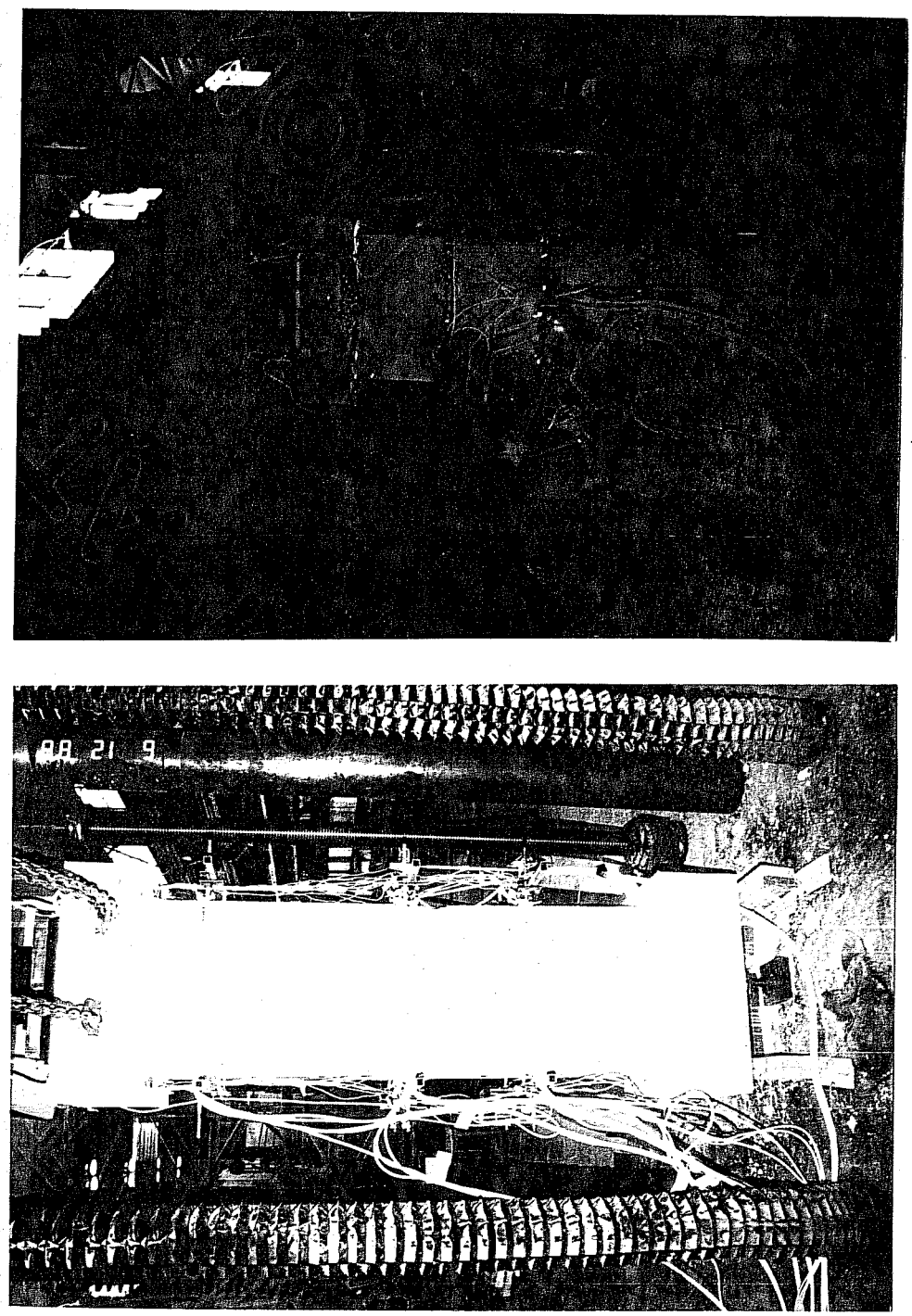

Figure 3.2a 600 kip Vertical Testing Machine

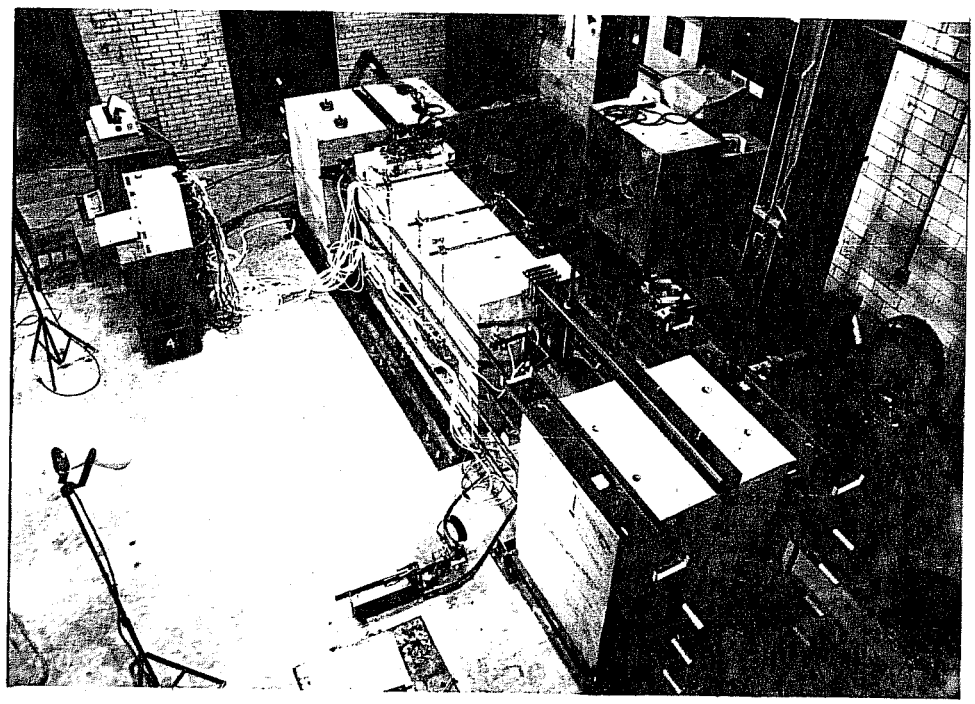

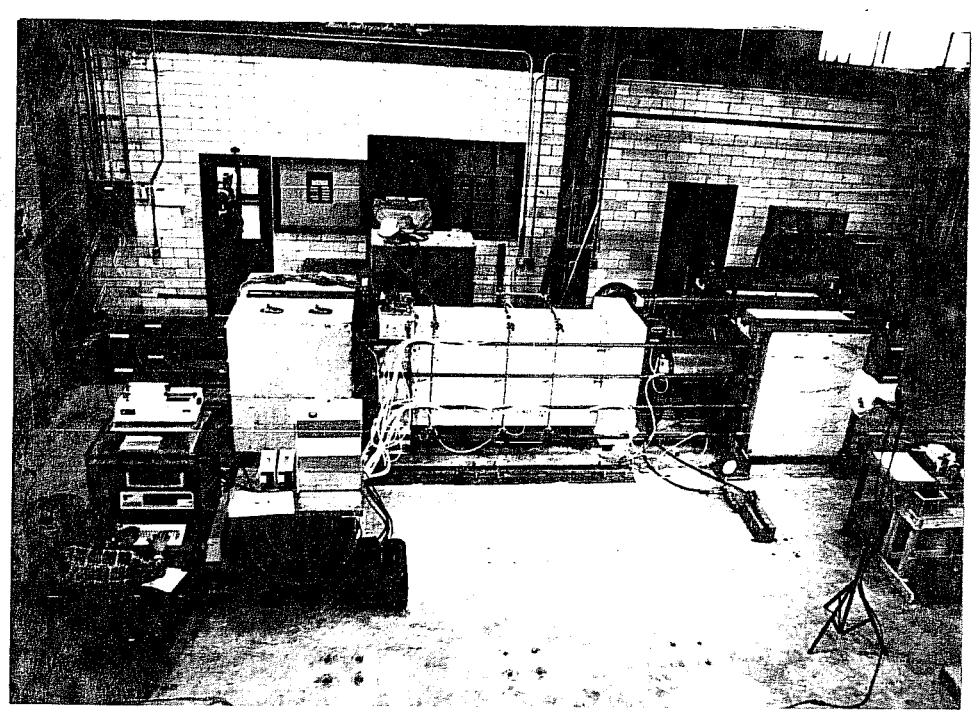

Figure 3.2b 1200 kip Horizontal Testing Machine

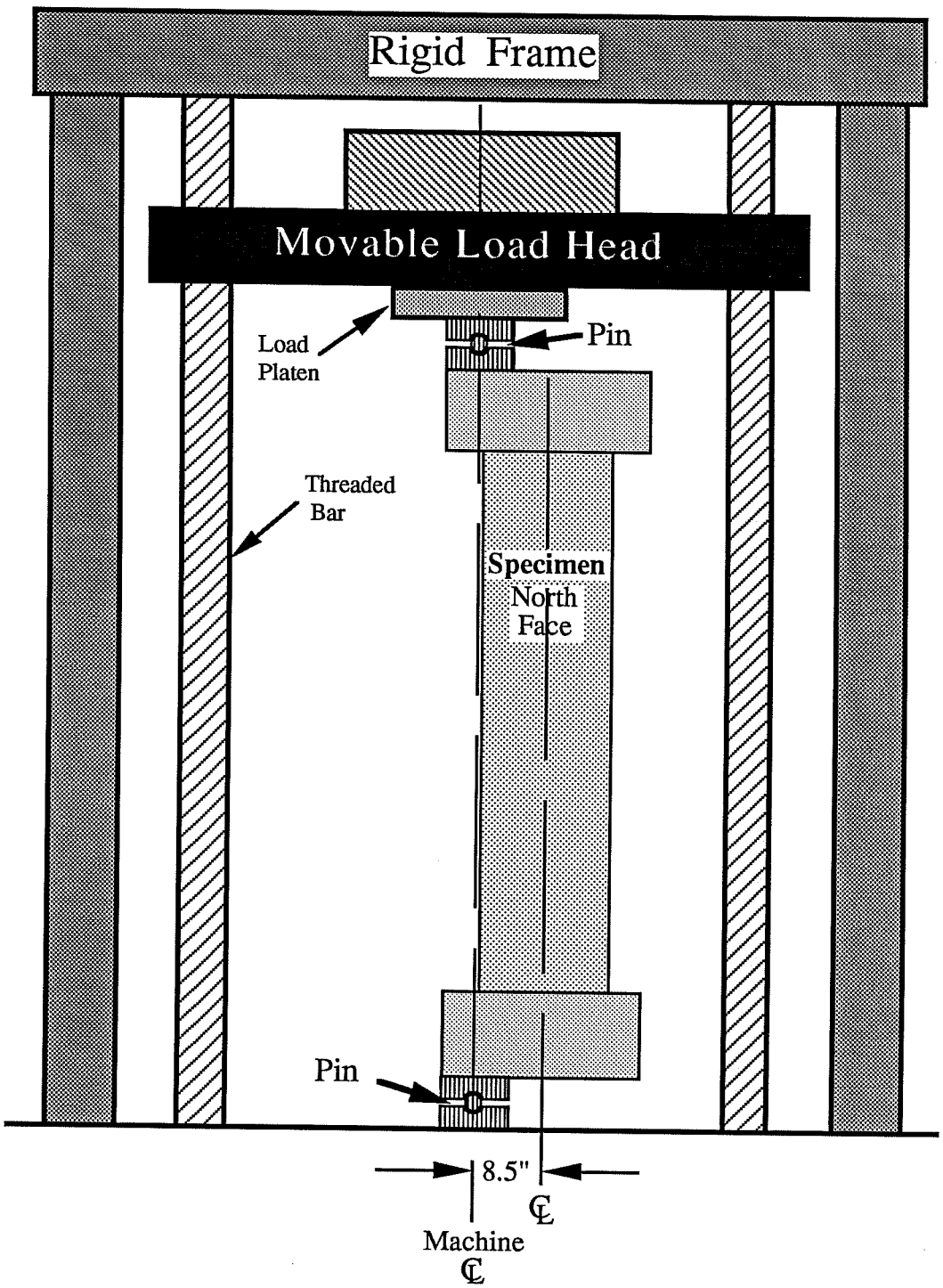

Figure 3.3 600 kip Testing Machine

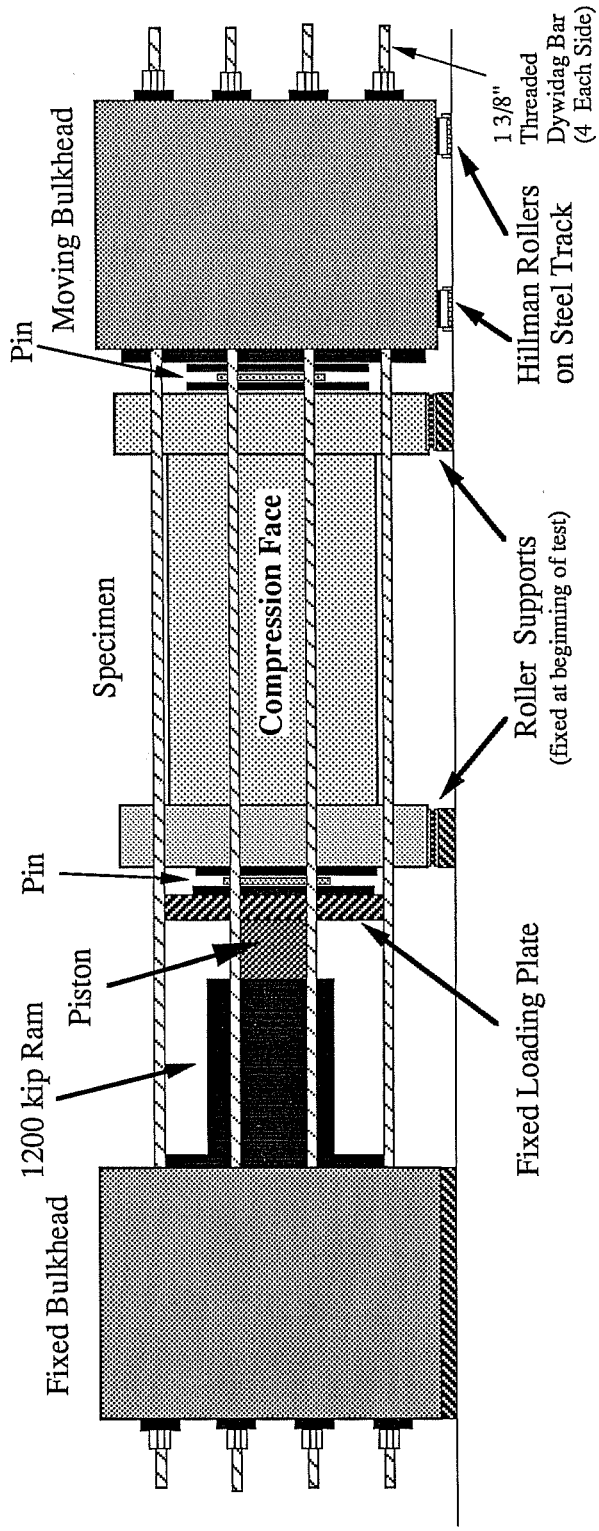

Figure 3.4 1200 kip Testing Machine

3.1.2 Loading Concept

3.1.2.1 Calibration

Both testing machines were calibrated using a 1000 kip load cell calibrated by the National Institute of Standards and Technology.

3.1.2.2 Boundary Conditions

To avoid the transfer of shear and moment from the testing machines to the test specimens, steel pins (see Figs. 3.3 and 3.4) were placed between the pier load heads and the testing machine. The pins were lubricated with an anti-seizing compound to reduce their internal friction.

All load on the specimens was transferred from the testing machine, through the pin connections, to the concrete load heads on either end of the pier. The load heads provided a uniform bearing surface to transfer and distribute load from the testing machine to the pier.

Hydrostone was used for level and uniform bearing between each steel to concrete interface.

3.1.2.3 Machine Limitations

The 600 kip machine was laterally rigid, therefore minimal accidental eccentricity from the test setup was expected. Contrarily, the 1200 kip machine was laterally flexible, creating the possibility of drift in the roller supported bulkhead. However, lateral restraint of the moving bulkhead was

provided by steel outriggers which limited its lateral movement to a maximum of 1/16th inch.

3.1.3 Instrumentation

Instrumentation was focused on the determination of strain distributions and local buckling effects in the specimen.

Strain gages were used to determine the longitudinal strain distribution in the pier by monitoring the behavior of the 6 mm diameter longitudinal reinforcing bars within each specimen. The type of strain gages used were from the Tokyo Sokki Kenkyujo Company, gage type FLA-5-3L-11. These gages had a 5 mm gage length.

Strain gages and potentiometers were concentrated on the compressive face of the specimen, the face where failure would initiate and local buckling would occur. Also, strain gages were placed at mid-height on all four sides of the specimen in order to gain information on the behavior of the pier cross-section. The locations of strain gages on each specimen are shown in Figures 3.5 through 3.8. All gages are located on the outer curtain of steel unless otherwise noted. Refer to Chapter 2 for the position of the longitudinal bars in the pier cross-section.

Linear potentiometers were utilized to indicate any distortion or buckling of the pier by monitoring the deflections and movements of the test specimen. The potentiometers used to

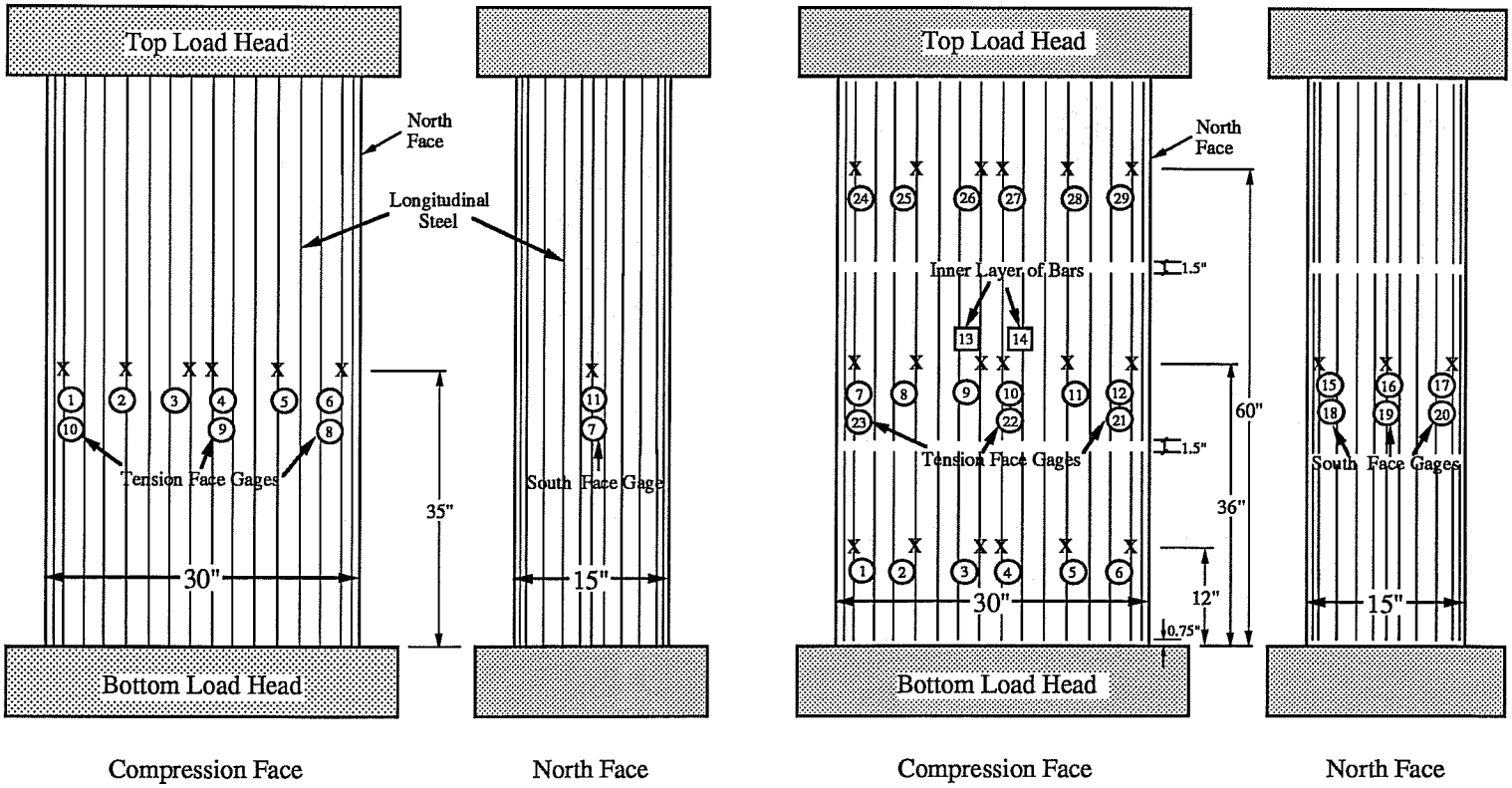

Figure 3.5 Specimens 1M and 1S Strain Gage Layout

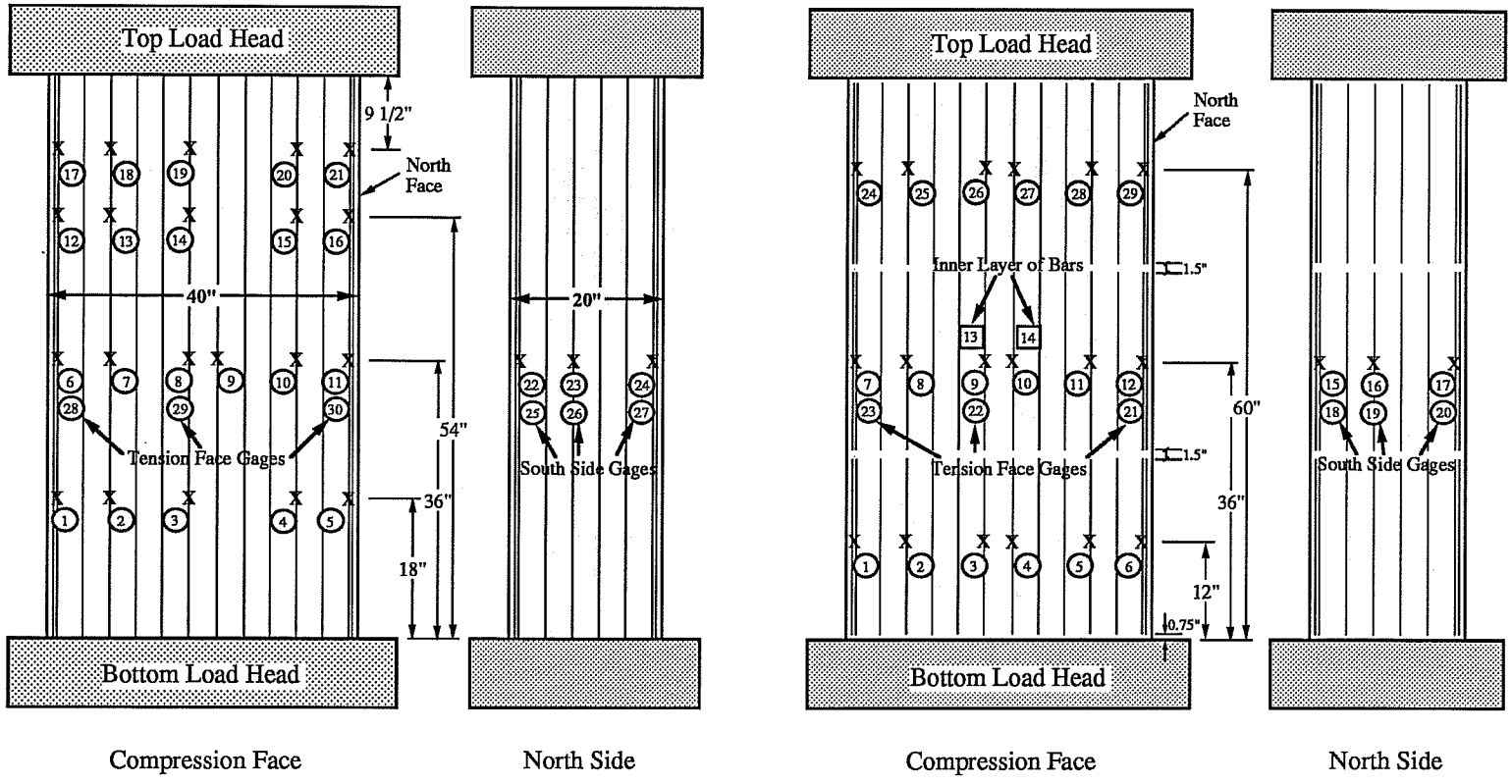

Figure 3.6 Specimens 2M and 2S Strain Gage Layout

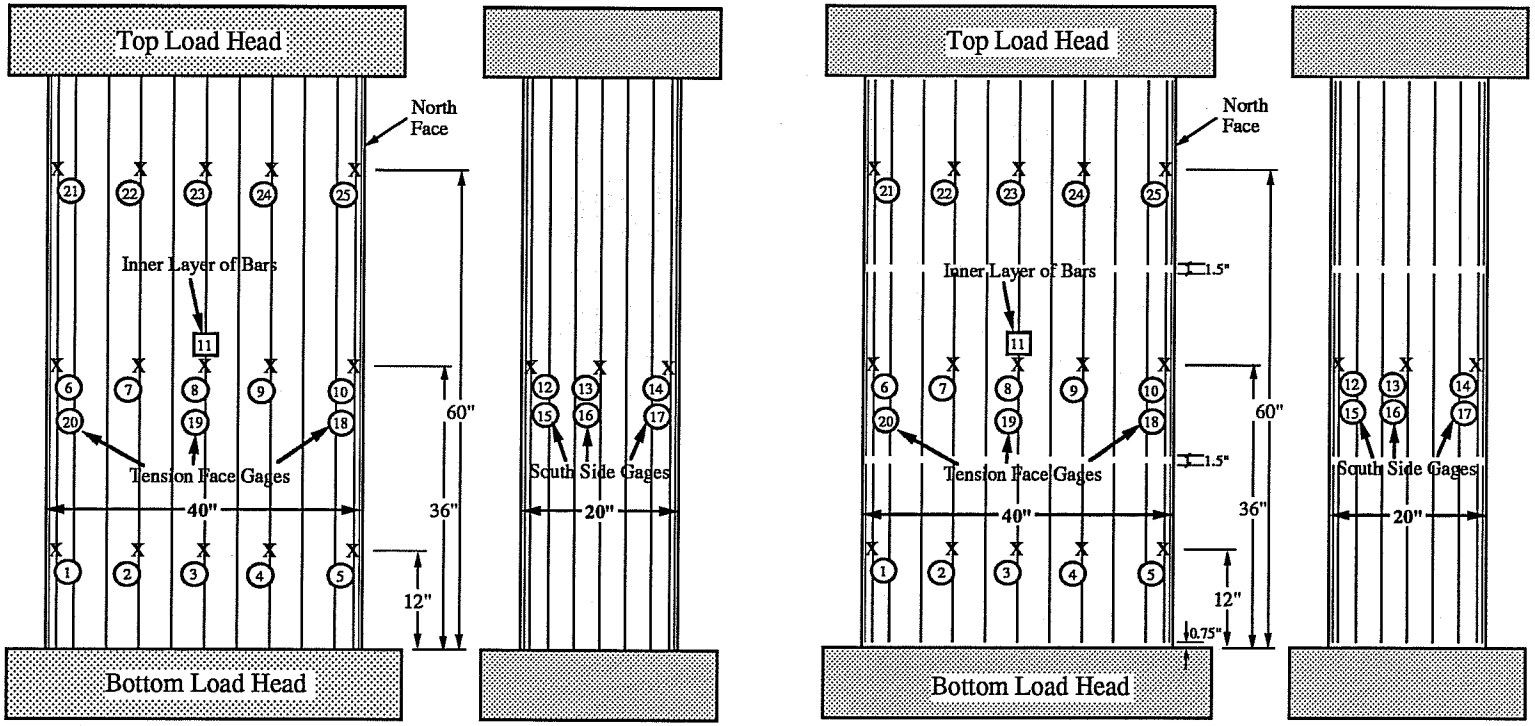

Figure 3.7 Specimens 3M and 3S Strain Gage Layout

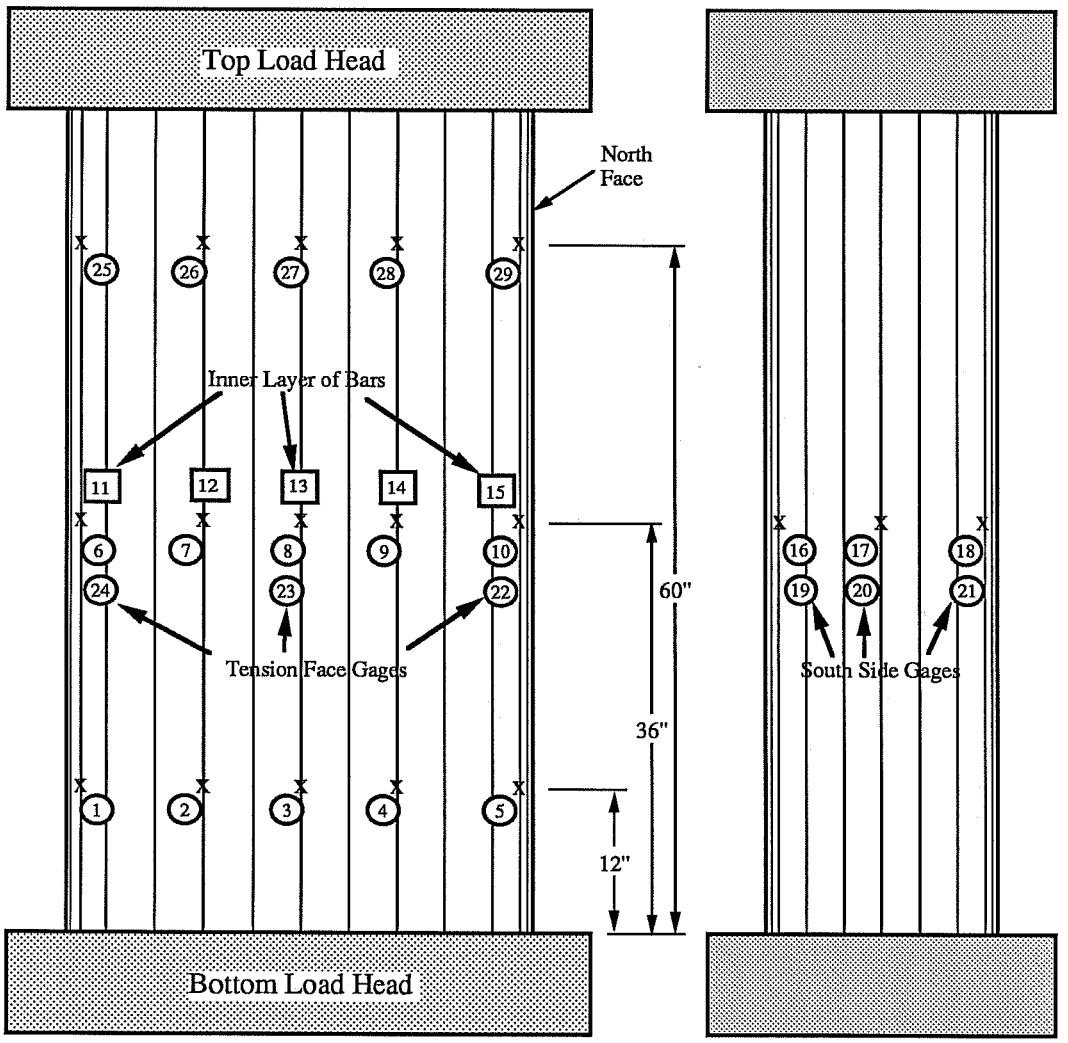

Figure 3.8 Specimen 3PM Strain Gage Layout

measure the profile of deflections across the pier face at several planes were mounted on the specimen through the use of a frame attached to studs cast into the short sides of the pier (Fig. 3.9). The locations of the potentiometers on each specimen are shown in Figure 3.10. Glass plates were attached on the specimen to provide a smooth contact surface for the potentiometer. Potentiometers were also used to measure curvatures along selected lengths of the pier and to measure rotation of the load heads on either end of the pier (Fig. 3.11). All potentiometers had a two inch range of movement.

In addition to the potentiometers already mentioned, one was used to measure the movement of the load head in the 600 kip machine and several others were used to measure the displacement of the ram and moving block in the 1200 kip machine.

A configuration using a string along with millimeter scales and mirrors was used to measure the centerline deformation of each specimen (Fig. 3.12). In this setup, a string was attached along the centerline located on the short sides of the specimen. This string was kept taught by passing it through a pulley and hanging a weight on its end. Millimeter scales and mirrors were then placed at specified stations along the centerline before testing. After aligning the string with its image in the mirrors, readings were taken from the scales at

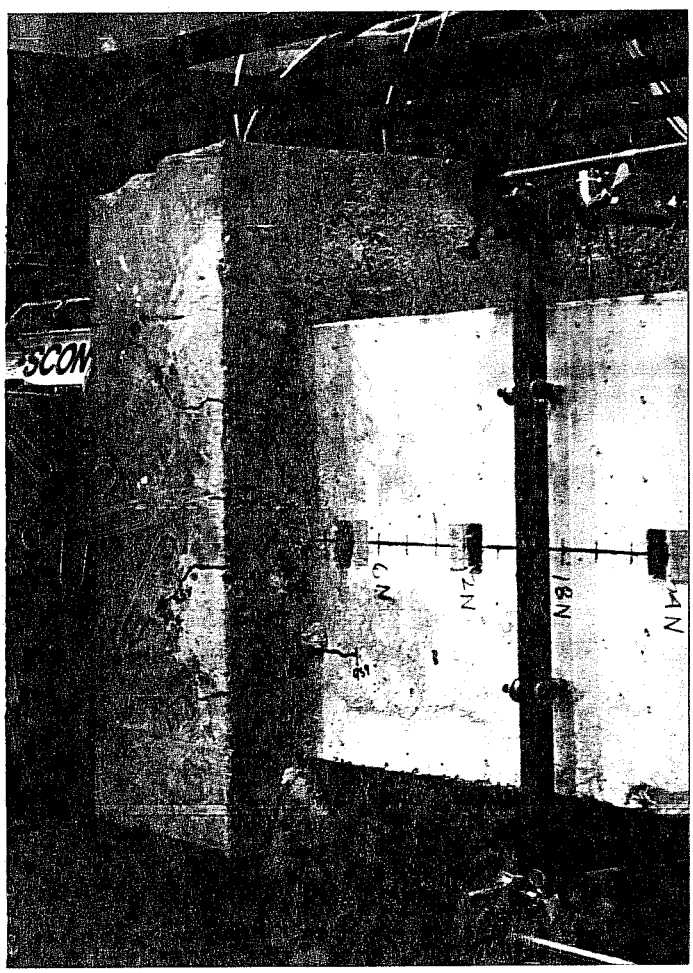

Figure 3.9 Potentiometer Frame

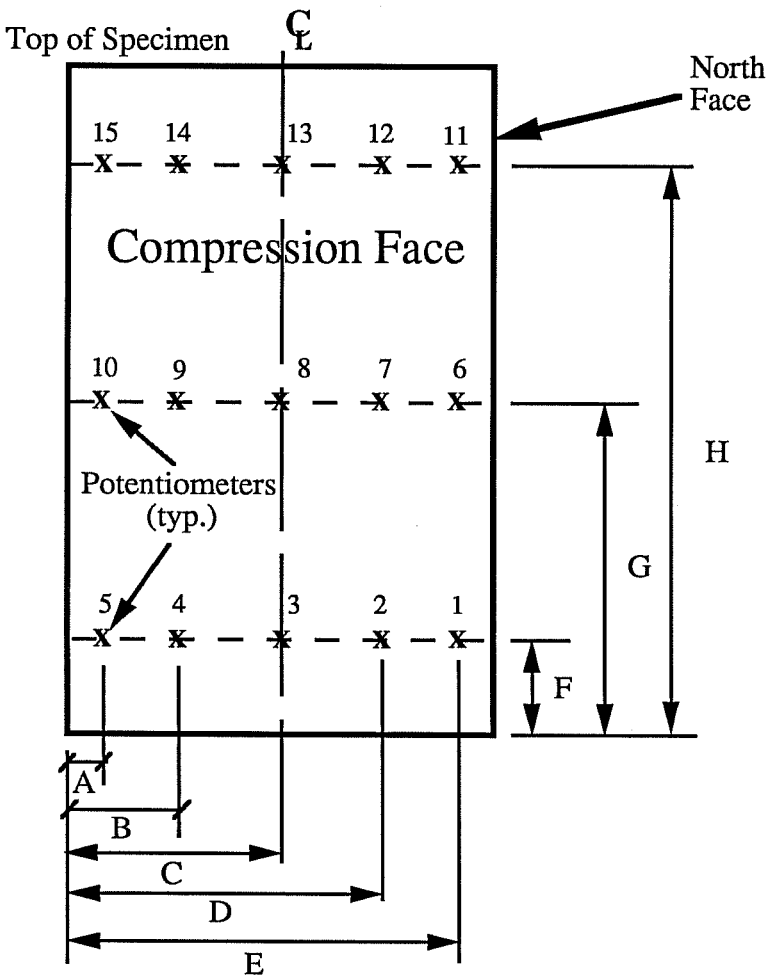

Specimen No.	"A"	"B"	"C"	"D"	"E"	"F"	"G"	"H"
1M	1.25"	7.5"	15"	22.5"	28.75"	18"	36"	54"
1S	1.25"	7.5"	15"	22.5"	28.75"	12"	36"	60"
2M	1"	10"	20"	30"	39"	18.75"	36.5"	63.75"
2S	1"	10"	20"	30"	39"	13"	35"	58.75"
3M	1"	10"	20"	30"	39"	11.5"	36.4"	59.25"
3S	1"	10"	20"	30"	39"	11.75"	35"	56"
3PM	1"	10"	20"	30"	39"	13.25"	35"	57.4"

Figure 3.10 Potentiometer Locations

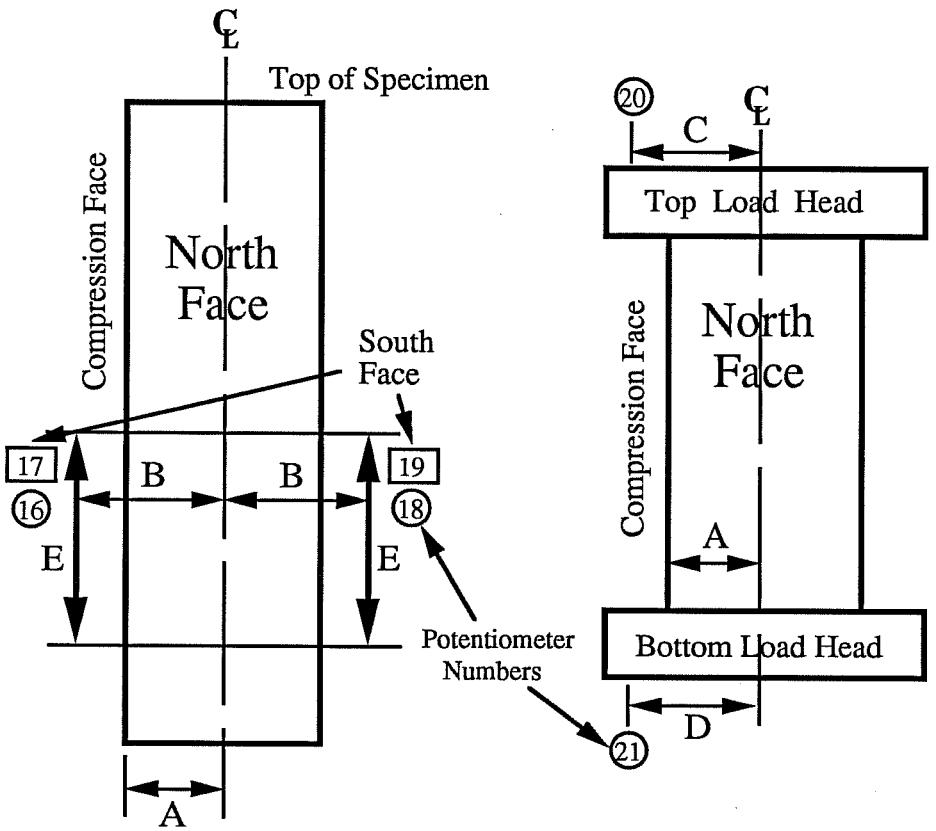

"E" is the distance between the studs holding potentiometer frames.

Specimen No.	"A"	"B"	"C"	"D"	"E"
1M	7.5"	12"	26 5/8"	31 1/8"	18"
1S	7.5"	10.5"	13 1/4"	9 3/8"	23"
2M	10"	14.5"	13 1/4"	13 3/4"	18"
2S	10"	15"	15"	15"	20 1/4"
3M	10"	15"	18 1/2"	18 1/4"	20"
3S	10"	15"	19 1/4"	18 1/4"	23 1/4"
3PM	10"	15"	18 1/4"	17 3/4"	23"

Figure 3.11 Curvature and Rotation Potentiometers

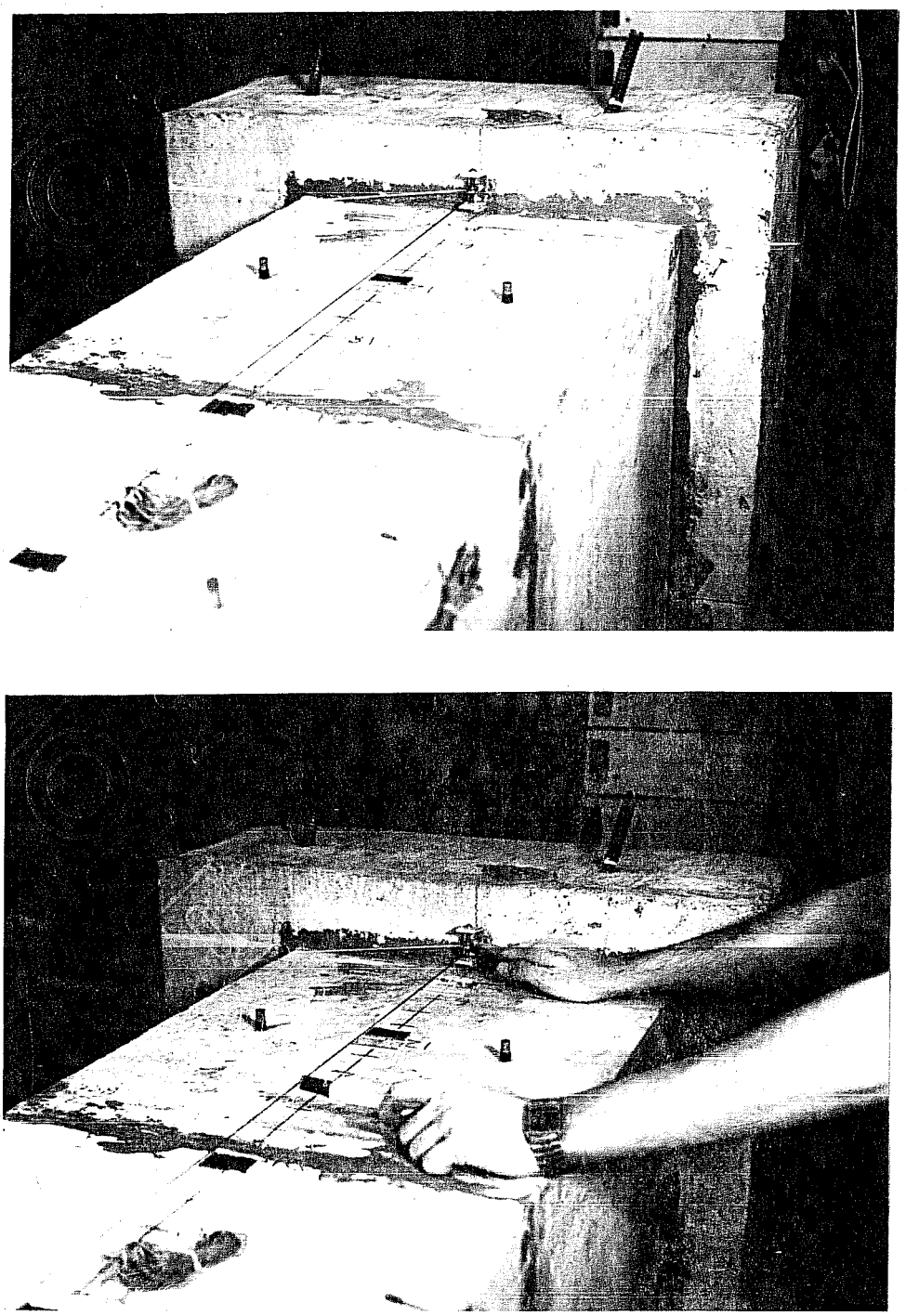

Figure 3.12 Centerline Deformation Instrumentation

each station. At certain load increments during the test, additional readings were taken. By recording the ruler readings throughout the test, the centerline deformation of the specimen was determined.

Four load cells were used to determine the forces being applied by the 600 kip testing machine. The average reading from the load cells was output on a digital display during the test.

A pressure transducer was used to determine the forces being applied by the hydraulic ram in the 1200 kip machine. The transducer was carefully calibrated to give accurate readings.

Specimens with complete instrumentation are shown in Figures 3.13a and 3.13b.

3.1.4 Data Acquisition

A personal computer (IBM AT) and an electronic data acquisition system (Hewlett Packard model no. 3852A) were used to record the data taken by the strain gages, potentiometers, and pressure transducer. The data were then converted into a form that could be read into a spreadsheet by an in-house program.

3.2 Procedure

Special care was taken with each specimen to make sure that it was properly aligned in the testing machine. The

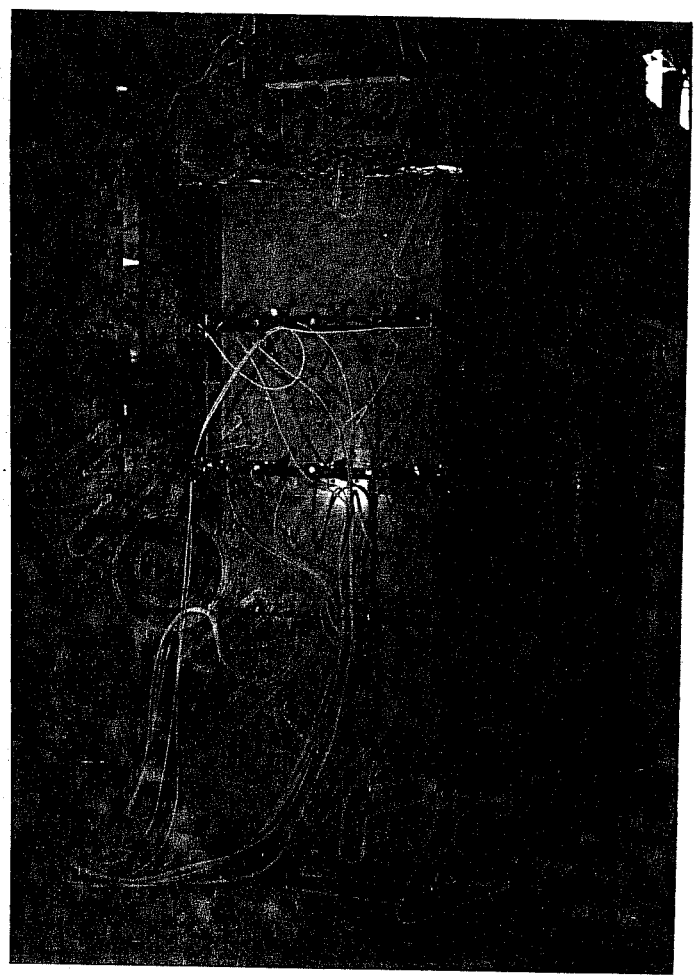

Figure 3.13a 600 kip Machine Instrumentation

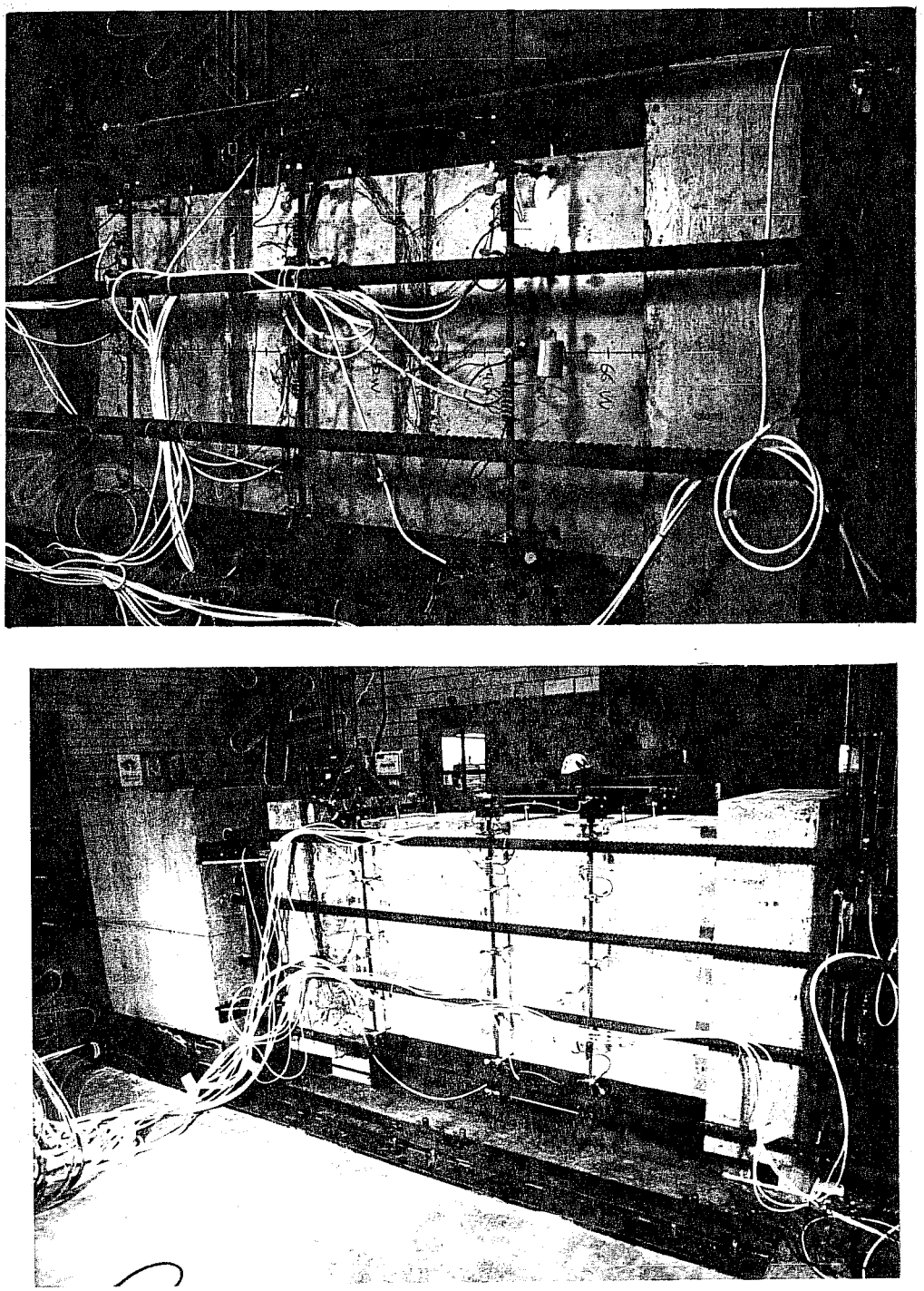

Figure 3.13b 1200 kip Machine Instrumentation

maximum tolerance established for alignment about the strong and weak axis of the specimen was ± 0.1 inch.

The average duration of each test was about 2 1/2 hours.

3.2.1 600 kip Machine Procedure

The bottom pin was positioned on the base of the machine in line with the center of the load platen (see Fig. 3.3). The specimen was moved into the machine and positioned vertically to provide an 8.5 inch eccentricity about the weak axis. The top pin was then positioned on the top load head in the same manner. Jacks were placed under the base of the specimen for support until it was loaded.

The test procedure was as follows:

1) An initial reading of the instruments was taken just before bringing the machine load platen into contact with the top pin.

2) The support jacks were removed from underneath the specimen after reaching a load of 40 kips.

3) The specimen was loaded in 20 kip increments from 0 to 100 kips and in 25 kip increments from 100 kips to failure.

4) Instrument readings were taken at each load increment. Readings were also taken immediately after failure and when all load was removed from the specimen.

3.2.2 1200 kip Machine Procedure

After fixing the roller supports against movement (see Fig. 3.4), the specimen was put into the testing machine and aligned with the ram in both the horizontal and vertical planes. Each specimen was positioned horizontally for the desired eccentricity about its weak axis. The pin assemblies were carefully aligned about the specimen centerlines to provide the following eccentricities.

Specimen Number	Eccentricity (inches)
1S	0.75
2M	2.75
2S	1.0
3M	1.0
3S	1.0
3PM	1.0

The test procedure was as follows:

1) An initial reading of the instruments was taken just before bringing the loading plate in contact with the pin.

2) The braces which fixed the roller supports were removed after reaching a load of 60 kips.

3) The specimen was loaded from 0 to 20 kips for the first increment and in subsequent increments of 40 kips until failure.

4) Instrument readings were taken at each load increment. Readings were also taken immediately after failure and when all load was removed from the specimen.

CHAPTER 4

TEST RESULTS

4.1 Introduction

The presentation of test results in this chapter includes a detailed summary of the physical behavior of each specimen and information from the instrumentation discussed in Chapter 3. The test data is presented in a form such that comparisons between the companion specimens in each series can be made. Specific conclusions will be made about the behavior of the specimens with regard to the information presented. However, final conclusions about the behavior of the piers will not be made until incorporating the analysis results of Chapter 5.

For each specimen, the following test results are presented:

1) General observations are presented concerning the behavior of each specimen, including photographs of the crack patterns, the failure region, and any other important details.

2) Strain gage data is presented in plots comparing the companion specimens for each series. Because the strain gage readings are very susceptible to fluctuations due to cracking and load redistribution, only general trends are mentioned. Unless otherwise noted, all strain gages are located on the

outer curtain of mild reinforcement and positive strain gage readings indicate compression.

3) Potentiometer data is presented in a series of figures. The figures include a three-dimensional plot showing the deflected shape of the compression face just before failure. Also, plots showing the moment-curvature relationship, load head movement, and shortening of the companion specimens for each series are presented.

4) Additional data from the instrumentation presented in Chapter 3 that is not included in this chapter can be found in the Appendix.

4.2 Specimens 1M and 1S

4.2.1 General Observations

The companion specimens in this series have the lowest wall slenderness ratios, X_u/t_f, of the three series compared. Specimen 1M has a wall slenderness ratio of 10. The addition of the corner bevels to include the post-tensioning tendons reduced the wall slenderness ratio, X_u/t_f, from 10 to 8.4 for Specimen 1S. Each specimen has a wall thickness of 2.5 inches. The mild reinforcement ratio and placement of the reinforcement is identical for each specimen. Unlike the monolithically cast Specimen 1M, Specimen 1S was segmentally constructed. Other than their method of construction, the only difference between

these two specimens is the addition of the post-tensioning tendons to Specimen 1S.

The cylinder strengths of the concrete near the failure region of each specimen are listed below.

Specimen 1M	7862 psi
Specimen 1S	6980 psi

4.2.1.1 Specimen 1M (Monolithic with end eccentricity of 8.5 inches and X_u/t_f of 10)

Sudden failure of this specimen occurred approximately 6 inches from the top of the pier at a load of 527 kips. The load was applied at an eccentricity of 8.5 inches. Adding the deflection observed at the critical section prior to failure, the total deflection at failure was approximately 8.6 inches. This deflection yields a failure moment of 4532 kip-inches.

The first visible cracks occurred on the "tension" face at a load of 175 kips. Cracks appeared in the load heads on the "tension" face side at a load of 400 kips. No cracks were observed on the compression face until after failure.

After failure, visible cracks were marked. As shown in Figure 4.1, the cracks on the compression face were much different than those on the "tension" face. The compression face cracks extended along the length of the specimen from the failure region. The "tension" face cracks were transverse to the length of the specimen and were spaced at regular intervals corresponding to the spacing of the lateral hoop reinforcement.

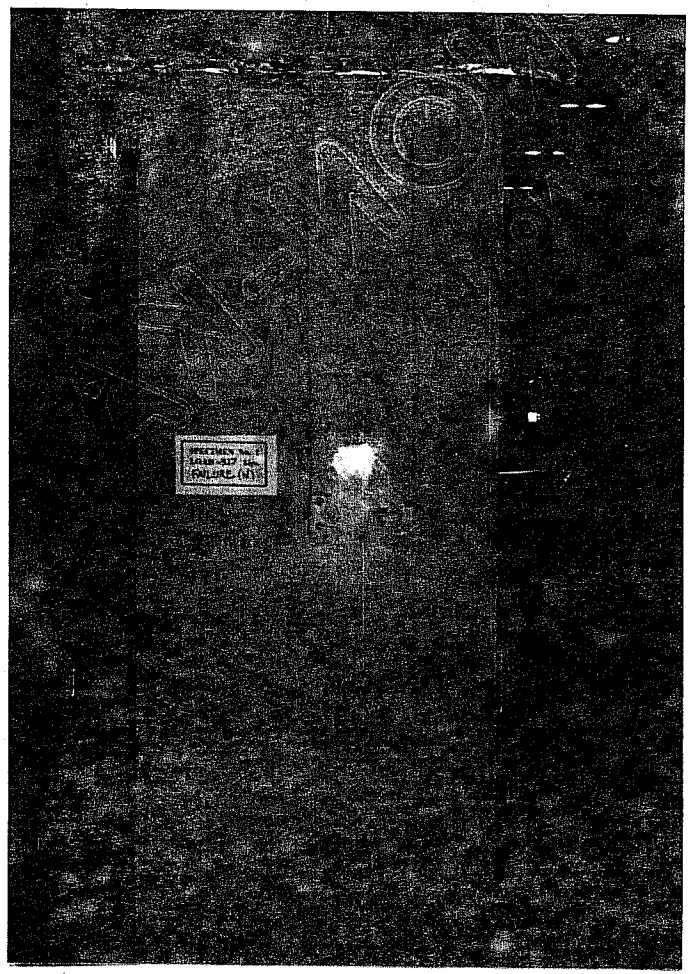

Compression Face

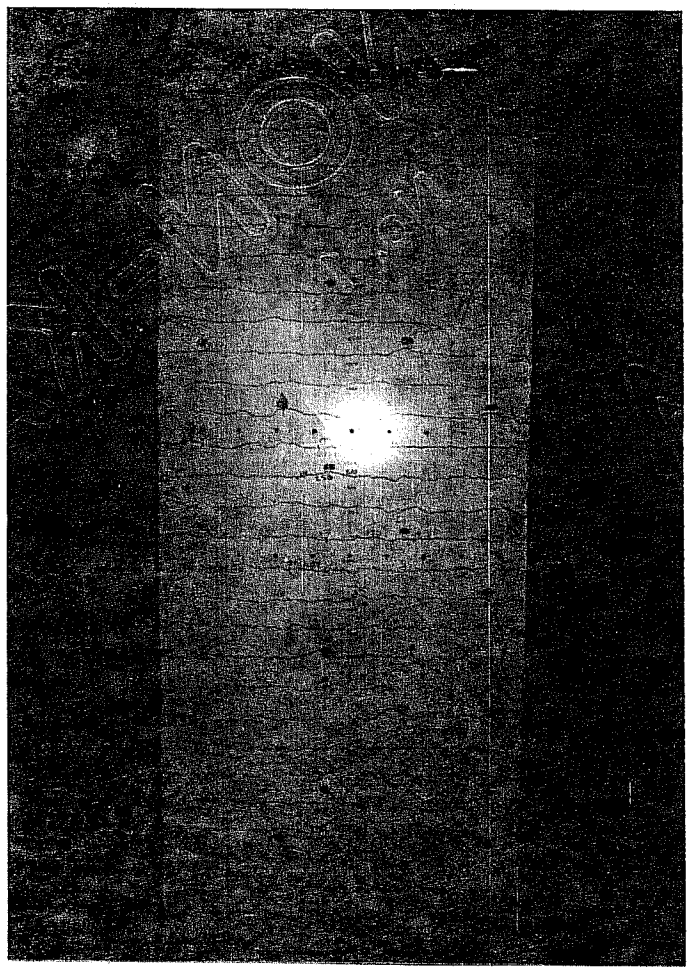

Tension Face

Figure 4.1 Specimen 1M Cracks Marked after Failure

In addition, the "tension" face cracks extended halfway across the north and south side faces of the specimen.

The different crack patterns on the compression and tension faces can be explained by the large eccentricity at which this specimen was loaded. Specimen 1M was the only specimen tested in which the "tension" face was truly in tension. Therefore, though the failure was initiated by material failure of the compression flange, the reinforcement in the tension flange proceeded to yield prior to final failure.

Several observations can be made about the failure region of this specimen:

1) The compression flange failure extended all the way through the wall thickness as evidenced by the crushing shown in Figure 4.2.

2) The lateral reinforcement seemed to perform well with the majority of longitudinal bars buckling between the levels of lateral reinforcement (Fig. 4.2).

3) No clearly defined failure plane was evident. Instead, the failure region extended over a 10 to 12 inch segment of the compression face.

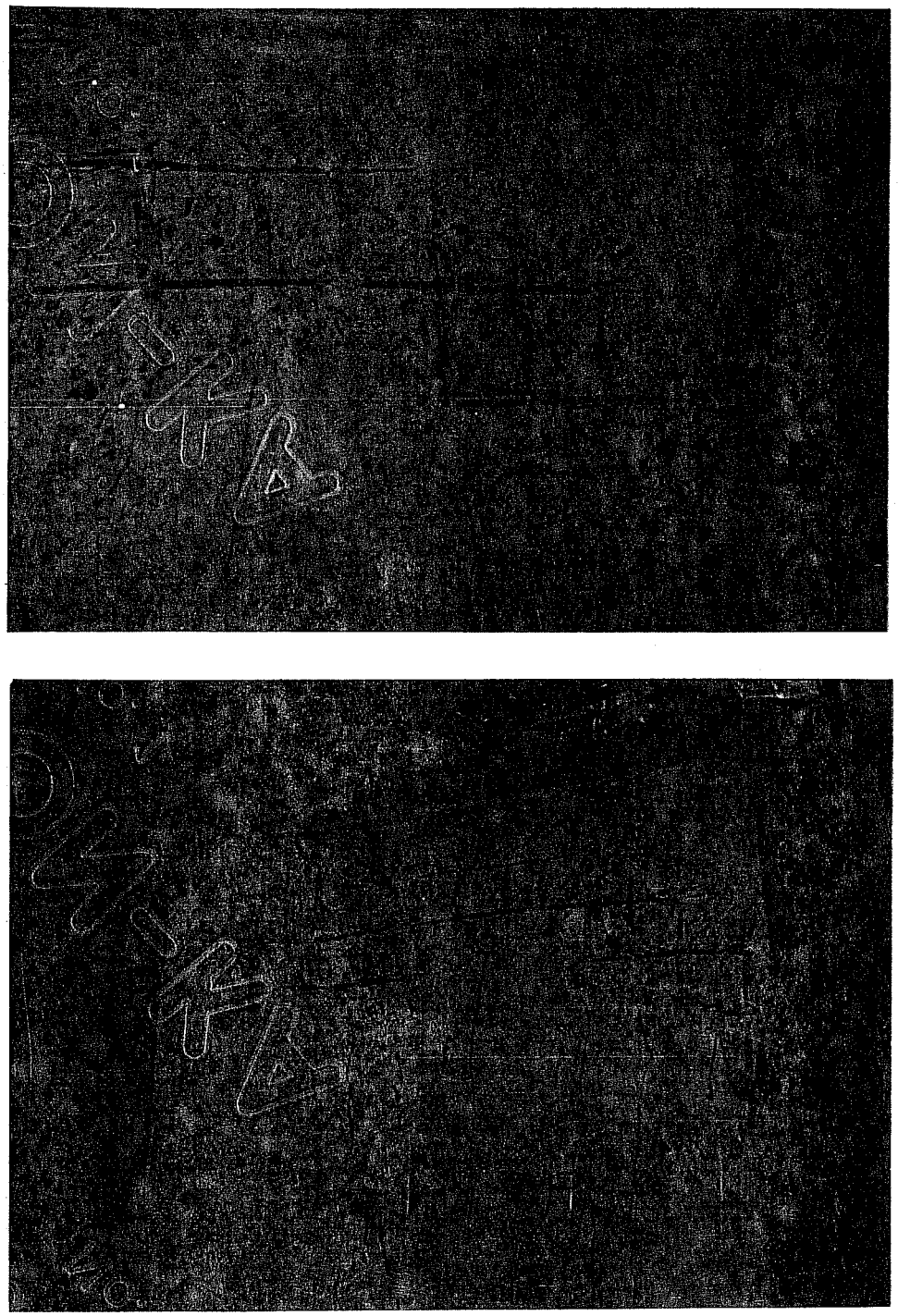

Figure 4.2 Specimen 1M Compression Face Failure Region

4.2.1.2 Specimen 1S (Segmental with end eccentricity of 0.75 inches and X_u/t_f of 8.4)

Failure of this specimen occurred approximately 30 seconds after reaching a load of 1137 kips. The failure was explosive. The location of failure was near the joint between the middle and bottom segments (Fig. 4.3). A deflection of approximately 1.5 millimeters was observed at the critical section prior to failure. Therefore, due to the 0.81 inch eccentricity at failure, the failure moment was 921 kip-inches.

First cracking occurred in each of the load heads at a load of 666 kips. Cracks appeared on the "tension" face at a load of 700 kips. First cracking on the compression face of the specimen occurred at a load of 861 kips. All of the cracks which formed ran longitudinally along the length of the specimen.

After failure, cracks were marked with a dashed line (Fig. 4.3) and several observations were noted:

1) Although there was extensive cracking of the compression face, the primary cause of failure appeared to be crushing of the concrete just below the joint (Fig. 4.4).

2) The two curtains of steel in the bottom segment were split apart. The confining hoop reinforcement broke loose from the top of the cage and the ends of the longitudinal bars at the top of the bottom segment were protruding out of the plane of

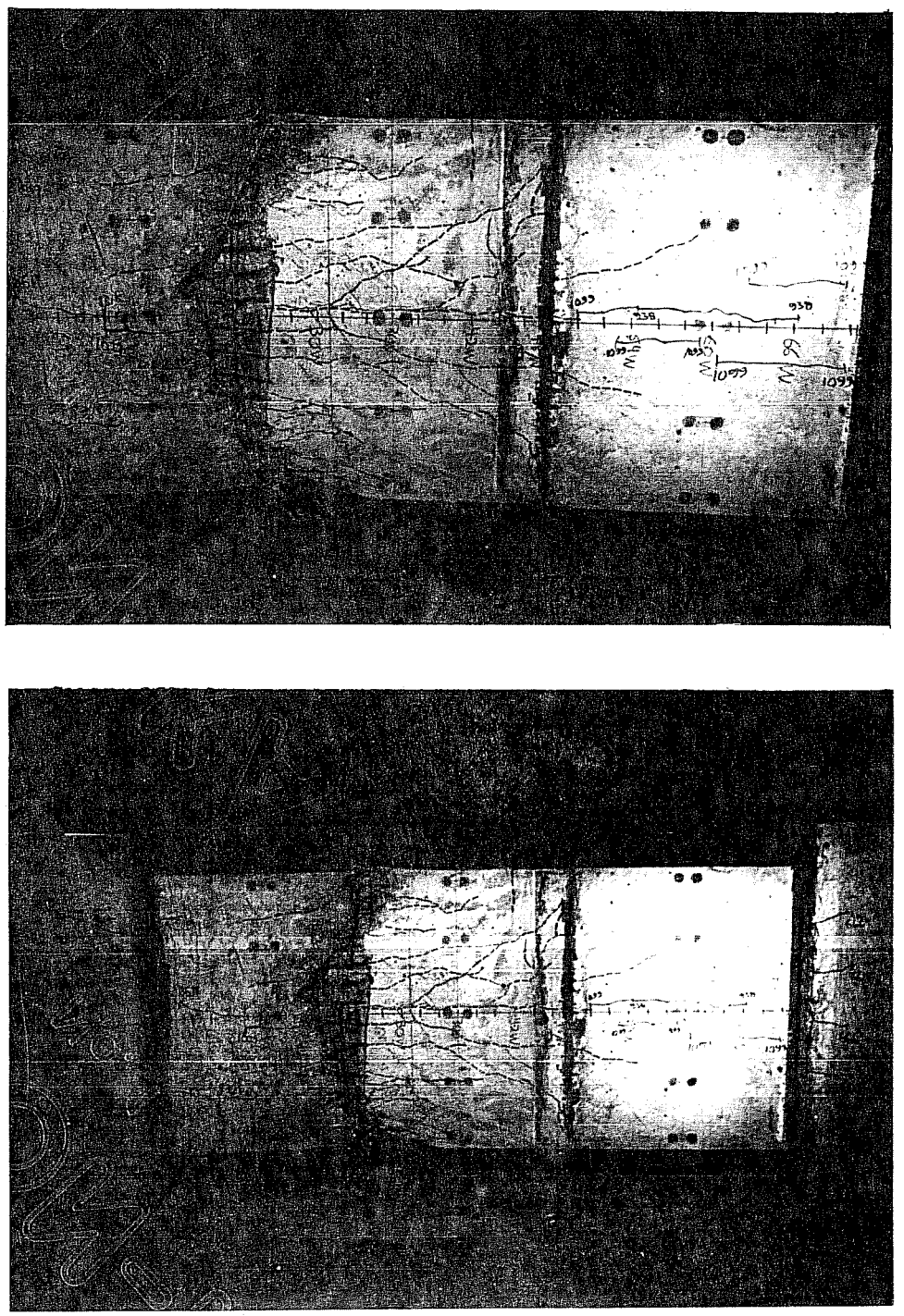

Figure 4.3 Specimen 1S Compression Face Cracks Marked after Failure

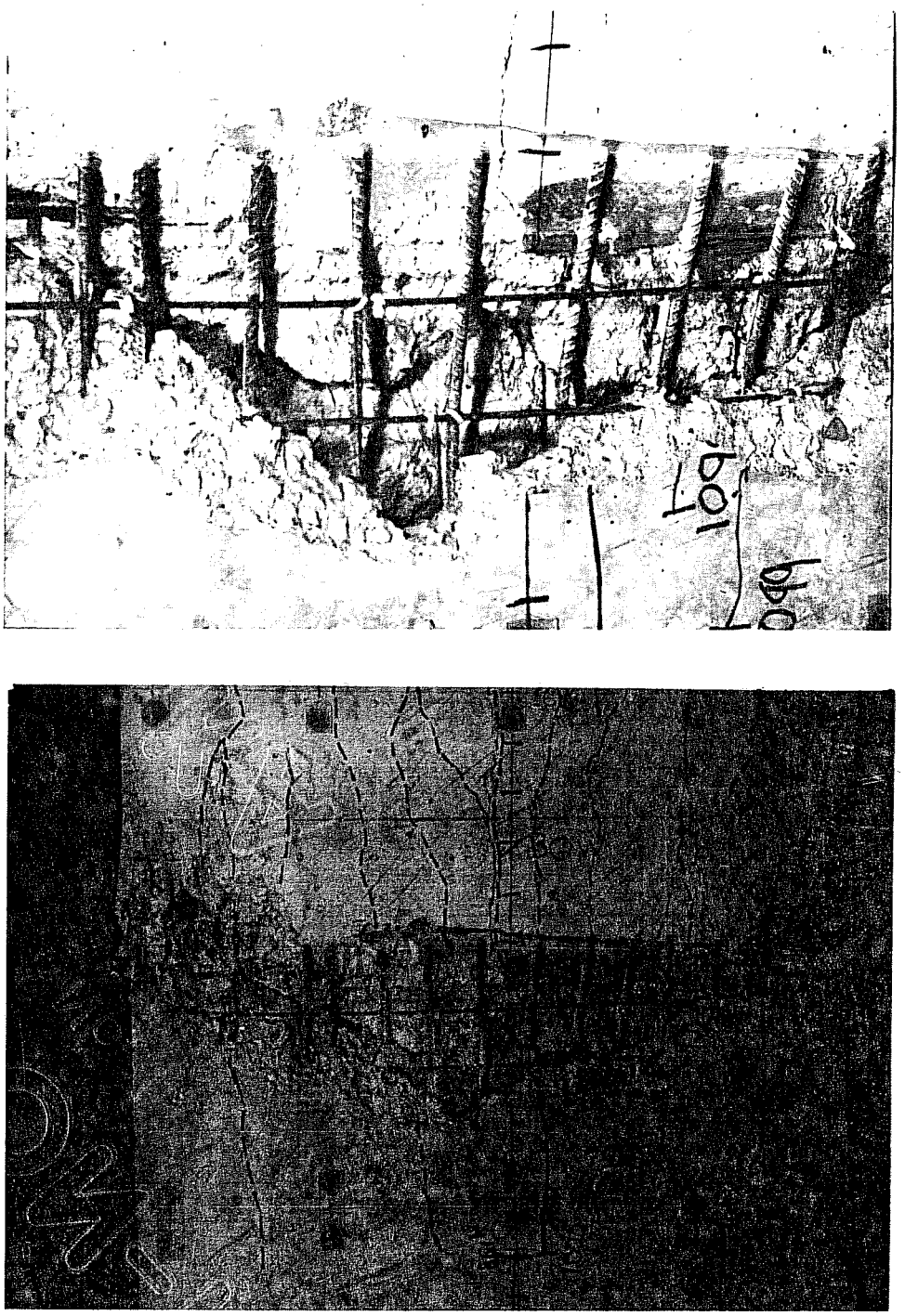

Figure 4.4 Specimen 1S Compression Failure Region

the wall (Fig. 4.4). However, the confining hoop reinforcement at the bottom of the middle segment remained in position and the longitudinal bars remained intact even though considerable crushing was evident (Fig. 4.5).

3) The "tension" face fracture occurred just below the joint between the bottom and middle segments. The fracture propagated along a line even with the ends of the longitudinal bars at the top of the bottom segment (Fig. 4.5). Unlike the other pier faces, all longitudinal bars and hoops remained confined in the concrete.

4) The post-tensioning tendons were all bent sharply at the location of the break. In addition, the two post-tensioning tendons on the compression face of the specimen were pushed out of the specimen about 3 inches (Fig. 4.6). This phenomena was likely caused by the absence of deformations in the smooth plastic ducts.

By removing the concrete cover around each joint, it was determined that for all three segments, the crossties in the top layer of lateral steel were missing. These ties were knocked loose by the concrete vibrator during casting. Unlike the other two segments, the top two layers of crossties seemed to be missing from the bottom segment.

The concrete cylinder strengths for each segment were as follows:

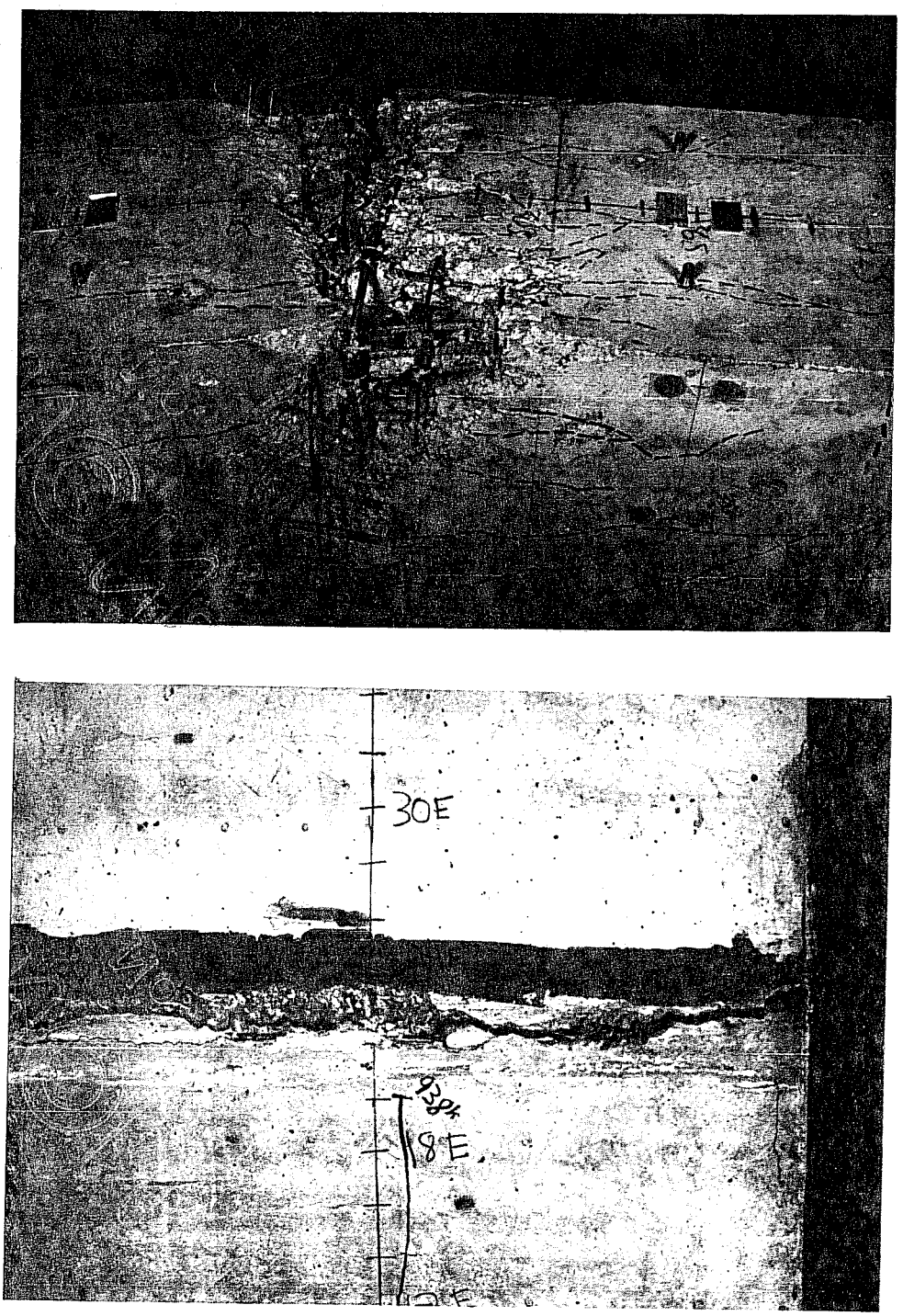

Figure 4.5 Specimen 1S Compression(top) and Tension Face Failure

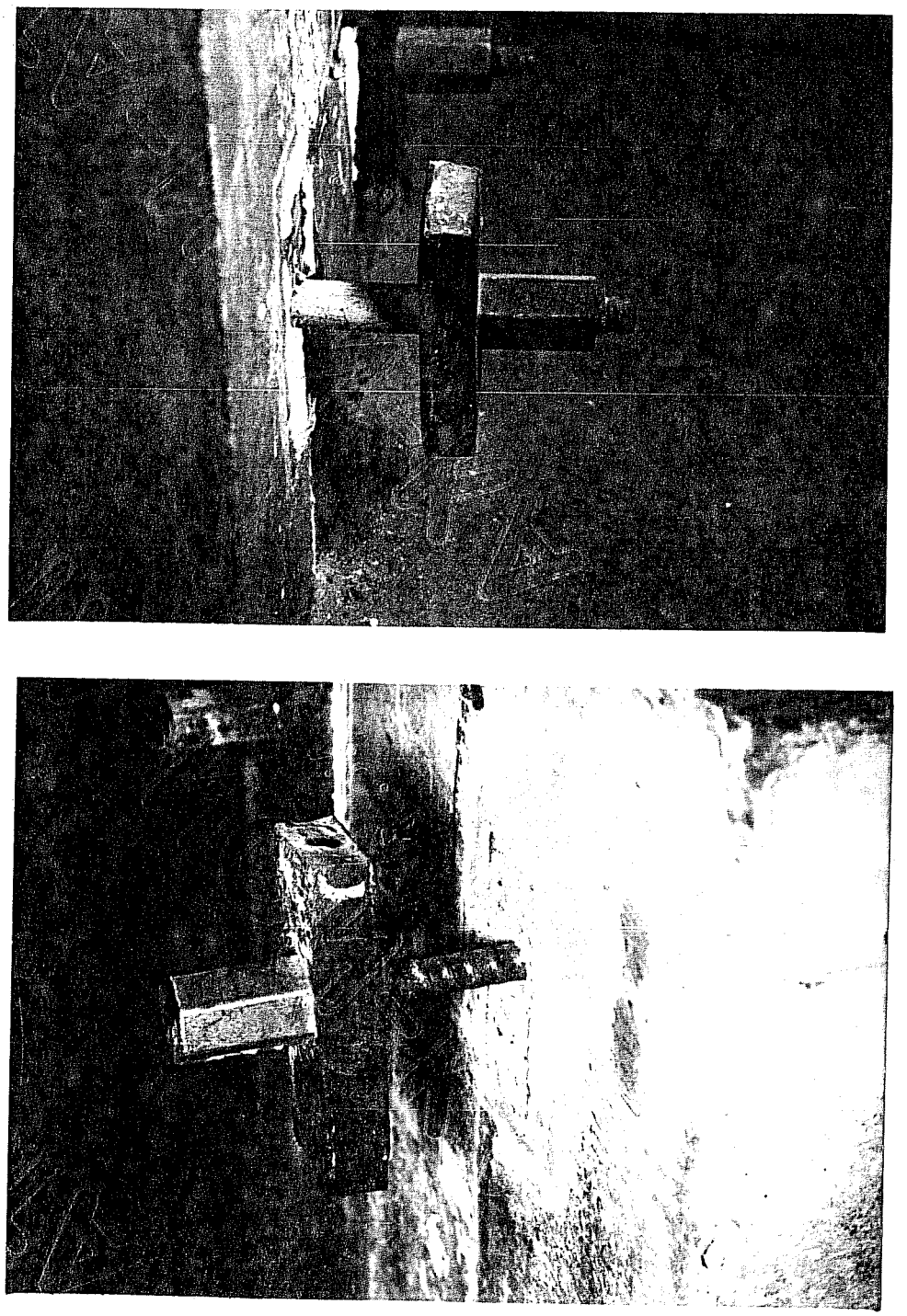

Figure 4.6 Specimen 1S Post-Tensioned Tendons after Failure

Top Segment 6.4 ksi
Middle Segment 5.7 ksi
Bottom Segment 7.0 ksi

Therefore, the bottom segment was where failure was thought least likely to occur. However, due to the problem with the crossties, the failure in the bottom segment may have been due to a lack of confinement as compared to the other segments. Since the failure occurred at the top of the bottom segment, it is also possible that the concrete was weaker than indicated due to the water gain effect.

Since the cylinder strengths indicated that failure was most likely in the middle segment, it is also interesting to note that considerable spalling and cracking was observed near the joint between the middle and top segments of the compression face after failure.

4.2.2 Comparison of Piers With 2.5 inch Wall Thickness

4.2.2.1 General Observations

Because of the different end eccentricities at which the specimens were loaded, the behavior of the two specimens was expected to be different. Nevertheless, several similarities were noted:

1) The failure of each specimen originated in the compression face.

2) Longitudinal cracks were observed on the compression flanges of each specimen after failure.

3) For both specimens, cracks were observed on the "tension" face before forming on the compression face.

Differences in the observed behavior of the two specimens were also noted:

1) There was more extensive cracking observed on the compression face of Specimen 1S.

2) No cracks which ran transverse to the length of the specimen were observed on the "tension" flange of the segmental specimen until after failure. Also, no longitudinal cracks were observed on the tension flange of the monolithic specimen.

3) Cracks in the compression face of Specimen 1M were not observed until after failure.

4) Unlike Specimen 1M, the segmental specimen had a clearly defined failure region.

4.2.2.2 Strains

It is difficult to compare the strain gage results of Specimens 1M and 1S because of the limited number of gages that were placed on Specimen 1M. In addition, strain gage 1 (as shown in Figure 3.5) was faulty for both specimens and strain gage 15 gave erroneous results for Specimen 1S.

Strains from strain gages located near the midheight of each specimen are shown in Figures 4.7 and 4.8. Figure 4.7 illustrates the strains at loads of 0.3 P_u, 0.7 P_u, and P_u (P_u is load just before failure) on the compression and "tension"

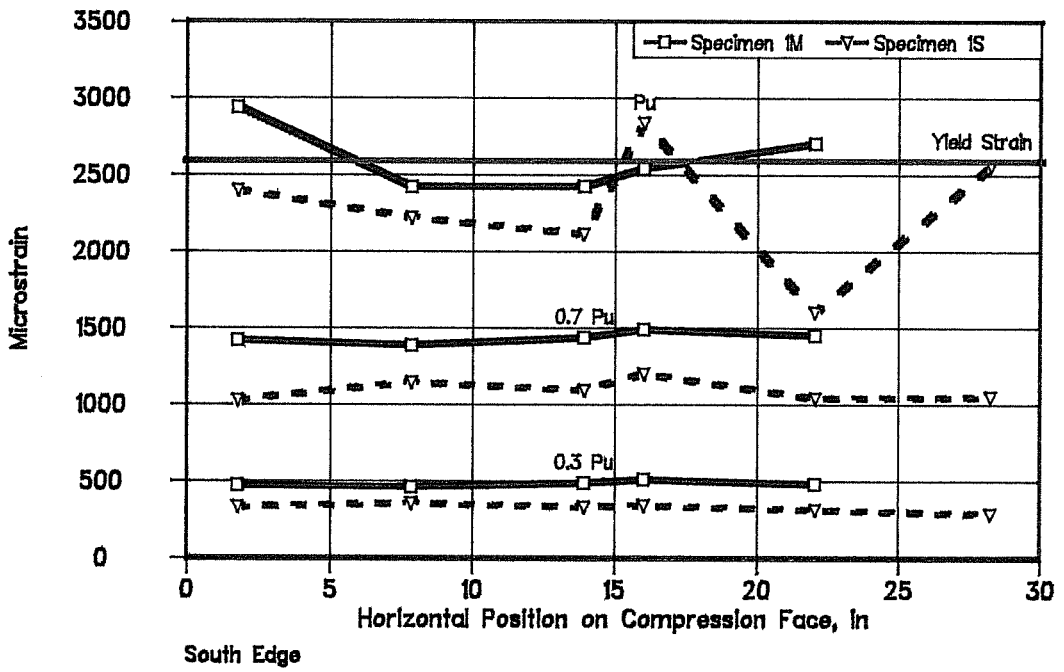

Compression Face Strains at Loads of 0.3 Pu, 0.7 Pu, and Pu
35" and 36" From Base

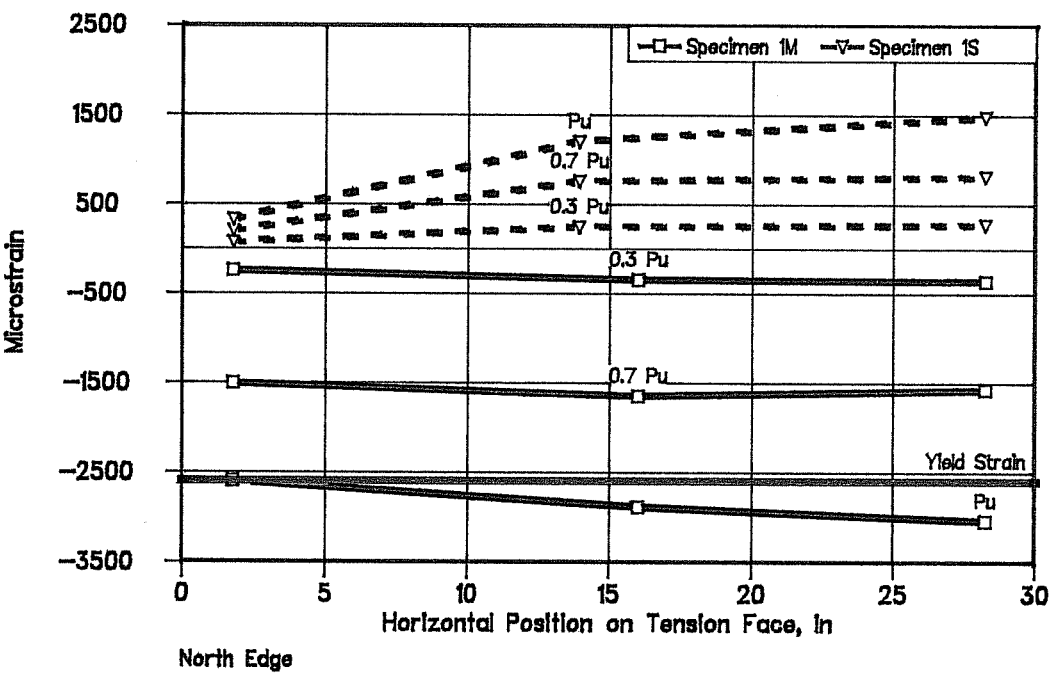

Tension Face Strains at Loads of 0.3 Pu, 0.7 Pu, and Pu
35" and 36" From Base

Figure 4.7 Specimens 1M and 1S Strain Gage Data

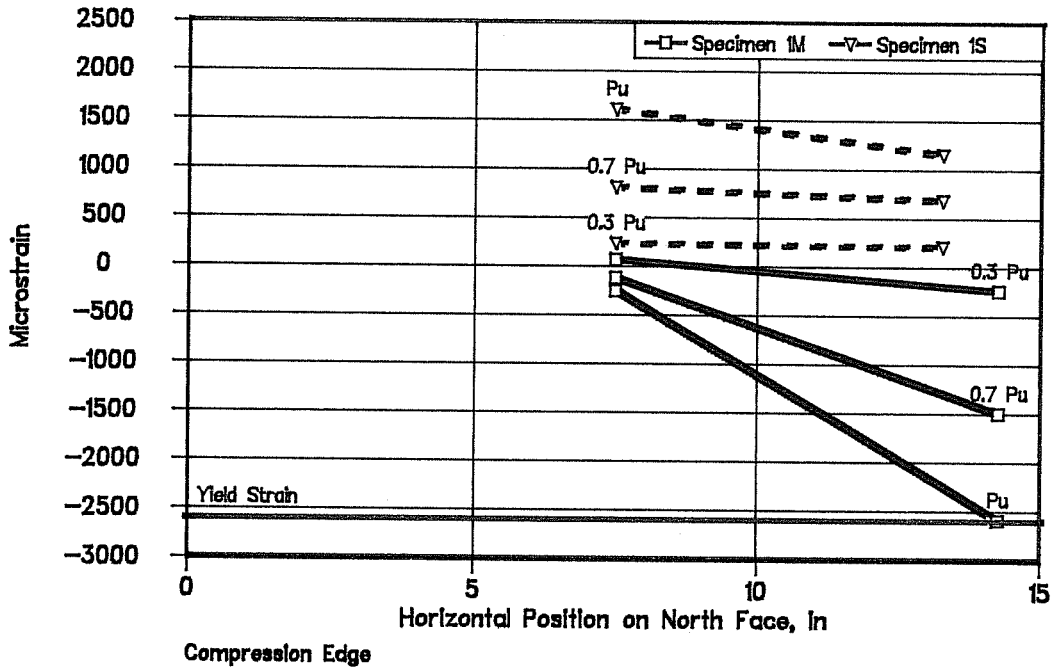

North Face Strains at Loads of 0.3 Pu, 0.7 Pu, and Pu
35" and 36" From Base

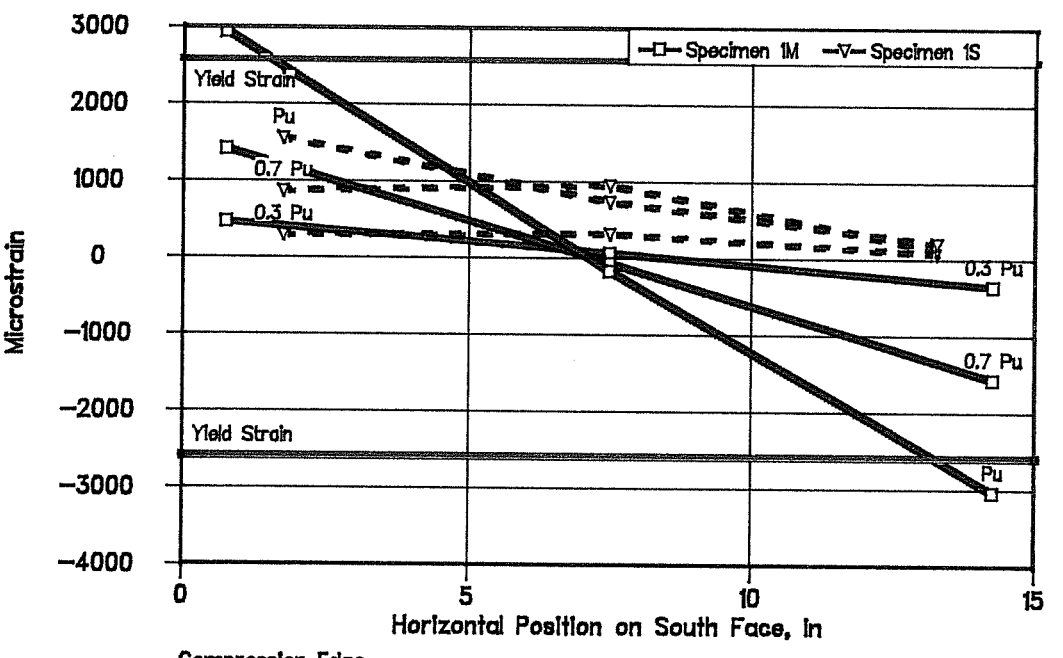

South Face Strains at Loads of 0.3 Pu, 0.7 Pu, and Pu
35" and 36" From Base

Figure 4.8 Specimens 1M and 1S Strain Gage Data

faces of each specimen. The compression face strains of Specimen 1M are fairly uniform across the width of the face. However, near the ultimate load of Specimen 1S, the strains become erratic across the width of the face. For each specimen, several of the longitudinal bars had yielded or were very near yield at ultimate. The strains across the "tension" face of each specimen seem to be consistent even though all of the longitudinal bars on the tension face of Specimen 1M had yielded before failure.

Strain gage results for gages located on the north and south faces of each specimen are shown in Figure 4.8. The gages located near the compression and tension edges of Specimen 1M are actually gage numbers 1, 6, 7, and 8 shown in Figure 3.5. Since both of the gages located near the compression edge were bad, it is difficult to compare the north face strains. However, the strains across the south face of each specimen behave as expected, decreasing linearly from near the compression face across to the "tension" flange.

Because additional strain gages were not placed on Specimen 1M, Figures 4.9 through 4.12 only show strain gage results from the test of Specimen 1S. The strains across the face of the specimen are fairly linear for loads of 0.3 and 0.7 Pu. However, the strains become highly nonlinear and erratic near ultimate. This phenomena can be attributed to cracks

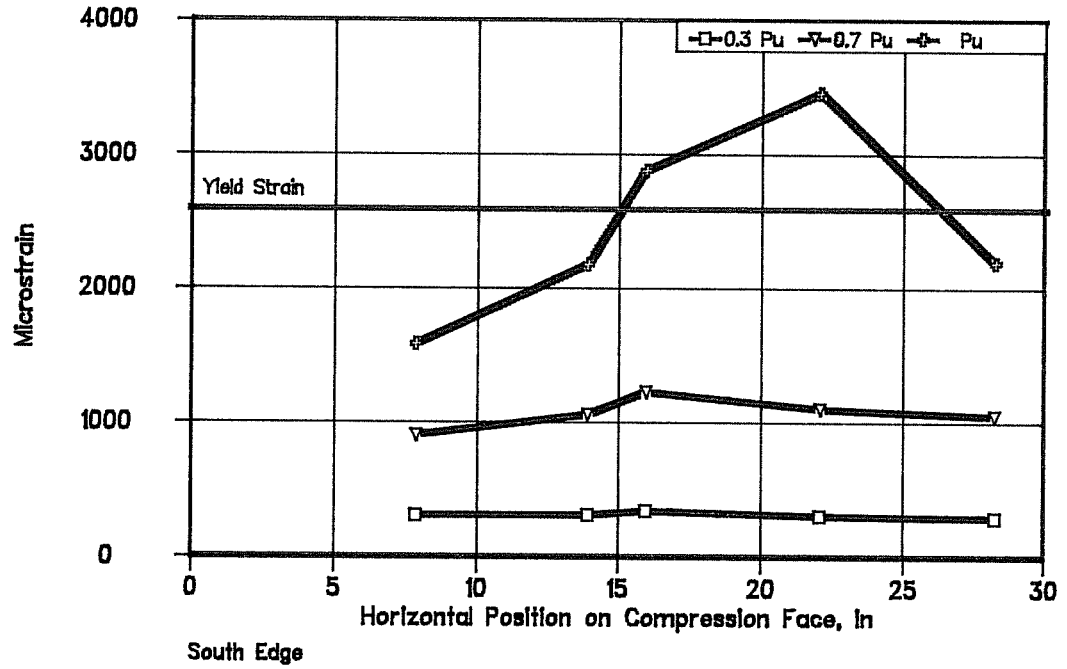

Compression Face Strains at Loads of 0.3 Pu, 0.7 Pu, and Pu
12" From Base

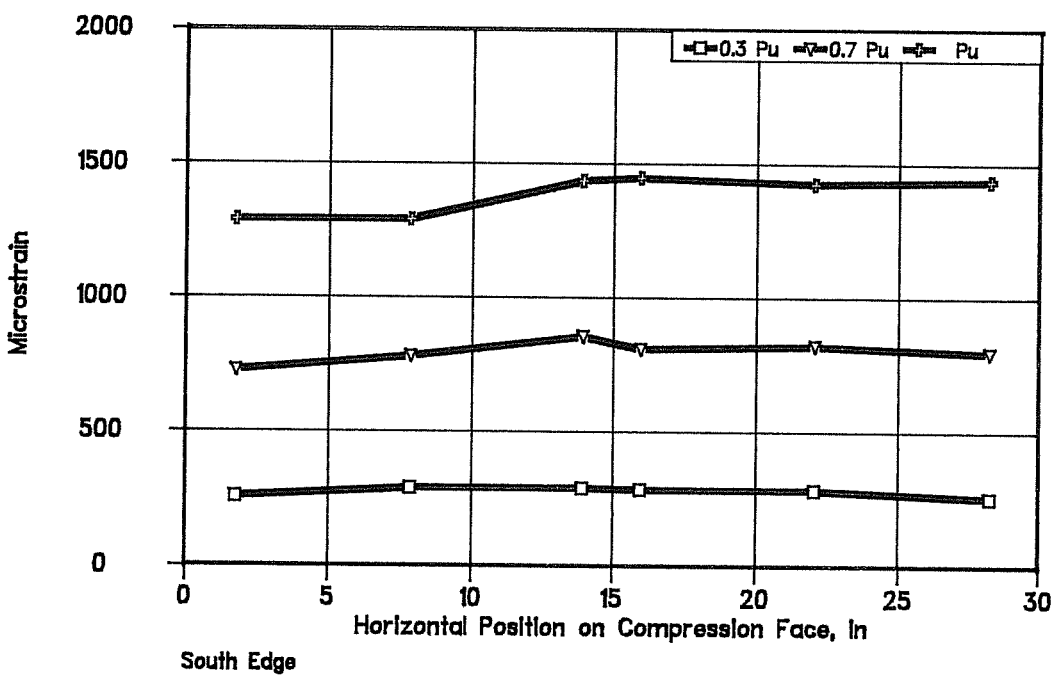

Compression Face Strains at Loads of 0.3 Pu, 0.7 Pu, and Pu
60" From Base

Figure 4.9 Specimen 1S Strain Gage Data

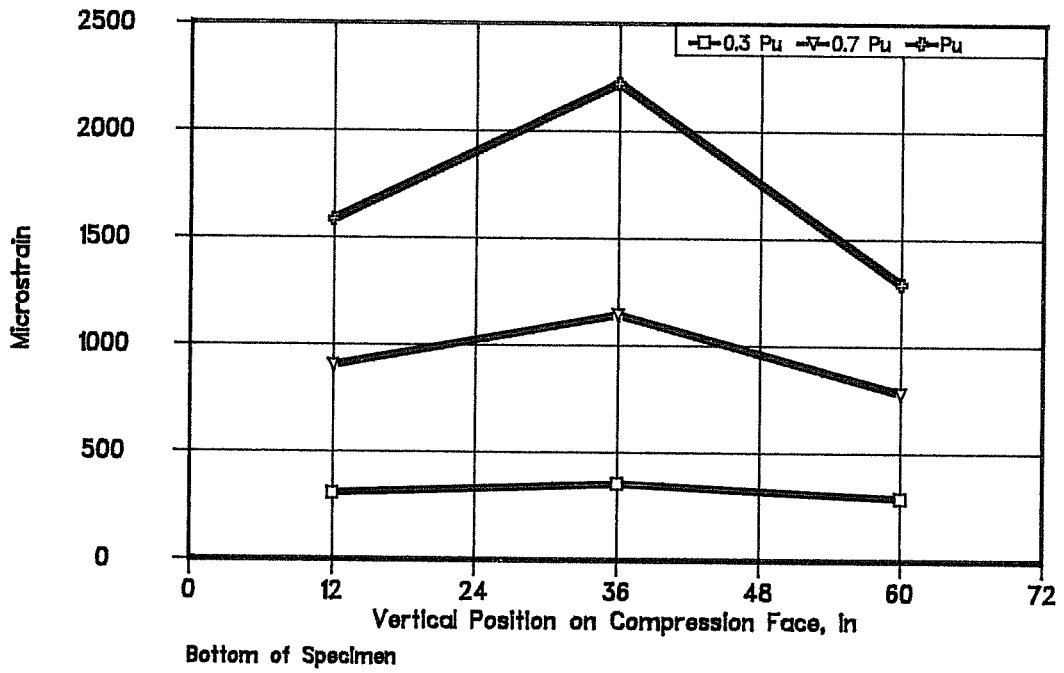

Compression Face Strains at Loads of 0.3 Pu, 0.7 Pu, and Pu
7.85" From South Face

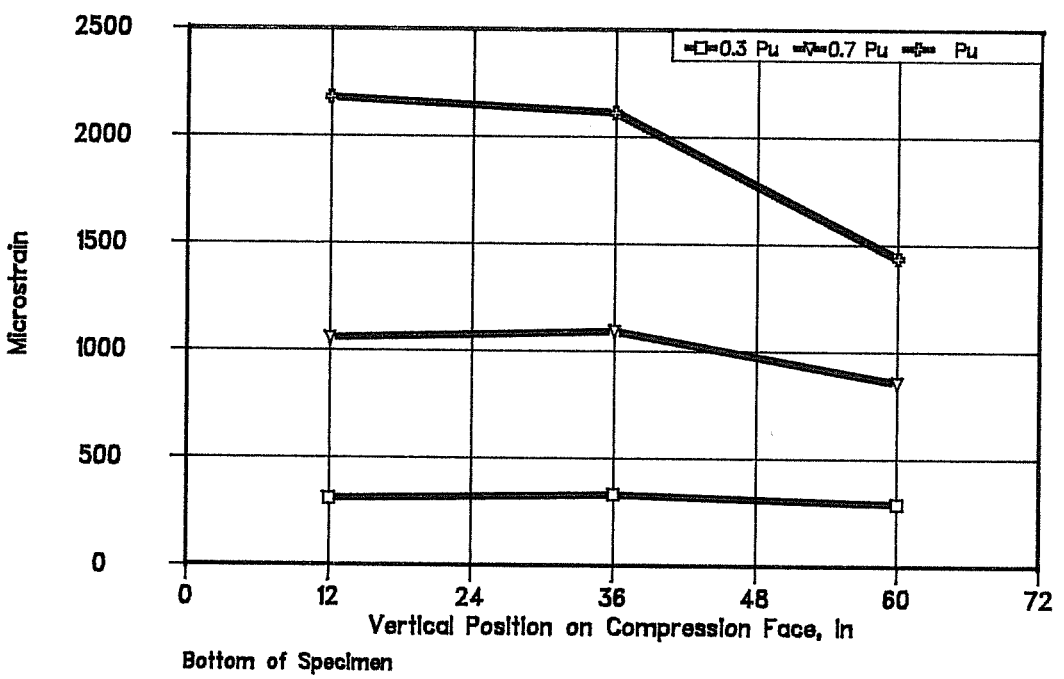

Compression Face Strains at Loads of 0.3 Pu, 0.7 Pu, and Pu
14" From South Face

Figure 4.10 Specimen 1S Strain Gage Data

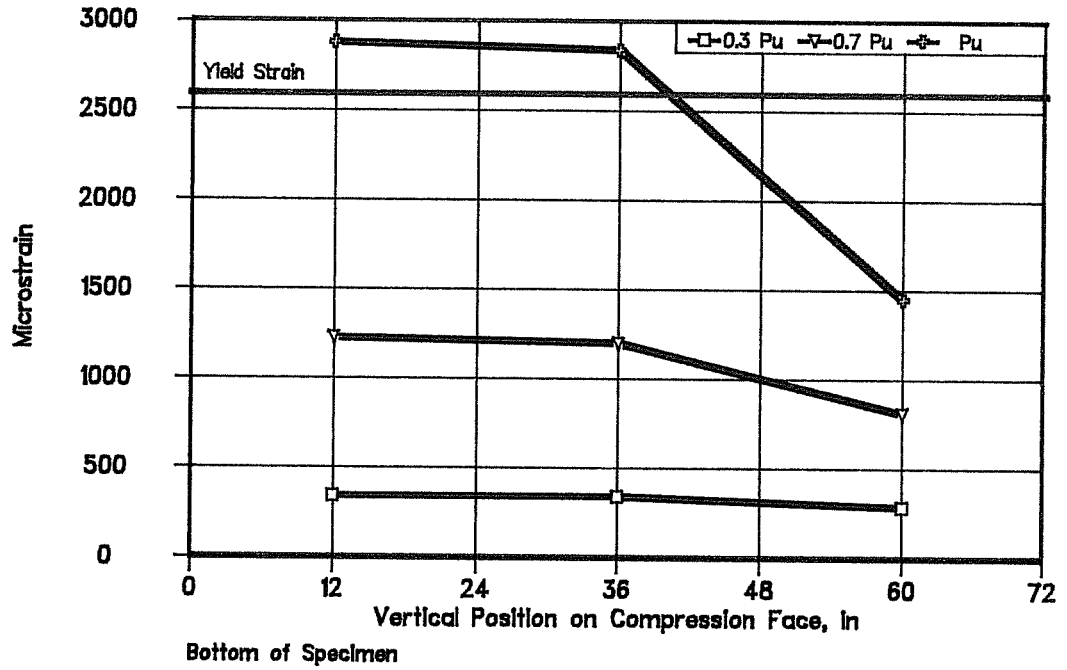

Compression Face Strains at Loads of 0.3 Pu, 0.7 Pu, and Pu
16" From South Face

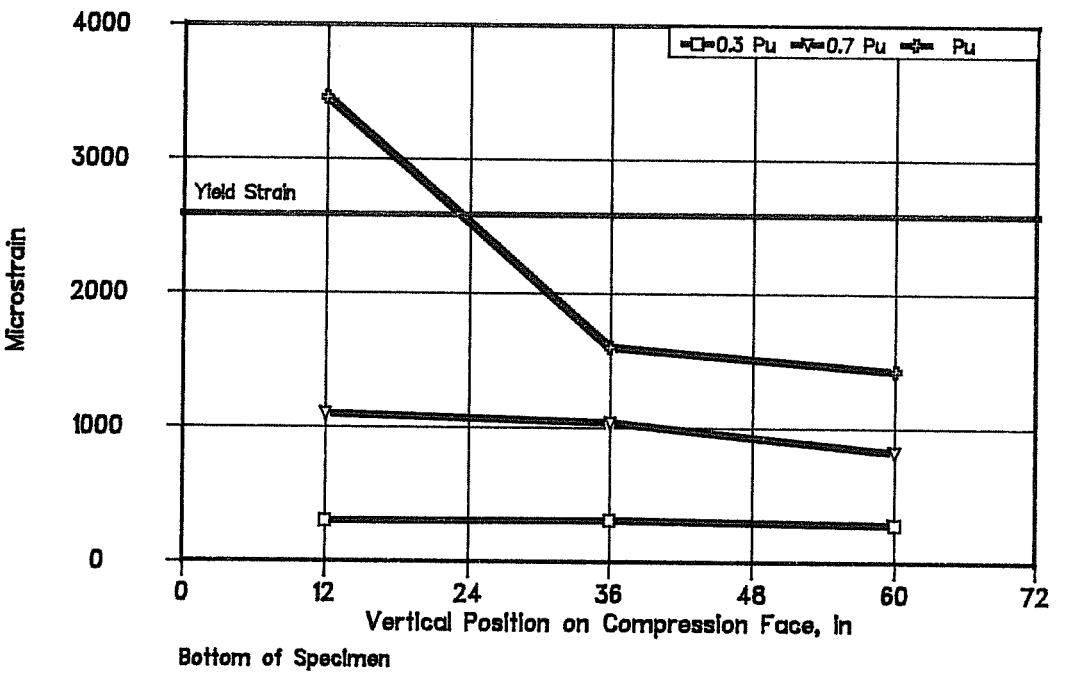

Compression Face Strains at Loads of 0.3 Pu, 0.7 Pu, and Pu
22" From South Face

Figure 4.11 Specimen 1S Strain Gage Data

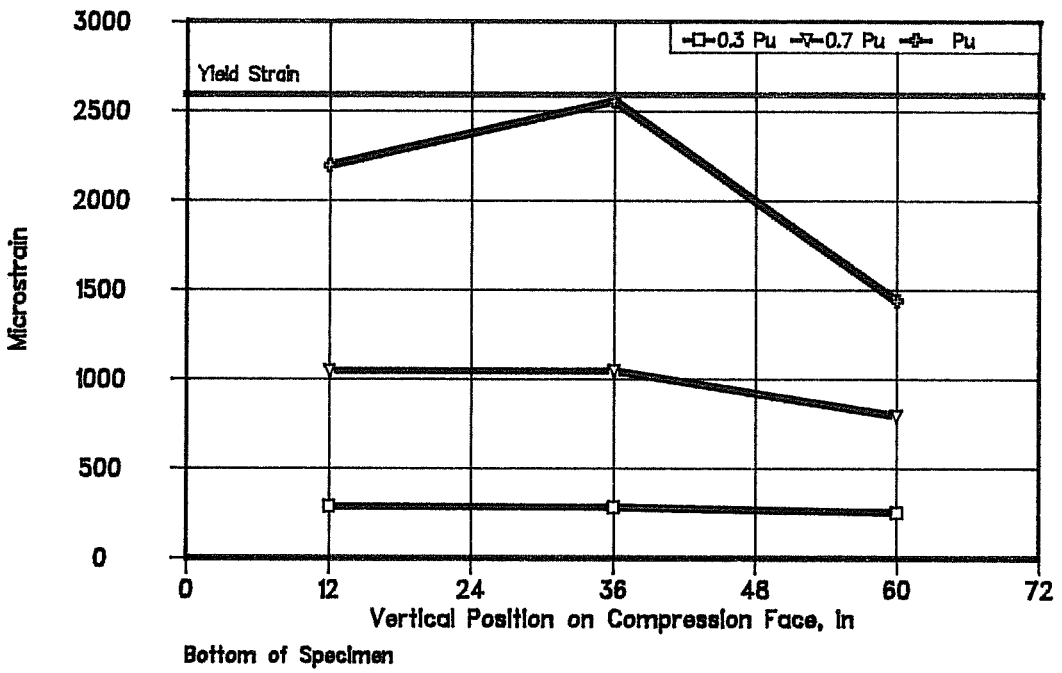

Compression Face Strains at Loads of 0.3 Pu, 0.7 Pu, and Pu
28.25" From South Face

Figure 4.12 Specimen 1S Strain Gage Data

forming in the concrete and yielding of the bars. From Figures 4.10 through 4.12, it appears that the bottom segment of Specimen 1S had the highest strains of the three segments.

4.2.2.3 Displacements

The compression face profile of Specimen 1M at ultimate is shown in Figure 4.13. (Refer to Chapter 3 for specific locations of the potentiometers.) The figure shows that the compression face was bowing inward at all locations except for potentiometer 3. The largest displacements of the compression face were located near the failure region, with decreasing displacements along the length of the pier.

Converse to that of Specimen 1M, the compression face of Specimen 1S was bowing outward as shown in Figure 4.14. In this case, the displacements are fairly uniform across the entire face, not just concentrated near the failure region. Also, the deformations near the edges of Specimen 1S are very small while the deformations near the edges of the monolithic specimen are similar to those found in the middle of the face.

The explanation for the differences in compression face displacements in the two specimens can be explained in regard to their overall behavior. Specimen 1M was loaded at an eccentricity which caused bending of the pier section with the neutral axis falling within the section. Thus the deformations shown in Figure 4.13 reflect the overall curvature of the

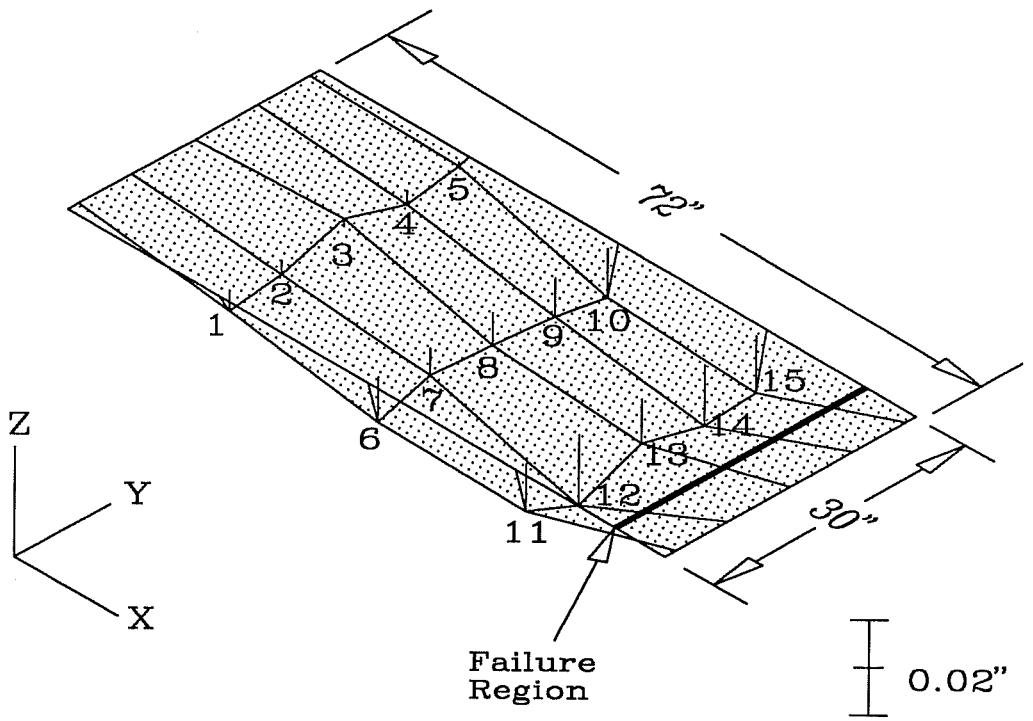

Compression Face Deflections Measured by Potentiometers Specimen 1M			
Potentiometer Number	Deflection (inches)	Potentiometer Number	Deflection (inches)
1	-0.0043	9	-0.0081
2	-0.0028	10	-0.0102
3	0.0016	11	-0.0100
4	-0.0028	12	-0.0149
5	-0.0008	13	-0.0092
6	-0.0094	14	-0.0128
7	-0.0057	15	-0.0120
8	-0.0068		

Figure 4.13 Specimen 1M Compression Face Profile at Failure Load

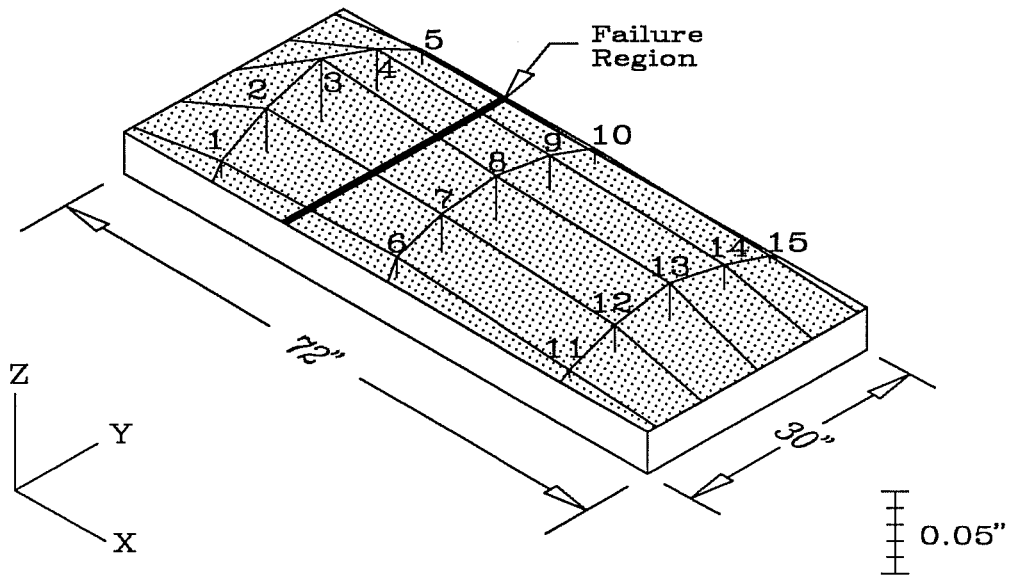

Compression Face Deflections Measured by Potentiometers Specimen 1S			
Potentiometer Number	Deflection (inches)	Potentiometer Number	Deflection (inches)
1	0.0096	9	0.0202
2	0.0261	10	0.0090
3	0.0375	11	0.0045
4	0.0244	12	0.0164
5	0.0085	13	0.0223
6	0.0122	14	0.0141
7	0.0222	15	0.0041
8	0.0267		

Figure 4.14 Specimen 1S Compression Face Profile at Failure Load

section. On the other hand, Specimen 1S was loaded such that the entire section was in compression. This caused the bulging of the section which is shown in Figure 4.14. The deformations of the edges of the compression face of Specimen 1S are limited by the confinement provided by the short sides of the pier.

Since the failure region of each specimen was located in an area of relatively large displacements, local instability of the compression face may have had some influence on the failure of the specimens.

The moment-curvature relationship along a length of each specimen was determined by manipulating test data (see Appendix) from the potentiometer setup shown in Chapter 3. Since Specimen 1M had a much greater eccentricity than that of Specimen 1S, only curvatures at similar moments can be compared. However, from the curvatures shown in Figure 4.15, it is evident that Specimen 1M withstood greater moment for the same amount of curvature as Specimen 1S.

From the plot of total shortening shown in Figure 4.15, it appears that Specimen 1S was axially stiffer than Specimen 1M. This is interesting because the cylinder strength of Specimen 1M was greater than that found in any segment of Specimen 1S (7862 vs. 6980 psi).

The load head rotations of each specimen are shown in Figure 4.16. Though the load heads of Specimen 1M behave as

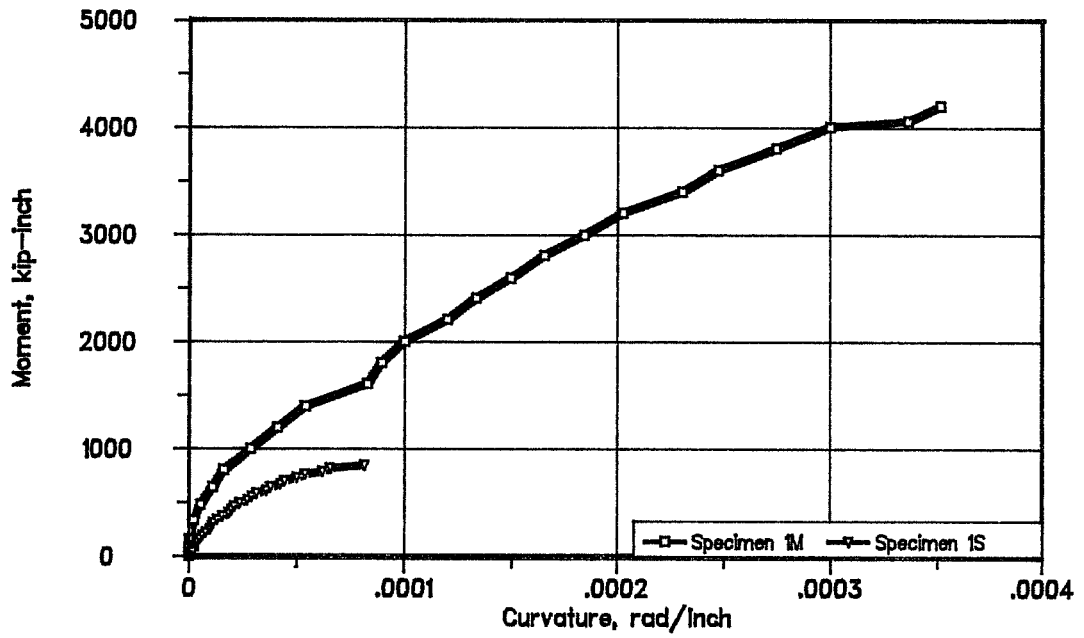

Moment-Curvature Relationship

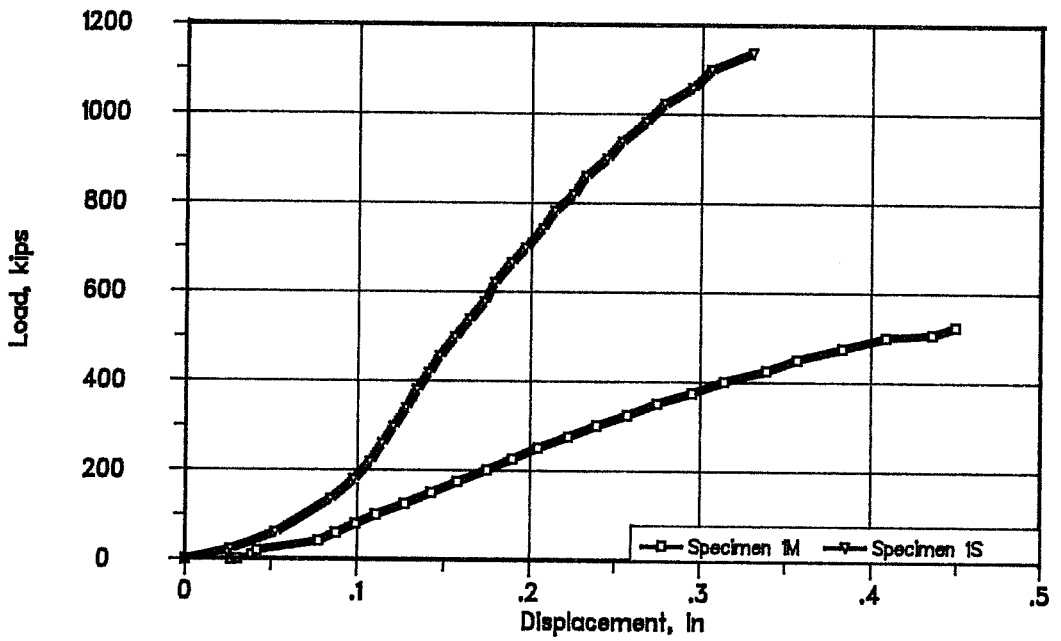

Total Shortening of Specimens

Figure 4.15 Specimens 1M and 1S Displacement Data

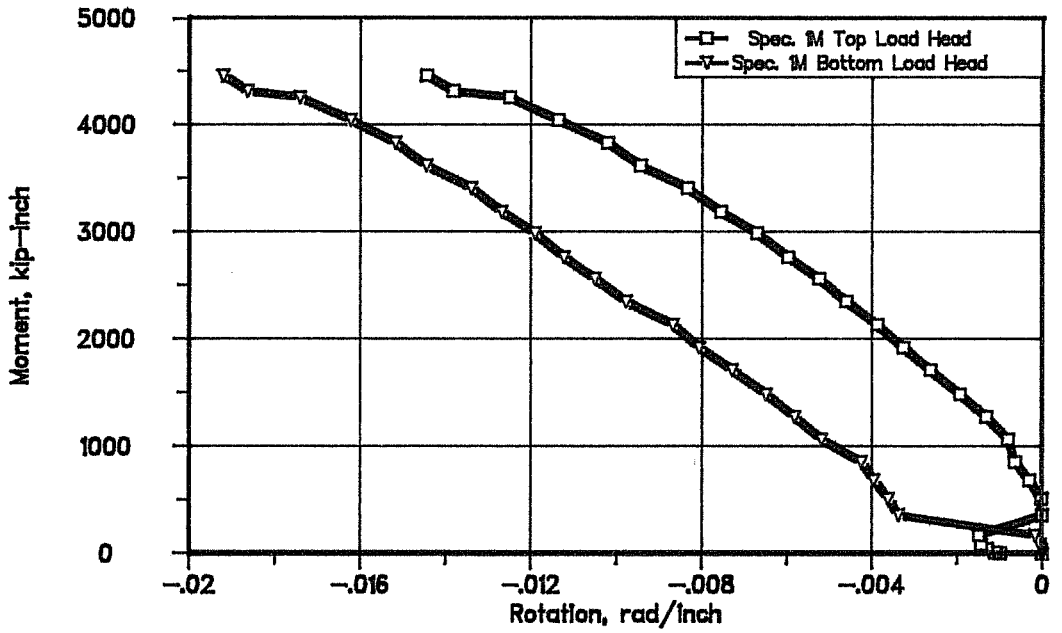

Specimen 1M

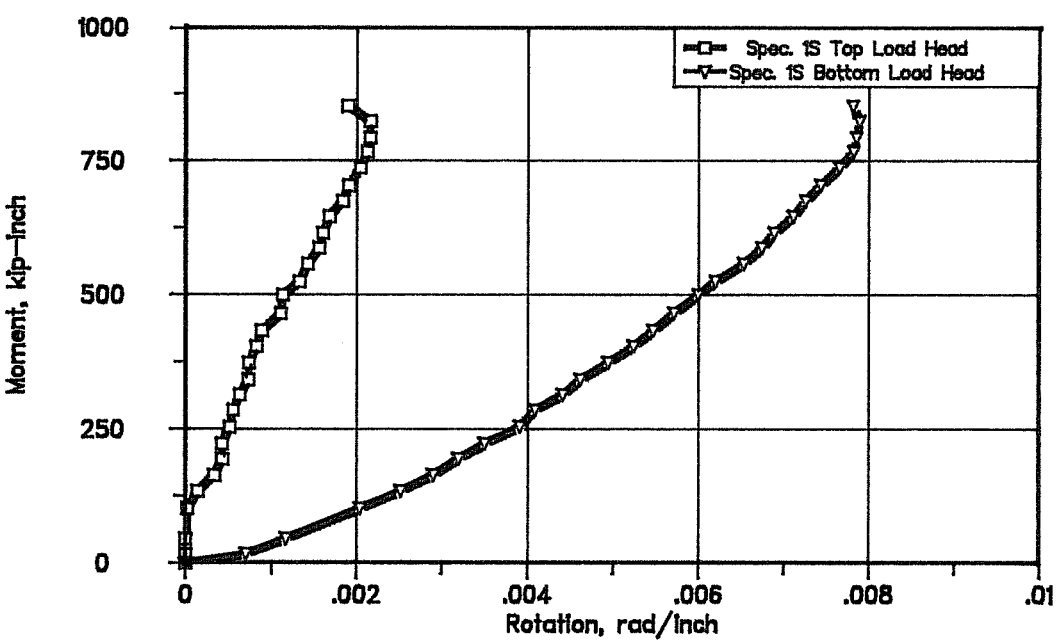

Specimen 1S

Figure 4.16 Specimens 1M and 1S Load Head Rotations

expected with rotation toward the pier, the load heads of Specimen 1S exhibit the interesting behavior of bowing outward from the center of load application. Thus, though Specimen 1S is shortening, the periphery of the load head is shortening less than the center of the load heads.

As discussed in Chapter 3, the centerline deformations of the short sides of the specimens are presented in Figure 4.17. The total deformation recorded and the load at the last reading taken is shown. Because of the large eccentricity at which Specimen 1M was loaded, the centerline deformation was consistent with the compression face profile shown in Figure 4.13. The centerline deformation of Specimen 1S was also substantial, even though it was loaded at a small eccentricity.

4.3 Specimens 2M and 2S

4.3.1 General Observations

Specimens 2M and 2S have wall slenderness ratios, X_u/t_f, of 18 and 15.5, respectively. Though fairly high, these ratios fall between the ranges compared in the other two series. Each specimen has a wall thickness of 2.0 inches. The mild reinforcement ratio and placement of the reinforcement is identical for each specimen. Specimen 2M was constructed monolithically while Specimen 2S was constructed segmentally. Other than their construction, the only difference between these

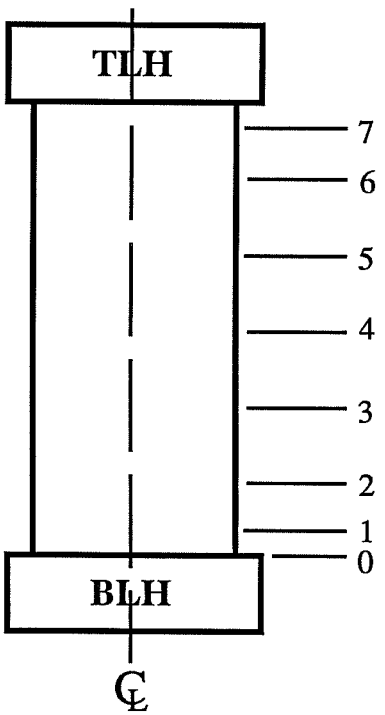

Specimen 1M
Load = 501 kips

Station	Location Above Base	Displacement (millimeters)
1	4"	1.25
2	12"	2.75
3	24"	4.50
4	36"	5.00
5	48"	4.25
6	60"	2.5
7	68"	1.0

**Note: For Specimen 1M, readings from the north and south faces were averaged.

Specimen 1S
Load = 1099 kips

Station	Location Above Base	Displacement (millimeters)
1	6"	0.5
2	12"	0.5
3	24"	1.5
4	36"	1.5
5	48"	1.5
6	60"	0.5
7	66"	0.5

Figure 4.17 Specimens 1M and 1S Centerline Deformations

two specimens is the addition of the post-tensioning tendons and associated bevels to Specimen 2S.

The cylinder strengths of the concrete near the failure region of each specimen are listed below.

Specimen 2M	7705 psi
Specimen 2S	4837 psi

4.3.1.1 Specimen 2M (Monolithic with end eccentricity of 2.75 inches and X_u/t_f of 18)

Explosive failure of this specimen occurred at a load of 938 kips. The load had been applied for approximately two minutes when failure occurred. Failure occurred about 5 inches from the top of the specimen. Since no additional deflection of the critical section was observed prior to failure, the failure moment was 2580 kip-inches.

First cracks appeared near the center of the "tension" face and on the load heads at a load of 458 kips. The first cracks on the compression face appeared near the centerline at a load of 496 kips. The first cracks ran along the length of the specimen and seemed to begin in the load heads. The last visible cracks before failure were marked at a load of 819 kips. All of the cracks that were marked before failure are shown in Figure 4.18.

After failure of the specimen, visible cracks were marked with dashed lines on the compression and "tension" faces (Fig.

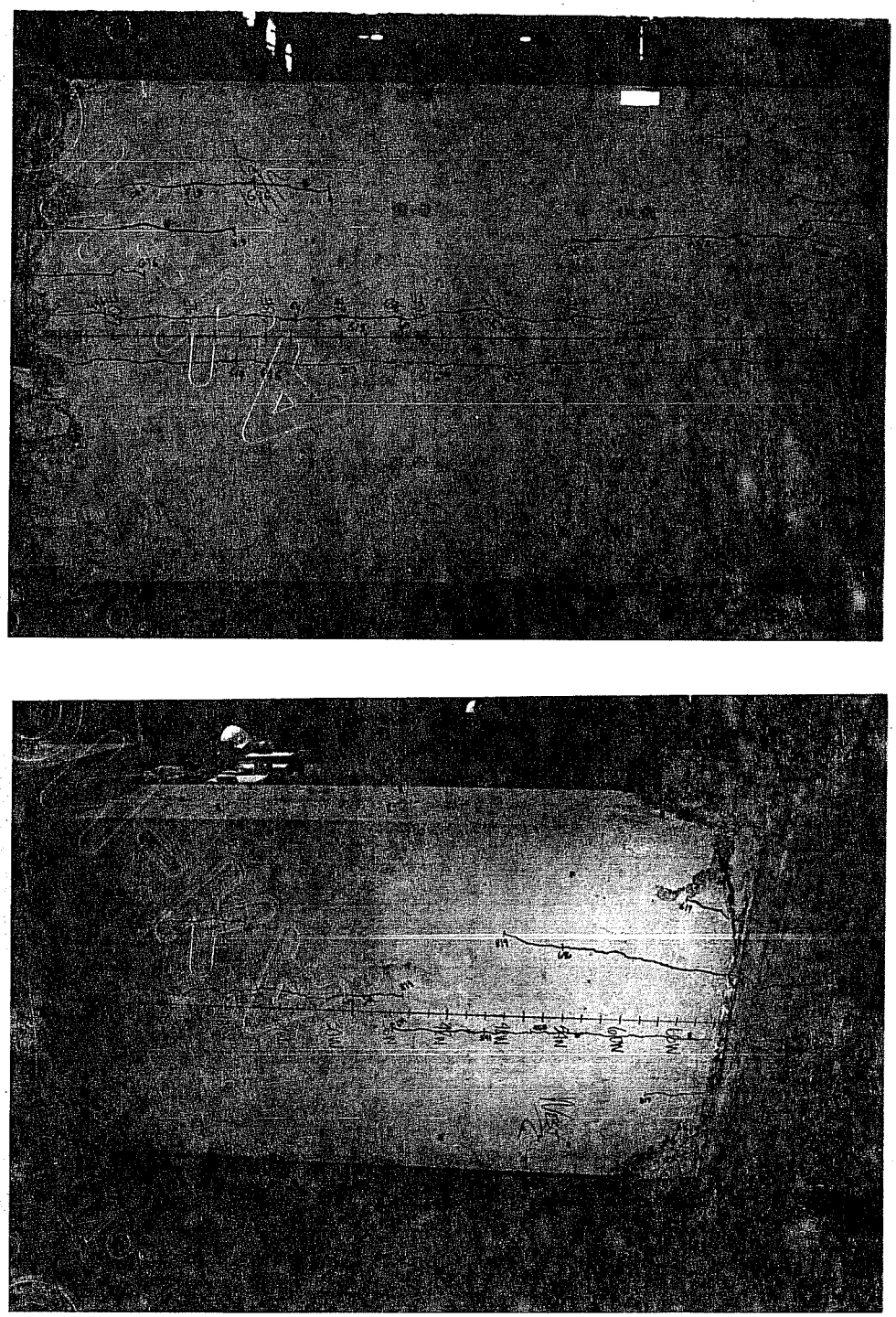

Figure 4.18 Specimen 2M Cracks Marked before Failure (compression face on top)

4.19). From Figure 4.19, it is evident that two different modes of failure occurred. Material failure of the compression face caused the "tension" flange to fail in flexure.

After failure, numerous cracks formed on the compression face. The tendency of the cracks to fan toward the side faces (Fig. 4.19) are probably a result of the restraint provided by the short sides and the confinement provided by the reinforcing cage. When the specimen failed, the collapse caused very high stresses in the longitudinal reinforcement. However, the bar stresses in the vicinity of the short sides were less because of the additional restraint. Therefore, the closely spaced (2 in.) lateral reinforcement distributed the high stresses found in the bars in the center of the section to those bars located near the edges.

Several observations were made after observing the failure region:

1) All of the longitudinal steel appeared to have buckled over one spacing of the transverse reinforcement.

2) The transverse reinforcement and crossties seemed to be in their proper positions.

3) The corners formed by the short sides and "tension" face seemed to fail in shear due to the increased flexural stiffness provided by the short sides of the pier. This is hypothesized because of the 45 degree cracking zones observed.

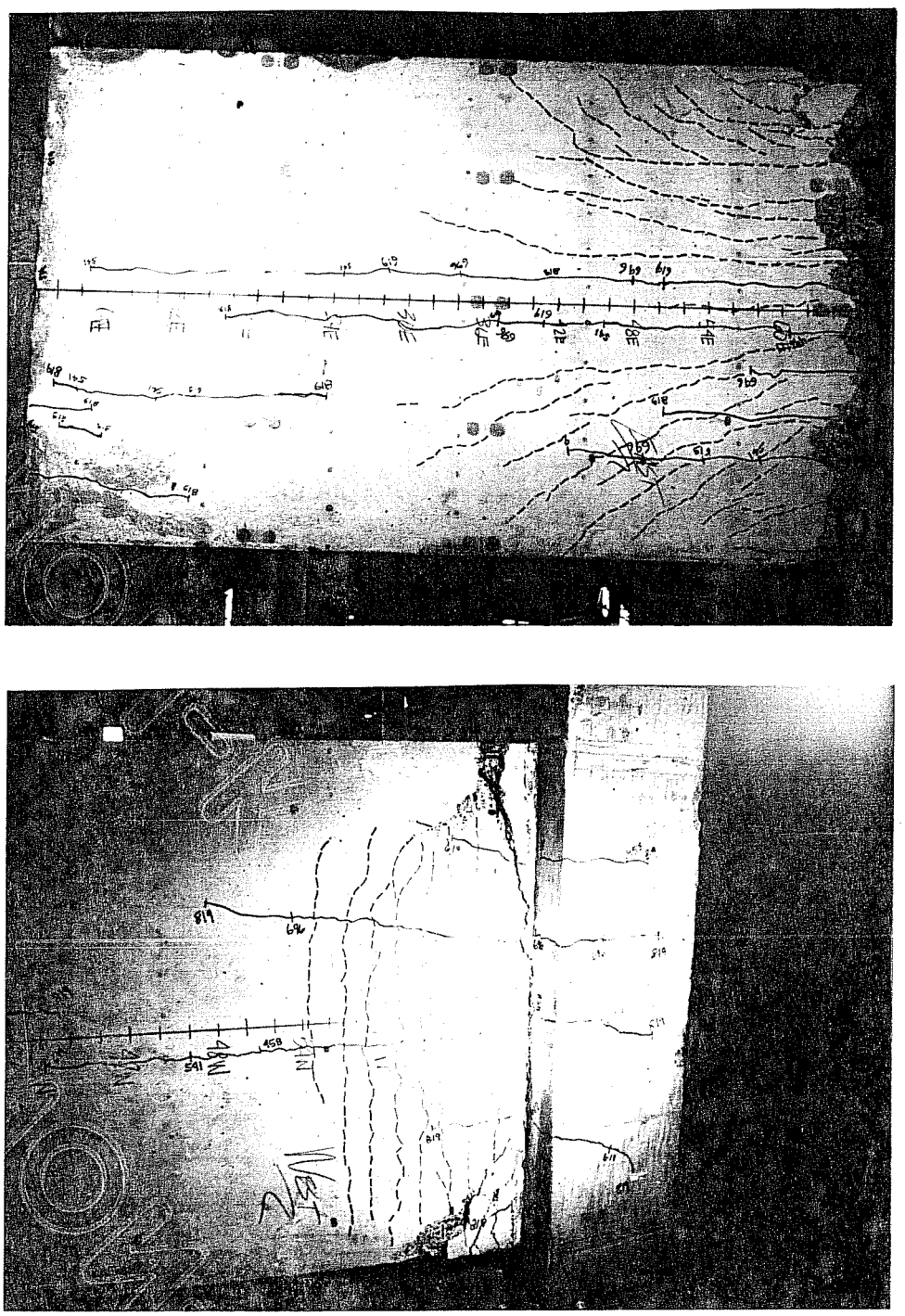

Figure 4.19 Specimen 2M Cracks Marked after Failure (compression face on top)

Typical of the other specimens, the acute angle caused by failure of the compression flange is shown in Figure 4.20.

4.3.1.2 Specimen 2S (Segmental with end eccentricity of 1.0 inch and X_u/t_f of 15.5)

This specimen failed at a load of 948 kips. Failure did not seem to be quite as explosive as other failures in the 1200 kip machine. Failure occurred approximately 4 inches below the joint between the top load head and the top pier segment. As with Specimen 2M, no additional deflection of the critical section was observed prior to failure. Therefore, the failure moment corresponding to the total eccentricity of 1 inch was 948 kip-inches. From Chapter 2, the cylinder strength of the concrete in the top segment was 4837 psi, the lowest of the three segments.

First cracking was observed in the load heads and the "tension" face at a load of 502 kips. Initial cracks were observed on the compression face at a load of 586 kips.

Final cracks were marked at a load of 824 kips. Long cracks along the length of the specimen were noted in all three segments on the compression and tension flanges (Fig. 4.21). Though the cracks extended the entire length of their respective segments, they did not appear to extend through the epoxied joint into the adjoining segment. Only one crack occurred in the center segment.

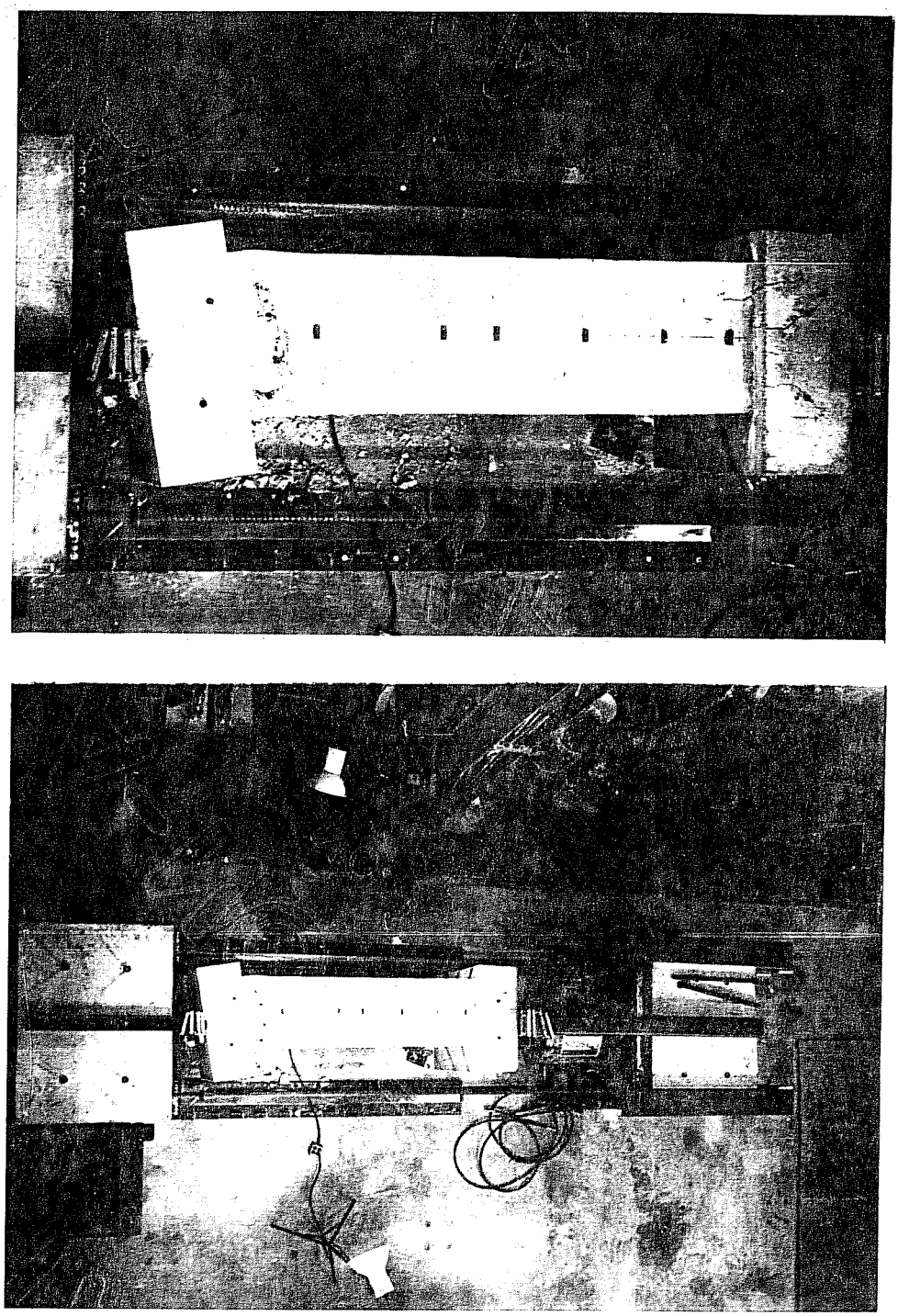

Figure 4.20 Typical Failure in 1200 kip Testing Machine

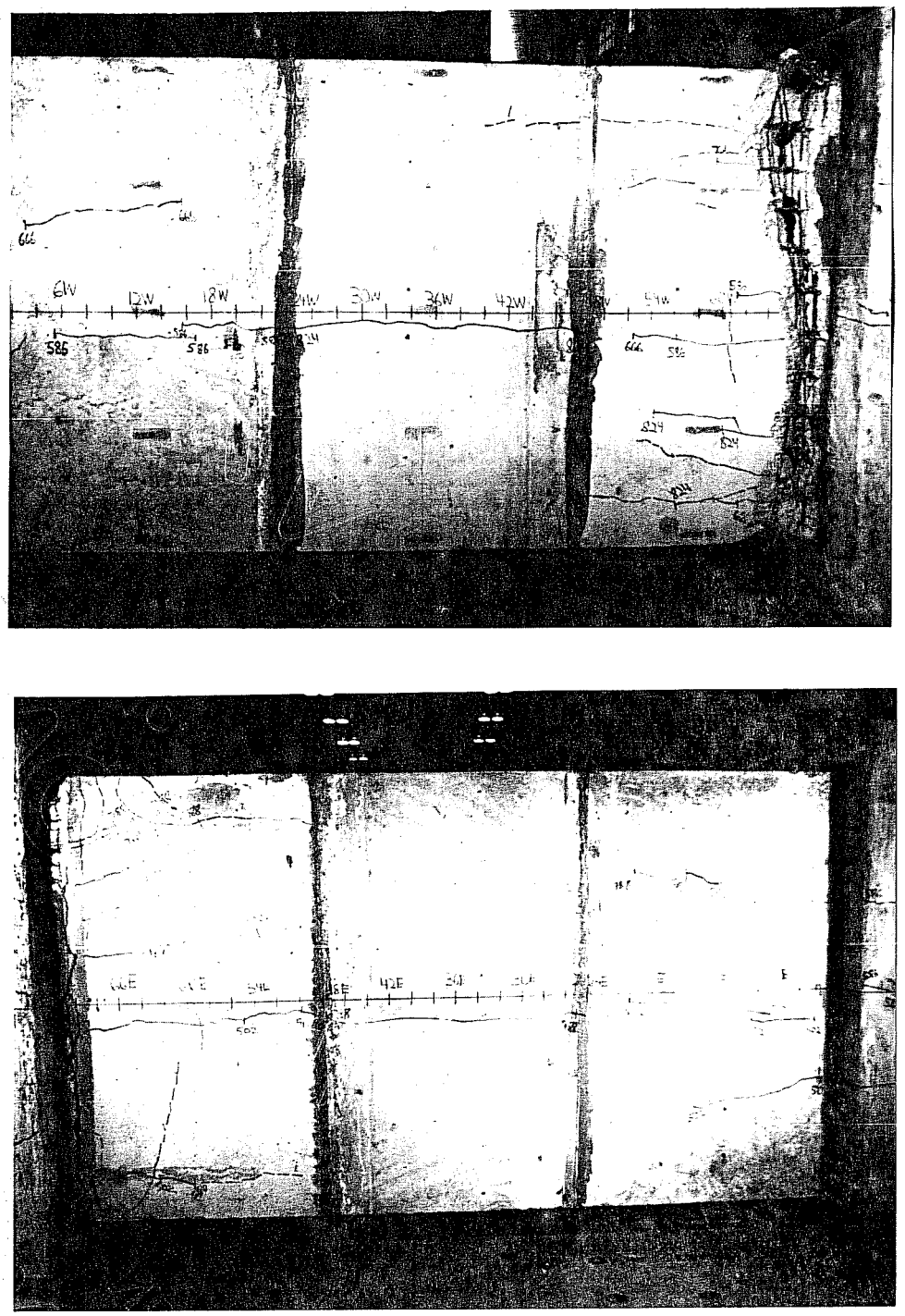

Figure 4.21 Specimen 2S Cracks Marked before Failure (compression face on top)

In addition to the longitudinal cracks found on the "tension" face, several cracks appeared at approximately 45 degree angles near the corners of the top segment (Fig. 4.22). This could be a combination of a compression field between the post-tensioned tendon and longitudinal reinforcement and a tension field caused by the edges of the load head pulling away from the center of the specimen. The latter part of this statement is verified by the measured load head displacements.

Cracks that appeared after failure on the compression and tension faces were marked with a dashed line (Fig. 4.23). As with the preceding specimens, these cracks seemed to indicate that the "tension" face was subjected to some bending after the material failure of the compression face.

From visual observation after failure, all of the longitudinal reinforcement crossing the failure plane buckled. Like Specimen 1S, the two post-tensioned tendons on the compression side of the specimen were protruding out about 2 to 3 inches from the top load head. This was apparently due to insufficient bond to resist the forces caused by the shortening of the specimen.

4.3.2 Comparison of Piers With 2.0 inch Wall Thickness

4.3.2.1 General Observations

Several similarities about the behavior of the specimens were observed:

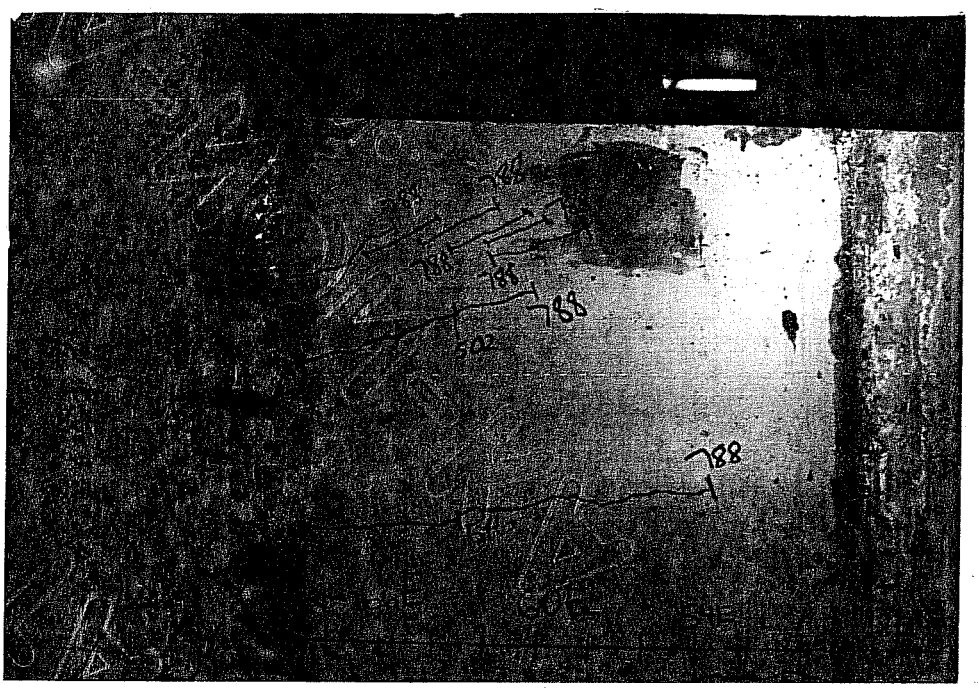

Figure 4.22 Specimen 2S Inclined Cracking on "Tension" Face

1) First cracking occurred on the "tension" face of each specimen. In addition, the initial cracks were located near the centerline of the face and ran along the length of the pier.

2) First cracking occurred in either the upper or lower third of each specimen.

3) The crack patterns before failure were very similar.

4) The locations of failure and failure regions were nearly identical.

Several differences were also noted:

1) The flexural mode of failure of the "tension" flange was not as obvious for the segmental specimen as it was for Specimen 2M.

2) Diagonal cracks were observed on the "tension" face of Specimen 2S before failure. The only diagonal cracks that were observed on Specimen 2M appeared in a similar location but were not formed until after failure.

3) After failure, there was more cracking evident in the monolithic specimen than Specimen 2S.

4.3.2.2 Strains

Referring to the gage numbers shown in Figure 3.6, gages 7, 12, 13, 16, 18, 19, 21, and 27 were found to give faulty results for Specimen 2M. Likewise, gages 6 and 24 were found to give erroneous results for Specimen 2S. Therefore, the data from these gages was left out of this section.

By comparing strain gage readings at loads corresponding to 30, 70, and nearly 100 percent of the failure load, several observations were made.

From the strains across the width of the compression face shown in Figures 4.24 and 4.25, it is apparent that the longitudinal steel strains in Specimen 2M were more uniform than those of Specimen 2S. Also, the longitudinal strains in the segmental specimen seem to be very erratic from one load step to the next.

The longitudinal steel strains across the "tension" face of each specimen are fairly linear (Fig 4.25). It is also interesting to note that the "tension" face strains are highest near the north edge of the pier for both specimens.

In Figure 4.26, the longitudinal steel strains across the north and south faces of the pier are shown. The strains across each face appear as expected with the largest strains occurring near the compression face of each specimen.

The longitudinal steel strains along the length of the specimens are shown in Figures 4.27 through 4.29. In each figure, the largest strains in Specimen 2S occur in the top segment. Other than the strains shown in Figure 4.27, the largest strains in Specimen 2M also occur in the top third of the pier.

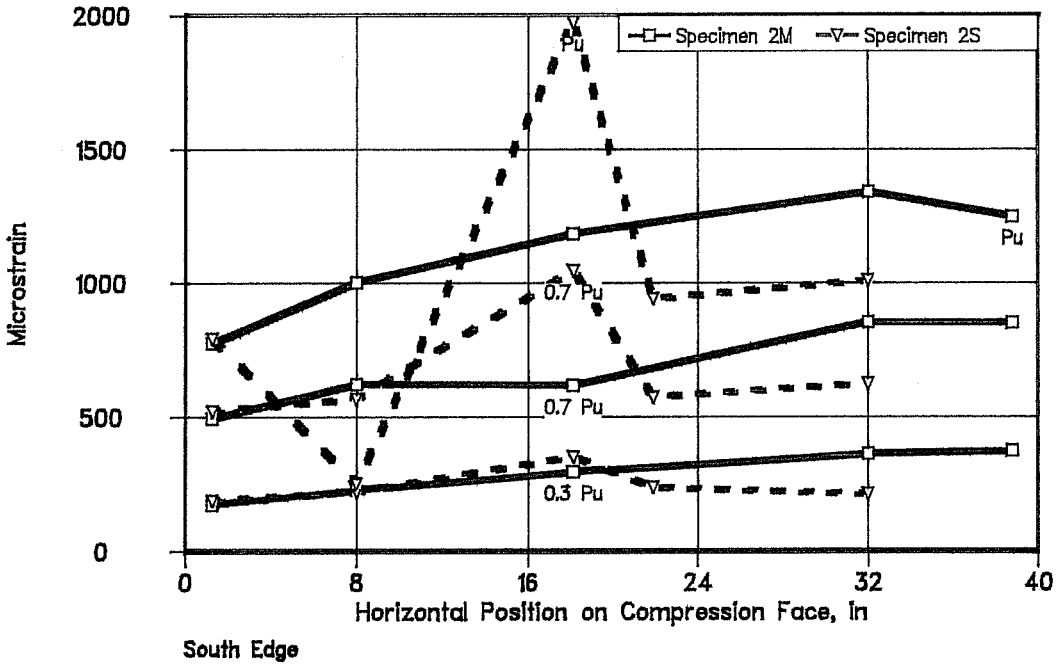

Compression Face Strains at Loads of 0.3 Pu, 0.7 Pu, and Pu
18" and 12" From Base

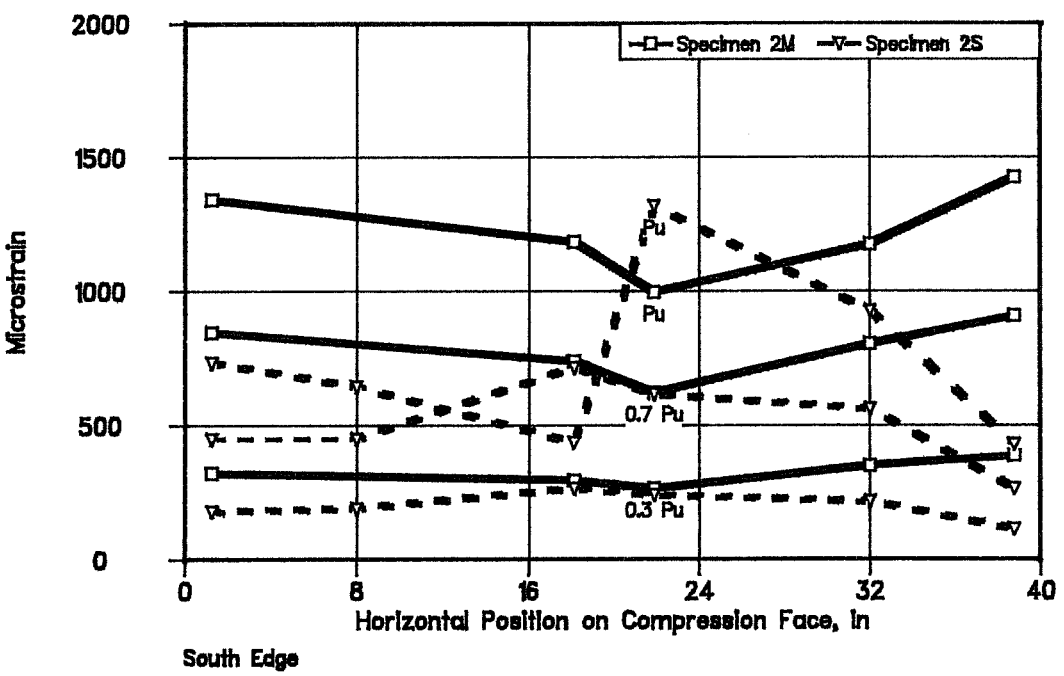

Compression Face Strains at Loads of 0.3 Pu, 0.7 Pu, and Pu
18" and 12" From Base

Figure 4.24 Specimens 2M and 2S Strain Gage Data

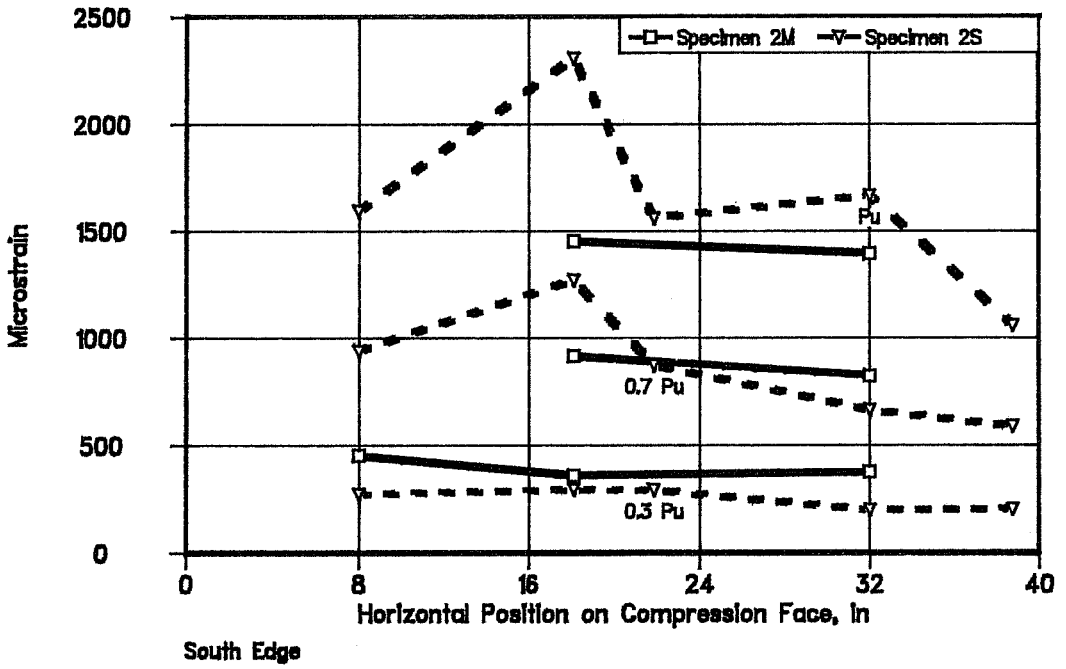

Compression Face Strains at Loads of 0.3 Pu, 0.7 Pu, and Pu
54" and 60" From Base

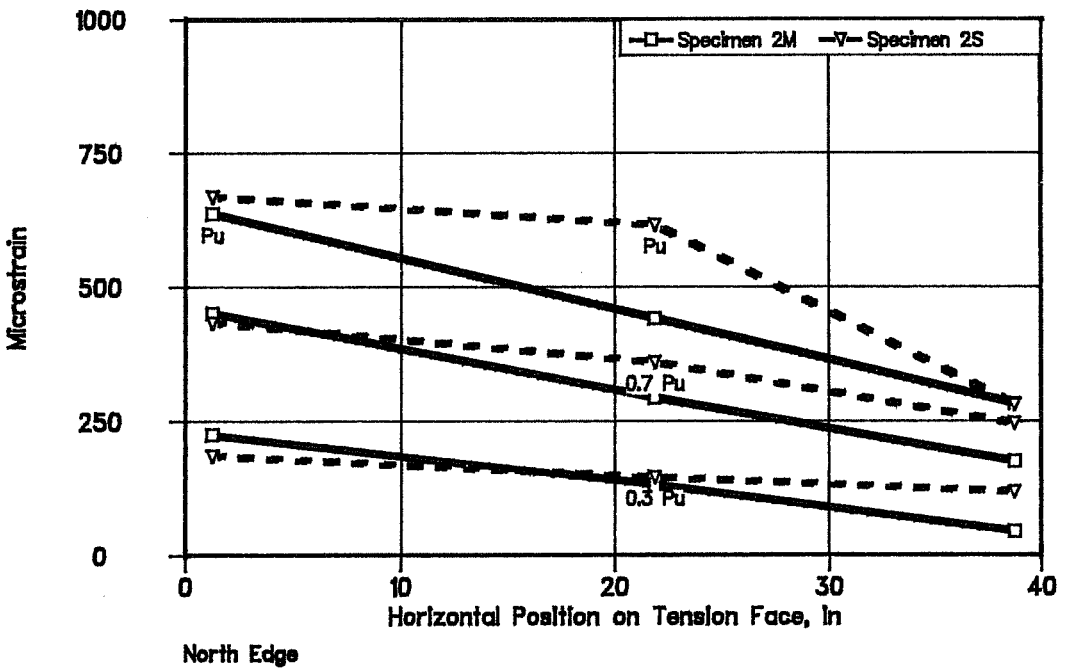

Tension Face Strains at Loads of 0.3 Pu, 0.7 Pu, and Pu
36" From Base

Figure 4.25 Specimens 2M and 2S Strain Gage Data

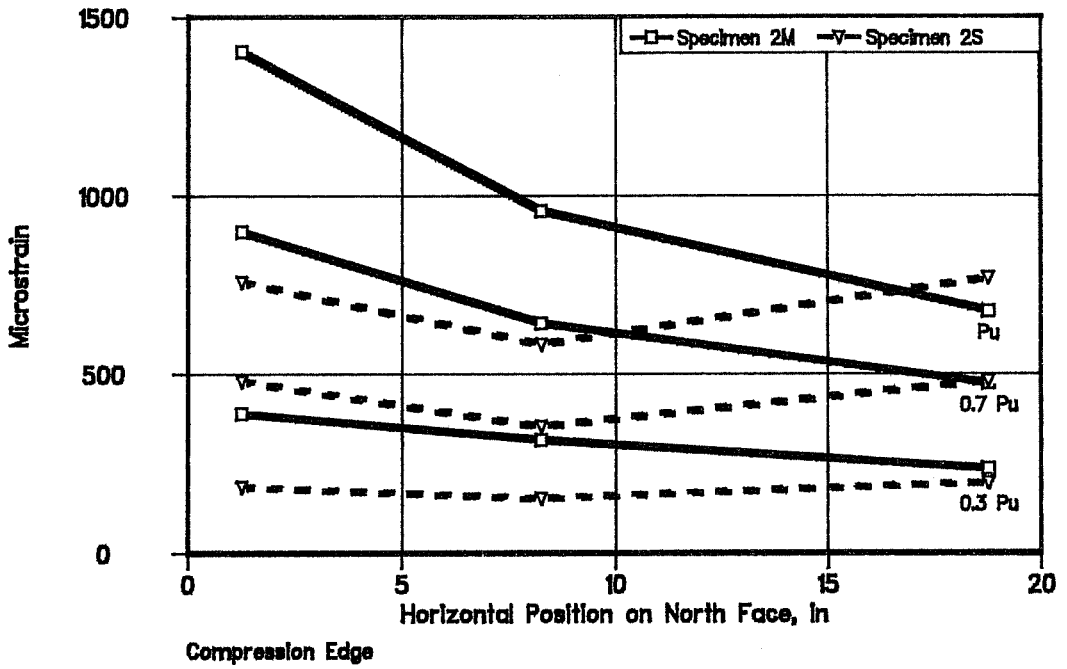

North Face Strains at Loads of 0.3 Pu, 0.7 Pu, and Pu
36" From Base

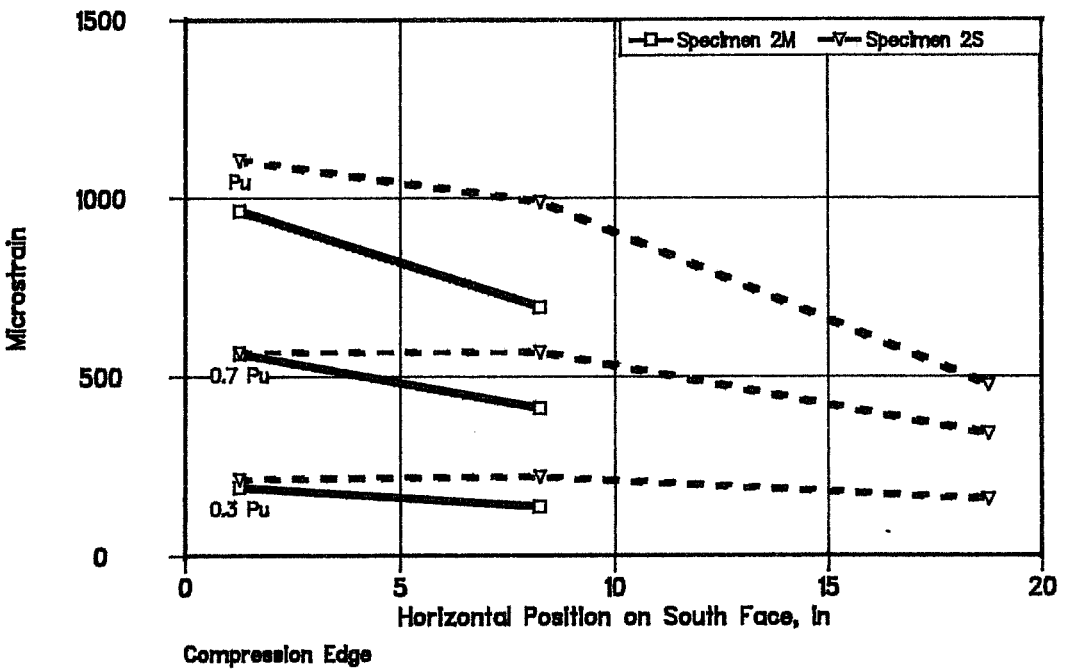

South Face Strains at Loads of 0.3 Pu, 0.7 Pu, and Pu
36" From Base

Figure 4.26 Specimens 2M and 2S Strain Gage Data

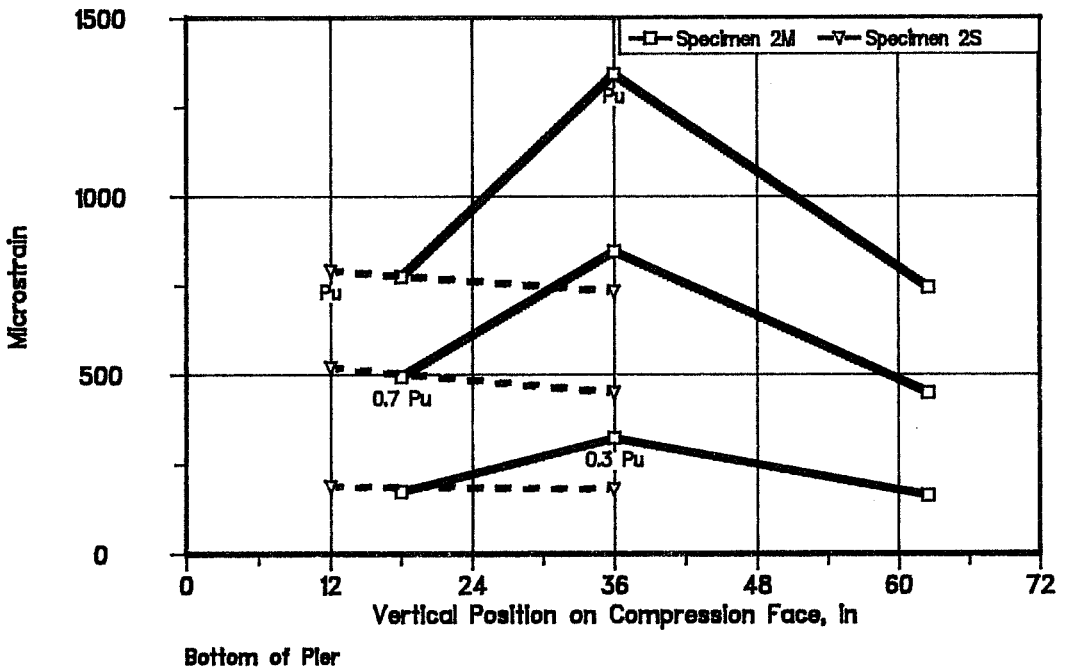

Compression Face Strains at Loads of 0.3 Pu, 0.7 Pu, and Pu
1.25" From South Face

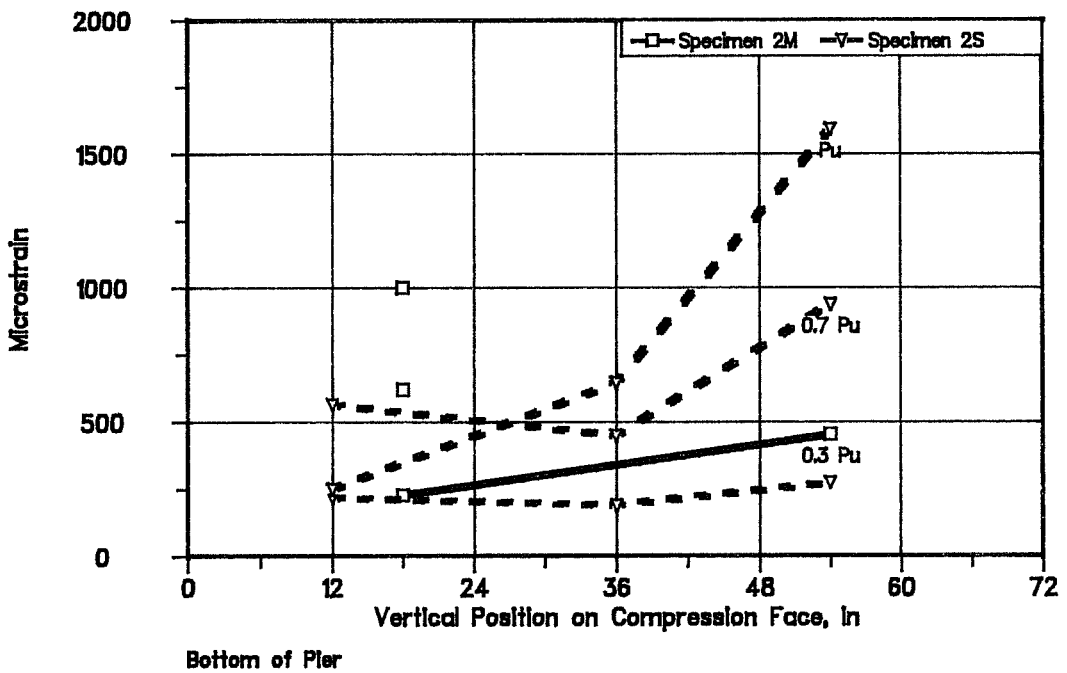

Compression Face Strains at Loads of 0.3 Pu, 0.7 Pu, and Pu
8.0" From South Face

Figure 4.27 Specimens 2M and 2S Strain Gage Data

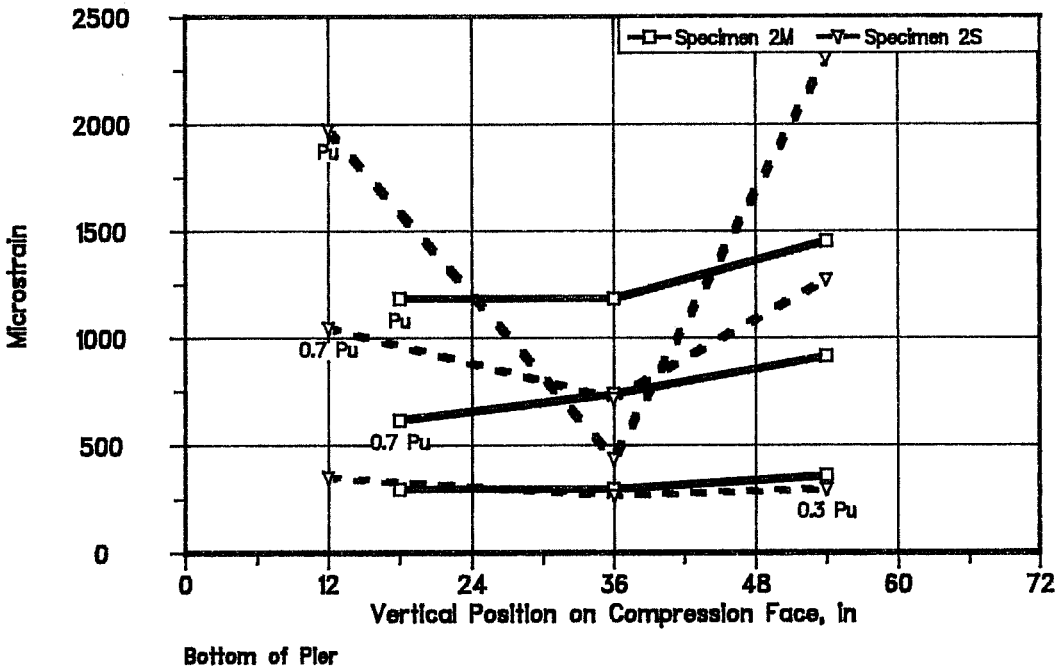

Compression Face Strains at Loads of 0.3 Pu, 0.7 Pu, and Pu
18.125" From South Face

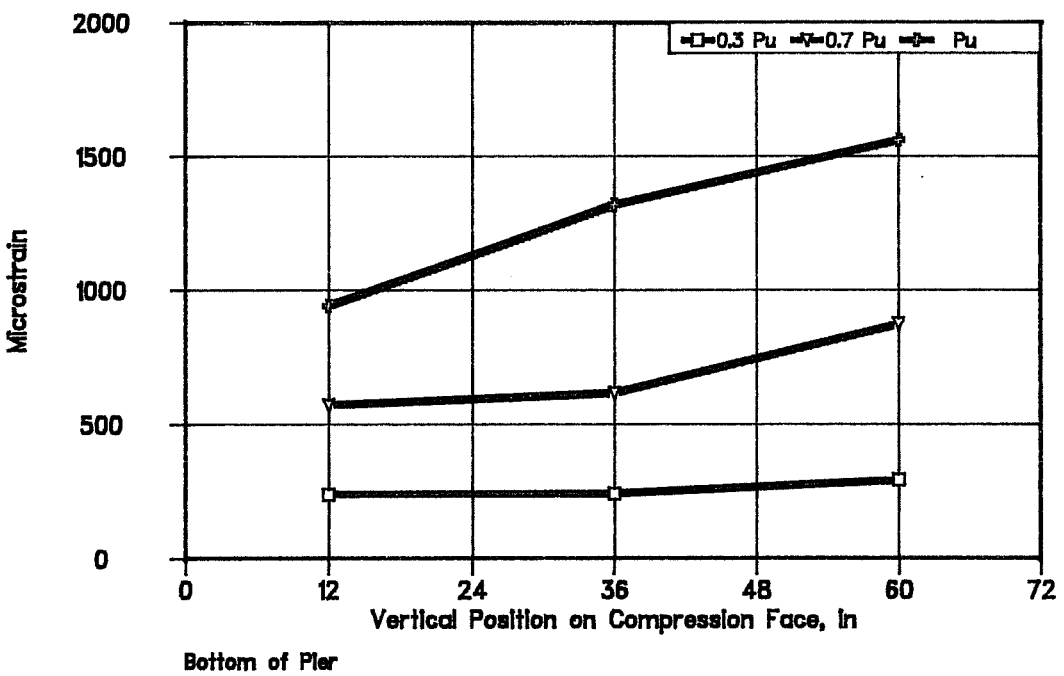

Specimen 2S Strains at Loads of 0.3 Pu, 0.7 Pu, and Pu
21.875" From South Face

Figure 4.28 Specimens 2M and 2S Strain Gage Data

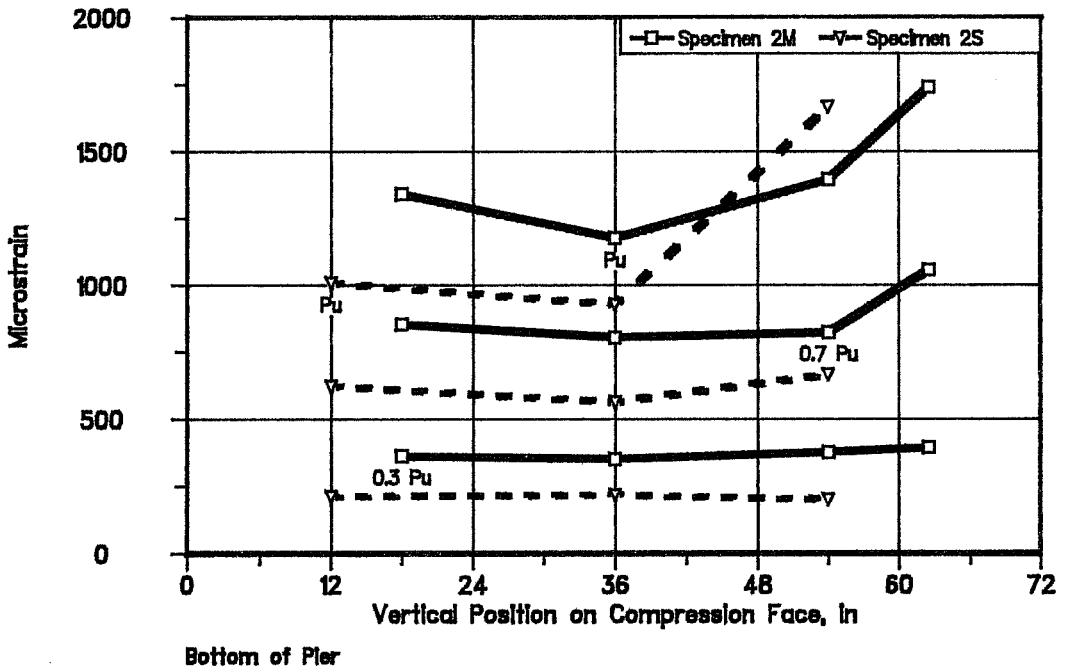

Compression Face Strains at Loads of 0.3 Pu, 0.7 Pu, and Pu
32" From South Face

Figure 4.29 Specimens 2M and 2S Strain Gage Data

No strain gage readings indicated that the bars had exceeded their yield strain (2590 microstrains).

4.3.2.3 Displacements

Three dimensional plots of the displacements measured by the potentiometers placed on the compression face of each specimen are shown in Figures 4.30 and 4.31. (Refer to Figure 3.10 for specific locations of the potentiometers.) All displacements were measured just prior to failure.

Several common observations can be made about the preceding figures:

1) The compression face of each specimen is bowing outward.

2) Deflections are smallest along the north and south edges.

3) The largest displacements occur in the bottom third of each specimen.

Several differences were also noted:

1) The smallest deflections of Specimen 2M are found in the center third of the pier.

2) The deflections of Specimen 2S are largest in the bottom segment of the pier and exhibit a downward slope toward the top segment.

3) The largest deflections of Specimen 2S are nearly twice those of Specimen 2M.

Because the failure region of Specimen 2M was located near an area of relatively large displacements, local instability may

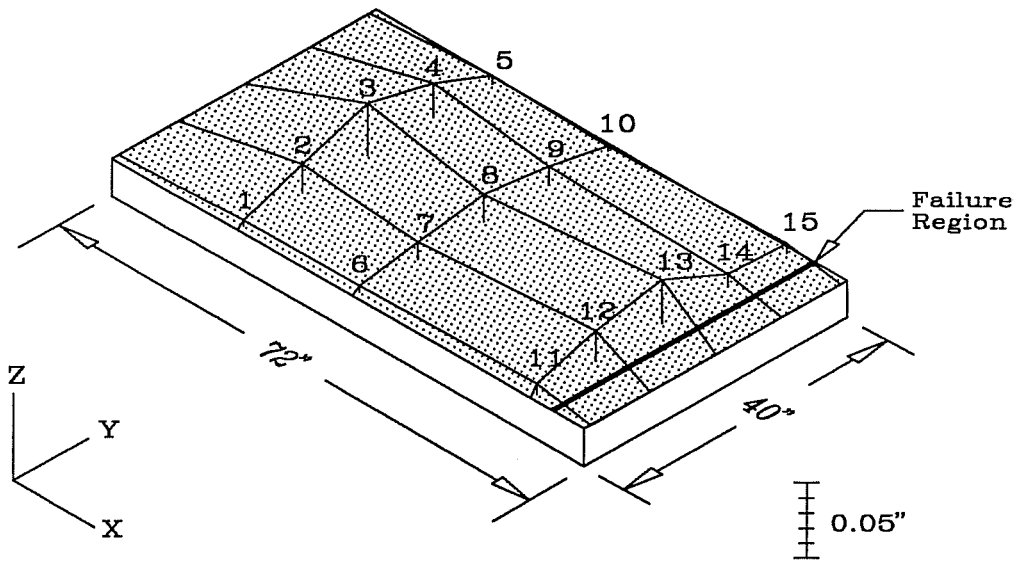

Compression Face Deflections Measured by Potentiometers Specimen 2M			
Potentiometer Number	Deflection (inches)	Potentiometer Number	Deflection (inches)
1	0.0037	9	0.0126
2	0.0188	10	0.0032
3	0.0340	11	0.0070
4	0.0230	12	0.0201
5	0.0057	13	0.0299
6	0.0044	14	0.0085
7	0.0113	15	0.0067
8	0.0187		

Figure 4.30 Specimen 2M Compression Face Profile at Failure Load

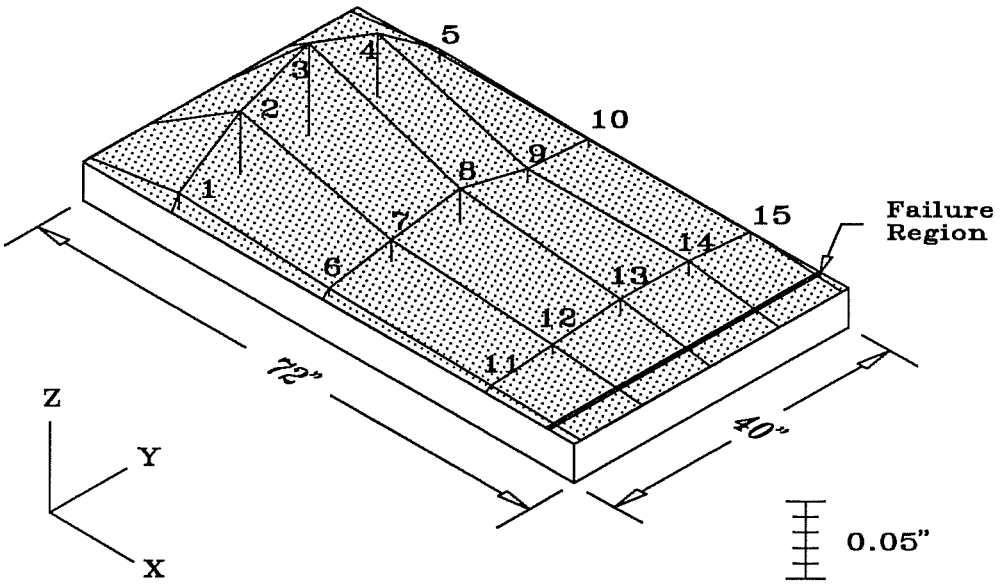

Compression Face Deflections Measured by Potentiometers Specimen 2S			
Potentiometer Number	Deflection (inches)	Potentiometer Number	Deflection (inches)
1	0.0102	9	0.0085
2	0.0402	10	0.0054
3	0.0589	11	0.0022
4	0.0406	12	0.0058
5	0.0079	13	0.0098
6	0.0048	14	0.0091
7	0.0131	15	0.0053
8	0.0208		

Figure 4.31 Specimen 2S Compression Face Profile at Failure Load

have contributed to the failure of the pier. On the other hand, the failure region of Specimen 2S seems to be located in an area with little displacement. Thus, from this figure, it seems that local instability did not influence the failure of Specimen 2S.

From the moment-curvature relationship shown in Figure 4.32, the specimens exhibit almost identical curvatures for similar values of moment. However, it should be noted that Specimen 2M has a substantially greater range of curvatures.

As with Specimen 1S, the load head rotations shown in Figure 4.32 indicate that the flanges of the load head are shortening less than the center of the specimen. However, for Specimen 2M, the skip shown near a moment of 1000 kip-inches and the shortening shown in Figure 4.33 indicate that the entire specimen shifted at a load of about 400 kips. This shift can be attributed to some slight lateral movement of the moving bulkhead in the 1200 kip testing machine. Also, as shown in Figure 4.33, Specimen 2S is axially stiffer than Specimen 2M.

No significant centerline deformations of the short sides were measured on either specimen.

4.4 Specimens 3M, 3S, and 3PM

4.4.1 General Observations

The companion specimens in this series have the highest wall slenderness ratios, X_u/t_f, of the three series compared.

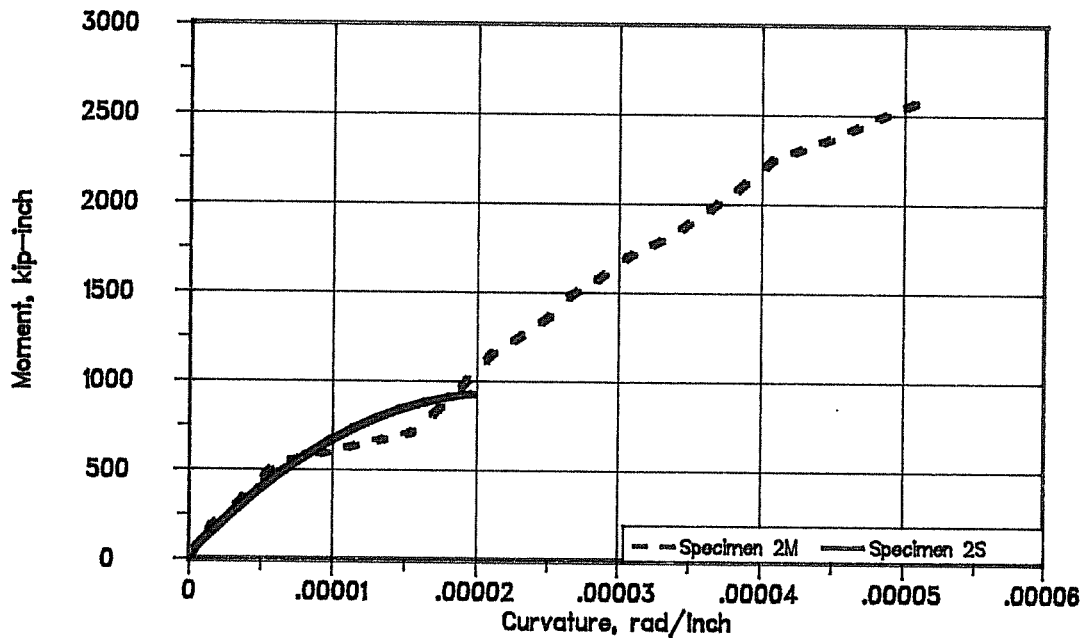

Moment-Curvature Relationship

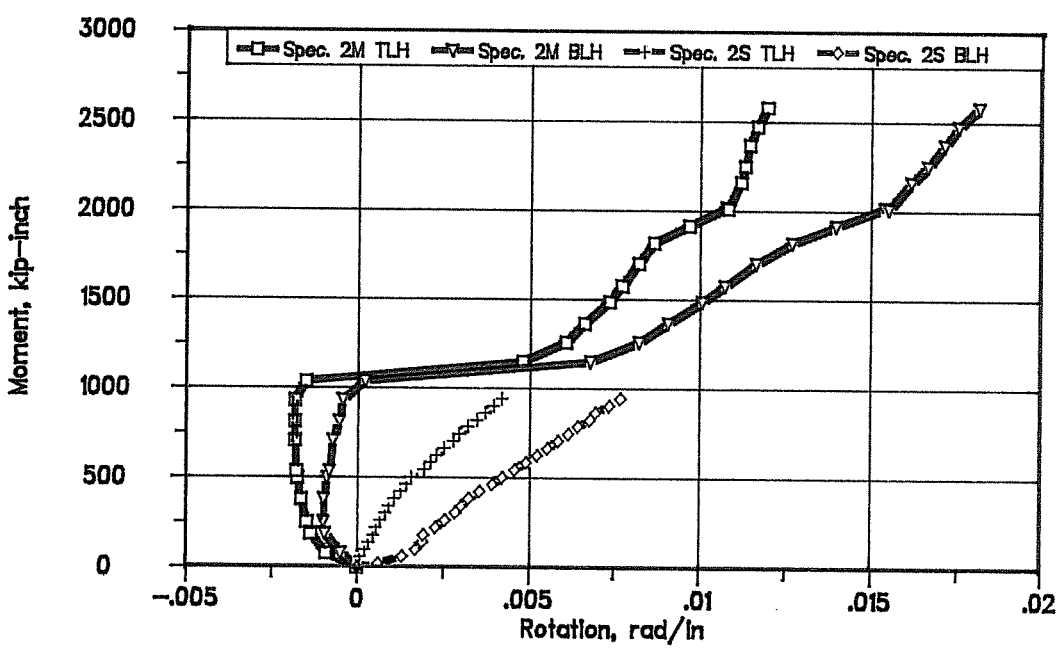

Load Head Rotations

Figure 4.32 Specimens 2M and 2S Moment-Rotation Relationships

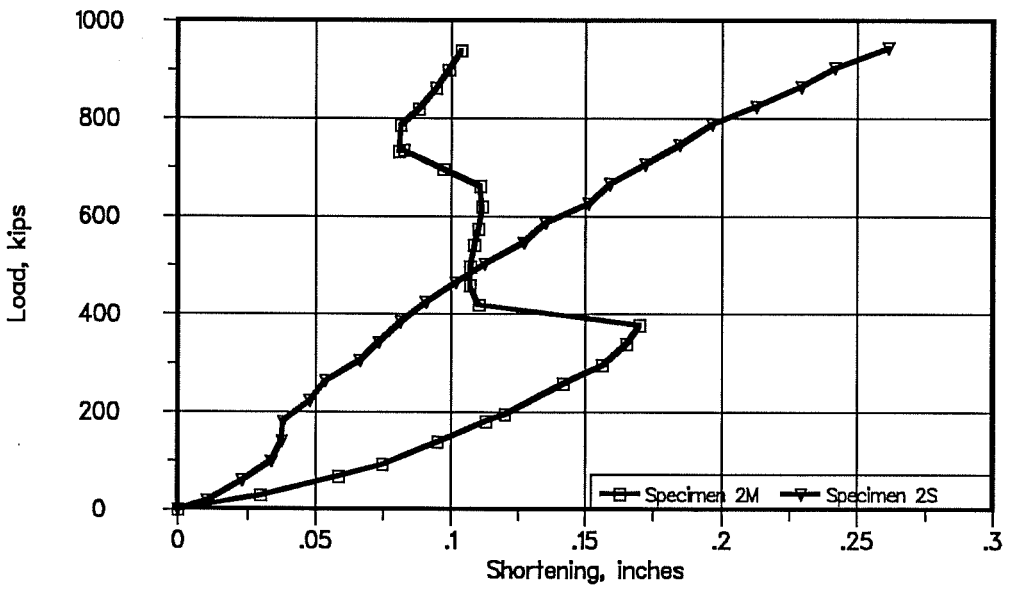

Figure 4.33 Specimens 2M and 2S Total Shortening

Specimen 3M has a wall slenderness ratio of 24.7, the highest of the seven specimens presented. The addition of the corner bevels to include the post-tensioning tendons reduced the wall slenderness ratio, X_u/t_f, from 24.7 to 22.3 for Specimens 3S and 3PM. Each specimen has a wall thickness of 1.5 inches. Mild reinforcement ratios and placement are identical. The only differences between these three specimens is in their construction method and the absence or presence of post-tensioning. Specimen 3M was monolithically constructed and was not post-tensioned. Specimen 3S was segmentally constructed and

post-tensioned. Specimen 3PM was monolithically constructed and post-tensioned.

The cylinder strengths of the concrete near the failure region of each specimen are listed below.

Specimen 3M	6311 psi
Specimen 3S	6916 psi
Specimen 3PM	6463 psi

4.4.1.1 Specimen 3M (Monolithic with end eccentricity of 1.0 inch and X_u/t_f of 24.7)

Failure occurred in a region approximately 68 inches from the bottom of the specimen at a load of 904 kips. The failure was not as explosive as that in other specimens. Since no deflection of the critical section was observed prior to failure, the failure moment was 904 kip-inches. The cylinder strength of concrete in the top section was 6311 psi, the lowest of the three sections.

The first cracks were observed in the load heads on the "tension" side of the specimen at a load of 300 kips. At a load of 502 kips, cracks were observed on the lower third of both compression and "tension" faces.

The last cracks before failure were marked at a load of 824 kips. The crack pattern before failure is shown by the solid lines in Figure 4.34. At this stage, there was substantial cracking in the lower third of the "tension" face. Though a few more cracks were found on the compression face, the

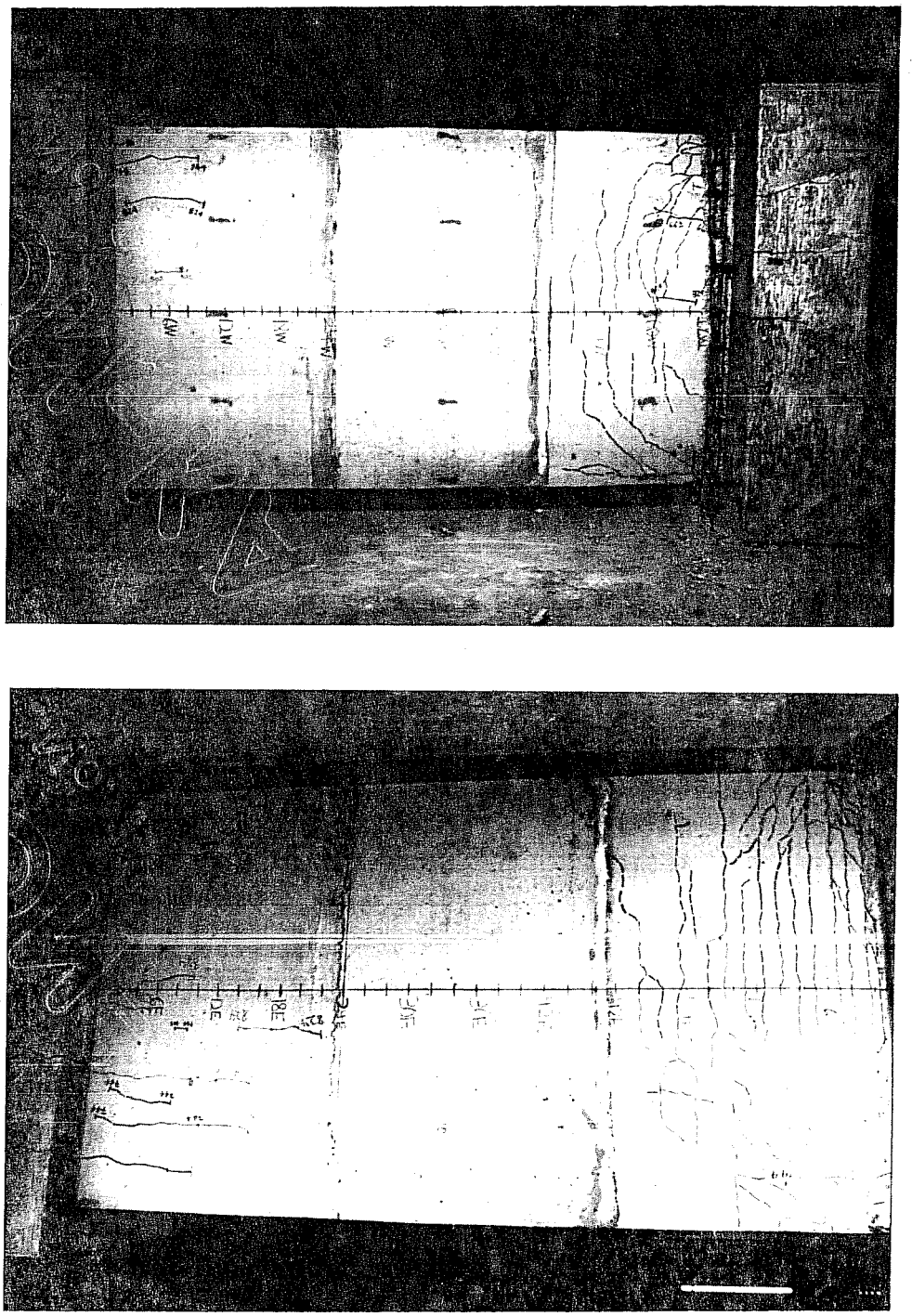

Figure 4.34 Specimen 3M Cracks Marked before (solid lines) and after Failure (compression face on top)

cracking was not nearly as extensive as that found on the "tension" face. Peculiarly, no cracks were found in the middle third of the specimen. All of the cracks observed prior to failure ran along the length of the specimen and were located in the upper and lower thirds of the pier.

Cracks observed after failure were marked with a dashed line and several observations were made:

1) Numerous cracks appeared on both the compression and "tension" faces at failure (Fig. 4.35). Most cracks appeared in the top third of the specimen, but one was found in the middle third. The compression face cracks seemed to begin in the failure region, extend longitudinally for about 3 inches, and then go parallel with the failure region.

This was the only specimen in which transverse cracks appeared on the compression face at failure. This may be the result of local instability which caused the compression flange to buckle outward and simultaneously fail.

2) The "tension" face appeared to have failed in bending after the compression face failure. Instead of one clearly defined failure crack, there were numerous similar looking cracks running along the entire width of the face about 1 inch apart (Fig. 4.35). Also, extensive diagonal cracking was found near the intersection of both side faces.

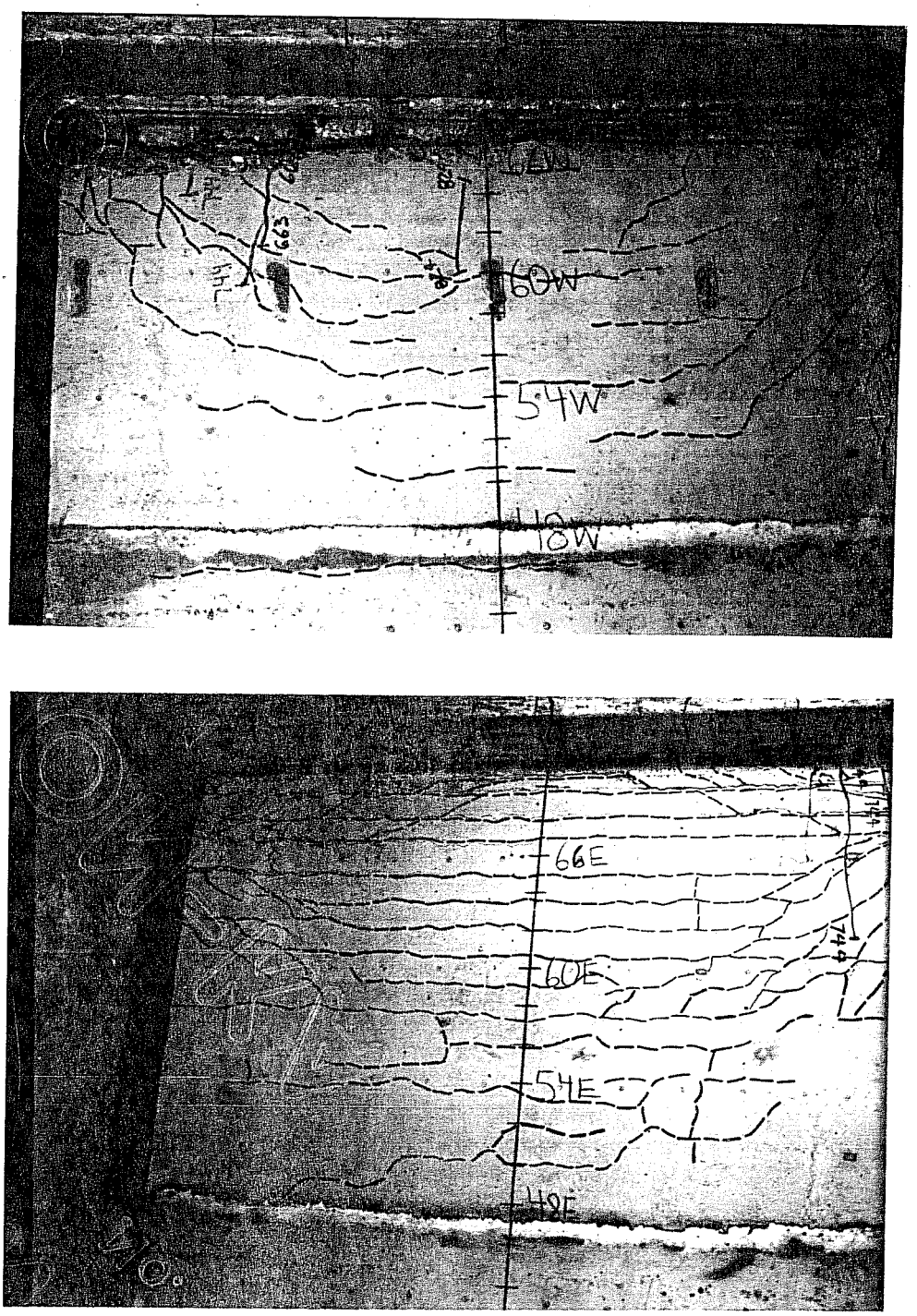

Figure 4.35 Specimen 3M Cracks Marked after Failure (compression face on top)

3) The concrete was fractured so that the inside of the specimen could be seen from all faces except the "tension" face. All of the mild longitudinal steel seemed to have buckled over one lateral tie spacing (Fig. 4.36).

4.4.1.2 Specimen 3S (Segmental with end eccentricity of 1.0 inch and X_u/t_f of 22.3)

Failure occurred in a region approximately 6 inches from the bottom of the specimen at a load of 999 kips. The failure was very explosive. A deflection of 0.5 millimeters was observed in the critical region prior to failure. Therefore, due to the 1.02 inch eccentricity at failure, the failure moment was 1019 kip-inches. The cylinder strength of concrete in the bottom segment was 6916 psi, similar to that of the other segments.

Cracks were first observed at a load of 302 kips in the load heads on the "tension" side of the specimen. The first cracks were found in the bottom segment of the "tension" face at a load of 423 kips. No cracks were observed on the compression face until a load of 744 kips was reached. The last cracks on the specimen were marked at a load of 820 kips. As shown by the solid lines in Figures 4.37 and 4.38, all of the cracks that formed before failure of the specimen were longitudinal.

After marking the cracks which appeared after failure with a dashed line, several observations were made:

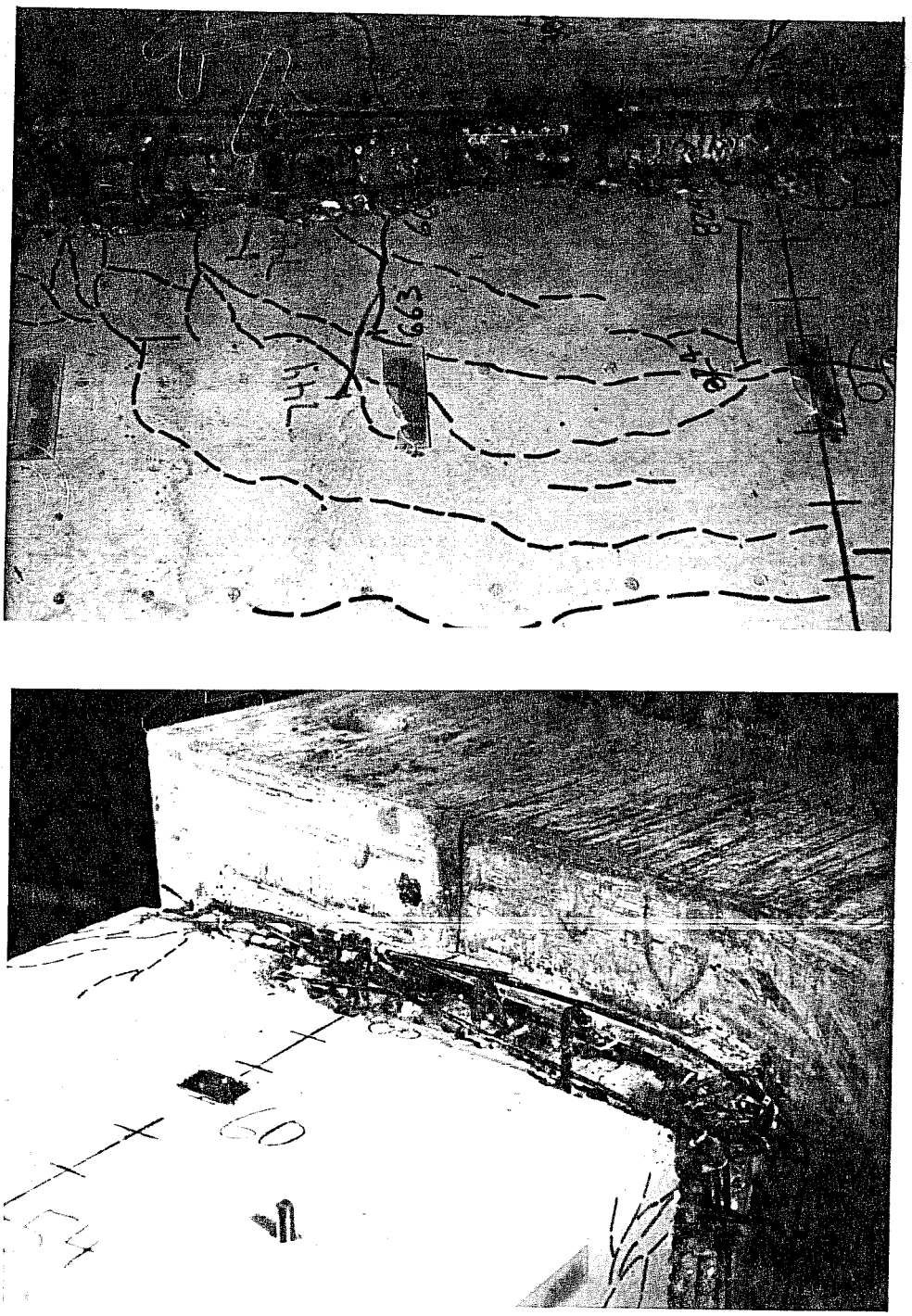

Figure 4.36 Specimen 3M Compression Failure Region

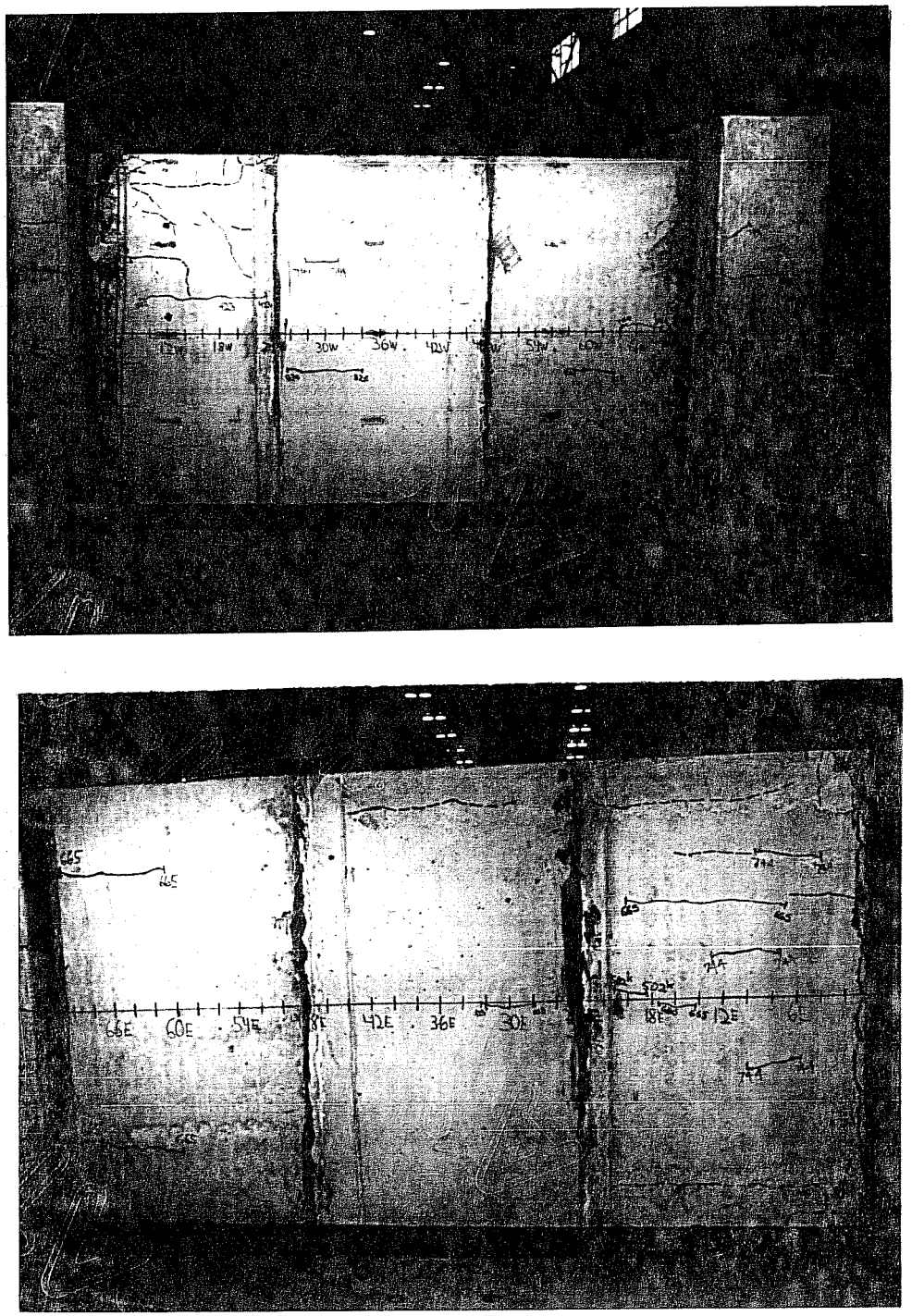

Figure 4.37 Specimen 3S Cracks Marked before and after Failure (compression face on top)

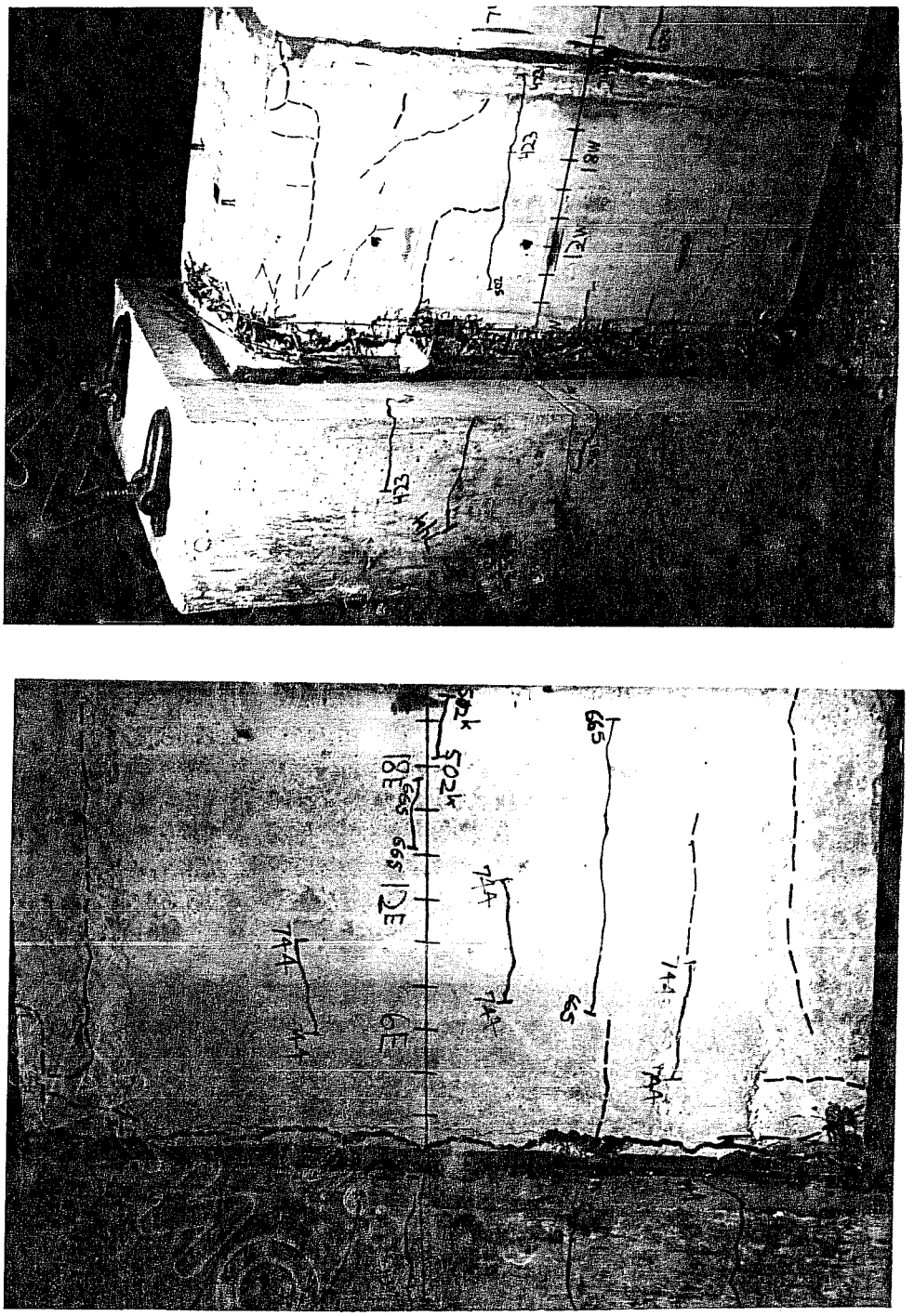

Figure 4.38 Specimen 3S Failure Regions
(compression face on top)

1) On the compression face, there were several longitudinal cracks extending from the fracture zone which were 8 to 10 inches in length (Fig. 4.38). After traveling about 10 inches, these cracks began to veer diagonally for short lengths. The diagonal cracks formed a failure zone at the intersection of the compression face and the south face extending from 12 to 18 inches above the pier base.

2) The "tension" face fracture is evidenced by the single 1/4 inch wide crack shown in Figure 4.38. The crack appears to run along the ends of the longitudinal bars at the bottom of the reinforcing cage. In addition, other hairline cracks were observed on the "tension" face. One crack which ran most of the length of the bottom and middle segments was located about 4 inches from the intersection with the south face (Fig. 4.37). Extensive diagonal cracking was found at the intersection of the "tension" face and the short sides of the pier. Figure 4.39 shows a close-up of the failure region.

3) After opening a hole to see inside of the specimen, both post-tensioning tendons on the compression side of the specimen were found to have fractured near the failure region. However, the ducts appeared to be well grouted and the corner ties which confined the tendons were still in place.

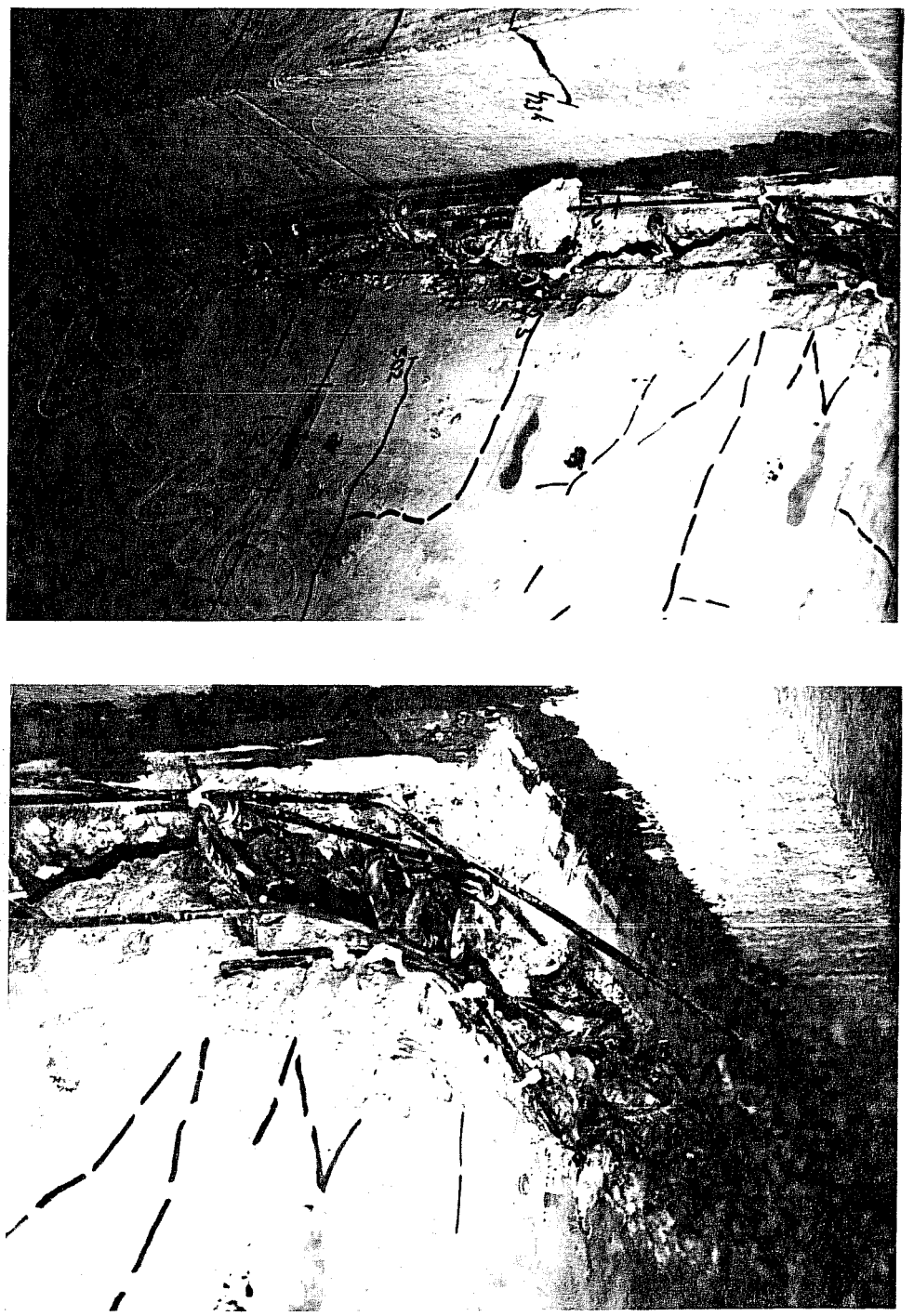

Figure 4.39 Specimen 3S Compression Failure Region Close-Ups

4) All of the longitudinal steel buckled within one lateral reinforcement spacing and all of the lateral reinforcement seemed to be in place.

4.4.1.3 Specimen 3PM (Post-Tensioned Monolithic with end eccentricity of 1.0 inch and X_u/t_f of 22.3)

Failure of this specimen occurred at a load of 961 kips. The failure was very explosive. Failure occurred in a region extending from approximately 64 inches above the bottom load head to the top of the pier section (Fig. 4.40). A deflection of 0.5 millimeters was observed in the critical region prior to failure. Therefore, with a total eccentricity of 1.02 inches, the failure moment was 980 kip-inches. From Chapter 2, the cylinder strength of the concrete in the top lift was 6463 psi, similar to that found in the other two lifts.

The first cracks appeared in the load heads on the "tension" side of the specimen at a load of 346 kips. Cracks were first observed in the bottom section on the compression and "tension" faces at a load of 505 kips.

The last cracks before failure of the specimen were marked with a solid line at a load of 785 kips (Fig. 4.41). At this stage, there was a considerable number of cracks which ran along the length of the "tension" face. On the compression face, there were only a few additional cracks found. Each of the cracks were fairly short and were located near the centerline of

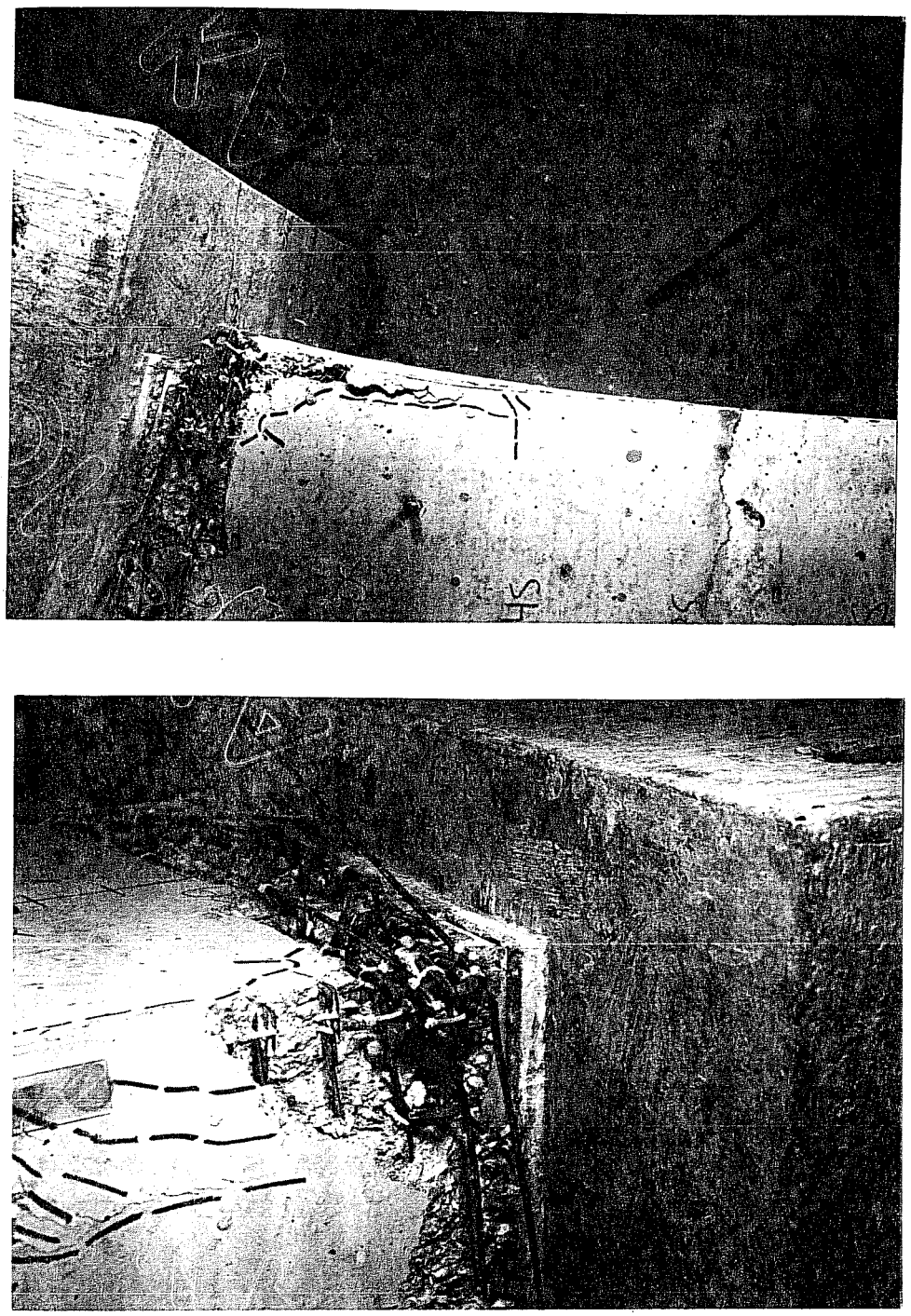

Figure 4.40 Specimen 3PM Failure Region on Compression and South Faces (compression face on top)

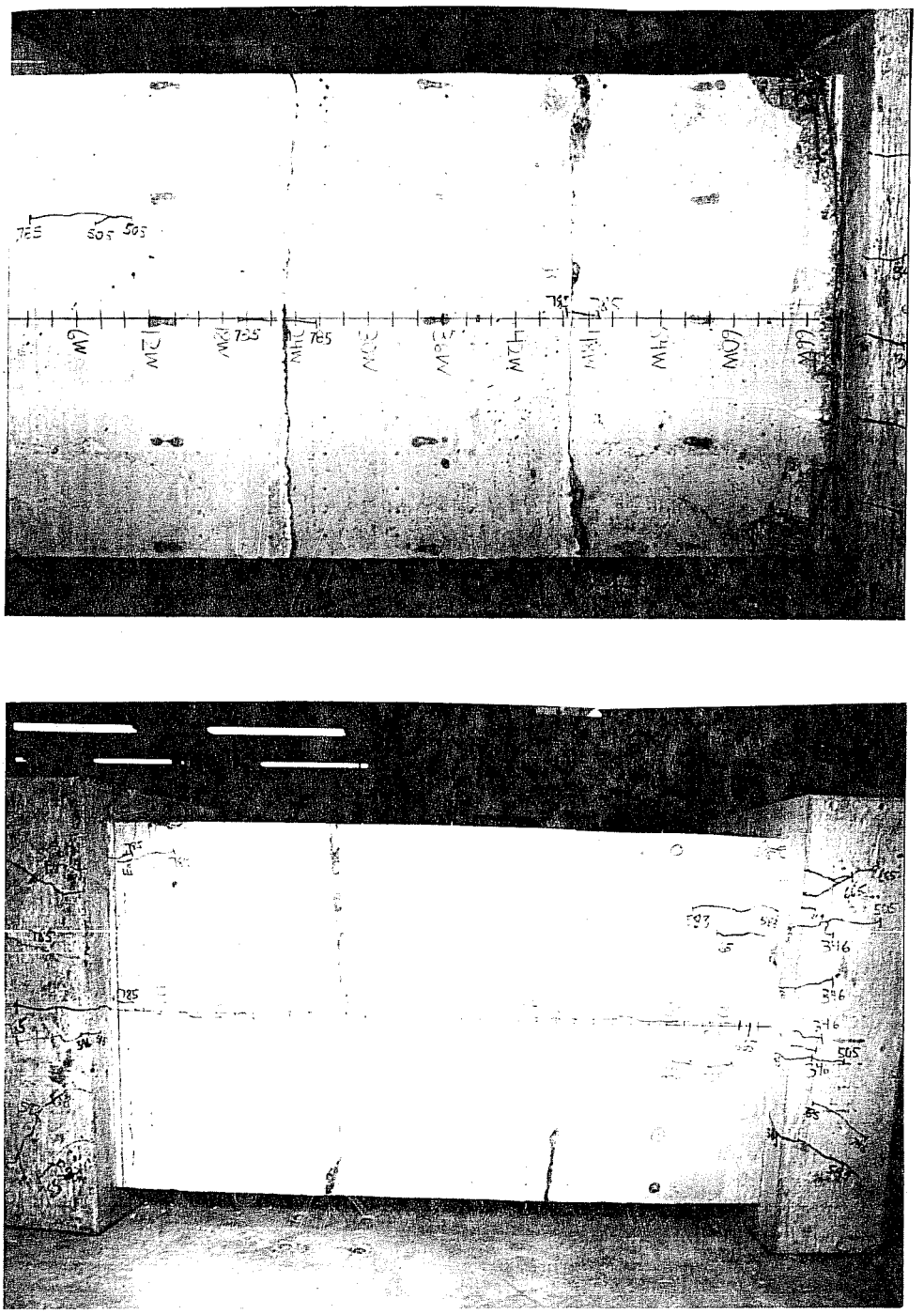

Figure 4.41 Specimen 3PM Cracks Marked before Failure (compression face on top)

the face. Extensive cracking was found in the load heads on both sides of the specimen. All of the cracks found on the pier ran along the length of the specimen.

After marking all failure cracks with a dashed line (Fig. 4.42), several observations were noted:

1) On the compression face, both layers of longitudinal steel buckled outward, outside the original plane of the wall (Fig. 4.40). In addition, it appeared that the entire width of the compression face was displaced outside of its original plane (about 1.5 in.) in a region stretching from 54 to 68 inches above the base (see Fig. 4.40). However, all of the lateral hoop reinforcement and crossties seemed to remain in place.

2) On the "tension" face there was no well-defined failure region, only a series of closely spaced (same as transverse reinforcement spacing) cracks which extended the width of the face (Fig. 4.42). These cracks were located over the upper 18 inches of the pier, though the widest (1/8 in.) were found near the top load head. Diagonal cracks which ran at almost 45 degree angles were found near the intersections of the "tension" face with the north and south sides (Fig. 4.42). These cracks were 8 to 10 inches in length.

3) The failure extended completely through the north and south faces with a pulverized failure region (Fig. 4.40).

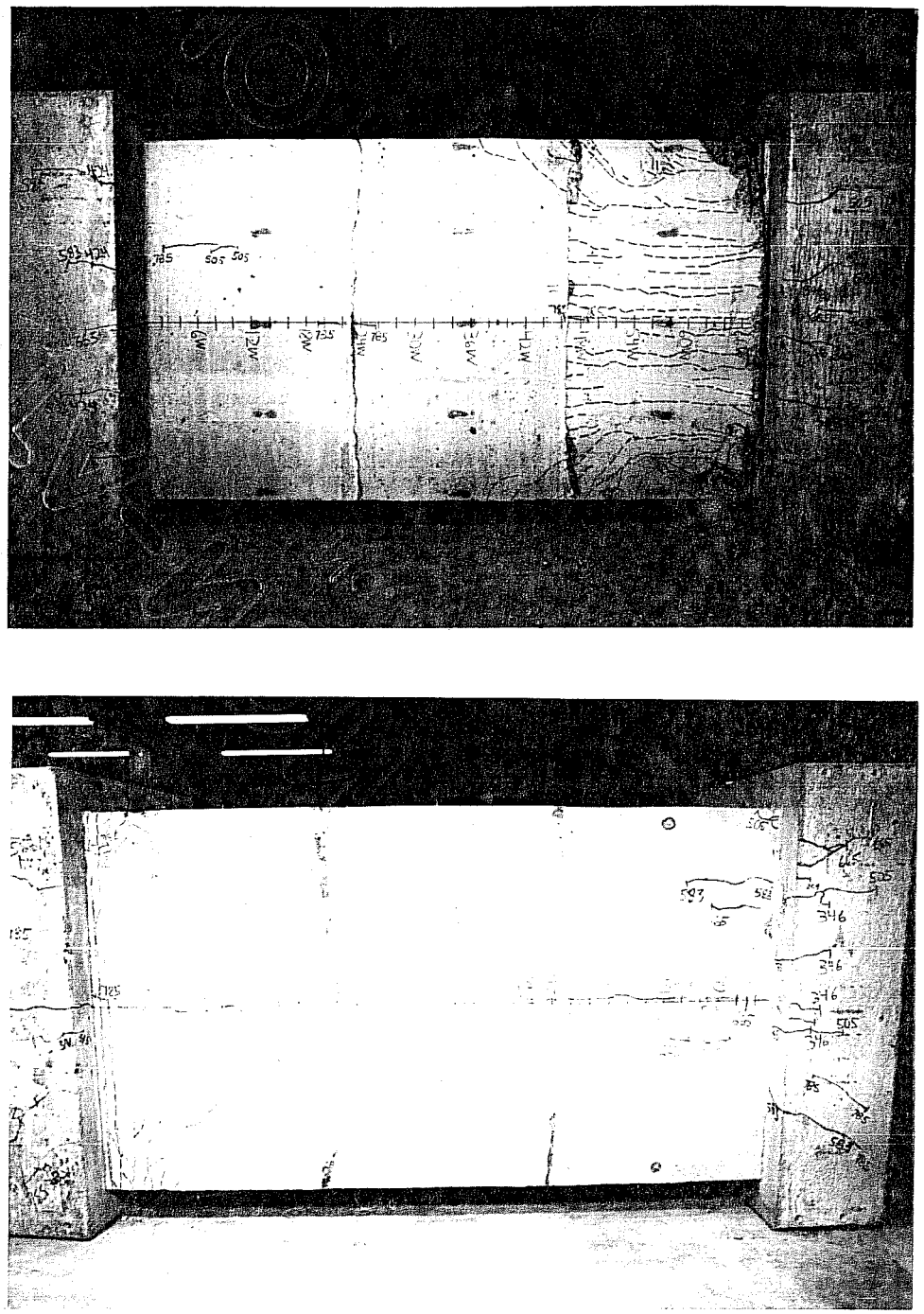

Figure 4.42 Specimen 3PM Cracks Marked after Failure (compression face on top)

Unlike Specimens 1S and 2S, the post-tensioning tendons did not get pushed out from the specimen due to shortening of the compression face. However, the tendons on the compression face buckled in the vicinity of the failure region.

4.4.2 Comparison of Piers With 1.5 inch Wall Thickness

4.4.2.1 General Observations

Several similarities about the behavior of the three specimens were observed:

1) There was only a slight amount of cracking in each specimen evident before failure.

2) First cracking occurred in either the upper or lower third of each specimen.

3) First cracking occurred at similar load levels for Specimens 3M and 3PM.

4) The "tension" face failure region and after failure cracks were almost identical for Specimens 3M and 3PM. The crack patterns indicated flexural failure of the "tension" face.

5) Diagonal cracks were located near the intersection of the "tension" face and side faces for all three specimens.

6) The post-tensioned tendons remained anchored in the ducts for Specimens 3S and 3PM.

Differences in the behavior of the specimens were also noted:

1) No cracks were observed in the middle section of Specimen 3M either before or after failure.

2) First cracking in the segmental specimen occurred at a lower load level than that of the monolithic specimens.

3) The crack pattern on the "tension" face of the segmental specimen did not exhibit evidence of a flexural failure.

4) There was very little cracking observed in Specimen 3S after failure. Also, none of the cracks seemed to propagate between the segments of Specimen 3S.

5) The failure region of Specimen 3PM was much different from that of any other specimen. The entire width of the compression face was displaced from its original plane.

6) The post-tensioned tendons on the compression side of Specimen 3S fractured at failure.

4.4.2.2 Strains

In order to better understand how the strain was distributed across the wall thickness of the compression face, Specimen 3PM was instrumented with a row of gages placed on the inner layer of longitudinal bars. The comparison of strains in the inner and outer layer of longitudinal bars is shown in Figure 4.43. As shown in the figure, the strains in the inner layer of bars are greater than those in the outer layer. However, in light of the outward bowing of the compression face

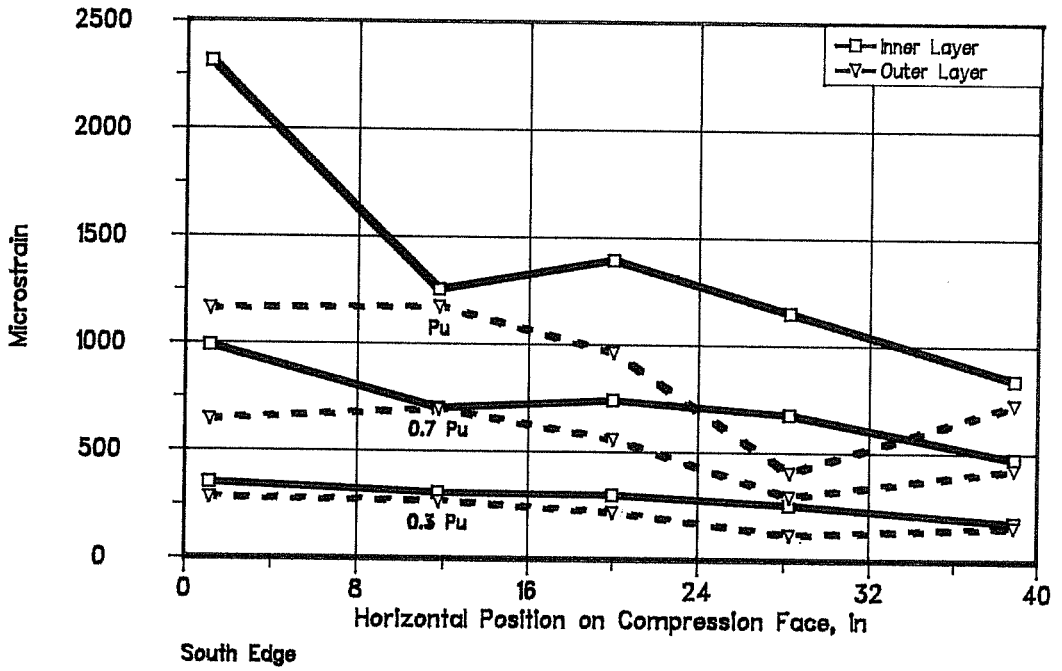

Strains on Inner and Outer Layers of Longitudinal Bars 36" From Base

Figure 4.43 Specimen 3PM Compression Face Strains

as illustrated by the compression face profiles to be presented later, this behavior was expected.

Figures 4.44 through 4.54 illustrate the comparison of strain gage data.

From the compression face strains across the width of the specimen shown in Figures 4.44 through 4.46, it appears that for all but the top segment, the strains in the monolithic specimen are higher than those found in the segmental specimen. This could be due to the fact that the longitudinal steel in the segmental specimen already has some initial strain due to the post-tensioning force, though only a few hundred microstrains. Except for the wide discrepancy shown in Figure 4.45 between the gages located 28.25 inches from the south edge, the strains in the segmental and post-tensioned monolithic specimens appear to be fairly similar. The discrepancy between the two gages seems to follow from Figures 4.44 and 4.46 which also indicate a smaller strain at that location.

Strains across the "tension" face of each specimen are shown in Figure 4.47. It is interesting to note that the strains in all three specimens are very similar for loads of $0.3P_u$ and $0.7P_u$. However, near ultimate, the segmental specimen has strains approximately 25 percent lower than those of either of the monolithic specimens.

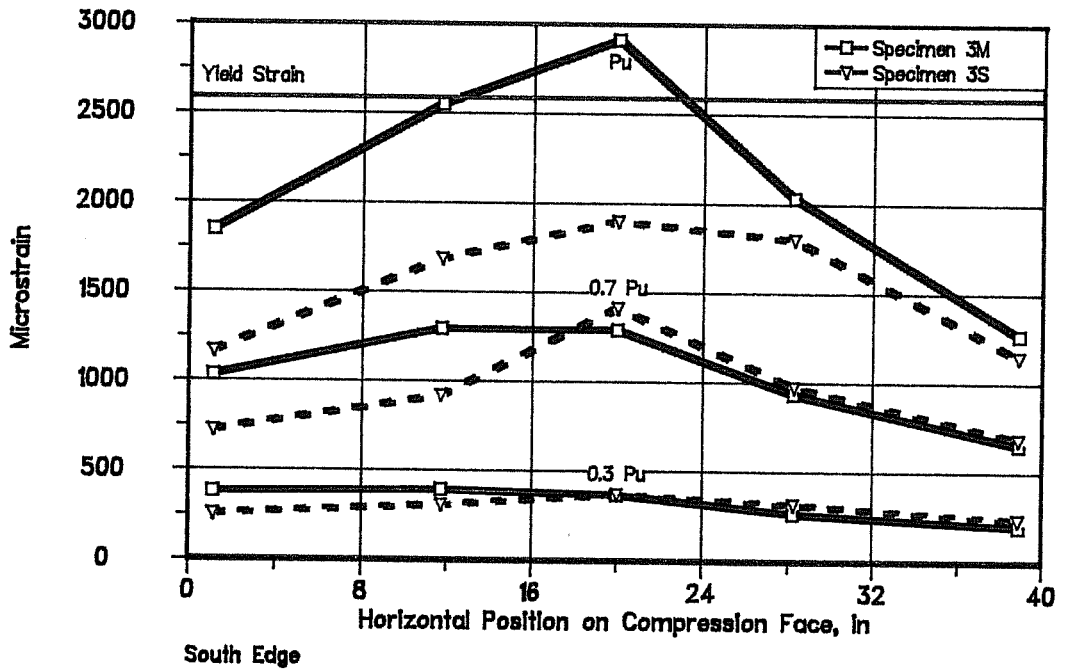

Compression Face Strains at Loads of 0.3 Pu, 0.7 Pu, and Pu
12" From Base

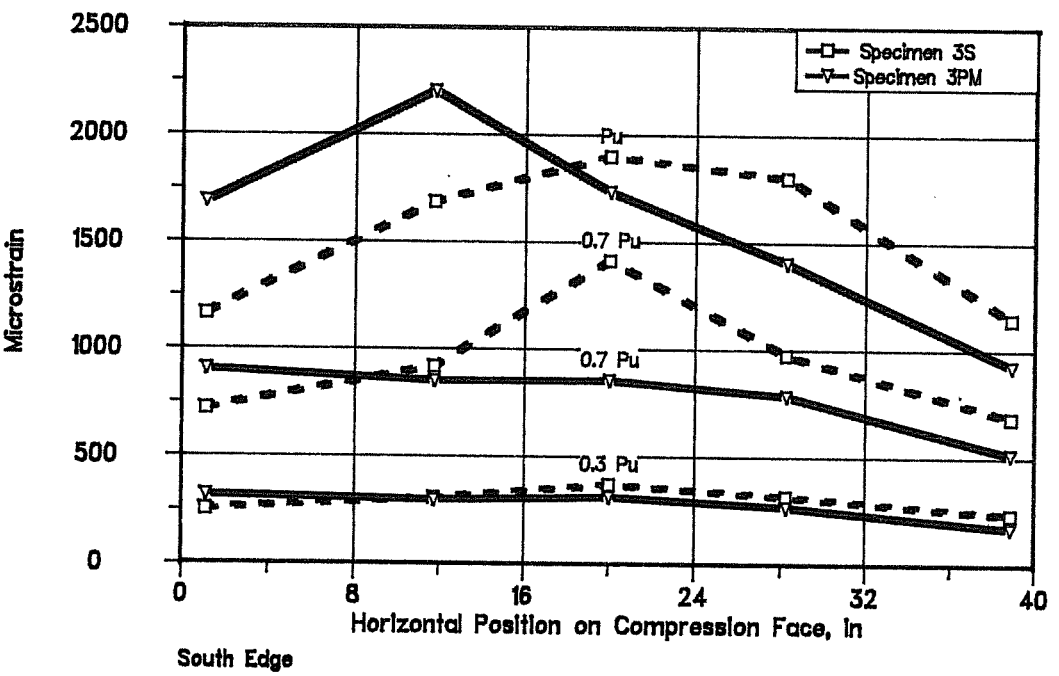

Compression Face Strains at Loads of 0.3 Pu, 0.7 Pu, and Pu
12" From Base

Figure 4.44 Specimens 3M, 3S, and 3PM Strain Gage Data

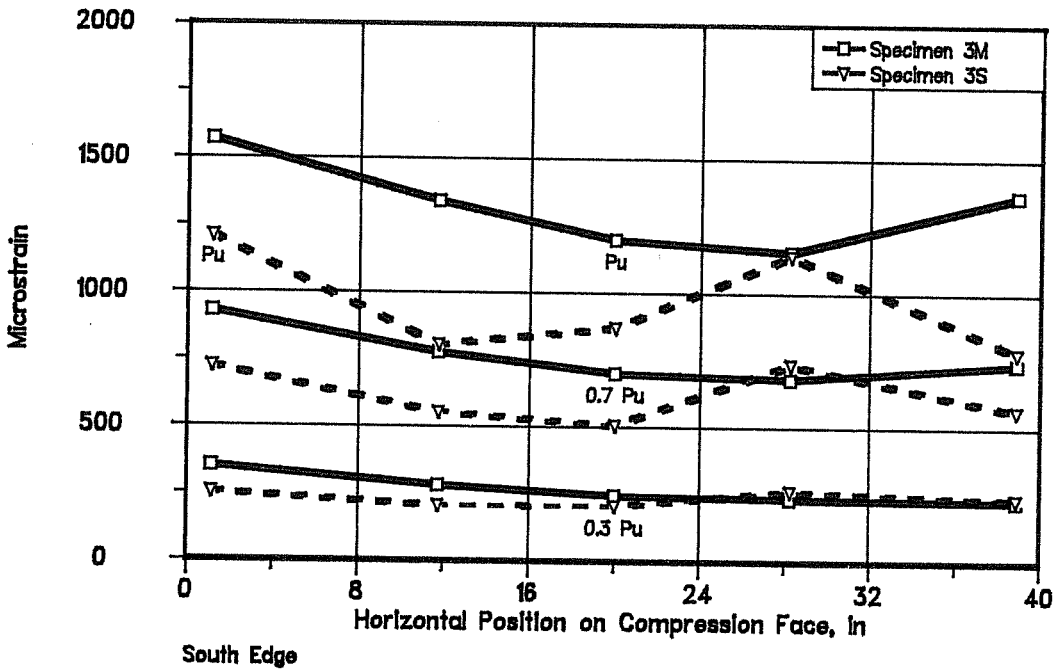

Compression Face Strains at Loads of 0.3 Pu, 0.7 Pu, and Pu
36" From Base

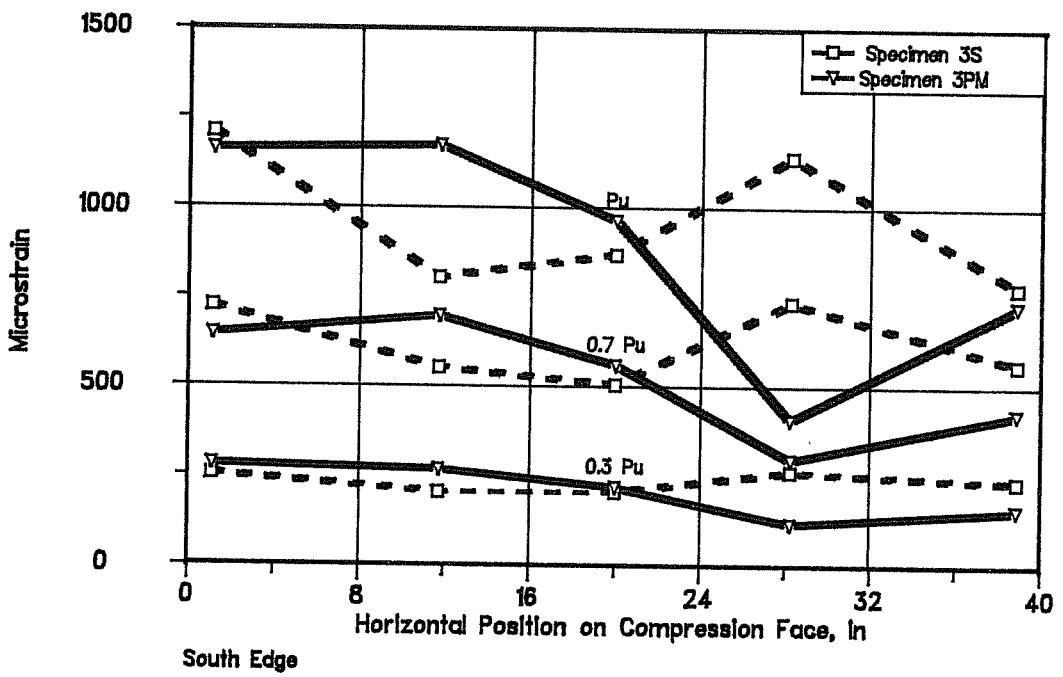

Compression Face Strains at Loads of 0.3 Pu, 0.7 Pu, and Pu
36" From Base

Figure 4.45 Specimens 3M, 3S, and 3PM Strain Gage Data

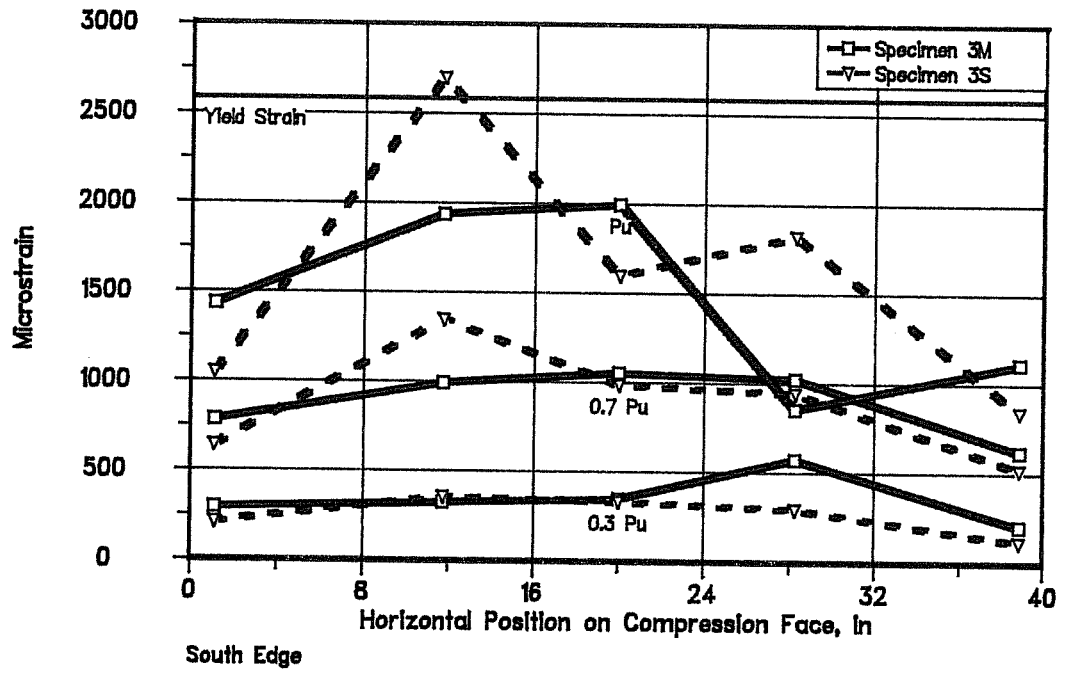

Compression Face Strains at Loads of 0.3 Pu, 0.7 Pu, and Pu
60" From Base

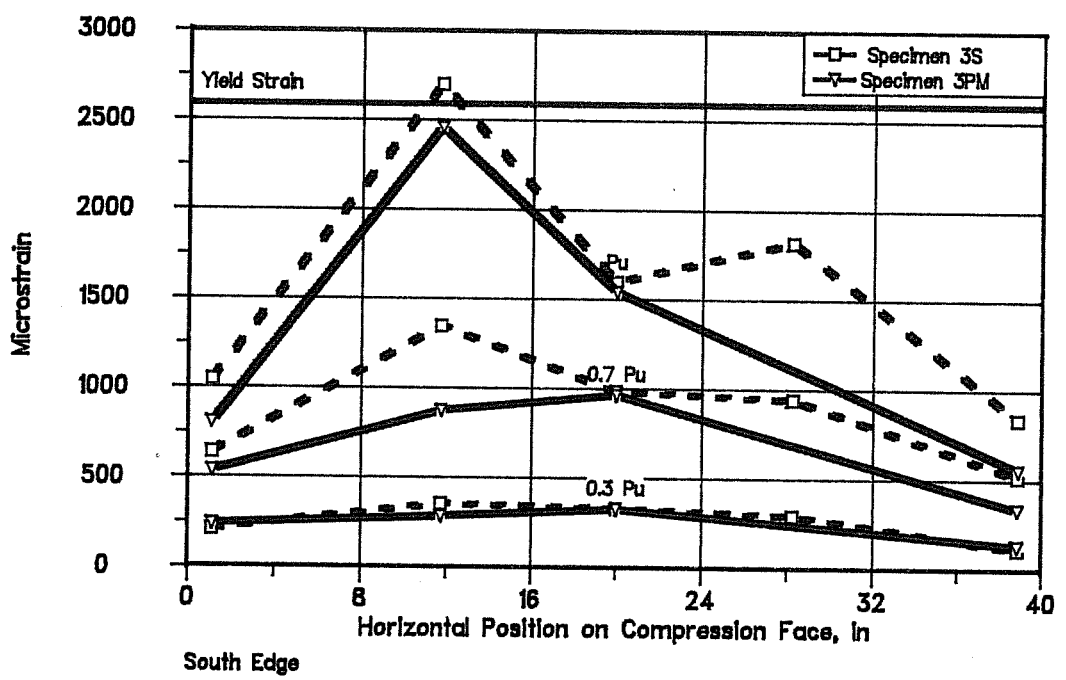

Compression Face Strains at Loads of 0.3 Pu, 0.7 Pu, and Pu
60" From Base

Figure 4.46 Specimens 3M, 3S, and 3PM Strain Gage Data

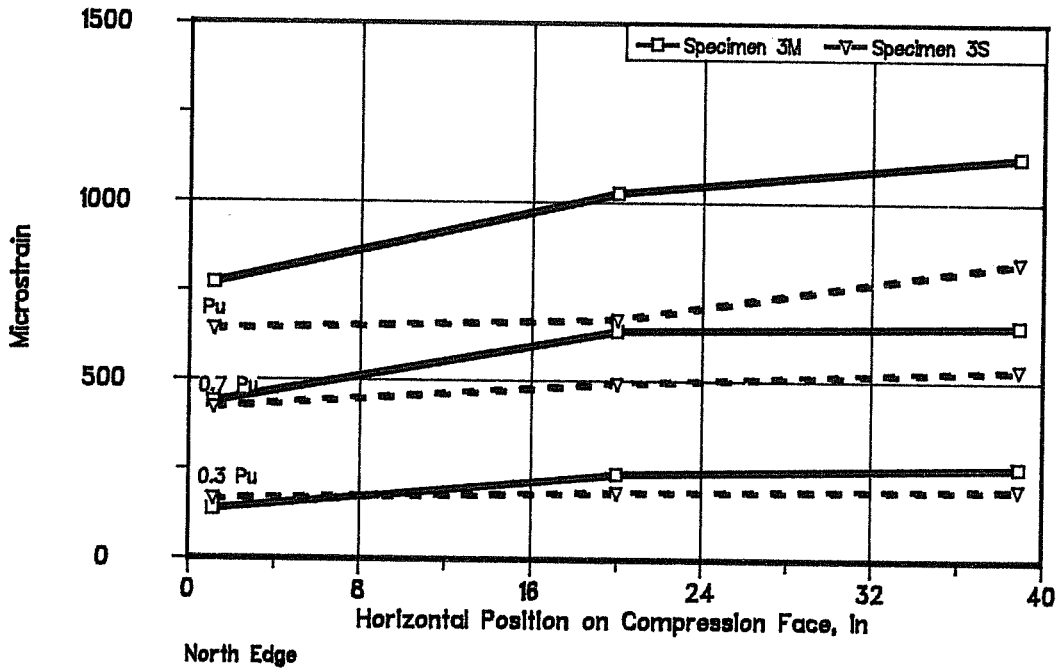

Tension Face Strains at Loads of 0.3 Pu, 0.7 Pu, and Pu
36" From Base

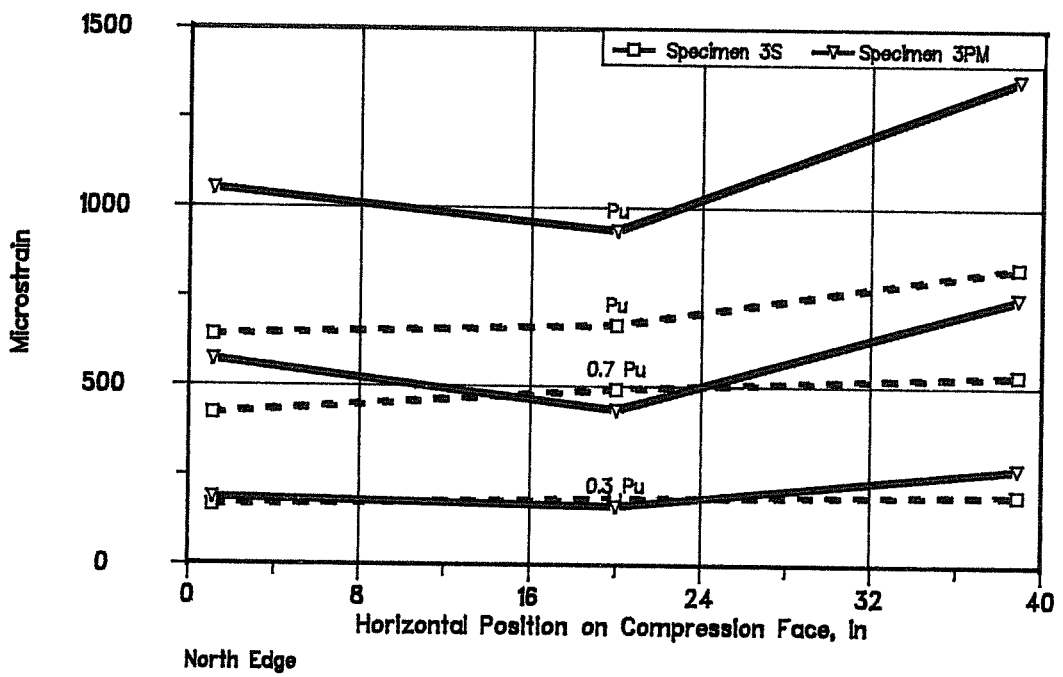

Tension Face Strains at Loads of 0.3 Pu, 0.7 Pu, and Pu
36" From Base

Figure 4.47 Specimens 3M, 3S, and 3PM Strain Gage Data

The strains on each of the side faces are shown in Figures 4.48 and 4.49. The strains across the north face of each specimen are fairly uniform with the largest strains occurring near the compression face. On the other hand, the strains across the south face of the segmental specimen are about 30 percent lower than those of either of the monolithic specimens. Also, there seems to be little strain gradient across the south face of the segmental specimen.

The compression face strains along the length of the specimen are shown in Figures 4.50 through 4.54. With the exception of those found in Figure 4.50, the smallest strains in the segmental specimen occur in the middle segment of the pier. This pattern also holds for the monolithic specimens except for gages located near the north and south faces.

Also, from observing Figures 4.50 through 4.54, the strains in Specimen 3M are either larger or very close to those found in the segmental specimen. However, the strains in Specimens 3S and 3PM seem to be similar. It is also interesting to note that for all three specimens, the patterns of strains shown in each plot are very similar.

4.4.2.3 Displacements

The compression face profiles for each of these specimens are shown in Figure 4.55 through 4.57. As observed from Figure 4.55, the largest deformations occur in the top third of the

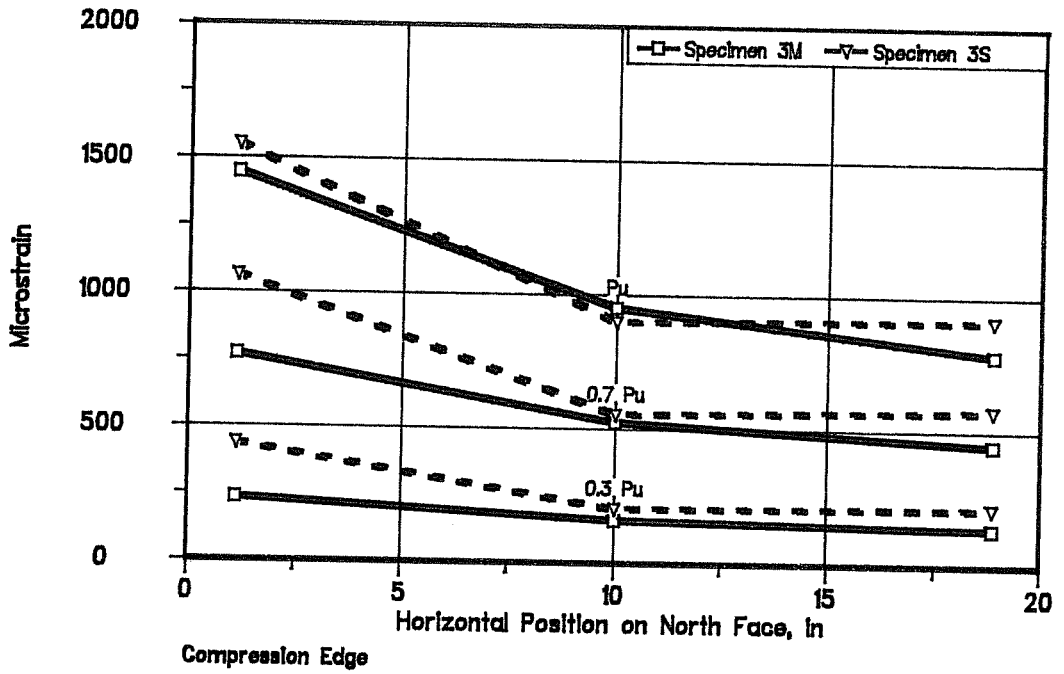

North Face Strains at Loads of 0.3 Pu, 0.7 Pu, and Pu
36" From Base

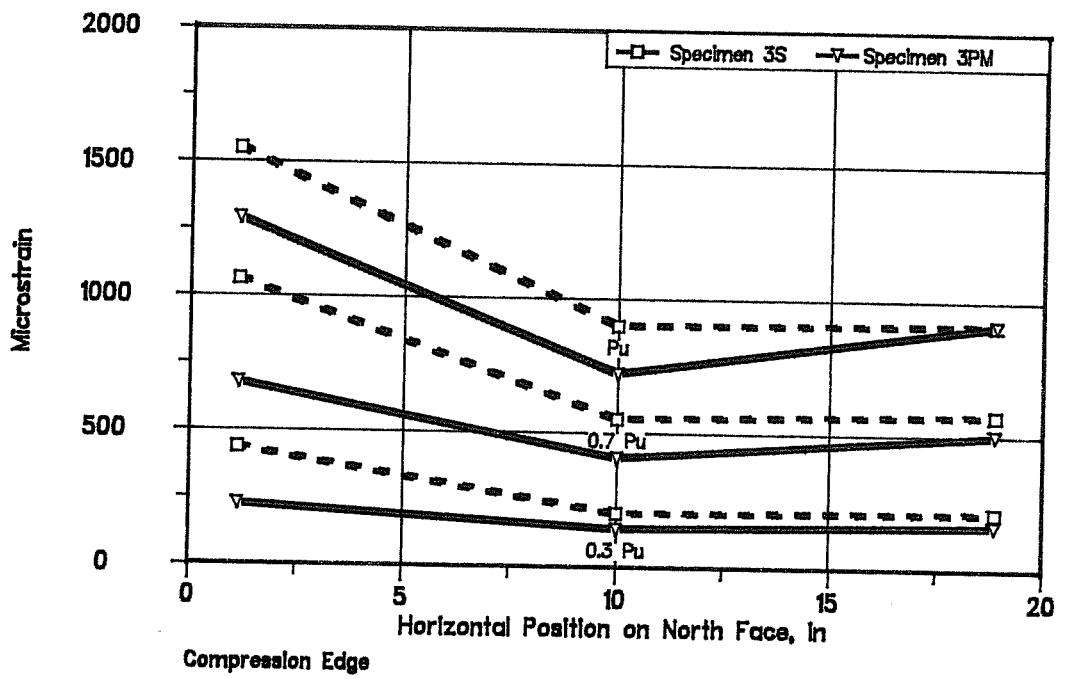

North Face Strains at Loads of 0.3 Pu, 0.7 Pu, and Pu
36" From Base

Figure 4.48 Specimens 3M, 3S, and 3PM Strain Gage Data

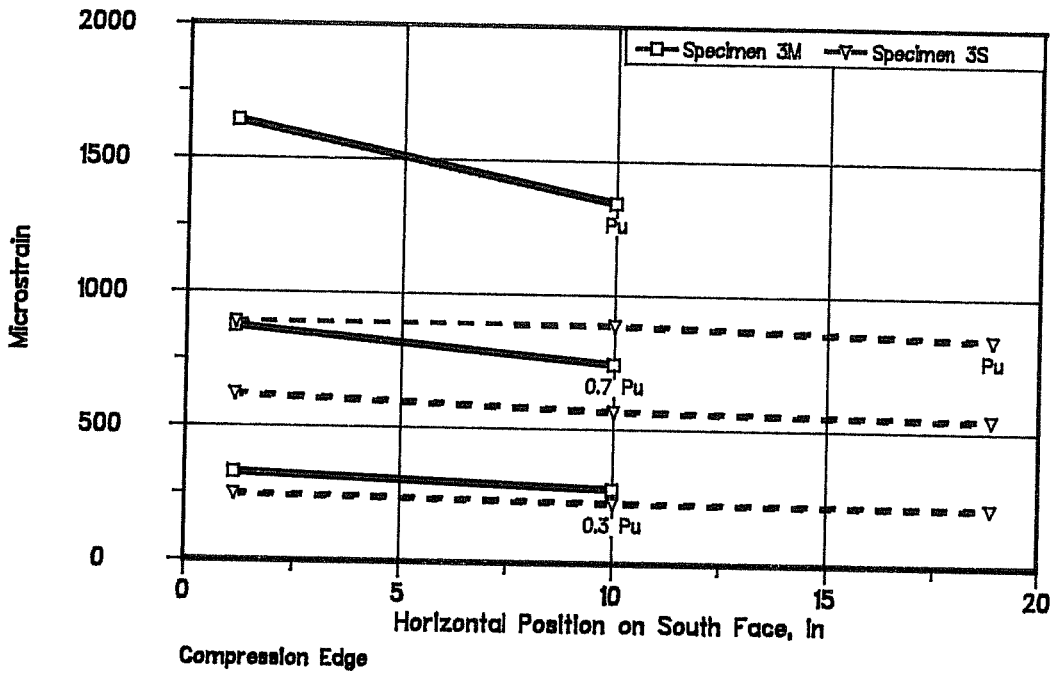

South Face Strains at Loads of 0.3 Pu, 0.7 Pu, and Pu
36" From Base

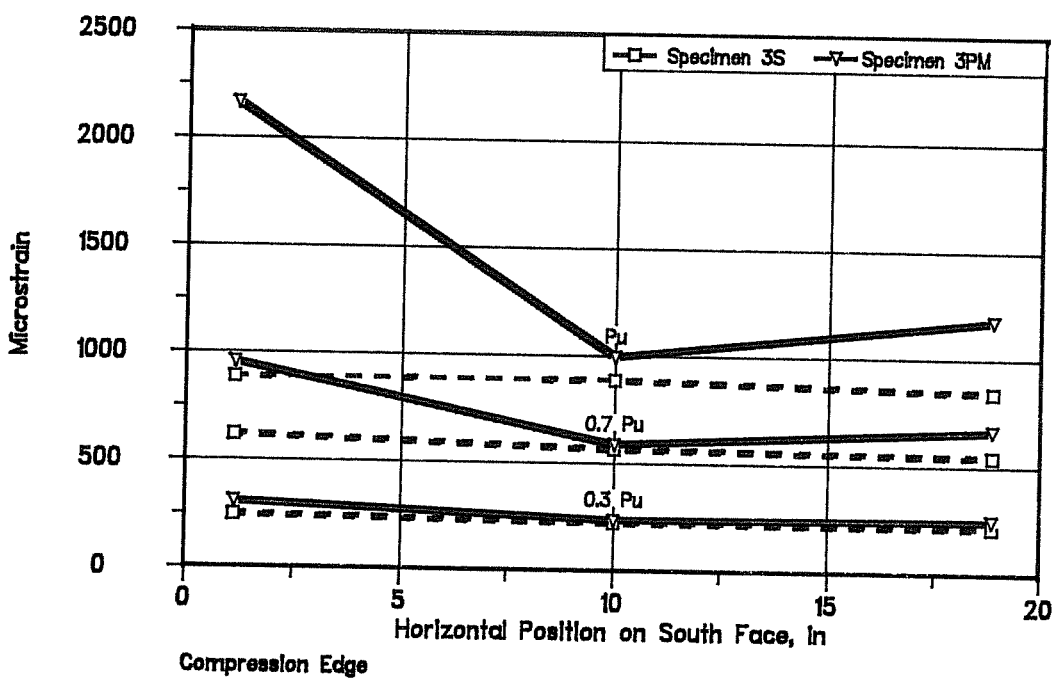

South Face Strains at Loads of 0.3 Pu, 0.7 Pu, and Pu
36" From Base

Figure 4.49 Specimens 3M, 3S, and 3PM Strain Gage Data

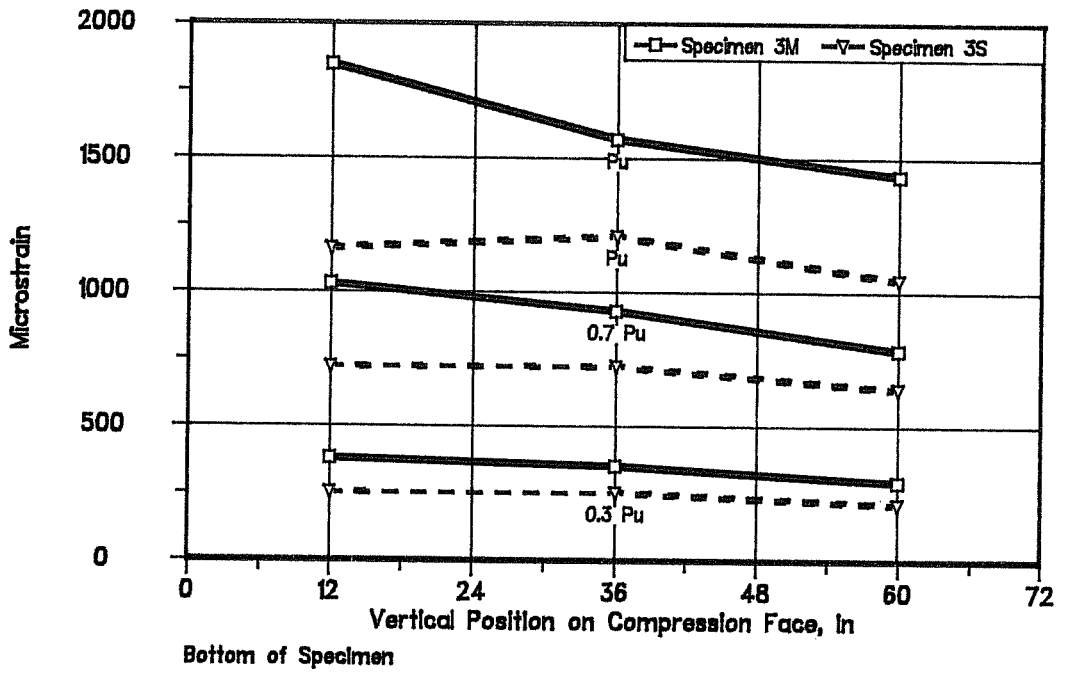

Compression Face Strains at Loads of 0.3 Pu, 0.7 Pu, and Pu
1.25" From South Face

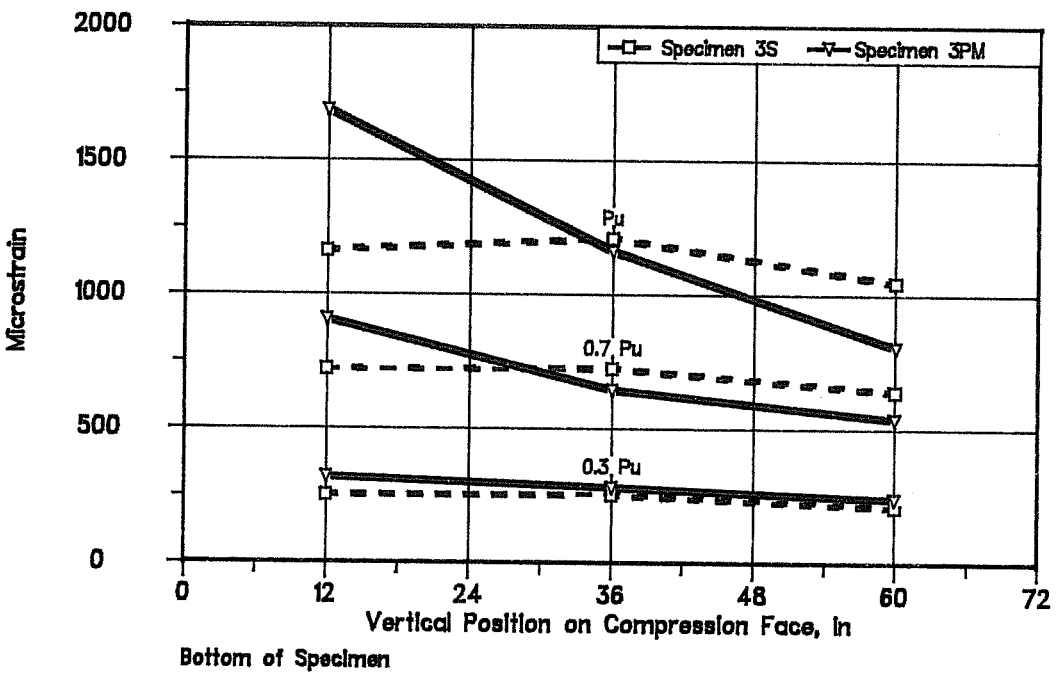

Compression Face Strains at Loads of 0.3 Pu, 0.7 Pu, and Pu
1.25" From South Face

Figure 4.50 Specimens 3M, 3S, and 3PM Strain Gage Data

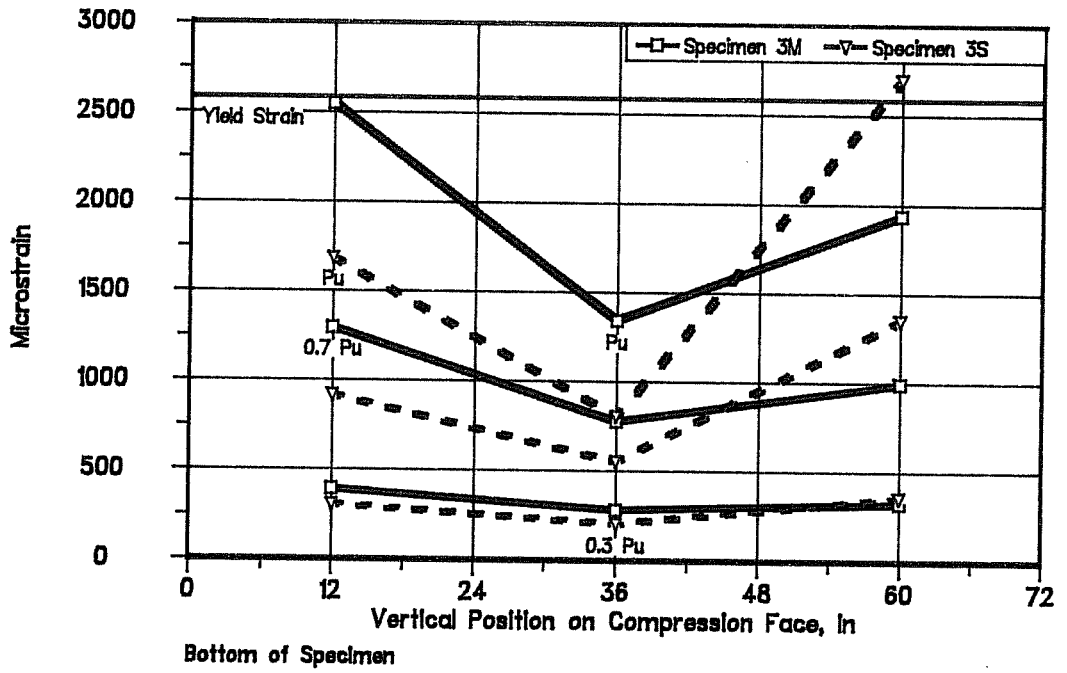

Compression Face Strains at Loads of 0.3 Pu, 0.7 Pu, and Pu
11.75" From South Face

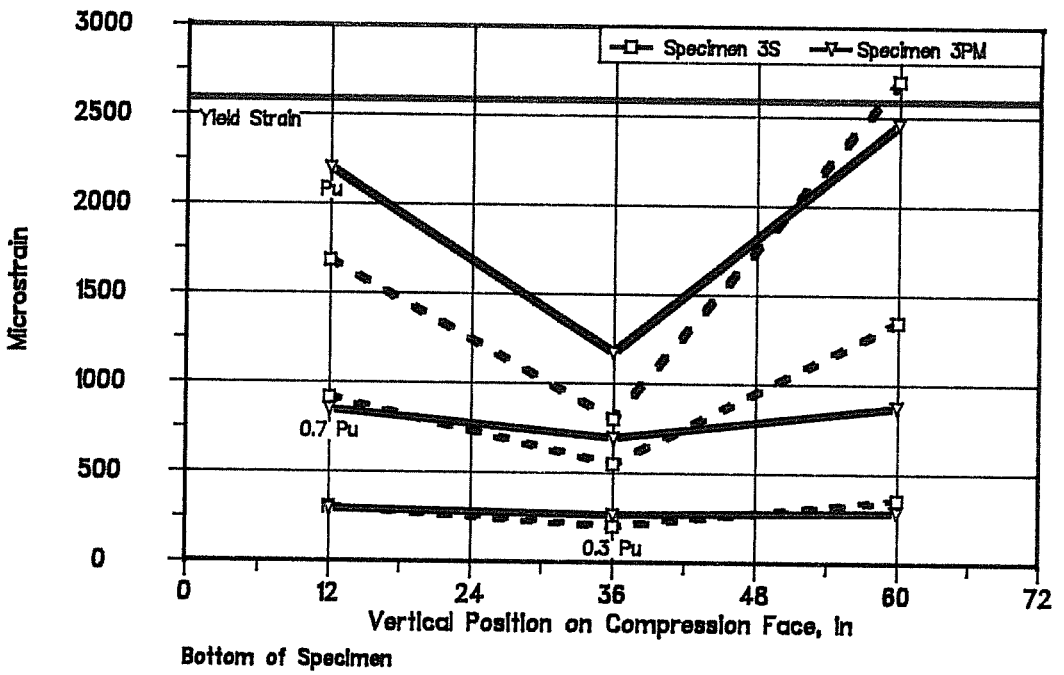

Compression Face Strains at Loads of 0.3 Pu, 0.7 Pu, and Pu
11.75" From South Face

Figure 4.51 Specimens 3M, 3S, and 3PM Strain Gage Data

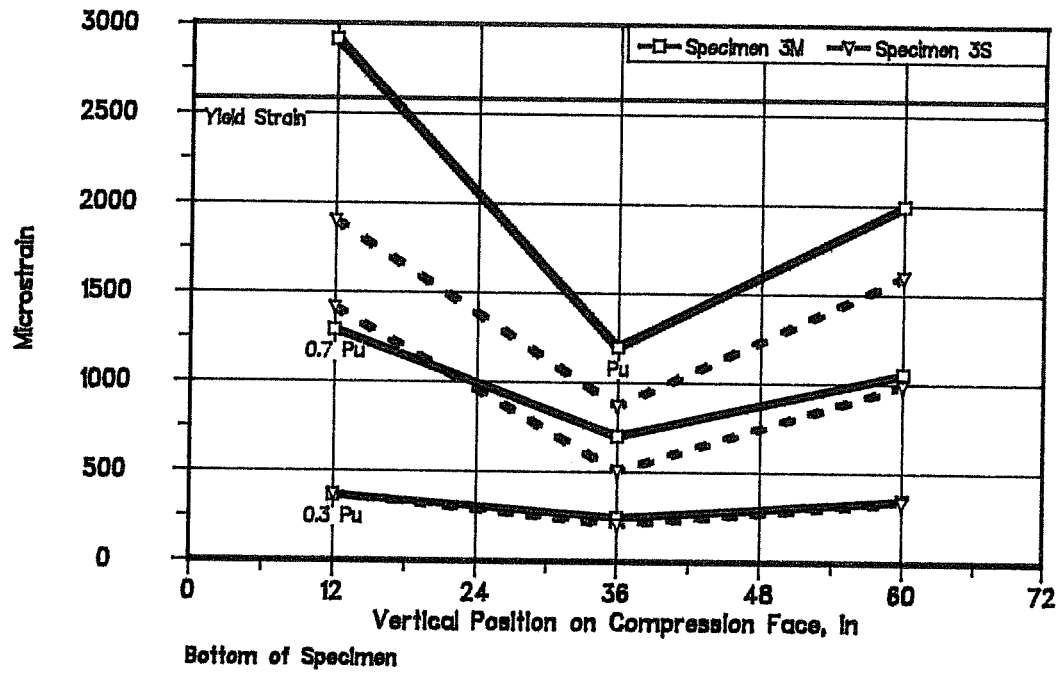

Compression Face Strains at Loads of 0.3 Pu, 0.7 Pu, and Pu
20" From South Face

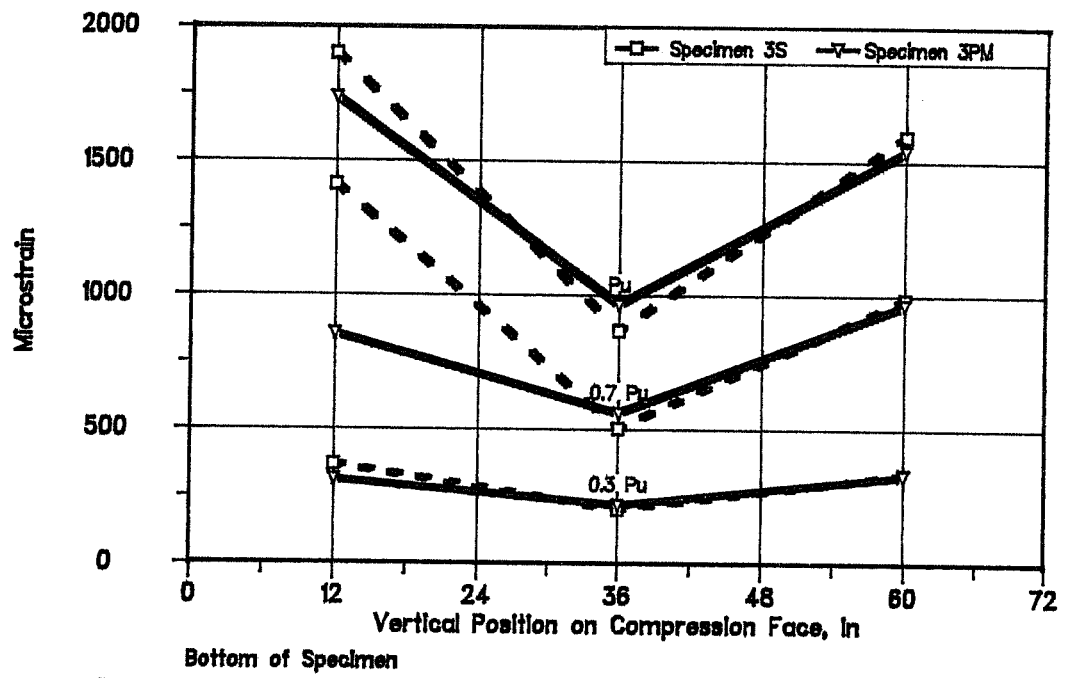

Compression Face Strains at Loads of 0.3 Pu, 0.7 Pu, and Pu
20" From South Face

Figure 4.52 Specimens 3M, 3S, and 3PM Strain Gage Data

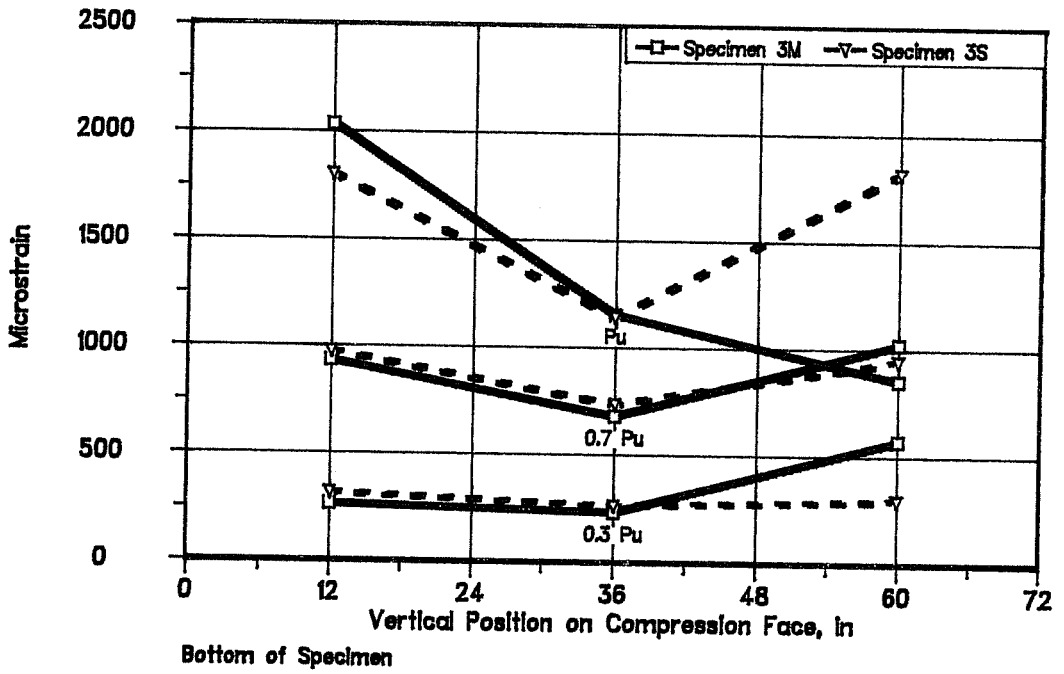

Compression Face Strains at Loads of 0.3 Pu, 0.7 Pu, and Pu
28.25" From South Face

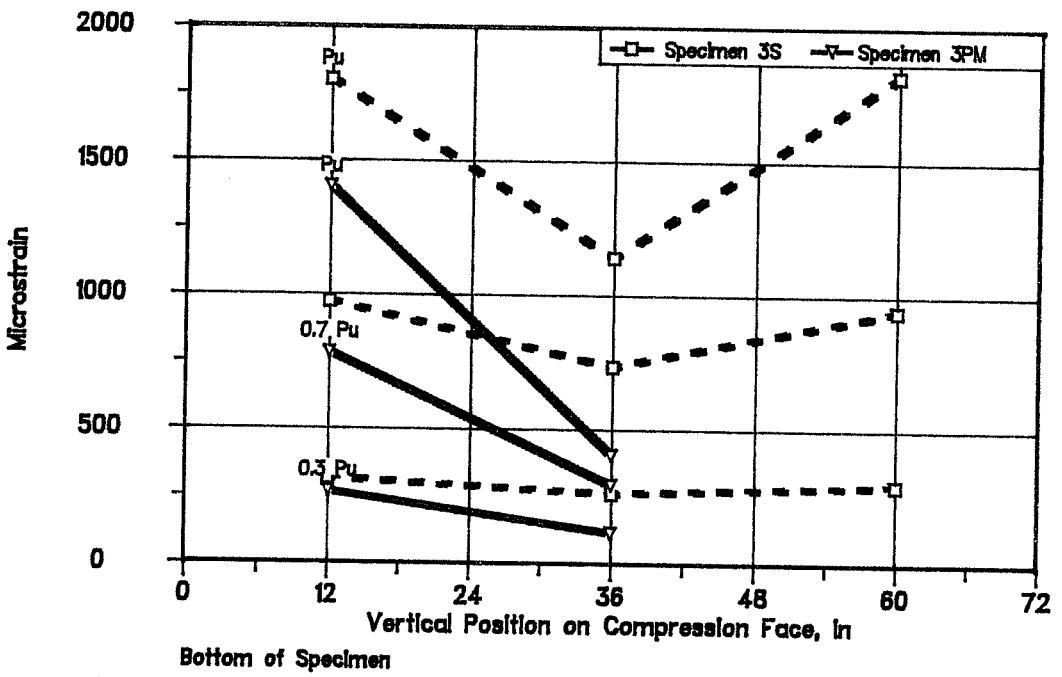

Compression Face Strains at Loads of 0.3 Pu, 0.7 Pu, and Pu
28.25" From South Face

Figure 4.53 Specimens 3M, 3S, and 3PM Strain Gage Data

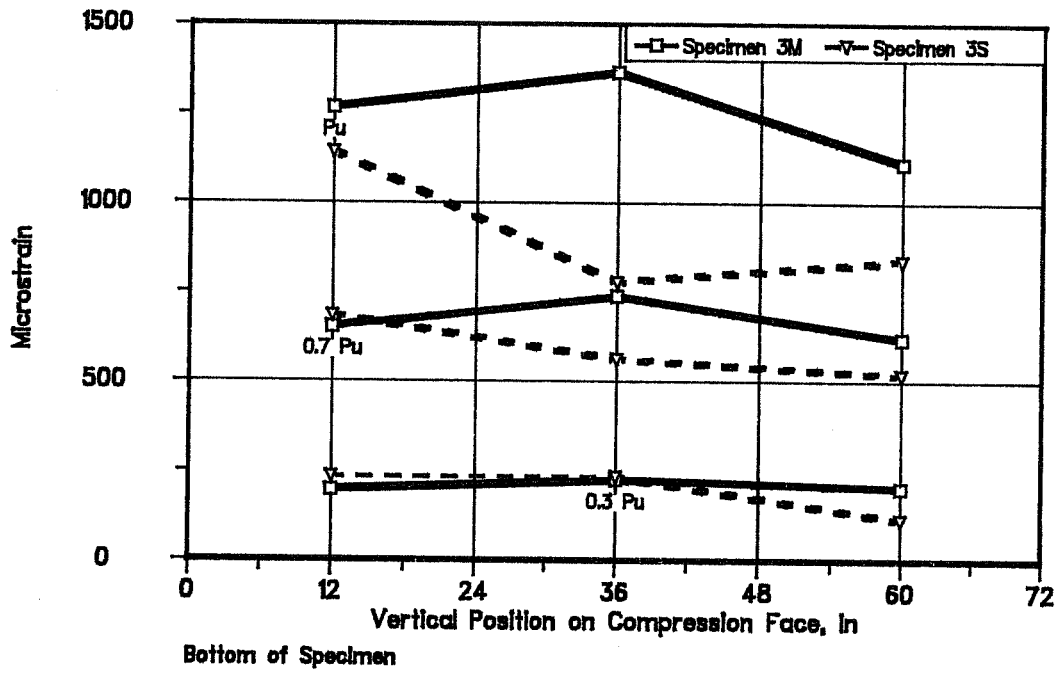

Compression Face Strains at Loads of 0.3 Pu, 0.7 Pu, and Pu
38.875" From South Face

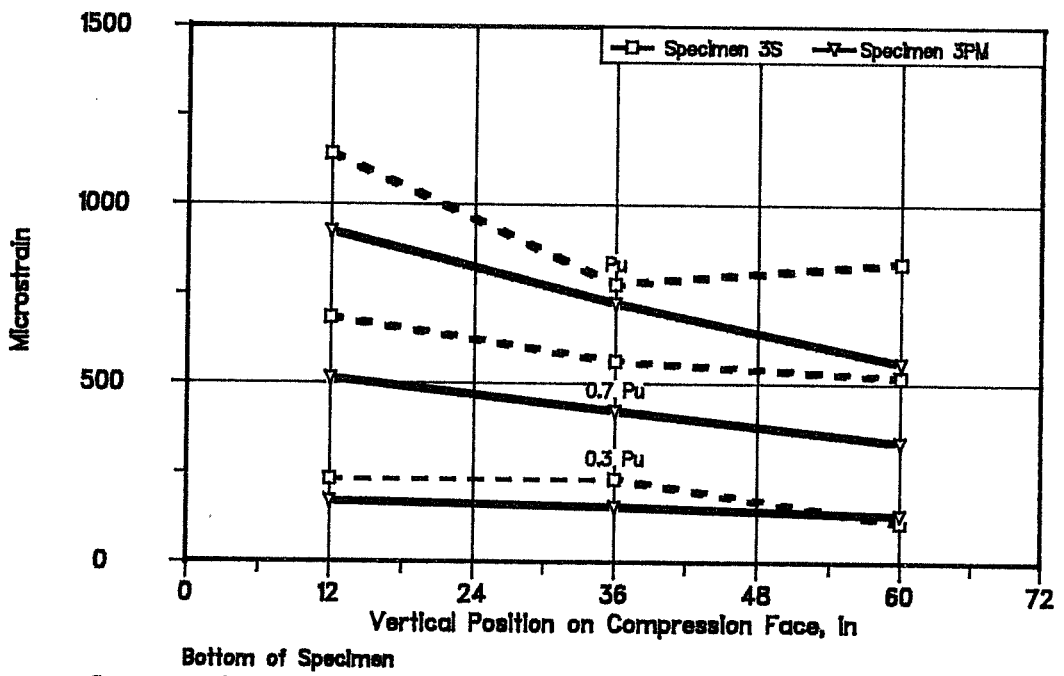

Compression Face Strains at Loads of 0.3 Pu, 0.7 Pu, and Pu
38.875" From South Face

Figure 4.54 Specimens 3M, 3S, and 3PM Strain Gage Data

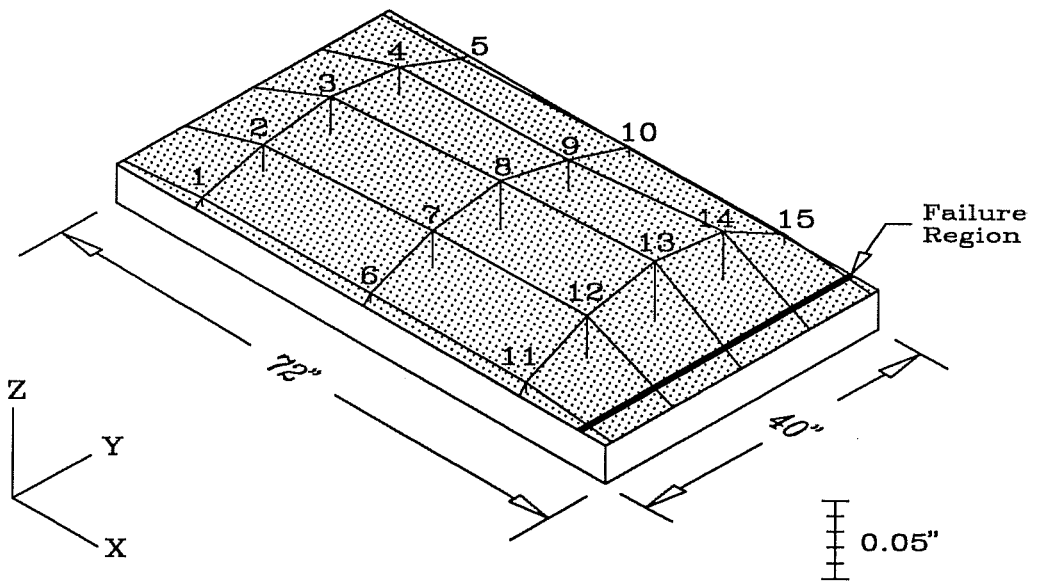

Compression Face Deflections Measured by Potentiometers Specimen 3M			
Potentiometer Number	Deflection (inches)	Potentiometer Number	Deflection (inches)
1	0.0046	9	0.0199
2	0.0166	10	0.0057
3	0.0230	11	0.0065
4	0.0177	12	0.0266
5	-0.0007	13	0.0364
6	0.0058	14	0.0308
7	0.0238	15	0.0069
8	0.0313		

Figure 4.55 Specimen 3M Compression Face Profile at Failure Load

specimen. The deformations of the face seem to be well behaved, linearly increasing from the bottom to the top of the specimen.

Though the compression face deformations shown in Figure 4.55 differ from those shown in Figures 4.56 and 4.57, the post-tensioned specimens seem to exhibit similar characteristics. The profiles of Specimens 3S and 3PM indicate that the largest deformations occurred in the bottom section of the pier, very small deformations occurred in the middle section of the pier, and moderate deformations occurred in the top section of the pier. In addition, the magnitudes of the deformations for each of the post-tensioned piers were nearly identical, though substantially larger than those found in Specimen 3M.

The fact that each of the piers failed in a region corresponding to an area in which relatively large displacements were measured seems to indicate that local instability contributed to their failure.

The moment-curvature relationship for Specimens 3M, 3S, and 3PM is shown in Figure 4.58. From the figure it is evident that the behavior of Specimens 3S and 3PM is almost identical. Specimens 3S and 3PM also seem to be stiffer against rotation than Specimen 3M, though the extra stiffness was expected since both specimens were post-tensioned. The total shortening of each specimen shown in Figure 4.58 seems to indicate that the post-tensioned specimens were also axially stiffer than Specimen

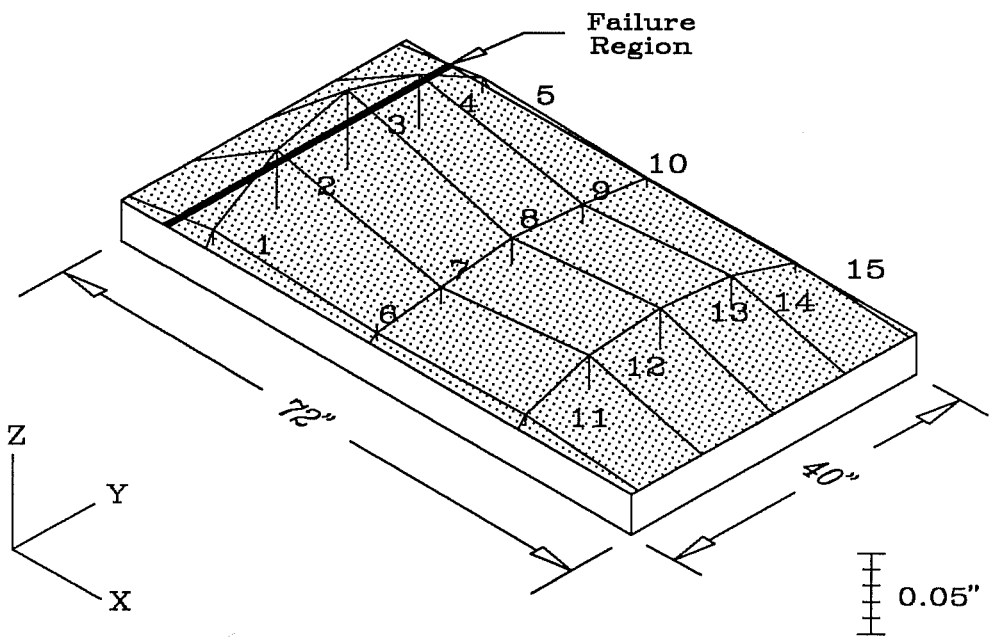

Compression Face Deflections Measured by Potentiometers Specimen 3S			
Potentiometer Number	Deflection (inches)	Potentiometer Number	Deflection (inches)
1	0.0090	9	0.0114
2	0.0360	10	0.0056
3	0.0486	11	0.0065
4	0.0332	12	0.0209
5	0.0095	13	0.0251
6	0.0039	14	0.0205
7	0.0099	15	0.0060
8	0.0155		

Figure 4.56 Specimen 3S Compression Face Profile at Failure Load

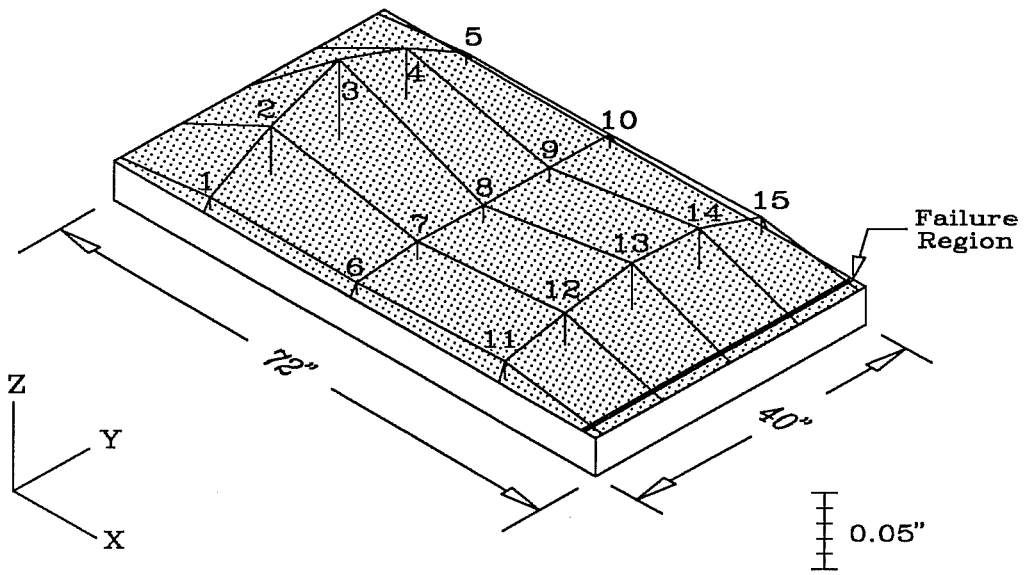

Compression Face Deflections Measured by Potentiometers Specimen 3PM			
Potentiometer Number	Deflection (inches)	Potentiometer Number	Deflection (inches)
1	0.0075	9	0.0091
2	0.0315	10	0.0084
3	0.0506	11	0.0111
4	0.0333	12	0.0208
5	0.0075	13	0.0286
6	0.0069	14	0.0259
7	0.0128	15	0.0107
8	0.0099		

Figure 4.57 Specimen 3PM Compression Face Profile at Failure Load

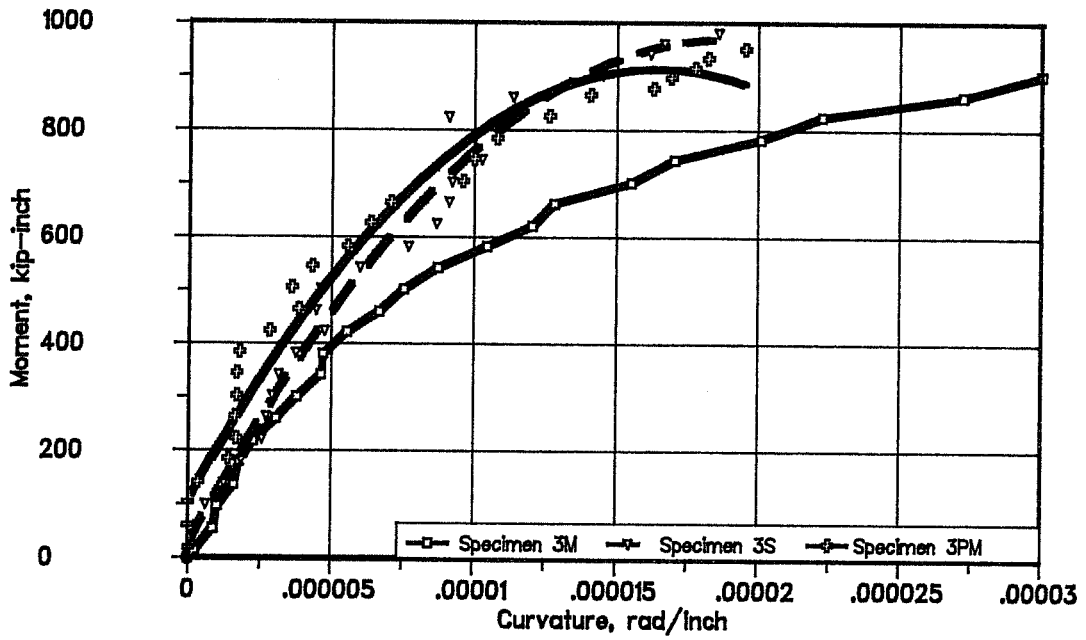

Moment-Curvature Relationship

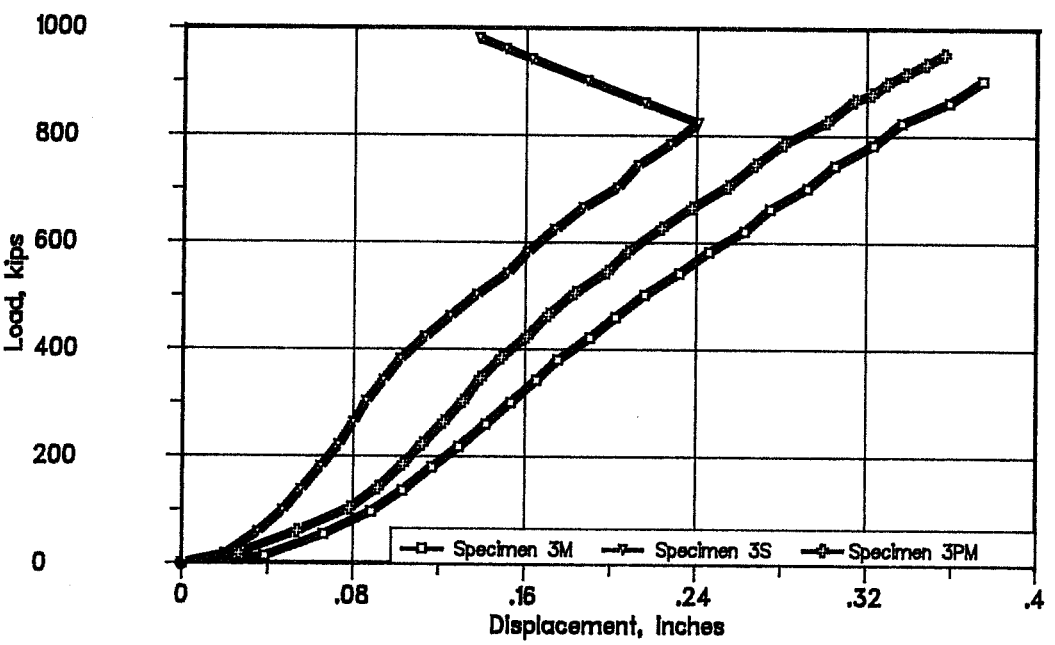

Total Shortening of Specimens

Figure 4.58 Specimens 3M, 3S, and 3PM Displacement Data

3M. The unusual trend seen at higher loads for Specimen 3S may be attributed to shifting of the moving bulkhead. Only one potentiometer was used to determine its movement.

As shown in Figures 4.59 and 4.60, the load head rotation in these specimens exhibited characteristics similar to that of the other segmental specimens.

No string readings are shown for these specimens because little or no movement of the specimen with respect to the string was recorded during the tests.

4.5 Conclusions

The test results are summarized in the following table.

Table 4.1 Summary of Failures

SPECIMEN NUMBER	FAILURE LOAD (kips)	TOTAL ECCENTRICITY (inches)	CYLINDER STRENGTH (psi)	LOCATION (inches from base)
1M	527	8.6	7862	66
1S	1137	0.81	6980	22
2M	938	2.75	7705	67
2S	948	1.0	4837	68
3M	904	1.0	6311	68
3S	999	1.02	6916	6
3PM	961	1.02	6463	68

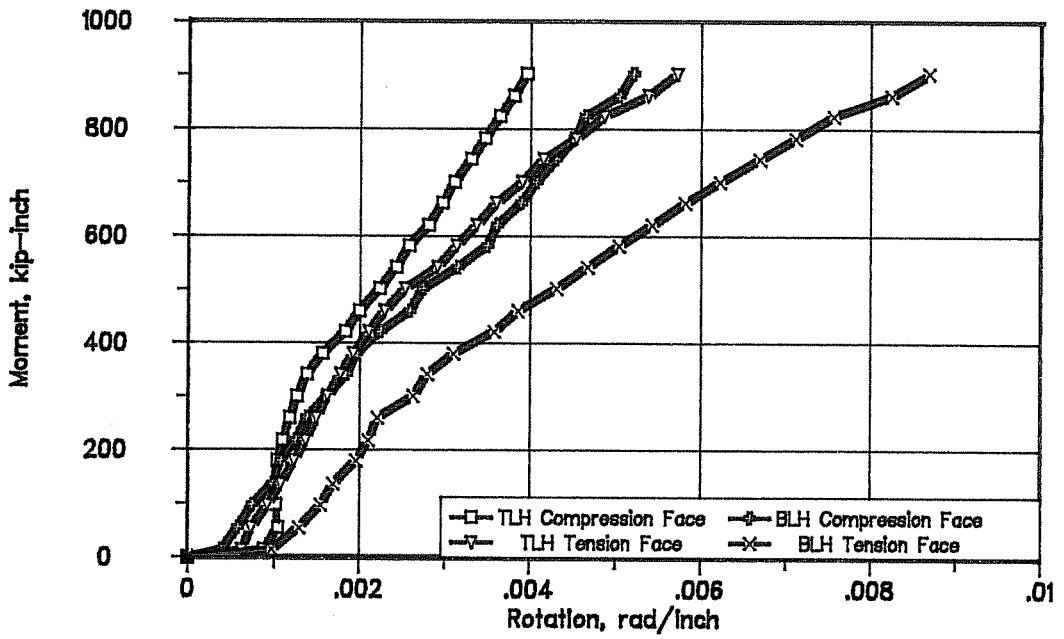

Specimen 3M

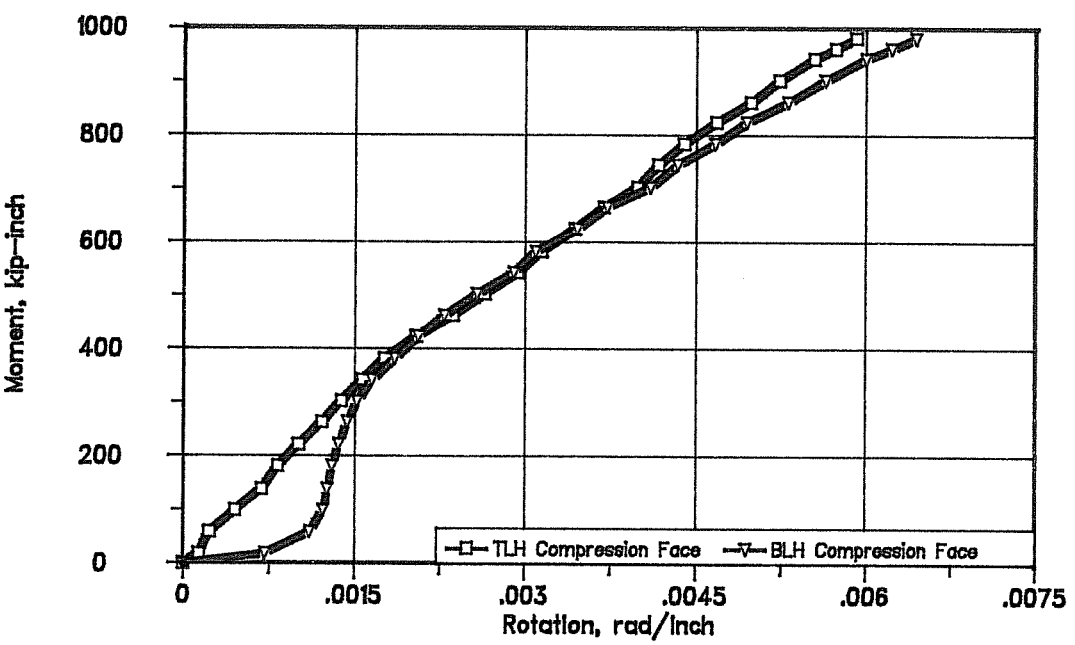

Specimen 3S

Figure 4.59 Specimens 3M and 3S Load Head Rotations

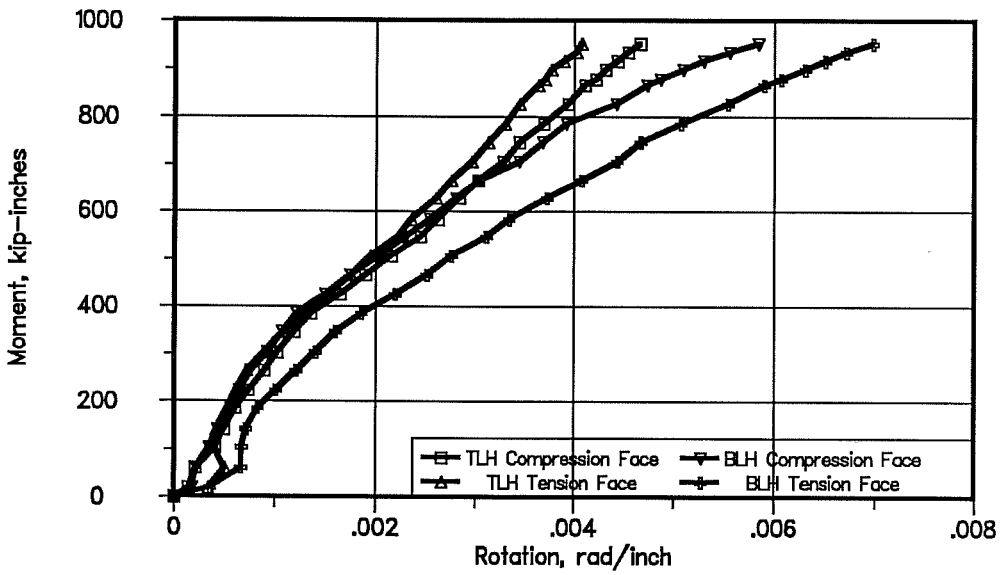

Figure 4.60 Specimen 3PM Load Head Rotations

Several preliminary conclusions regarding the behavior of the monolithic and segmental specimens can be made from the information presented in this chapter:

1) Local buckling of the thin-walled compression face seemed to contribute to the failure of each specimen. Each of the piers appeared to fail due to crushing of the concrete in the compression flange. With the exception of Specimen 2S, the failure region of each specimen coincided with an area of relatively large compression face displacements.

2) The location of the failure was not greatly influenced by segmental construction. This statement is based on the fact

that, with the exception of Specimen 1S, the compression flange failure plane occurred within the reinforcing cage with buckling of the longitudinal reinforcement. As previously indicated, it is felt that the failure location of Specimen 1S had more to do with the lack of confinement than the absence of mild reinforcement through the joint.

3) The propagation of the failure region was influenced by segmental construction. Because of the extreme deformations of the section caused by failure, the "tension" face of each specimen was forced into flexure. Though the continuous reinforcement present in the monolithic specimens offered some resistance against failure of the "tension" flange, the "tension" flange of the segmental specimens fractured in the cross-section with no reinforcement.

4) The discontinuity of mild steel at the joint of the segmental specimens had little influence on the strains in the section. The only difference between the longitudinal steel strains found in the monolithic and segmental specimens was that the segmental specimen strains were sometimes more erratic.

5) The component plates which formed the pier were not influenced by the segmental construction. From the longitudinal steel strains and compression face profiles, it seems that the thin walls were not influenced by the lack of continuity at the epoxied joint.

6) The reinforcement details performed well. Observations made after failure indicated that the longitudinal steel usually buckled over one lateral tie spacing and the concrete and post-tensioning steel seemed to be well-confined.

7) Cracks that appeared before failure were greatly influenced by the transfer of load through the load heads. The initial cracks appeared in the upper and lower thirds of the pier for all except Specimen 1M. As indicated by the load head deflections, the load heads exhibited flexural behavior in the transfer of load from the testing machine to the specimen. Therefore, it must be concluded that the pier section was not subjected to a uniform loading and that initial cracks observed in the specimens might have originated in the load heads.

8) The longitudinal cracks which formed in each specimen prior to failure may be attributed to Hooke's law. For a homogeneous isotropic material, it can be shown that with the large normal stresses present in the specimens, a tension field sufficient to cause cracking will form perpendicular to the direction of the applied load. Even though Poisson's ratio for concrete is low and reinforced concrete is an orthotropic material, it is felt that the hypothesis holds in this instance. Evidently, the tension forces present in the compression face of Specimen 1M were not large enough to form visible cracks.

9) The longitudinal cracks which formed on the compression faces of each specimen after failure were caused by large compressive stresses along the longitudinal bars which caused tension in the surrounding concrete. The large compressive stresses were initiated by the gross deformation of the section at failure which pulverized the concrete and shifted the load to the steel.

10) As evidenced in Figure 4.61, the initial cracks almost always occurred on the "tension" face. One reason for the additional load required for visible cracking on the

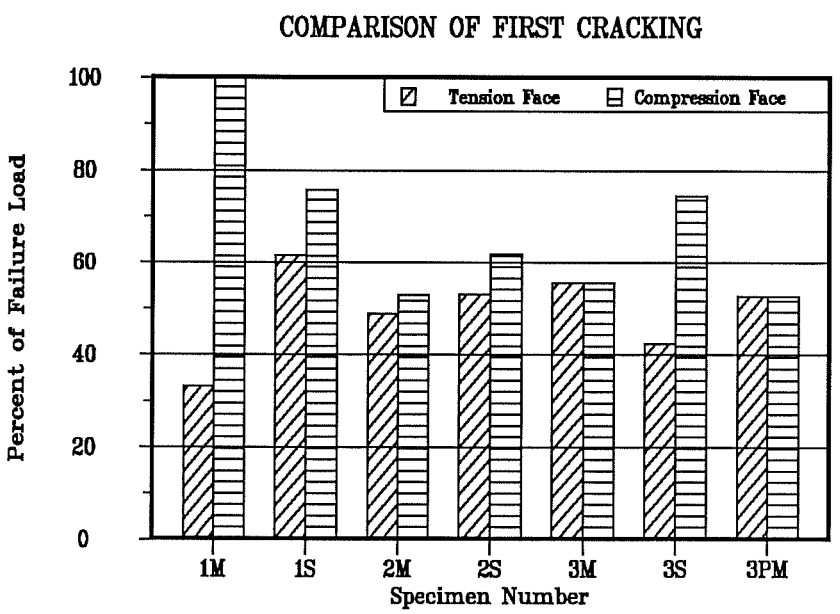

Figure 4.61 First Cracking of Specimens

compression face might have been due to the increased confinement from the greater compressive load.

11) The monolithic specimens exhibited more ductility than the segmental specimens. The moment-curvature relationship for each specimen indicates that the monolithic specimens are capable of undergoing more rotation than the segmental specimens. The ductile failure evident on the "tension" face of each of the monolithic specimens verifies this conclusion. In addition, the post-tensioned specimens were expected to have more rotational stiffness than the other specimens. However, Specimens 3M, 3S, and 3PM comprised the only group of specimens in which higher rotational stiffnesses were observed in the post-tensioned specimens.

12) The post-tensioned specimens were axially stiffer than the other specimens. From observation of the load versus shortening plots, it appears that the post-tensioned specimens undergo less shortening than the other specimens. This may be attributed to the presence of the post-tensioning tendons and the fact that the specimens had already experienced some shortening due to the post-tensioning.

CHAPTER 5

ANALYSIS OF TEST RESULTS

5.1 Introduction

This chapter summarizes the development of an analytical model for predicting the strength and stiffness of segmentally constructed bridge piers. The analytical model presented is in the form of a computer program written to calculate the interaction diagram and moment-curvature relationship for each pier. By comparing the analytical behavior of the segmental specimens to the companion series of monolithic specimens, a better understanding of segmental pier behavior was obtained.

Conclusions drawn from the analysis and recommendations for the design of segmentally constructed bridge piers are presented at the end of the chapter.

Notation used throughout this chapter is as follows:

A_c = concrete area

A_{cr} = cross-sectional area

A_s = area of longitudinal mild reinforcement

b = width of section

c = distance from neutral axis to extreme compression fiber

e = eccentricity of load with respect to mid-depth of the section

E_c = secant modulus of elasticity of concrete at $0.45f''_c$

E_o = modulus of elasticity of concrete

f_c = concrete stress

f_{cr} = stress which causes local buckling of the pier's component plates

f'_c = compressive strength of 6 X 12 inch cylinders

f''_c = compressive strength of concrete in flexure = $k_3 f'_c$

f_y = yield stress of mild reinforcement

F_i = initial force applied to section due to post-tensioning

k_3 = reduction factor accounting for casting position and size and shape of member

NU = Poisson's ratio for concrete

P_n = nominal axial load capacity at a given eccentricity

P_o = value used to normalize the axial load capacity of a cross-section = $f''_c A_{cr}$

t = depth of section

t_f = wall thickness

ϵ_c = concrete strain

ϵ_{cr} = strain at which local buckling will occur; calculated from critical buckling stress f_{cr}

ϵ_{lim} = maximum usable concrete strain = ϵ_{cr} or ϵ_u

ϵ_o = compressive strain in concrete corresponding to maximum stress

ϵ_u = ultimate concrete strain

ϵ_4 = extreme concrete compression fiber strain

Φ = curvature of specimen = ϵ_4/c

5.2 Analytical Model

5.2.1 Stress-Strain Models

In order to make an accurate comparison between the test results and results from the analytical model, realistic stress-strain models for materials were incorporated into the analysis.

5.2.1.1 Concrete Models

Numerous models for the relationship between stress and strain in concrete have been proposed. However, most consist of either a variation on the classic model presented by Hognestad (14) or fitting the experimental data by a series of curves (15,16,17). Though several of these models were reviewed, it was determined that a representative of each type of model would be used in an attempt to model the stress-strain behavior determined by testing the concrete used in the pier specimens.

5.2.1.1.1 Hognestad Model

In 1951, Hognestad presented a comprehensive study of combined bending and axial load in reinforced concrete members (14). As part of the investigation, Hognestad proposed a

stress-strain relationship for concrete in flexure which correlated well with the test results. The Hognestad stress-strain curve is shown in Figure 5.1.

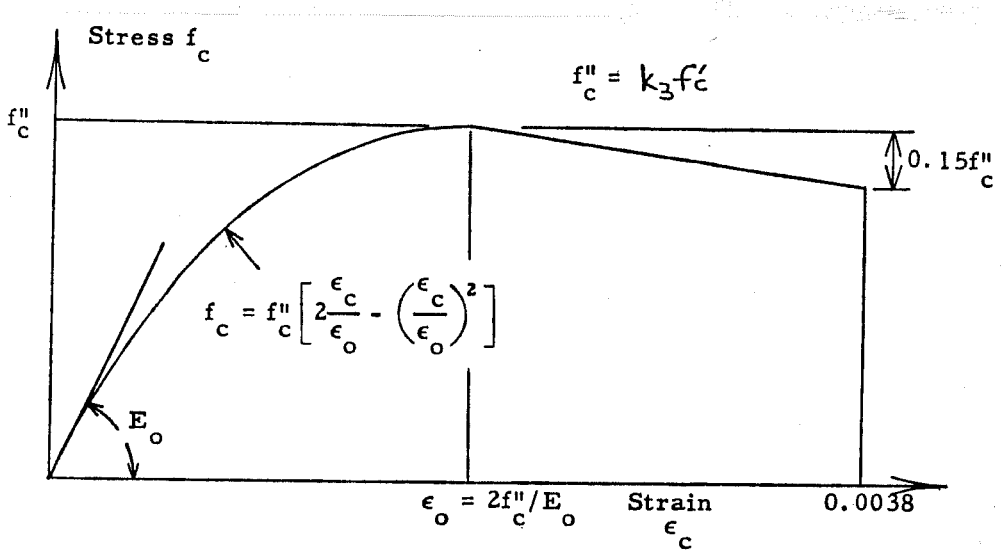

Figure 5.1 Hognestad Stress-Strain Model
(taken from reference 18)

The initial part of the curve is defined by the equation:

$$f_c = f''_c \{2\epsilon_c/\epsilon_o - (\epsilon_c/\epsilon_o)^2\} \qquad (5.1)$$

where f''_c = maximum compressive stress of concrete in flexure = $k_3 f'_c$;

ϵ_c = strain in concrete corresponding to stress f_c;

ϵ_o = strain in concrete corresponding to maximum stress = $2k_3 f'_c/E_o$.

The descending portion of the curve is given by the equation:

$$f_c = f''_c - 0.15f''_c(\epsilon_c - \epsilon_o)/(\epsilon_u - \epsilon_o) \qquad (5.2)$$

where ϵ_u = ultimate concrete strain.

Hognestad proposed that the maximum concrete stress be limited to $f''_c = k_3 f'_c$ with $k_3 = 0.85$. In addition to the effect of casting position, this reduction factor is thought to include the size and shape of the member. Since all of the pier specimens were cast vertically, this reduction factor can be expected to apply in the analysis of the piers.

The initial slope of Hognestad's original curve was given by:

$$E_o = 1{,}800{,}000 + 460f''_c \qquad (f''_c \text{ in psi}) \qquad (5.3)$$

However, for a given ϵ_o,

$$E_o = 2f''_c/\epsilon_o \qquad (5.4)$$

Hognestad also proposed that the ultimate concrete strain be limited to a value of $\epsilon_u = 0.0038$.

5.2.1.1.2 Wang Model

Wang, Shah, and Naaman (15) have proposed an analytical expression for the stress-strain relationship of concrete that depends on stress-strain data obtained from cylinder tests. The

following expression was used to fit a curve through the data points.

$$Y = (Ax + Bx^2)/(1 + Cx + Dx^2) \qquad (5.5)$$

where $Y = f_c/f''_c$

$X = \epsilon_c/\epsilon_o$

f''_c = maximum compressive stress of concrete in flexure = $k_3 f'_c$

ϵ_c = strain in concrete corresponding to stress f_c

ϵ_o = strain in concrete corresponding to maximum stress

E_o = secant modulus of elasticity at the peak stress = f''_c/ϵ_o

E_c = secant modulus of elasticity at $0.45f''_c$

A,B,C,D = constants

A curve developed from this expression is shown in Figure 5.2.

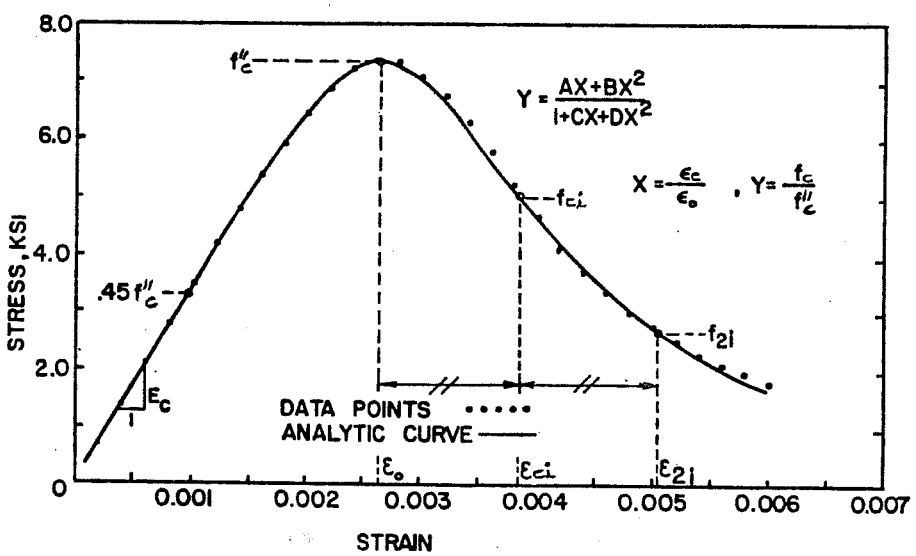

Figure 5.2 Wang Stress-Strain Model

Two separate sets of values of the four constants are used for the ascending and descending parts of the curve. The values of the four constants for the ascending part were evaluated from the following four conditions:

$Y = 1$ for $X = 1$

$Y = 0.45$ for $X = 0.45/(E_c/E_o)$

$dY/dX = E_c/E_o$ at the origin ($Y = 0$, $X = 0$)

$dY/dX = 0$ for the peak point ($Y = 1$, $X = 1$)

The values of the four constants for the descending part were evaluated from four other conditions:

$Y = 1$ for $X = 1$

$dY/dX = 0$ for the peak point ($Y = 1$, $X = 1$)

$Y = f_{ci}/f''_c$ for $X = \epsilon_{ci}/\epsilon_o$

$Y = f_{2i}/f''_c$ for $X = \epsilon_{2i}/\epsilon_o$

where f_{ci} = stress at the inflection point

ϵ_{ci} = strain at the inflection point

$\epsilon_{2i} = 2\epsilon_{ci} - \epsilon_o$

f_{2i} = stress corresponding to ϵ_{2i}

From the preceding information, an analytic stress-strain curve can be generated from four key points of the experimental curve: the strain corresponding to peak stress (ϵ_o), the secant modulus of elasticity at a stress of $0.45f''_c$ (E_c), the stress and strain at the inflection point (ϵ_{ci},f_{ci}), and stress

and strain at a point symmetric to the peak with respect to the inflection point (ϵ_{2i},f_{2i}).

In order to generate the stress-strain curve from the compressive strength, the four points required were statistically related to the compressive strength. The following expressions serve to relate the required data points to the compressive strength of normal weight concrete:

$$\epsilon_o = 0.000125f''_c + 0.00230$$

$$f_{ci} = 0.580f''_c + 0.774 \qquad \text{(ksi)}$$

$$\epsilon_{ci} = 0.00005f''_c + 0.00401$$

$$f_{2i} = 0.085f''_c + 2.024 \qquad \text{(ksi)}$$

$$E_c = 271f''_c + 978 \qquad \text{(ksi)}$$

where f''_c = maximum compressive stress of concrete in flexure = $k_3 f'c$ (in ksi)

From evaluating this expression, it was found that for f''_c less than 6500 psi, $f_{2i} = 0.085f''_c + 1.5$.

By using an experimental technique which enabled the stress-strain curve to be developed up to a strain of 0.006, Wang was able to successfully reproduce the descending portion of the stress-strain curve. However, one must question whether the descending portion of the curve can be obtained for such large strains in the absence of a controlled testing apparatus.

5.2.1.1.3 Comparison of Actual Data to Models

The cylinder strengths of concrete at the time each pier was tested are shown in the following table.

Specimen Number	f'_c
1M	7862
1S	6980
2M	7705
2S	4837
3M	6311
3S	6916
3PM	6463

Representative plots of measured stress-strain data along with the two analytical models are shown in Figures 5.3 and 5.4. (additional stress-strain plots are shown in the Appendix) Since data from the tests had to be manually recorded, the rate of load application to the cylinders was much slower than a standard cylinder test (about 1-1/2 hours for stress-strain test). Therefore, the maximum stress evident from the stress-strain curves is lower than f'_c found from standard cylinder tests.

It is evident from the figures that each model has its benefits. Although Wang's model represents the descending portion of the curve very well, it indicates less stiffness in the initial portion of the curve. On the other hand, Hognestad's model seems be more representative of the initial

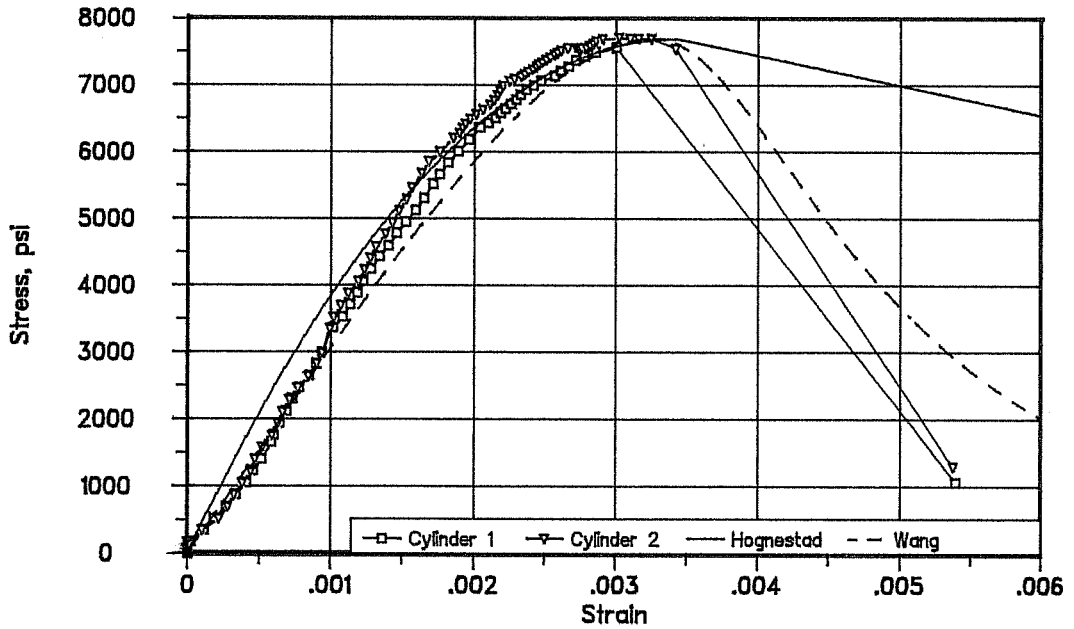

Specimen 2M Concrete Stress-Strain Comparison

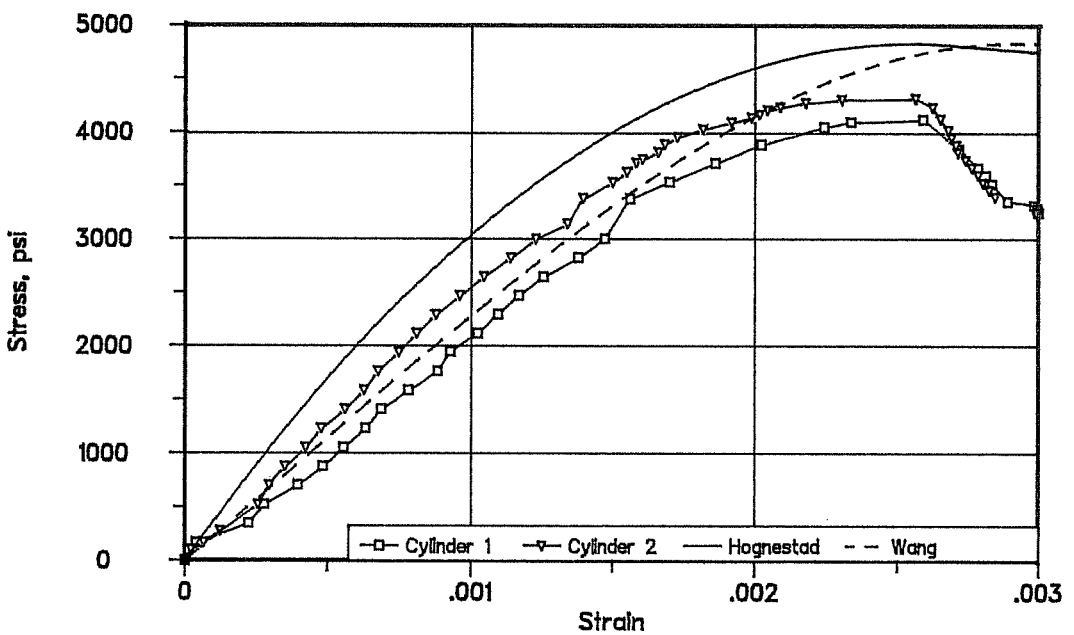

Specimen 2S Concrete Stress-Strain Comparison

Figure 5.3 Comparison of Concrete Stress-Strain Relationships

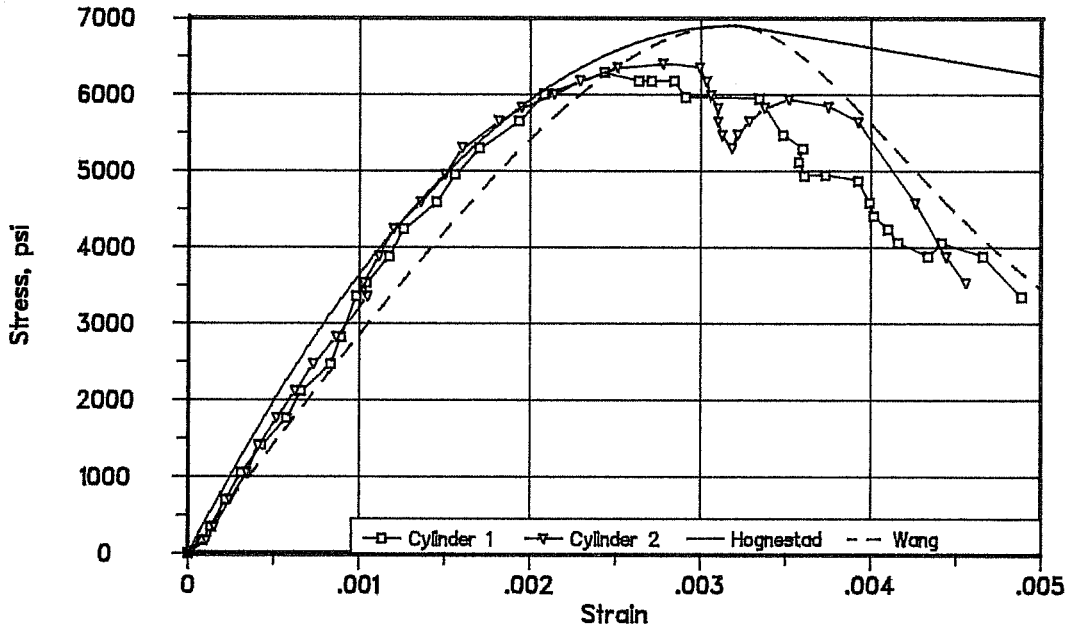

Specimen 3S Concrete Stress-Strain Comparison

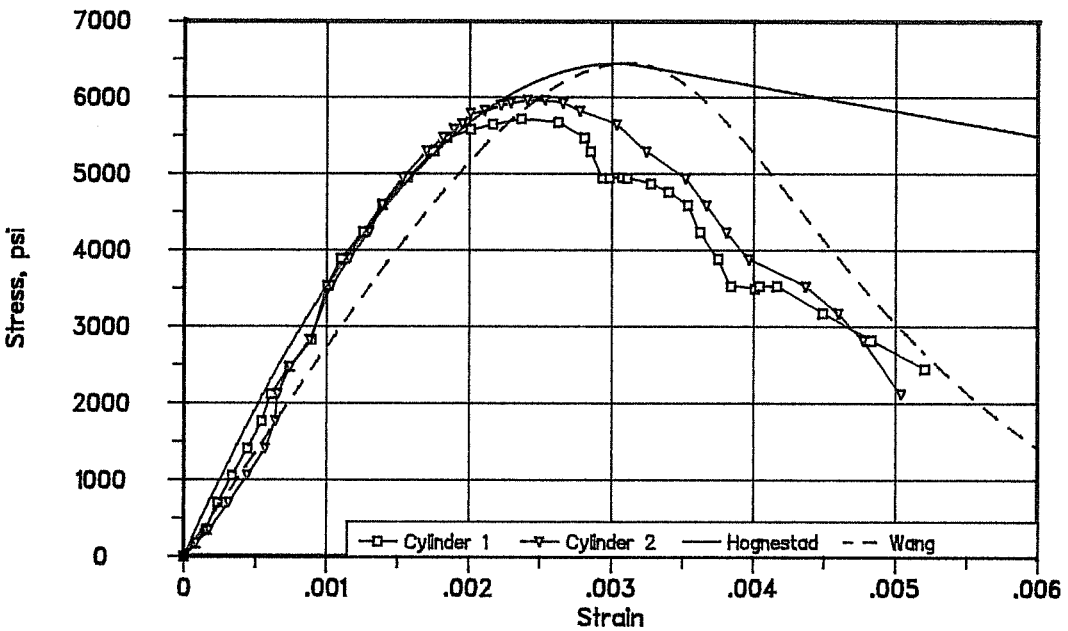

Specimen 3PM Concrete Stress-Strain Comparison

Figure 5.4 Comparison of Concrete Stress-Strain Relationships

stiffness, but does not represent the descending portion very well. Since the development of the descending portion of the curve in the test specimens is questionable, and since Hognestad's model represents the initial stiffness fairly accurately, it seemed that Hognestad's model would be the better model to use in the analysis.

The experimental stress-strain data was obtained by performing a controlled test on 6 by 12 inch cylinders with thin sulfur caps immediately following the test to failure of each specimen. The cylinders were carefully loaded while manually recording load head displacement and the associated load. Load head displacement was measured by two linear potentiometers placed on opposite sides of the cylinder.

Since the specimens were made of high strength concrete, it was felt that the modulus of elasticity used in Hognestad's model would yield artificially high results. Therefore, an expression developed at Cornell (19) was substituted for Hognestad's original equation. The expression developed at Cornell is as follows:

$$E_o = 40{,}000 \sqrt{f''_c} + 1.0 \times 10^6 \quad (f''_c \text{ in psi}) \qquad (5.6)$$

Because the reduction factor k_3 is a result of factors related to casting position and geometry of the section, it is not applicable when comparing the analytical models to the stress-strain results measured from a cylinder test.

Key points from the experimental stress-strain curve and the Hognestad stress-strain curve used in the analysis are presented in the following table. Stress-strain tests were not conducted for concrete from Specimen 1S.

Table 5.1 Concrete Stress-Strain Data

Specimen	Experimental Data			Analytical Model		
	f''_c (ksi)	ϵ_o	E_o (ksi)	f''_c (ksi)	ϵ_o	E_o (ksi)
1M	6.611	0.00324	3700	6.683	0.00313	4270
2M	6.497	0.00356	3700	6.549	0.00309	4237
3M	5.050	0.00279	3500	5.364	0.00273	3930
1S	*****	*******	****	5.933	0.00291	4081
2S	3.590	0.00258	2500	4.111	0.00231	3565
3S	5.401	0.00261	3700	5.879	0.00289	4067
3PM	4.976	0.00245	3500	5.494	0.00277	3965

5.2.1.2 Reinforcement Models

5.2.1.2.1 Mild Reinforcement

From the results of tension tests with a two-wire strain gage in conjunction with a Measurements Group Model P-350A strain indicator, the stress-strain curves of five representative 6 mm diameter longitudinal reinforcing bars were obtained. With a yield stress of 75.1 ksi and an ultimate stress of 90.4 ksi, the steel was subjected to substantial strain hardening before fracture. With an elongation at break of 9.9%, the strain hardening coefficient is calculated to be

1.577%. The results of four of the stress-strain tests are shown along with the idealized curve used in the analysis in Figure 5.5. The portion of the idealized curve before yield is based on the modulus of elasticity, 29000 ksi.

5.2.1.2.2 Post-Tensioning Tendons

The stress-strain curve for the Dywidag bars used for post-tensioning the specimens was obtained from mill tests and other standard information provided by the Dywidag company. Though the bars are subject to strain hardening, the strain hardening is not appreciable until a strain of approximately 0.04 is reached. This strain was not obtained in any of the pier tests and is unlikely to be obtained in practice. Therefore, the elastoplastic relationship shown in Figure 5.6 was used in the analysis. From mill tests on the bars that were used, their yield stress was 138.2 ksi and their modulus of elasticity was 29000 ksi.

5.2.2 Buckling Program

The possibility of local buckling in the test specimens was considered by running a program, PLCRST, developed by Tran (20) which calculates the critical buckling stress, f_{cr}, of a hollow pier wall. The reader is referred to Tran's work (20) for the development of this program.

Tran's program, PLCRST, considers the inelastic stress-strain curves of concrete and reinforcement. However, it does

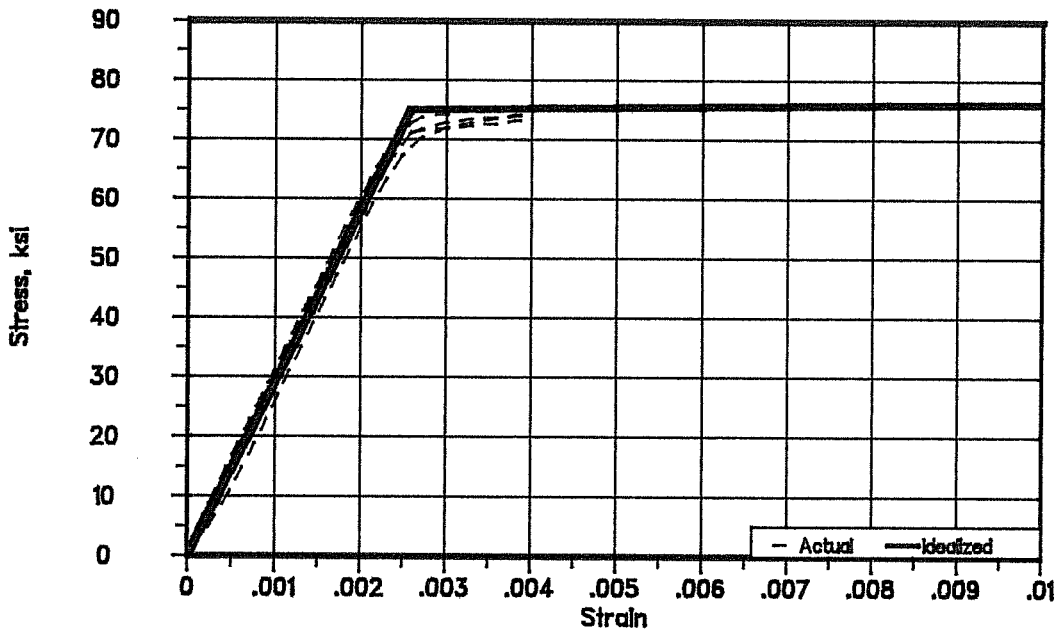

Figure 5.5 Mild Reinforcement Stress-Strain Relationship

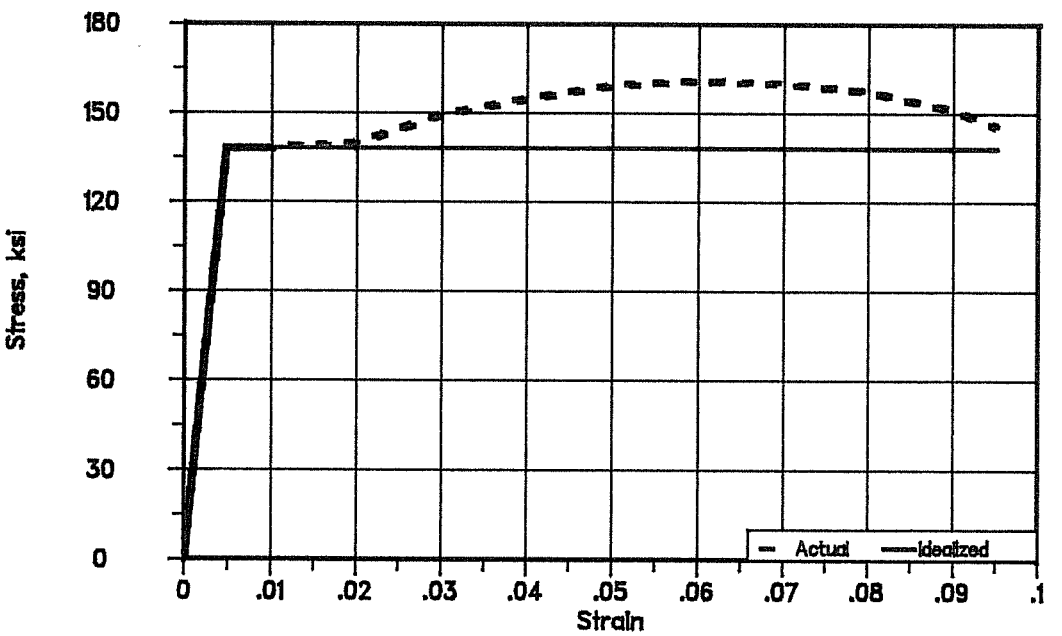

Figure 5.6 Post-Tensioning Tendon Stress-Strain Relationship

not consider reductions in stiffness due to the type of longitudinal cracking observed on the compression faces of many of the physical test specimens. Thus it probably overestimates the actual stiffness of the compression flange and therefore gives somewhat higher estimates of the flange buckling load than may occur in reality. However, the program is useful in indicating a probable upper bound for such buckling loads.

PLCRST was based on Hognestad's stress-strain model (14) for properties of the concrete. Therefore, the program was slightly modified by this author to include additional subroutines which would calculate the concrete stress-strain relationship based on Wang's model or user-defined input fitted through the equation presented by Wang (15).

The modifications to PLCRST are shown in the flowcharts in Figures 5.7 and 5.8 which were originally presented by Tran (20). Flowcharts for the added subroutines are shown in Figure 5.9. The source code for the modified version of PLCRST as well as a guide for using the program are given in the Appendix.

5.2.3 Interaction Diagram Program

Program MOMINT was developed to calculate the capacity of the pier cross-section by studying procedures developed by Pfrang, et. al., (21) and Breen (22) .

The concrete strain distribution shown in Figure 5.10 was assumed in the development of the program.

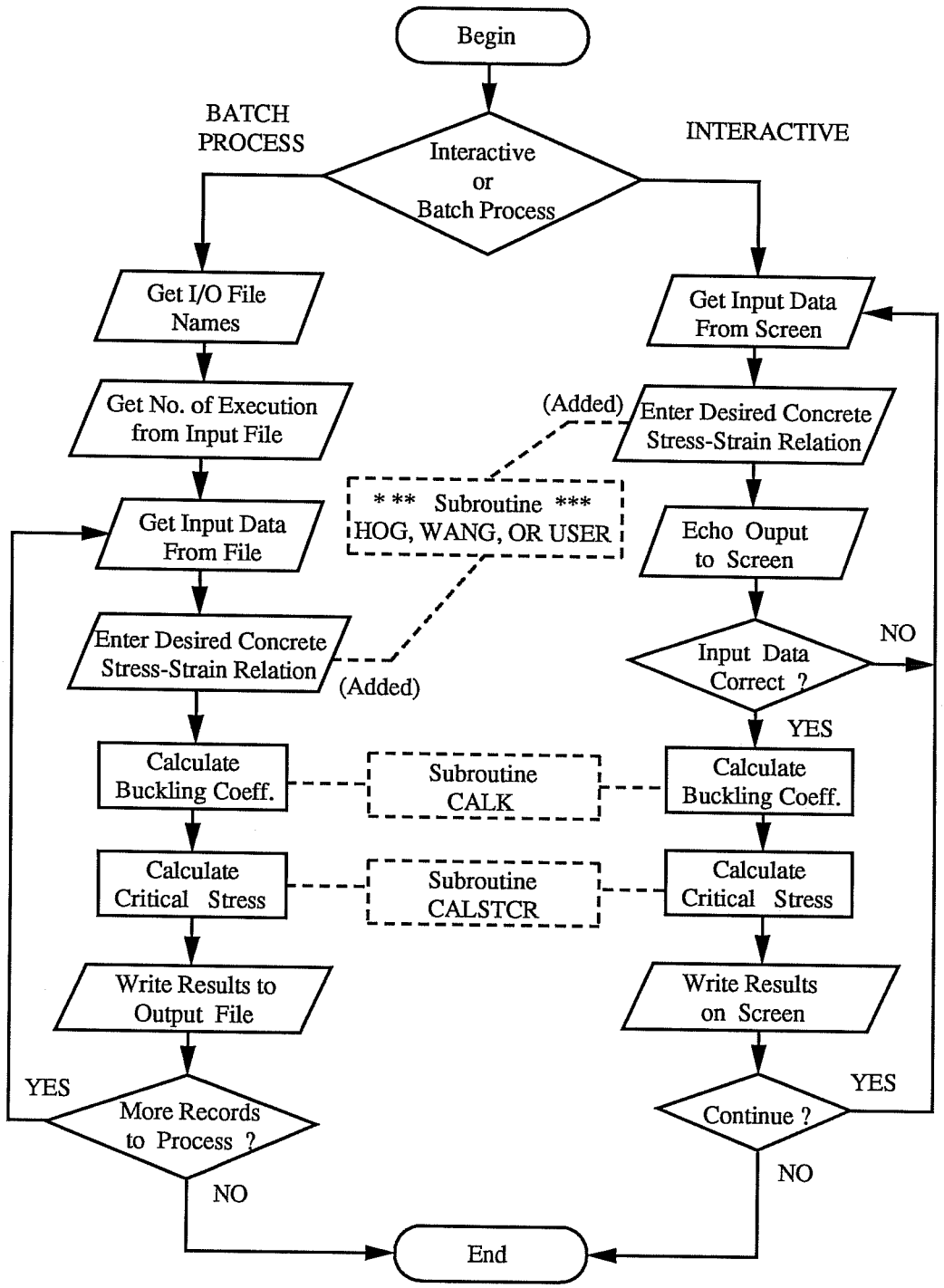

Figure 5.7 Flow Chart of the Computer Program PLCRST

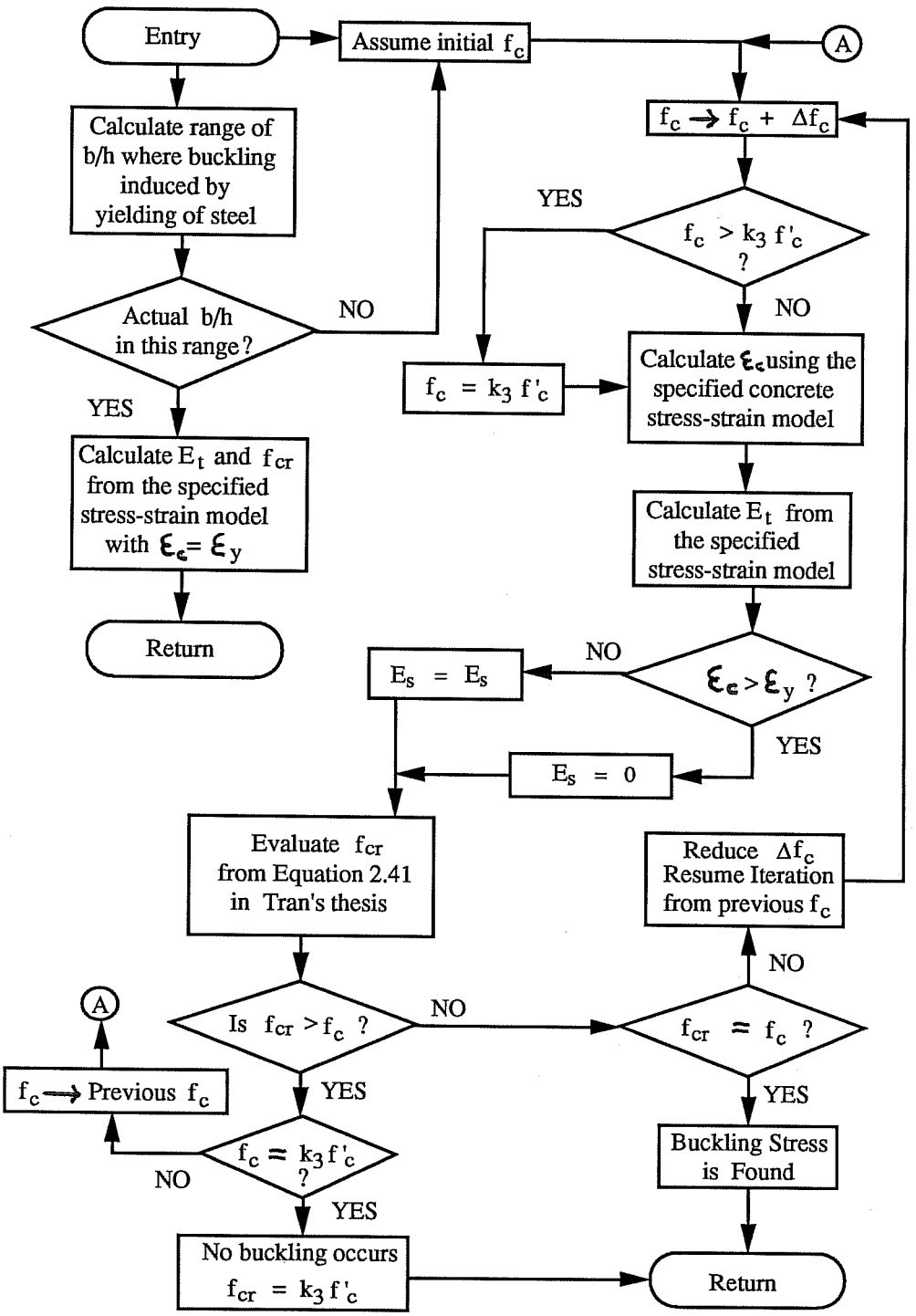

Figure 5.8 Flow Chart of Subroutine CALSTCR

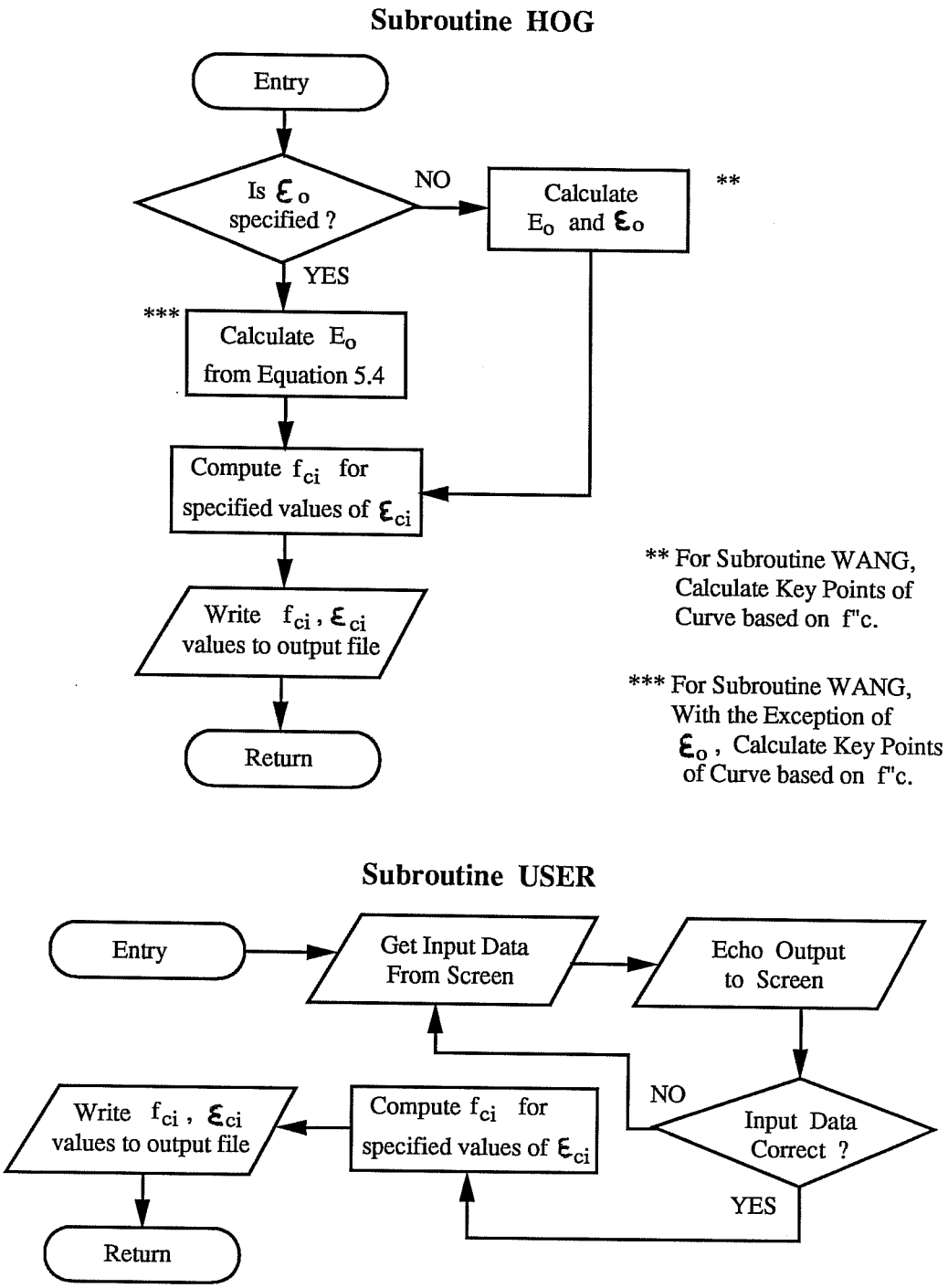

Figure 5.9 Flow Charts for Subroutines HOG, WANG, and USER

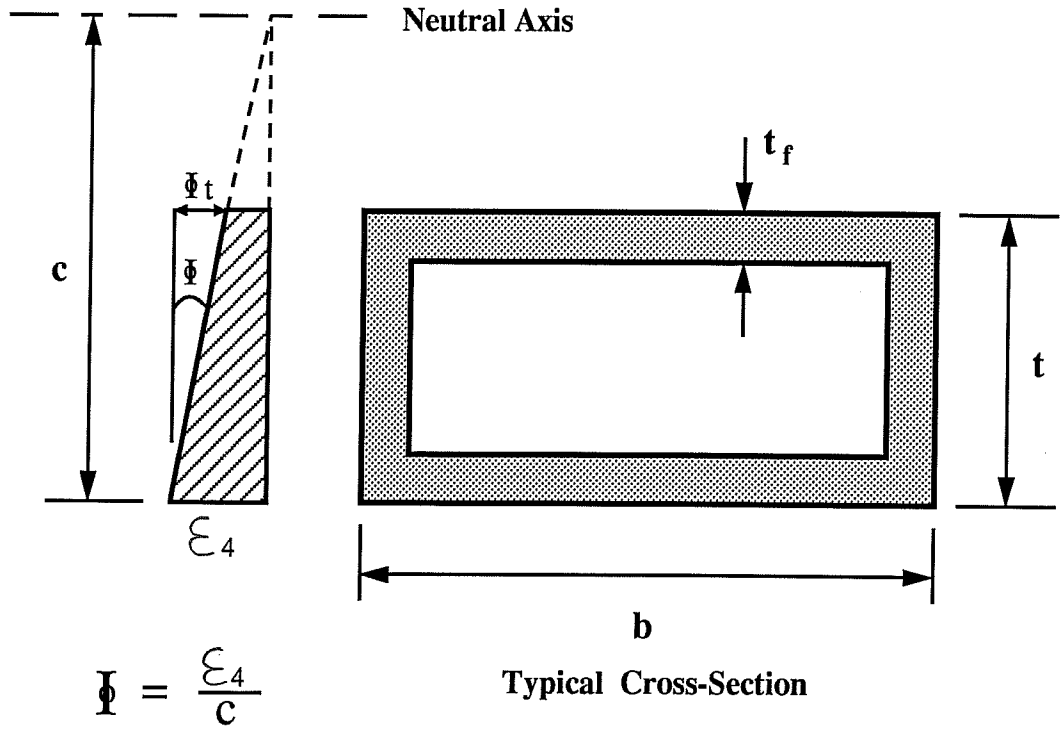

Figure 5.10 Assumed Concrete Strain Distribution

The basic scheme of the program is as follows. For a specified axial load the maximum moment is desired. To calculate the moment, two other values must be known; strain, ϵ and curvature, Φ. However, the moment calculated for particular values of ϵ and Φ might not correspond to the specified value of axial load. Breen (22) has shown that for a particular value of axial load, P, and curvature, Φ, there exists a unique value for strain, ϵ. Therefore, by assuming a value of curvature, Φ, for a specified value of axial load, there can be an iteration performed on ϵ until a value of axial load within a certain range of the specified value is found. The moment corresponding to the value found for ϵ and the assumed value of Φ can then be calculated.

By assuming a wide range of curvatures, the moment-curvature relationship for the specified axial load can be determined. A search of the values of moment for the specified axial load can be performed to find the maximum value of moment. This maximum value of moment for the specified axial load corresponds to one point on the interaction diagram of the section. Because the moment-curvature diagram for a particular axial load may have a descending branch terminated by the moment corresponding to the maximum strain, this traditional value of maximum moment may be lower than the moment corresponding to a

lesser value of strain. The same procedure can be followed for each of the desired number of points on the interaction diagram.

Flowcharts for the program code developed to perform the preceding procedure are shown in Figures 5.11 through 5.13. The main program reads in material and geometrical properties. It then calculates the value of ϵ_u including consideration of the critical stress, f_{cr}, from program PLCRST. For the number of points required for construction of the interaction diagram, the program calls subroutine CALMC which iterates on values of ϵ for various values of Φ. This subroutine also stores values of moment and curvature for each axial load and finds the maximum moment corresponding to a specified axial load. Subroutine CALMC calls subroutine CALPM which calculates the moment and axial load corresponding to particular values of ϵ and Φ using numerical integration of the stress-strain data. For the segmental specimens, the program calculates the capacity of the cross-section available after post-tensioning.

The strains due to the post-tensioning can either be input to the program directly or calculated from inputting the total post-tensioning force applied to the section. Subroutine ISTRN was written to calculate the initial strain in the section due to the total post-tensioning force applied to the cross-section. The flowchart for ISTRN is shown in Figure 5.14. By assuming strain compatibility in the cross-section between the

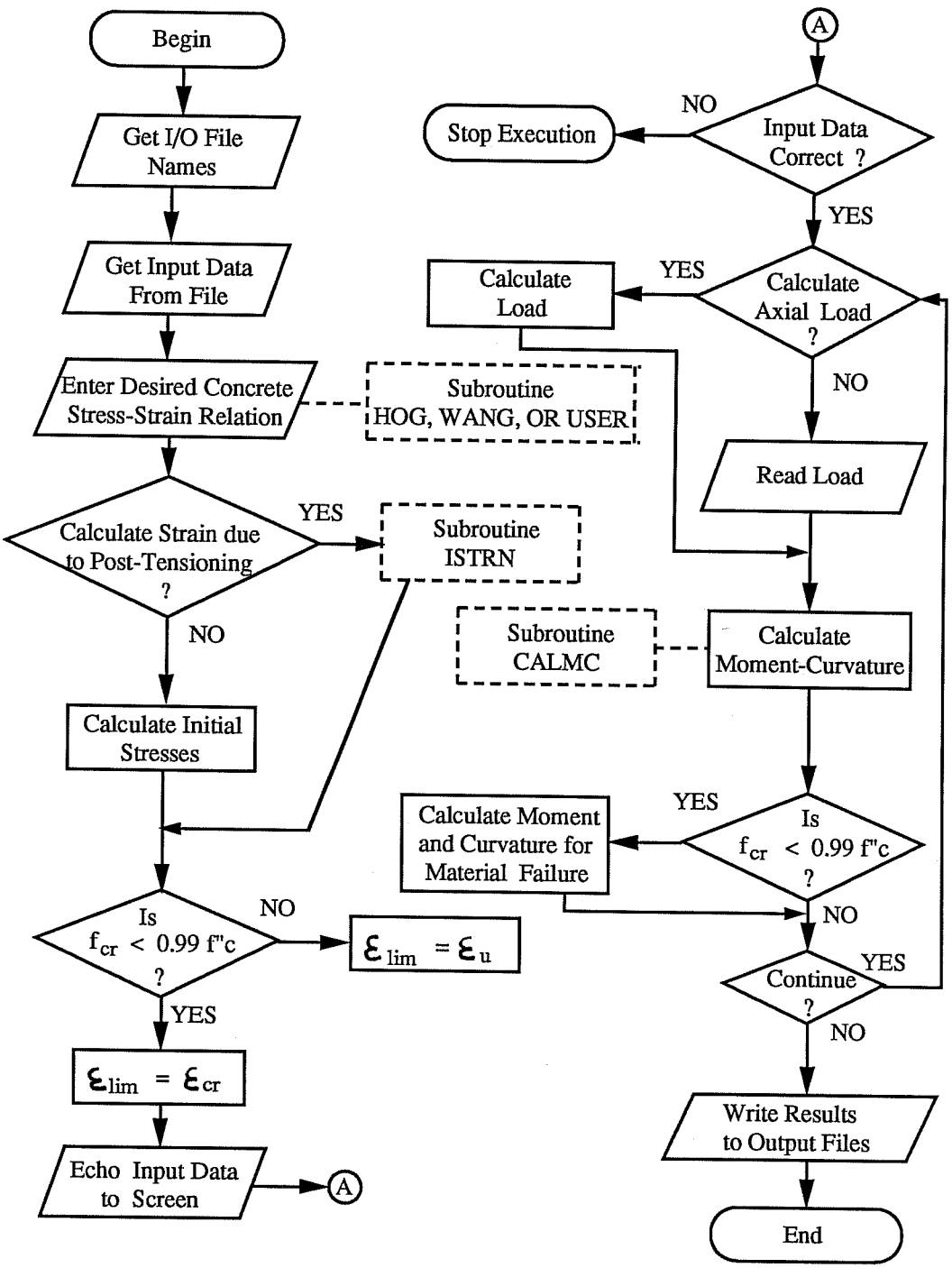

Figure 5.11 Flow Chart of the Computer Program MOMINT

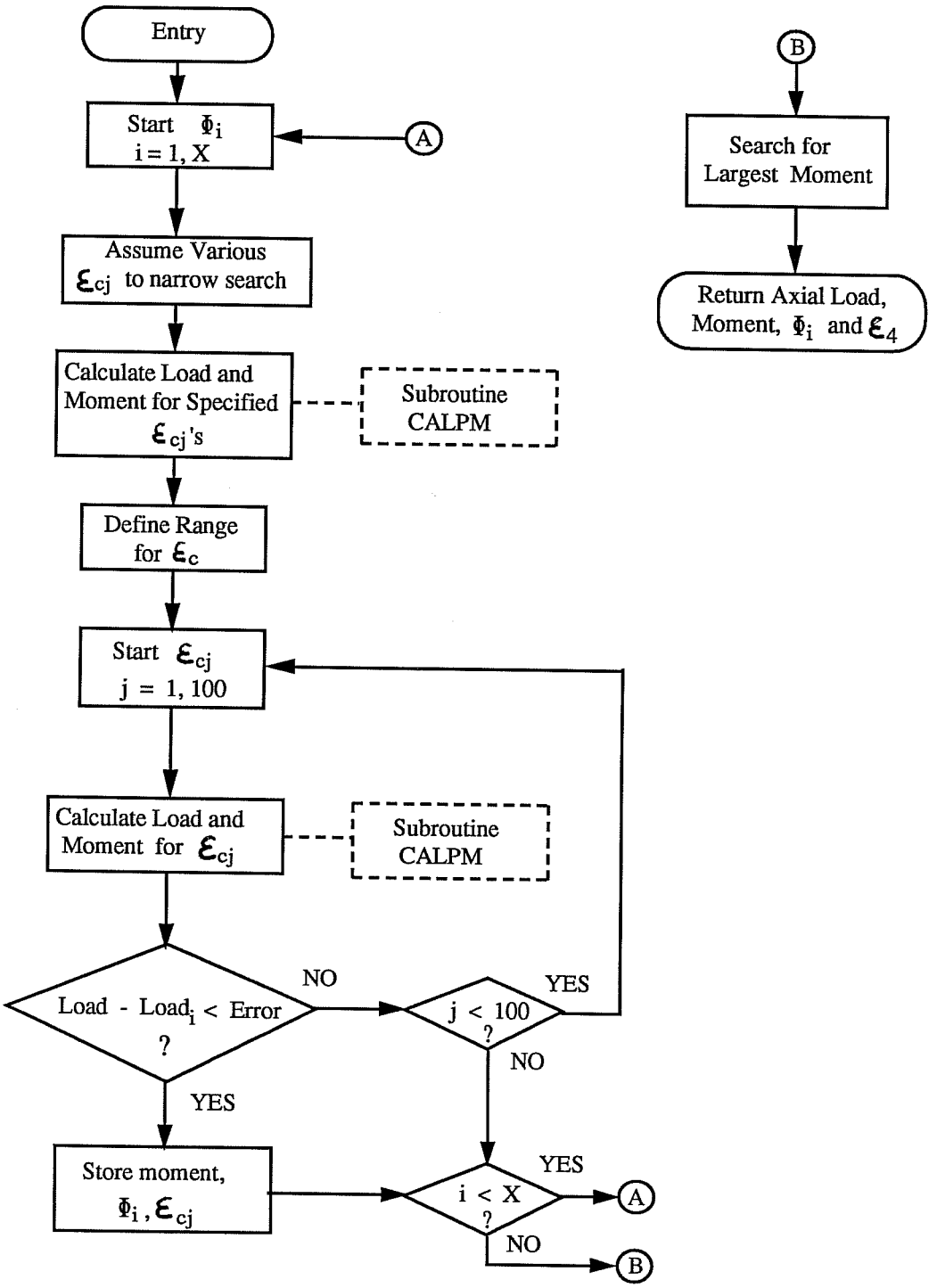

Figure 5.12 Flow Chart of Subroutine CALMC

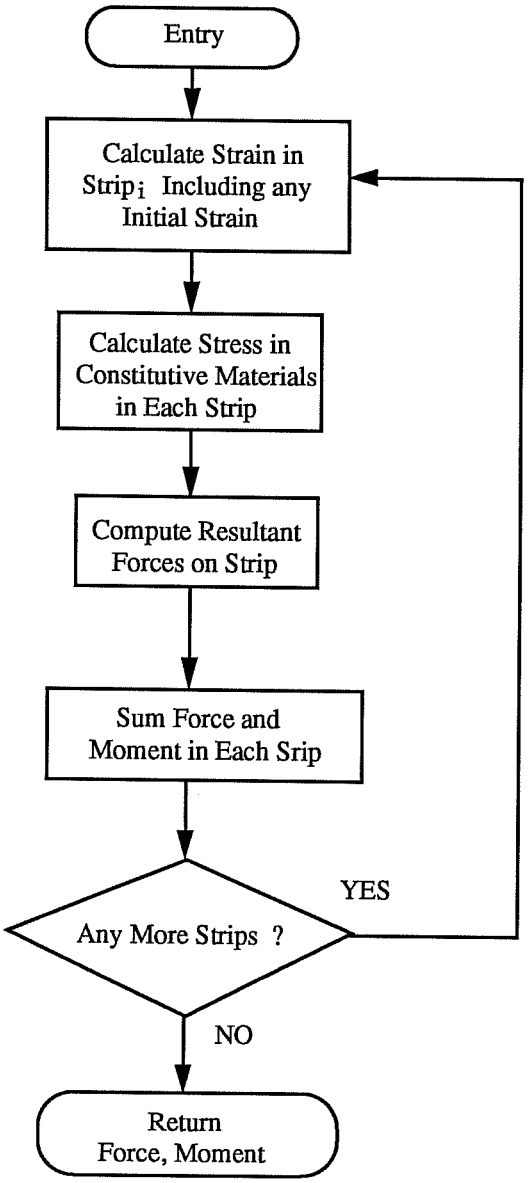

Figure 5.13 Flow Chart of Subroutine CALPM

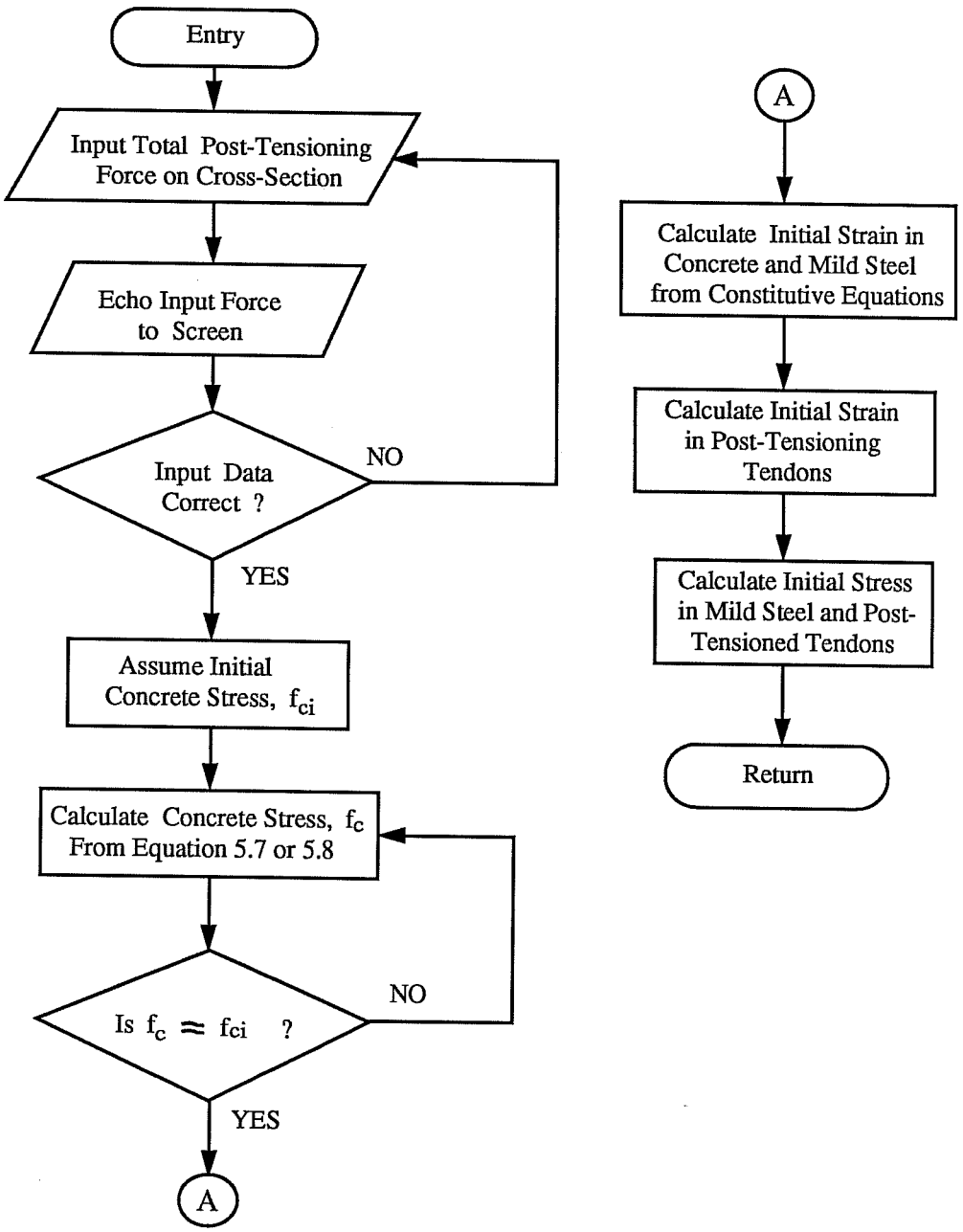

Figure 5.14 Flow Chart of Subroutine ISTRN

constitutive materials, the following equations were developed to calculate the concrete stress due to a uniform post-tensioning force applied to the section.

Assuming the initial concrete strain to be on the ascending portion of the stress-strain curve:

for Hognestad's stress-strain model,

$$f_c = \{F_i - \epsilon_o E_s A_s (1 - \sqrt{1 - f_c/f''_c})\}/A_c \qquad (5.7)$$

and for Wang's stress-strain model,

$$f_c = \{F_i - \epsilon_o E_s A_s (-S - \sqrt{S^2 - 4R})/2R\}/A_c \qquad (5.8)$$

where $R = D - Bf''_c/f_{cr}$ $\qquad S = C - Af''_c/f_{cr}$

and

$$A = E_c/E_o$$

$$D = (A^3 - 2.45A^2 + 1.9A - 0.45)/(0.55A - 0.2475)$$

$$C = -1 - 0.55D/(1-A)$$

$$B = C + D + 1 - A$$

Flowcharts for the subroutines used to define the stress-strain relationship for concrete were shown in Figure 5.9. The source code of program MOMINT as well as a guide for using the program are given in the Appendix.

Because of the uncertainty involved in calculating the critical buckling stress of each specimen, the interaction diagram program does not calculate the interaction diagram based on the critical stress, f_{cr}, unless it falls below $0.99f''_c$. There is no significant difference in strength at this level

between the section capacity based on material failure and the section capacity based on critical stress.

5.3 Comparison of Test Results to Analytical Model Predictions

5.3.1 Assumptions for Analysis of Cross-Section

5.3.1.1 Concrete Stress-Strain Model

For reasons previously mentioned, Hognestad's stress-strain model was used for the analysis.

5.3.1.2 Concrete Flexural Stress, f''_c

Based on Hognestad's work, the fact that these specimens were vertically cast, and the reasoning behind the reduction factor k_3, the maximum concrete flexural stress used in the analysis was:

$$f''_c = k_3 f'_c = 0.85 f'_c$$

5.3.1.3 Ultimate Compression Strain, ϵ_u

Although Hognestad recommended a value of $\epsilon_u = 0.0038$, from observing the experimental stress-strain data, it seemed that the recommended ACI (11) value of 0.003 was more applicable.

5.3.1.4 Modulus of Elasticity of Concrete, E_o

As previously mentioned, the value of E_o recommended by researchers at Cornell (19) for higher strength concrete (above 6000 psi) is used in the analysis. The modulus of elasticity is as follows:

$$E_o = 40{,}000 \sqrt{f''_c} + 1.0 \times 10^6 \quad (f''_c \text{ in psi})$$

5.3.1.5 Concrete Tensile Stress

It was assumed that the concrete was not able to develop tensile stresses.

5.3.1.6 Strain Distribution

The linear concrete strain distribution shown in Figure 5.10 was assumed throughout the analysis.

5.3.1.7 Cross-Sectional Area

The average wall thickness from the measurements recorded in Chapter 2 was used in defining the cross-sectional area used in the analysis.

5.3.1.8 Plane Sections

Plane sections are assumed to remain plane after bending.

5.3.2 Monolithic Specimens

5.3.2.1 Critical Stress

In calculating the theoretical pier capacity, the pier strength is assumed to be dependent on the critical buckling stress of the component plate subjected to the largest compressive force. Therefore, the geometric and material properties of the compression flange were input into the program PLCRST for calculation of the critical buckling stress for each specimen. Using the program's notation (see Appendix), key input data for each specimen is listed below.

Table 5.2 Properties for Calculating Critical Stress of Plates

Specimen	f'_c (ksi)	ϵ_o	a (in)	b (in)	h (in)	b_f (in)	ZBAR (in)	RO (%)
1M	7.862	0.00313	72	25	2.554	10	0.5	1.82
2M	7.705	0.00309	72	36	2.132	16	0.375	1.32
3M	6.311	0.00273	72	37	1.551	17	0.375	1.54

Notes: -Reinforcement properties: f_y = 75.1 ksi, E_s = 29000 ksi
-k_3 = 0.85, ϵ_u = 0.003, NU = 0.2

The value of 0.2 used for Poisson's ratio, NU, is based on the work with higher strength concretes done at Cornell (19).

Since the critical stress of each specimen is assumed to be a function of the wall slenderness ratio, X_u/t_f, the critical stress of each specimen is listed along with the appropriate X_u/t_f in the following table.

Table 5.3 Critical Stress of Monolithic Specimens

Specimen	X_u/t_f	f_{cr}	f''_c	f_{cr}/f''_c
1M	10	6.673	6.683	0.999
2M	18	6.491	6.549	0.991
3M	24.7	5.350	5.364	0.997

Since f_{cr}/f''_c is not below 0.99, the interaction diagram program, MOMINT, did not calculate the capacity of the monolithic specimens based on local buckling of the compression flange.

5.3.2.2 Strength and Stiffness

The strength and stiffness of the monolithic specimens is shown through the use of interaction diagrams and moment-curvature diagrams constructed from output of the interaction diagram program, MOMINT.

In order to understand how the value selected for ultimate strain, ϵ_u, and a particular stress-strain model influences the interaction diagram, interaction diagrams are also shown for Wang's stress-strain model and $\epsilon_u = 0.0038$. With the exception of ϵ_o, which was set equal to Hognestad's value, Wang's model is presented in its original form.

5.3.2.2.1 Strength

Interaction diagrams for each specimen are shown in Figures 5.15 and 5.16. From these figures it is evident that the capacity of the piers was less than their theoretical strength. A comparison of failure loads and theoretical capacities is given in Table 5.4.

Table 5.4 Comparison of Failure Loads and Calculated Capacities for Monolithic Specimens

Specimen	X_u/t_f	P_{test} (kips)	P_n (kips)	P_{test}/P_n
1M	10	527	550	0.96
2M	18	938	1300	0.72
3M	24.7	904	1000	0.90

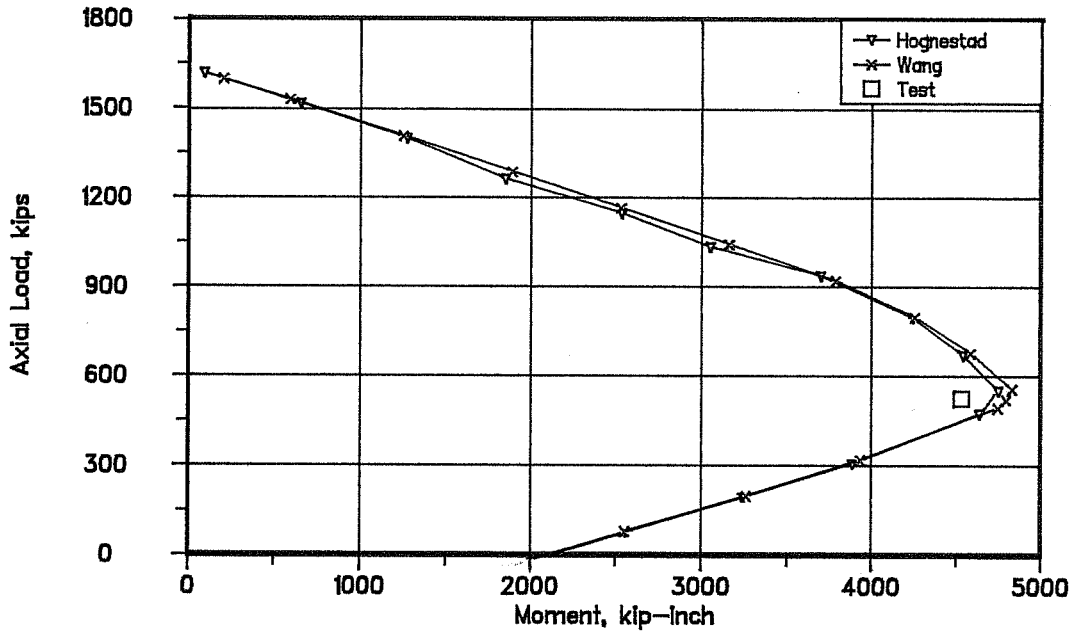

Specimen 1M Interaction Diagram, $X_u/t_f = 10$

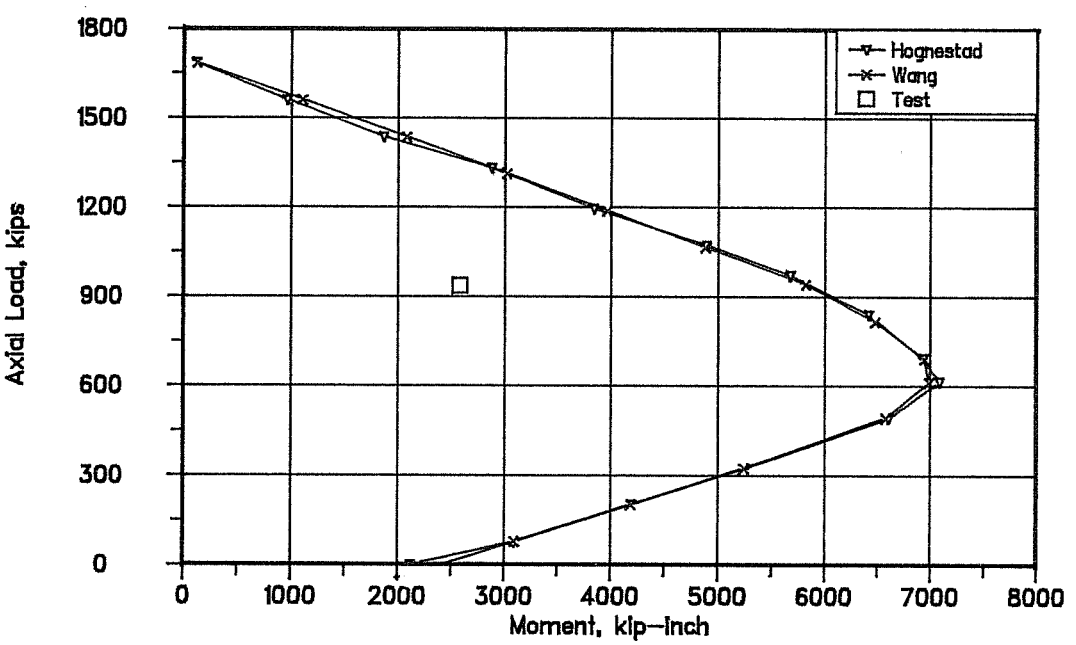

Specimen 2M Interaction Diagram, $X_u/t_f = 18$

Figure 5.15 Interaction Diagrams for Specimens 1M and 2M

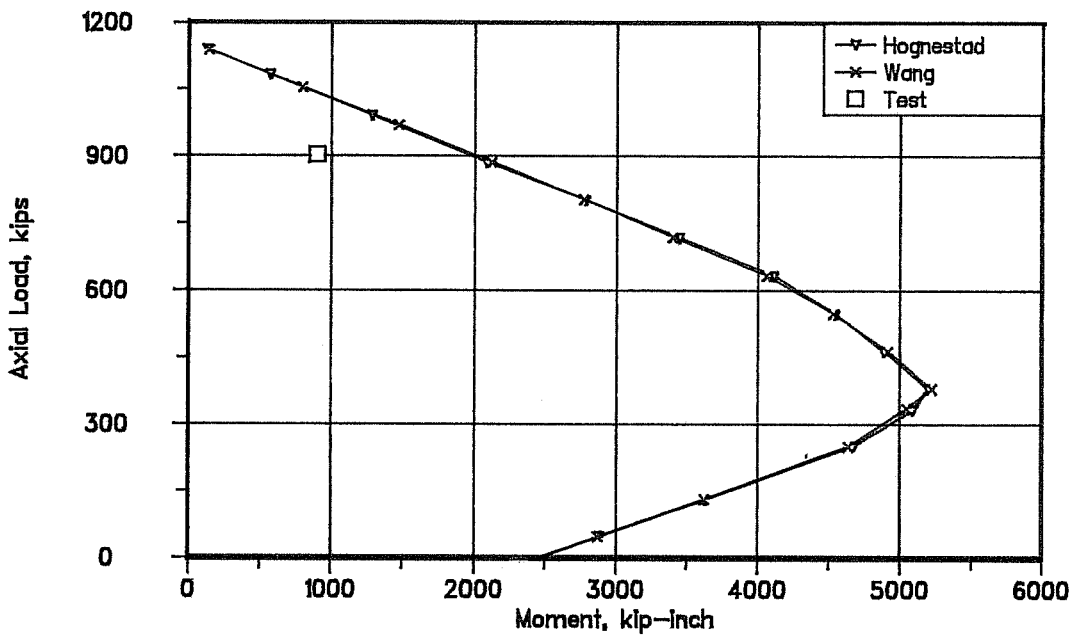

Figure 5.16 Interaction Diagram for Specimen 3M, X_u/t_f = 24.7

Experimental errors that may contribute to the understrength of the specimens include the accuracy of the flexural concrete stress reduction factor, k_3, stress concentrations at the discontinuity of the cross-section between the load heads and the pier, and construction errors. The stress reduction factor is introduced into the analysis to take into account the casting position. However, unlike the ordinary columns on which Hognestad recommended the use of $k_3 = 0.85$, there was extensive vibrating to insure proper consolidation of the concrete in the thin-walled piers. Because of the additional vibration, water tended to rise, increasing the water-to-cement ratio near the top of the specimen. Therefore, it is theorized that the concrete at the top of the pier may have been weaker than that found in the remainder of the pier or cylinders. This hypothesis may be one reason why failure occurred near the top of each of the monolithic piers. However, this problem should have been limited primarily to Specimens 1M and 2M which, unlike the other specimens, were cast in one continuous lift.

As evidenced by the crack patterns and displacements discussed in Chapter 4, the transfer of load from the load heads to the pier section caused stress concentrations in that vicinity. These stress concentrations may provide another reason for premature failure of the specimens. Stress

concentrations were also evident at the bottom of the pier section. However, the lap splices between the steel in the bottom load head and the pier specimen effectively doubled the amount of reinforcement extending 8 inches into the bottom of the pier.

In addition, construction errors may contribute to the premature failure of the monolithic specimens. Referring to Figure 2.6 in Chapter 2, the measured wall thicknesses in Specimens 1M and 2M show a general decrease near the top of the pier section. Since the average of the measured wall thicknesses was used in the analysis, the strength of the cross-section at which failure occurred may be less than that shown in Figure 5.15.

More important than the experimental errors previously discussed, there are several other possible reasons for the premature failure of the monolithic specimens. From the behavior of the specimens presented in Chapter 4, it seems that the compression flange failure of each specimen may have been influenced by local instability. As observed in Figure 4.18, there was extensive longitudinal cracking in the compression face of Specimen 2M before failure. This may have caused the plate stiffness to be reduced more than that predicted by program PLCRST so as to cause a premature local instability problem. Since there was not much cracking observed on the

compression faces of Specimens 1M and 3M, the loss of stiffness is considered to be less severe.

More convincing evidence of the participation of local buckling in the failure of the monolithic specimens is evident in the compression face profiles shown in Figures 4.13, 4.30, and 4.55. It is evident from these figures that the failure region of each specimen coincided with substantial deflections of the compression plate. Also, the cracking pattern observed in Figure 4.35 seems to indicate that failure of Specimen 3M was initiated by local buckling of the compression flange.

As shown in Figures 5.15 and 5.16, the use of an increased value of ϵ_u (0.0038 vs. 0.003) and the stress-strain relationship defined by Wang (15) does not significantly influence the predicted capacity of the cross-section.

5.3.2.2.2 Stiffness

Theoretical moment-curvature diagrams for each specimen are shown in Figures 5.17 and 5.18. In each figure, the horizontal axis is represented by Φt, the curvature multiplied by the depth of the cross-section. Each figure shows the moment-curvature relationship for three levels of axial load; $P_n/P_o = 0.85$, $P_n/P_o = 0.40$, and $P_n/P_o = 0.15$, where $P_o = f"_c A_{cr}$. These diagrams indicate similar patterns, with little or no ductility at high levels of axial load, somewhat ductile behavior at intermediate load levels, and ductile behavior at

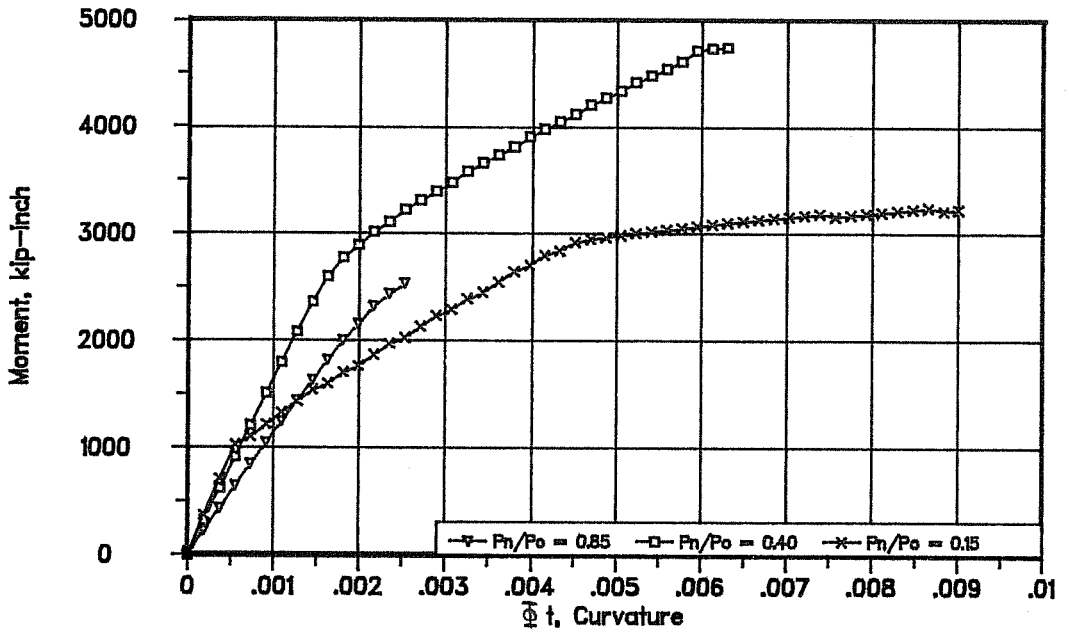

Specimen 1M Moment-Curvature Relationship, $X_u/t_f = 10$

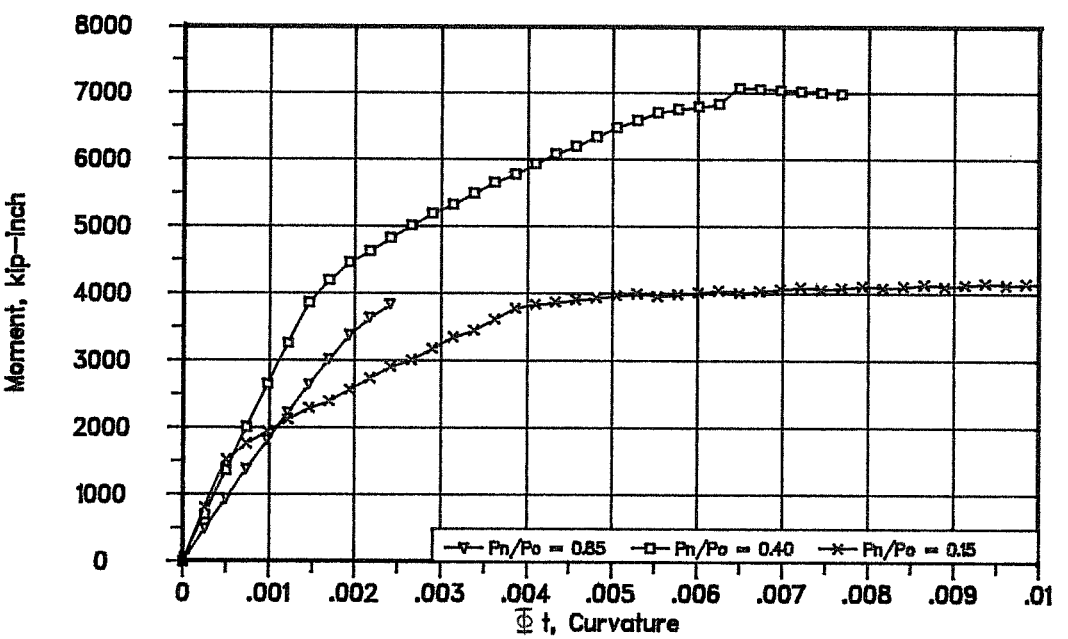

Specimen 2M Moment-Curvature Relationship, $X_u/t_f = 18$

Figure 5.17 Moment-Curvature Diagrams for Specimens 1M and 2M

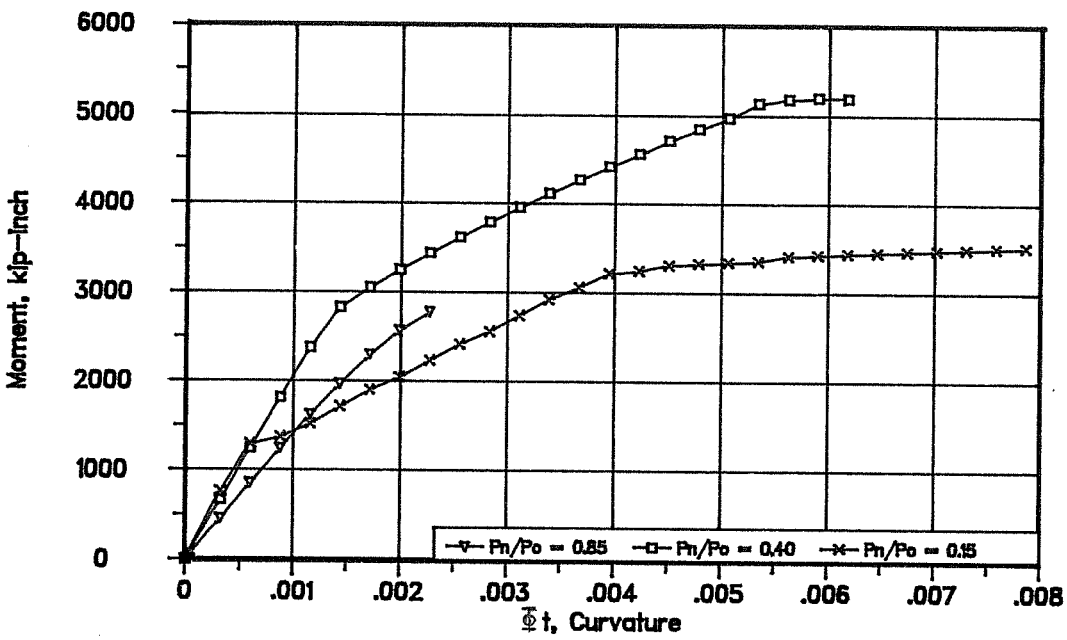

Figure 5.18 Moment-Curvature Diagram for Specimen 3M, $X_u/t_f = 24.7$

low levels of axial load. It is also interesting to note that the initial stiffness of each specimen increases as the level of axial load is reduced.

5.3.3 Segmental Specimens

5.3.3.1 Post-Tensioning Force and Losses

As recommended by ACI (11) and PCI (23), post-tensioning losses due to elastic shortening, anchorage seating, creep, shrinkage, and relaxation were all considered.

The force applied to each tendon during post-tensioning was carefully controlled so that the force in each tendon was measured after seating losses and elastic shortening of the concrete. Therefore, losses due to these factors were not considered. However, following the guidelines set forth by PCI (23), losses due to creep, shrinkage, and relaxation of the tendons were considered.

The following table lists the initial post-tensioning force present in each tendon, the total loss due to the aforementioned factors, and the force assumed to be present in each tendon at the time of the test.

Table 5.5 Initial Post-Tensioning Force and Losses in Segmental Specimens Per Tendon

Specimen	Initial Force (kips)	Total Loss (kips)	Force Present at Time of Test (kips)
1S	35.0	3.5	31.5
2S	42.6	7.4	35.2
3S	32.1	3.4	28.7

5.3.3.2 Critical Stress

The critical stress for each specimen was calculated using the analysis program PLCRST. However, since the mild longitudinal reinforcement was discontinuous, the analysis was performed twice; once including the mild longitudinal reinforcement, and once without including the mild longitudinal reinforcement. Using the program's notation, key input data for each specimen is listed below.

Table 5.6 Properties for Calculating Critical Stress of Segmental Specimens, Including Longitudinal Steel

Specimen	f'_c (ksi)	ϵ_o	a (in)	b (in)	h (in)	b_f (in)	ZBAR (in)	RO (%)
1S	6.980	0.00291	72	21	2.443	6	0.5	1.81
2S	4.837	0.00231	72	31	2.036	11	0.375	1.53
3S	6.916	0.00289	72	33.5	1.521	13.5	0.375	1.70

Notes: -Reinforcement properties: f_y = 75.1 ksi, E_s = 29000 ksi
-k_3 = 0.85, ϵ_u = 0.003, NU = 0.2

The properties for the analyses excluding the longitudinal steel were identical except for the reinforcement ratio, RO, which was set equal to 0.0 for each specimen.

The critical stress and wall slenderness ratio, X_u/t_f, of each specimen is listed in the following table.

Table 5.7 Critical Stress of Segmental Specimens

Specimen	X_u/t_f	f_{cr}	f''_c	f_{cr}/f''_c
Including Mild Reinforcement				
1S	8.4	5.930	5.933	0.999
2S	15.5	4.111	4.111	1.000
3S	22.3	5.815	5.879	0.989
Excluding Mild Reinforcement				
1S	8.4	5.930	5.933	0.999
2S	15.5	4.097	4.111	0.997
3S	22.3	5.740	5.879	0.976

As evidenced from the values presented in Table 5.7, the absence of reinforcement had little influence on the critical buckling stress, f_{cr}. Since the ratio of f_{cr} to f''_c for Specimen 3S was below 0.99, the interaction diagram program calculated the interaction diagram based on both the critical stress due to local buckling of the unsupported walls and material failure of the specimen.

5.3.3.3 Strength and Stiffness

In order to investigate the effect of the discontinuous mild longitudinal reinforcement, each of the segmental specimens was analyzed for two cases:

(1) Including the mild longitudinal reinforcement.

(2) Excluding the mild longitudinal reinforcement.

5.3.3.3.1 Strength

It is evident from the interaction diagrams shown in Figures 5.19 and 5.20 that the mild longitudinal reinforcement has a significant influence on the strength of the cross-section. It seems that there is roughly a 20 percent decrease in calculated strength with the exclusion of the mild longitudinal reinforcement.

As shown in Figures 5.19 and 5.20, each specimen failed below the section capacity defined by the analysis including the mild reinforcement, and above that capacity derived from the analysis excluding the mild reinforcement. Considering all three specimens, it seems that the analysis including the mild longitudinal reinforcement predicts the strength for Specimens 1S and 3S fairly accurately. On the other hand, it seems that the analysis excluding the mild reinforcement would be more appropriate for predicting the strength of Specimen 2S.

Results from the failure load analysis of the segmental and monolithic specimens are compared in Table 5.8. The

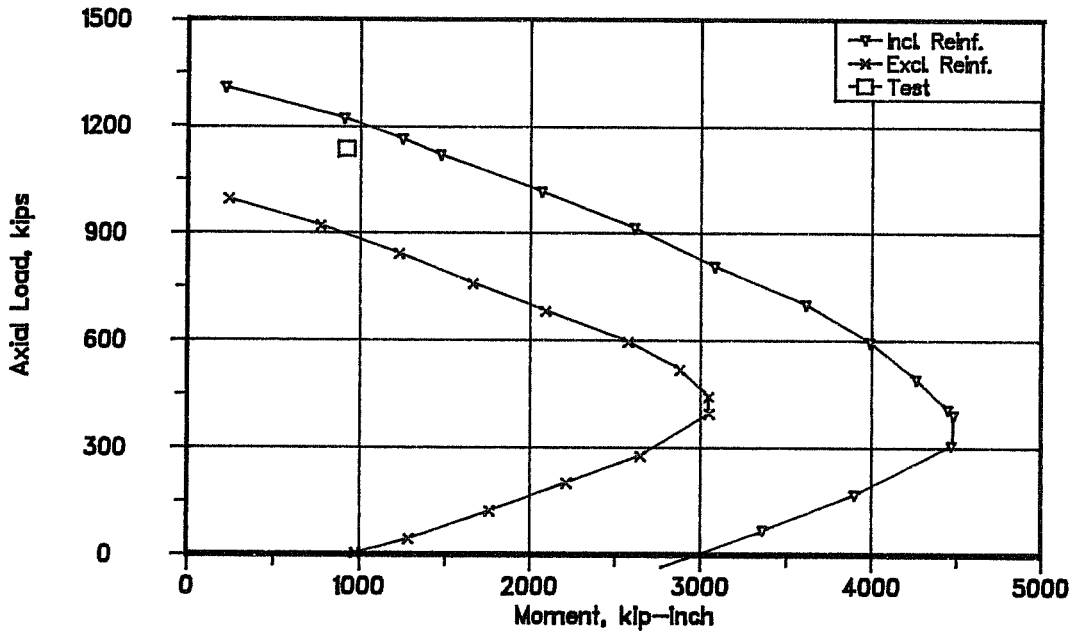

Specimen 1S Interaction Diagram, $X_u/t_f = 8.4$

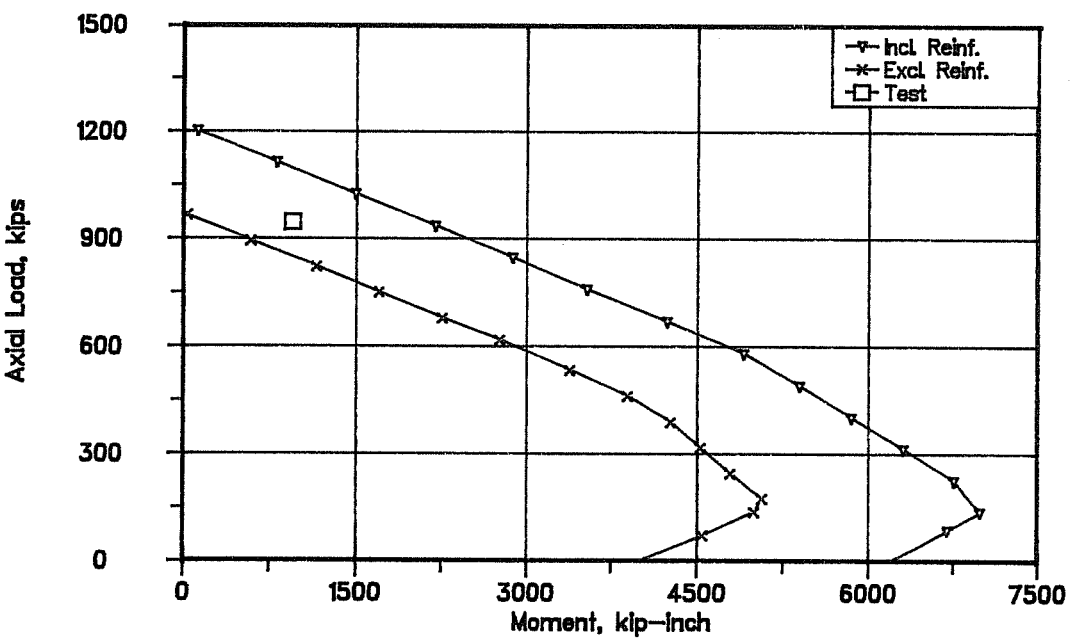

Specimen 2S Interaction Diagram, $X_u/t_f = 15.5$

Figure 5.19 Interaction Diagrams for Specimens 1S and 2S

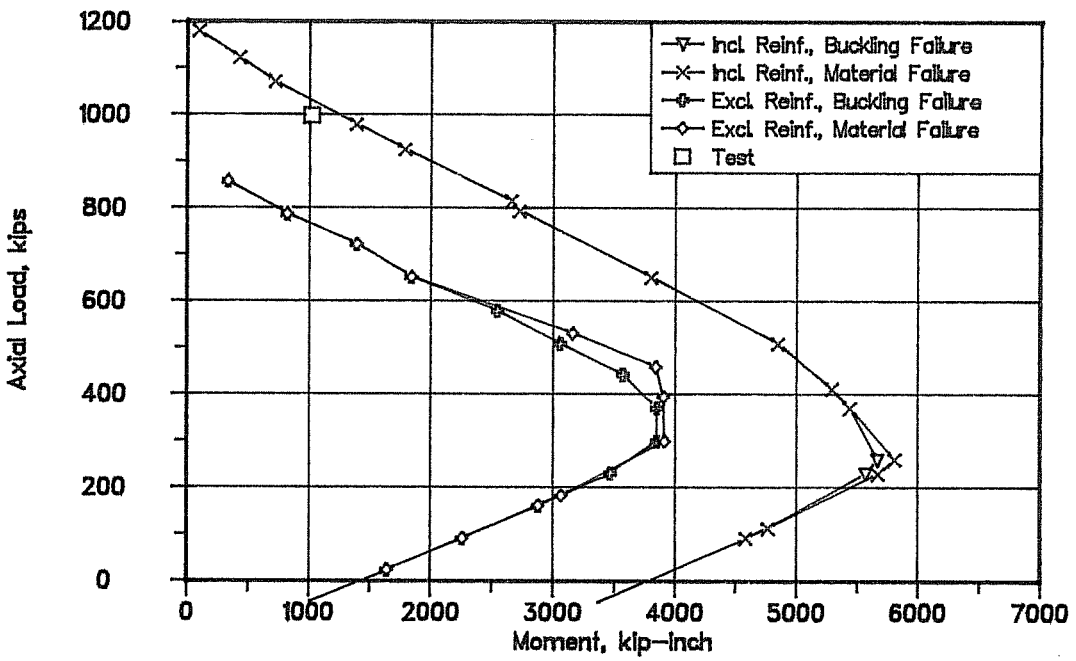

Figure 5.20 Interaction Diagram for Specimen 3S, X_u/t_f = 22.3

understrength of the segmental specimens compared to their capacity from the analysis for the case including the mild reinforcement is shown in the table. The comparison between the failure load and theoretical capacity, P_{test}/P_n, is similar for the segmental and monolithic specimens. Therefore, part of

Table 5.8 Comparison of Failure Loads and Calculated Capacities for Monolithic and Segmental Specimens

Specimen	X_u/t_f	P_{test}	P_n	P_{test}/P_n
1M	10	527	550	0.96
1S	8.4	1137	1250	0.91
2M	18	938	1300	0.72
2S	15.5	948	1125	0.84
3M	24.7	904	1000	0.90
3S	22.3	999	1050	0.95

the strength reduction may be attributed to the same factors discussed for the monolithic specimens. A reduction as severe as that shown for the analysis excluding the mild reinforcement seems unjustified since the experimental strength of each specimen exceeded the strength predicted from the analysis in all cases. Therefore, it appears that the use of discontinuous mild longitudinal reinforcement in the segmental specimens resulted in behavior similar to that of the continuous reinforcement found in the monolithic specimens.

Like the monolithic specimens, the failure of the segmental specimens seemed to be influenced by local instability of the compression flange. As noted in the discussion of the failure of Specimen 2M in the previous section, cracking of the compression flange may cause local buckling of the flange to occur prematurely. From the test results presented in Chapter 4, it was found that there was substantial cracking observed in the compression flange of Specimens 1S and 2S. It is interesting to note that these specimens have a lower P_{test}/P_n ratio than Specimen 3S in which very little cracking was observed. The compression face profiles shown in Figures 4.14 and 4.56 seem to confirm the influence of local instability. However, the compression face profile of Specimen 2S shown in Figure 4.31 does not seem to indicate any influence from local buckling.

As shown in Figure 5.20, the theoretically predicted strength reduction due to local buckling of Specimen 3S was only present near the balance point of the interaction diagram.

5.3.3.3.2 Stiffness

Theoretical moment-curvature curves for the segmental specimens are shown in Figures 5.21 and 5.22. As with the monolithic specimens, the segmental specimens seem to exhibit an increasing initial stiffness with decreasing axial load, though the initial stiffnesses for the two lower levels of axial load

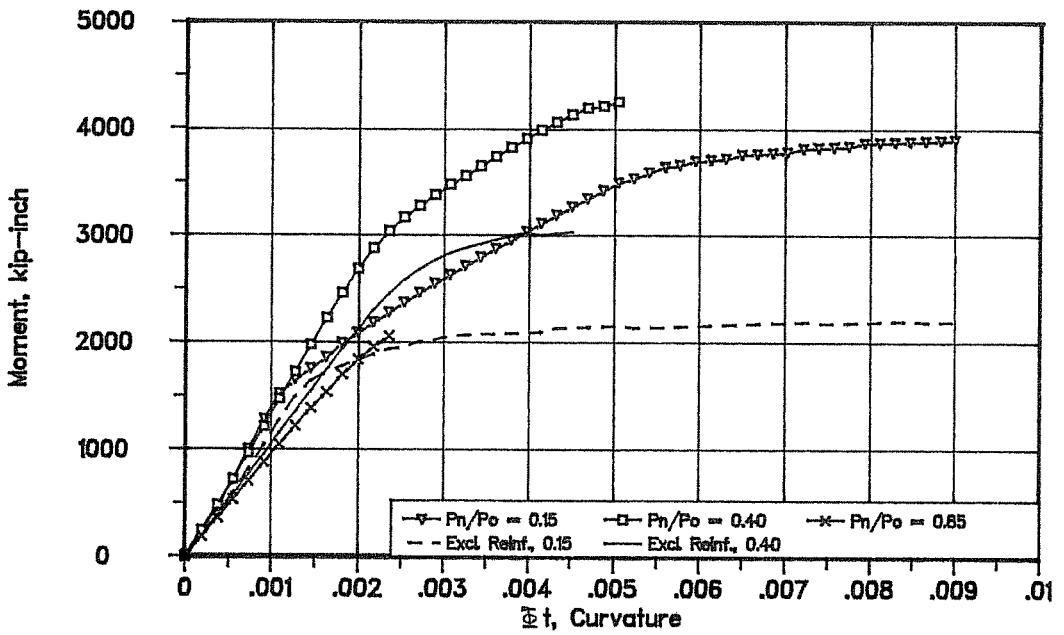

Specimen 1S Moment-Curvature Relationship, X_u/t_f = 8.4

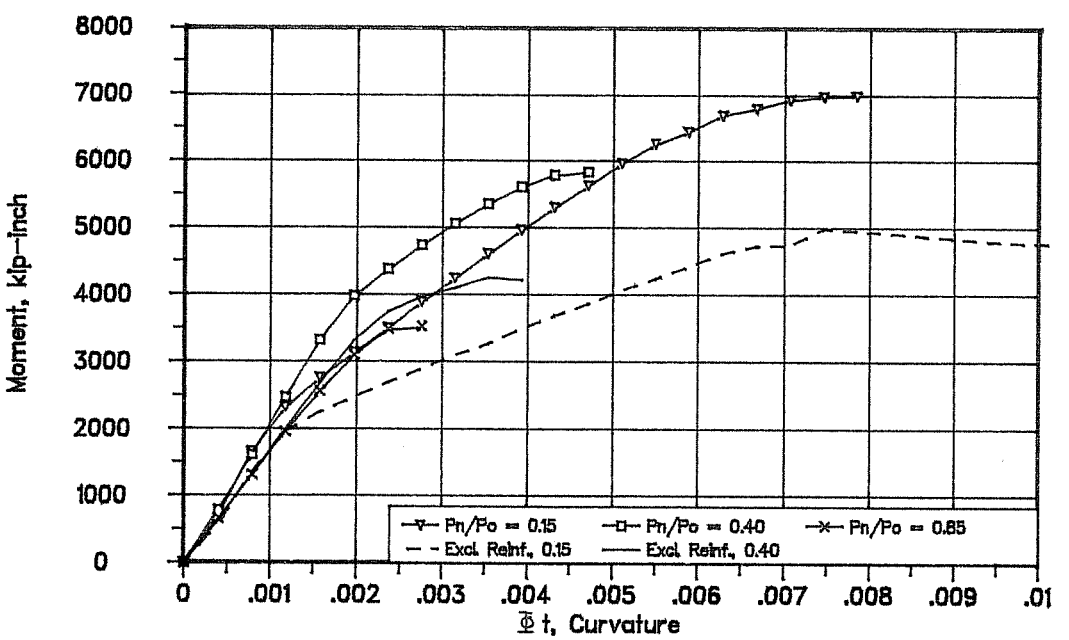

Specimen 2S Moment-Curvature Relationship, X_u/t_f = 15.5

Figure 5.21 Moment-Curvature Diagrams for Specimens 1S and 2S

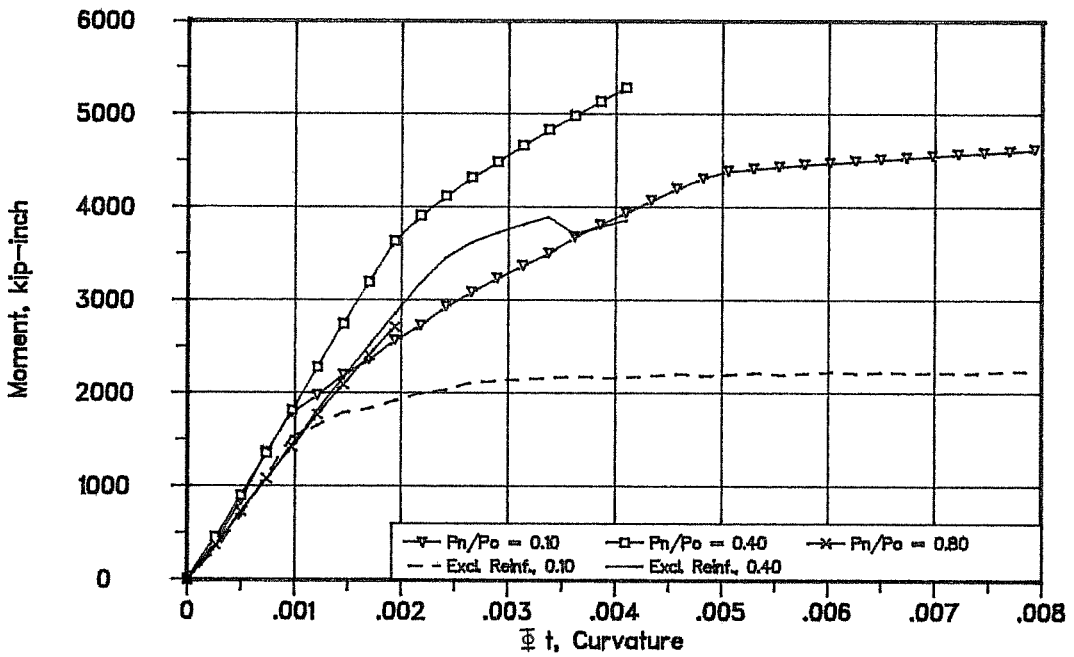

Figure 5.22 Moment-Curvature Diagram for Specimen 3S, $X_u/t_f = 22.3$

appear to be nearly identical. As expected, the ductility of each specimen increases with decreasing axial load.

In comparing the results from the analyses including and excluding the mild reinforcement, several observations can be made.

1) For comparative levels of axial load, the initial stiffness of the specimens excluding the mild reinforcement is less than the stiffness from the analysis including the mild reinforcement.

2) The amount of curvature ductility available in each section seems to be independent of the inclusion or exclusion of the mild steel.

3) The analysis which includes the mild longitudinal steel indicates a much larger moment capacity (40 to 100%) than the capacity determined from the analysis excluding the mild steel.

5.3.4 Post-Tensioned Monolithic Specimen

5.3.4.1 Post-Tensioning Force and Losses

As with the segmental specimens, losses due to elastic shortening, anchorage seating, creep, shrinkage, and relaxation were all considered.

The initial post-tensioning force present in each tendon, the total loss due to the aforementioned factors, and the force assumed to be present in each tendon at the time of the test were as follows:

Specimen	Initial Force (kips)	Total Loss (kips)	Force Present at Time of Test (kips)
3PM	32.1	3.3	28.8

5.3.4.2 Critical Stress

As for the other specimens, the critical stress was calculated for Specimen 3PM using the analysis program PLCRST. Since the mild longitudinal reinforcement was continuous, only one computer run was required. Using the program's notation, key input data for the specimen is listed below.

Table 5.9 Properties for Calculating Critical Stress of Specimen 3PM

f'_c (ksi)	ϵ_o	a (in)	b (in)	h (in)	b_f (in)	ZBAR (in)	RO (%)
6.463	0.00277	72	33.5	1.486	13.5	0.375	1.72

Notes: -Reinforcement properties: f_y = 75.1 ksi, E_s = 29000 ksi
-k_3 = 0.85, ϵ_u = 0.003, NU = 0.2

The critical stress and wall slenderness ratio, X_u/t_f, for Specimen 3PM is given below.

X_u/t_f	f_{cr}	f''_c	f_{cr}/f''_c
22.3	5.470	5.494	0.996

Since f_{cr}/f''_c was not below 0.99, the interaction diagram was calculated for material failure only.

5.3.4.3 Strength and Stiffness

5.3.4.3.1 Strength

As shown in Figure 5.23, the failure of this specimen was very close to the predicted pier capacity. However, from observing the test data presented in Chapter 4, it seems that local instability may have contributed to the failure. Though little cracking of the compression flange was observed prior to failure, the compression face profile shown in Figure 4.57 indicates relatively large deflections in the failure region. Observations of the failure region after failure also seemed to indicate some sort of buckling failure. As shown in Figure 4.40, the entire compression face was displaced outside of its original plane (about 1.5 inches).

5.3.4.3.2 Stiffness

The theoretical moment-curvature relation of Specimen 3PM is shown in Figure 5.23. Similar to that of the segmental specimens, the initial stiffness of Specimen 3PM is nearly identical for the two lower levels of axial load. In addition, the initial stiffness at the higher axial load is less than that of the two lower levels of load.

5.3.5 Wall Slenderness Effect, X_u/t_f

Since local instability seemed to contribute to the premature failure of the specimens, it was felt that there should be some correlation between the slenderness, X_u/t_f, of

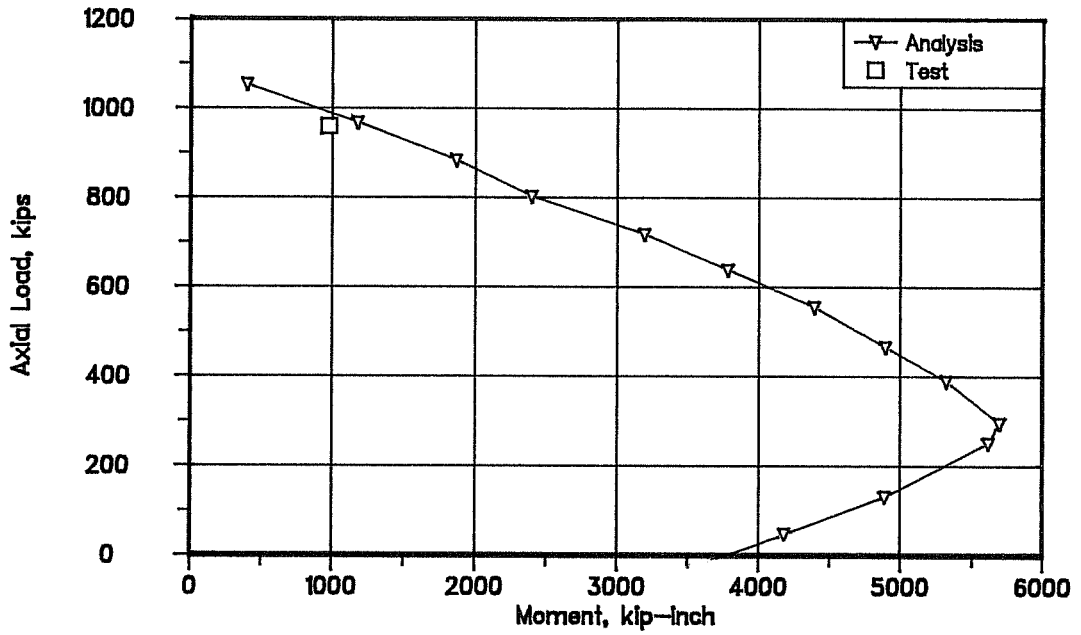

Specimen 3PM Interaction Diagram, X_u/t_f = 22.3

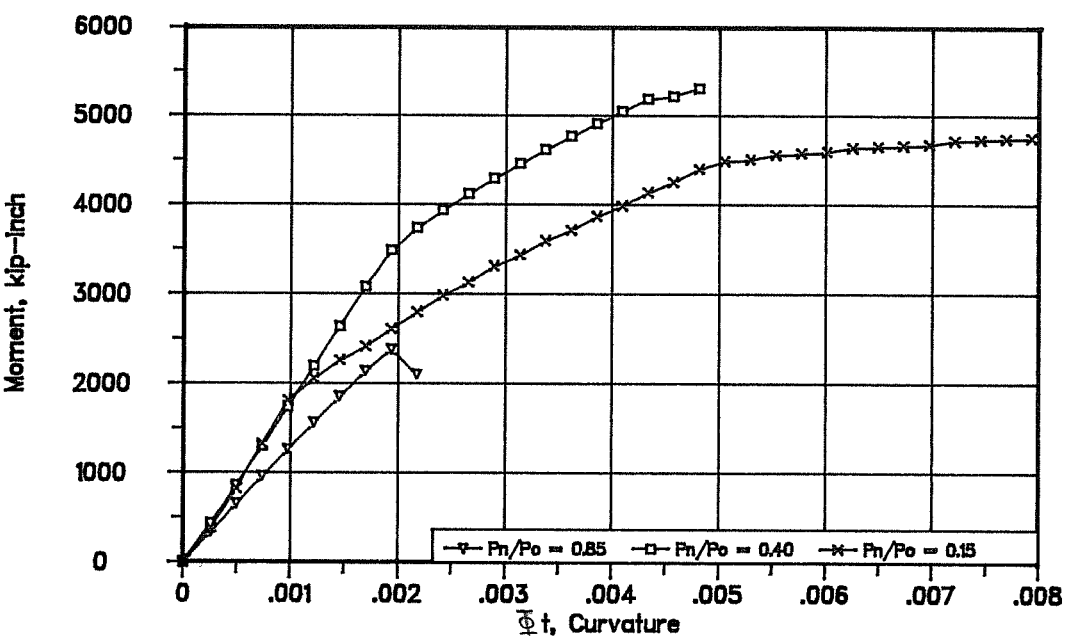

Specimen 3PM Moment-Curvature Relationship

Figure 5.23 Strength and Stiffness of Specimen 3PM

the piers' compression flange and the amount of strength reduction. In order to show the relationship between X_u/t_f and strength, the values listed in the following table are illustrated in Figure 5.24.

Table 5.10 Comparison of Failure Loads and Calculated Capacities for Specimens

Specimen	X_u/t_f	P_{test}	P_n	P_{test}/P_n
1M	10	527	550	0.96
1S	8.4	1137	1250	0.91
2M	18	938	1300	0.72
2S	15.5	948	1125	0.84
3M	24.7	904	1000	0.90
3S	22.3	999	1050	0.95
3PM	22.3	961	985	0.98

It is evident from Figure 5.24 that there is no clearly defined relationship existing between wall slenderness, X_u/t_f, and degree of understrength in the specimens presented in this thesis. However, it is interesting to note that the segmental specimens seemed to perform about as well as or better than the monolithic specimens, although it was somewhat expected because of their lower X_u/t_f ratios.

The interaction diagram program, which ignored the effect of reductions in stiffness due to the longitudinal cracking observed in the test specimens, does not predict a significant

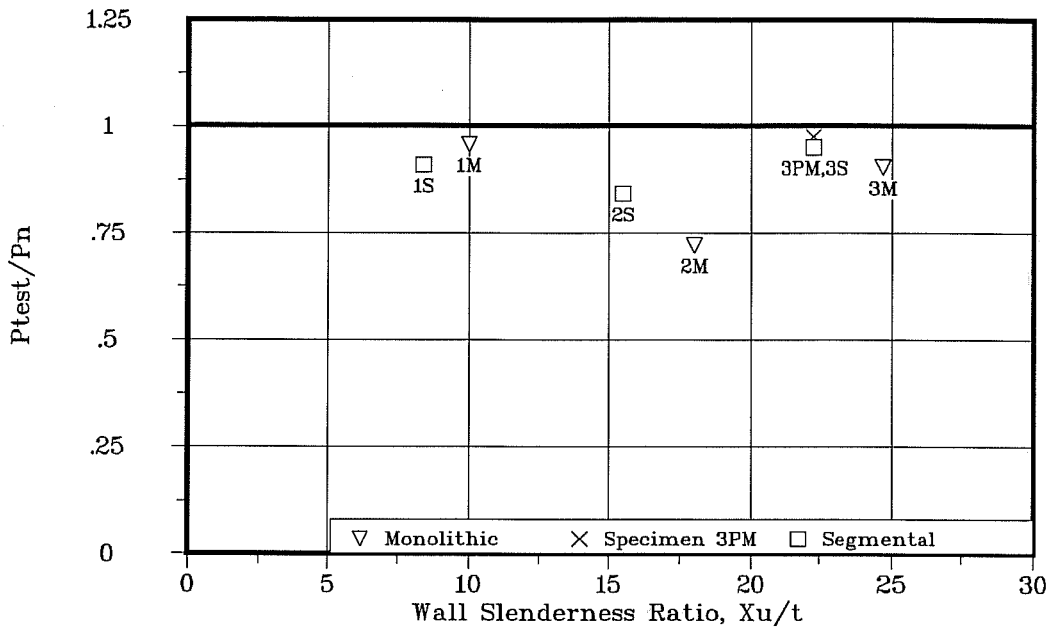

Figure 5.24 Effect of Wall Slenderness Ratios

strength reduction due to local instability of the component plates. It is probable that due to the observed cracking, the actual stiffness of the plates in the test specimens was less than that assumed in the analytical model. Therefore, problems due to local instability may occur at a lower slenderness ratio than predicted. The analytical model needs to be refined to consider such stiffness reduction effects.

5.3.6 Comparison of Strength and Stiffness

Using the following definitions, the data was normalized so that it could be better compared.

Axial Load ..... $R = P_n/(f"_c A_{cr})$

Moment ..... $Re/t_f = P_n e/(f"_c A_{cr} t_f)$

Since the effect of the discontinuous steel has already been investigated, the following comparison primarily addresses the differences between the behavior of the two sets of specimens due to post-tensioning. The mild longitudinal reinforcement was included in the analysis of the segmental piers. Therefore, the only significant differences between the following comparisons are concrete strength and the absence or presence of post-tensioning reinforcement and post-tensioning force.

5.3.6.1 Strength

Interaction diagrams for each specimen are shown in Figures 5.25 and 5.26. These figures further confirm that the test specimens were often less stiff than expected and that compression flange instability reduces the actual capacity below the predicted capacity.

In addition, since the understrength of Specimen 3PM appears nearly identical to that of Specimen 3S, the hypothesis that the discontinuous mild reinforcement has little effect on the capacity of the cross-section seems to be verified. Since the predicted reduction in strength due to local buckling was only present near the balance point, the interaction diagram shown for Specimen 3S includes the reduction for local buckling.

The comparison of Specimens 3M and 3PM is shown in Figure 5.27. Since these specimens differed only in the addition of

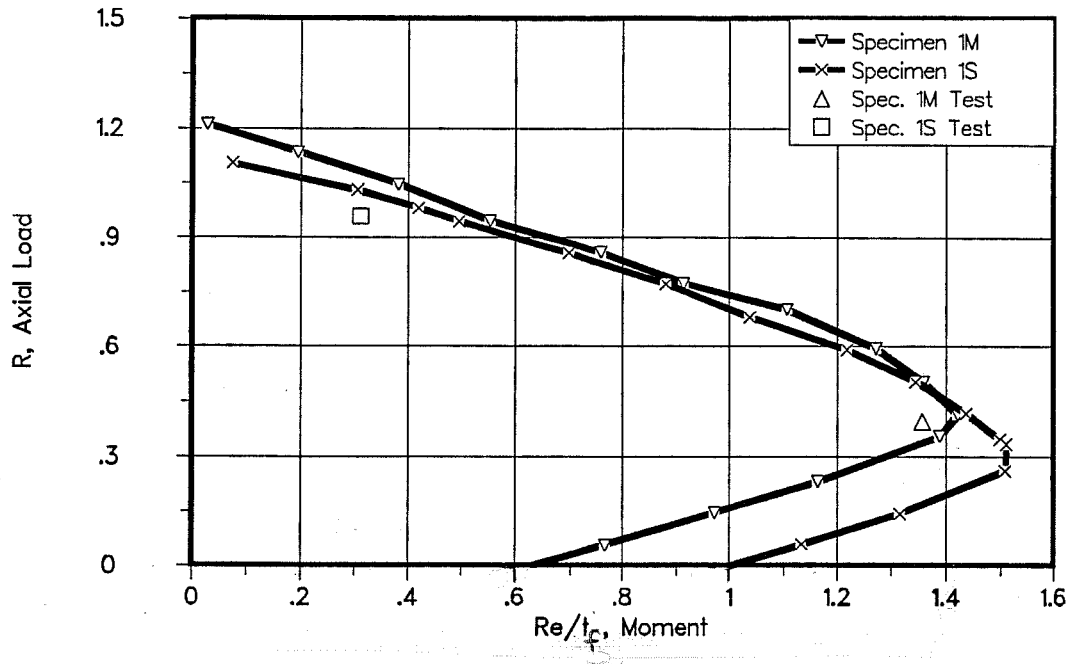

Specimens 1M and 1S Interaction Diagrams

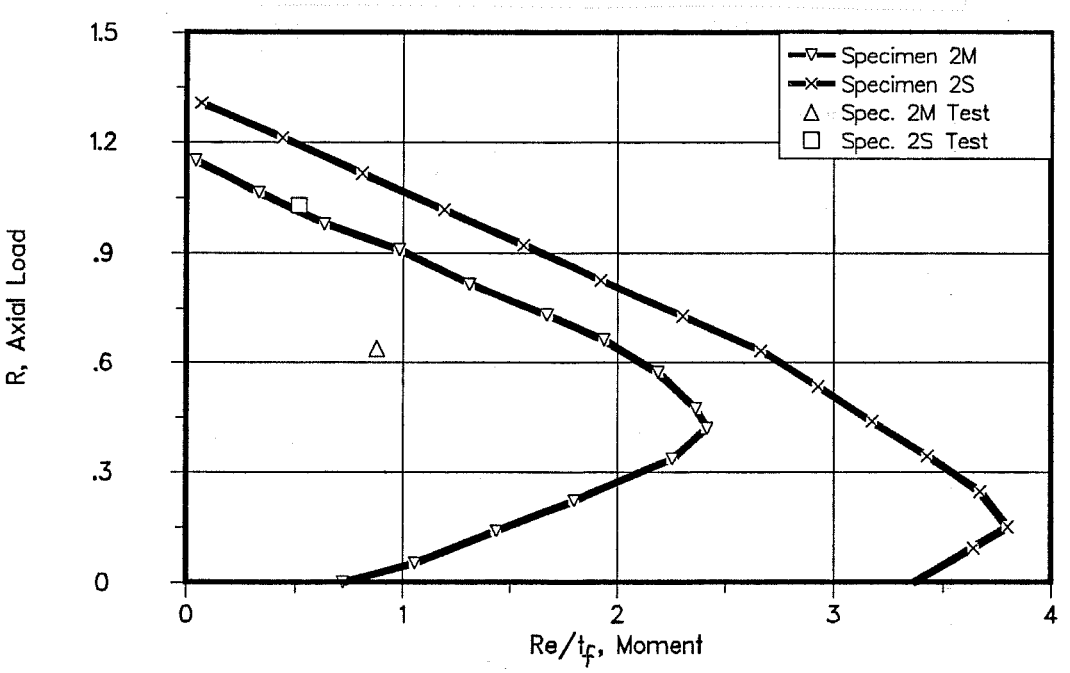

Specimens 2M and 2S Interaction Diagrams

Figure 5.25 Comparison of Interaction Diagrams

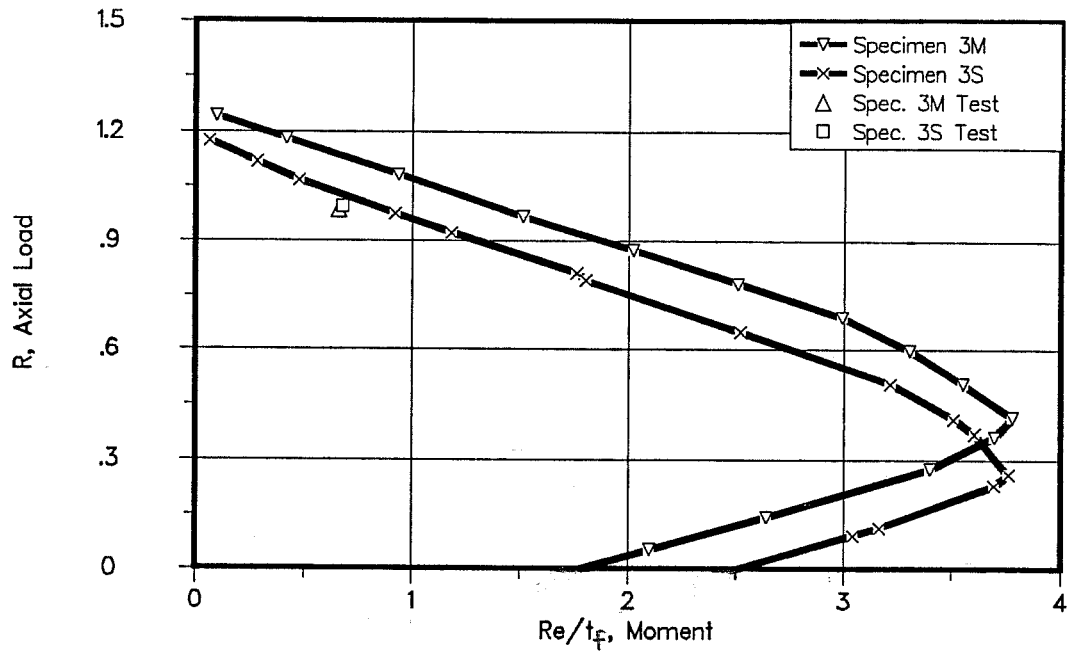

Specimens 3M and 3S Interaction Diagrams

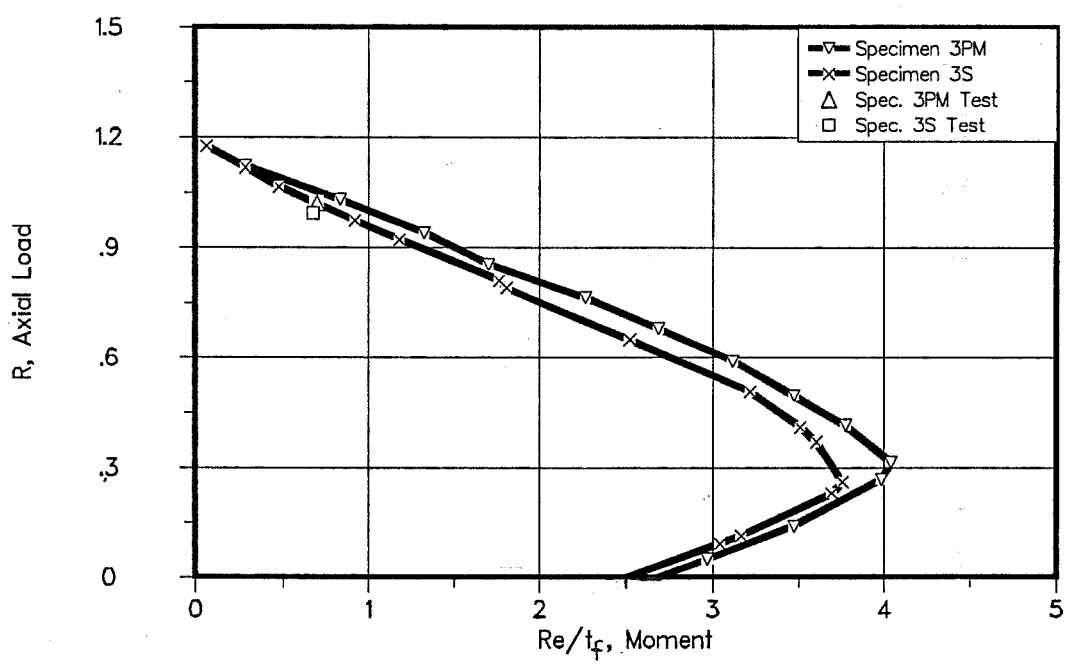

Specimens 3PM and 3S Interaction Diagrams

Figure 5.26 Comparison of Interaction Diagrams

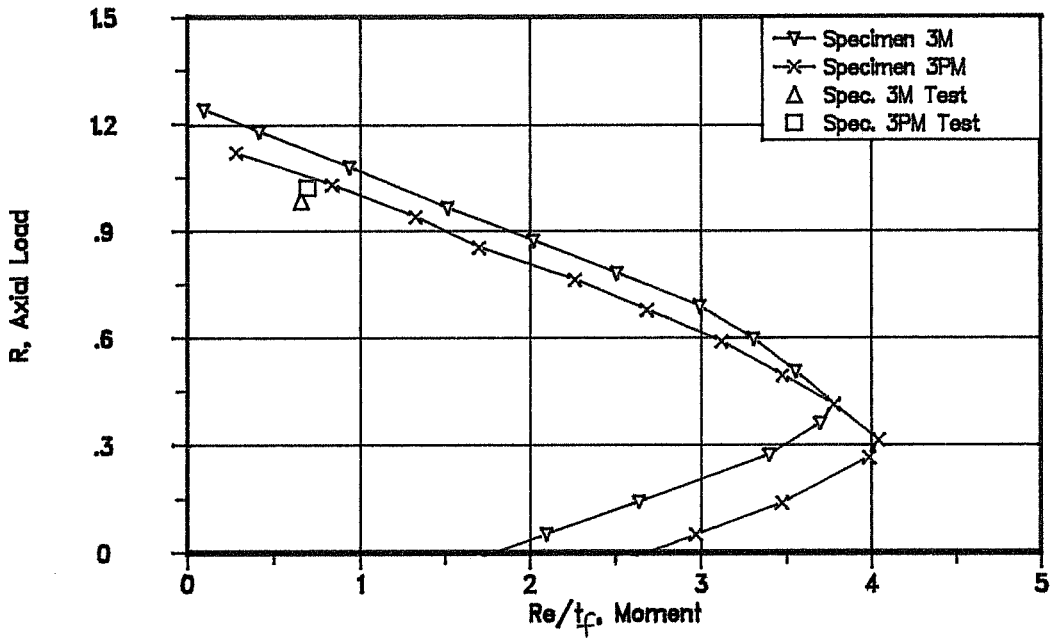

Specimens 3M and 3PM Interaction Diagrams

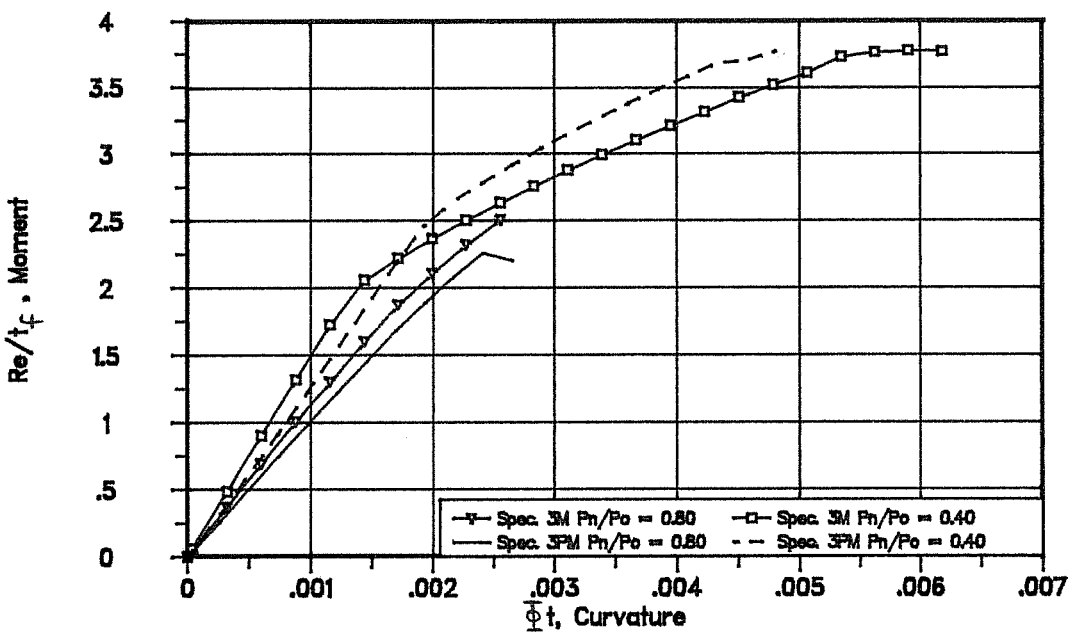

Specimens 3M and 3PM Moment-Curvature Relationships

Figure 5.27 Comparison of Diagrams for Specimens 3M and 3PM

the post-tensioning reinforcement and associated post-tensioning force, their effect can be closely examined. It is evident from the interaction curve of Figure 5.27 that there is a reduction in the axial load capacity of Specimen 3PM compared to Specimen 3M. However, this reduction can be attributed to the capacity taken by the post-tensioning force. On the other hand, the addition of the post-tensioning reinforcement seems to increase the moment capacity of the section.

5.3.6.2 Stiffness

The effect of the post-tensioning force and post-tensioning tendons can be more clearly seen in the theoretical moment-curvature plots shown in Figures 5.28 and 5.29.

Based on these moment-curvature curves, several observations were noted.

1) Additional rotational capacity is evident in the monolithic specimens which were not post-tensioned.

2) With the exception of Specimens 2M and 2S which had widely differing concrete strengths, the initial stiffness of the monolithic specimens seems to be slightly larger than that of the post-tensioned specimens.

3) In general, the moment capacity of the segmental specimens seems to be very similar to that of the monolithic specimens. The difference in moment capacity between Specimens

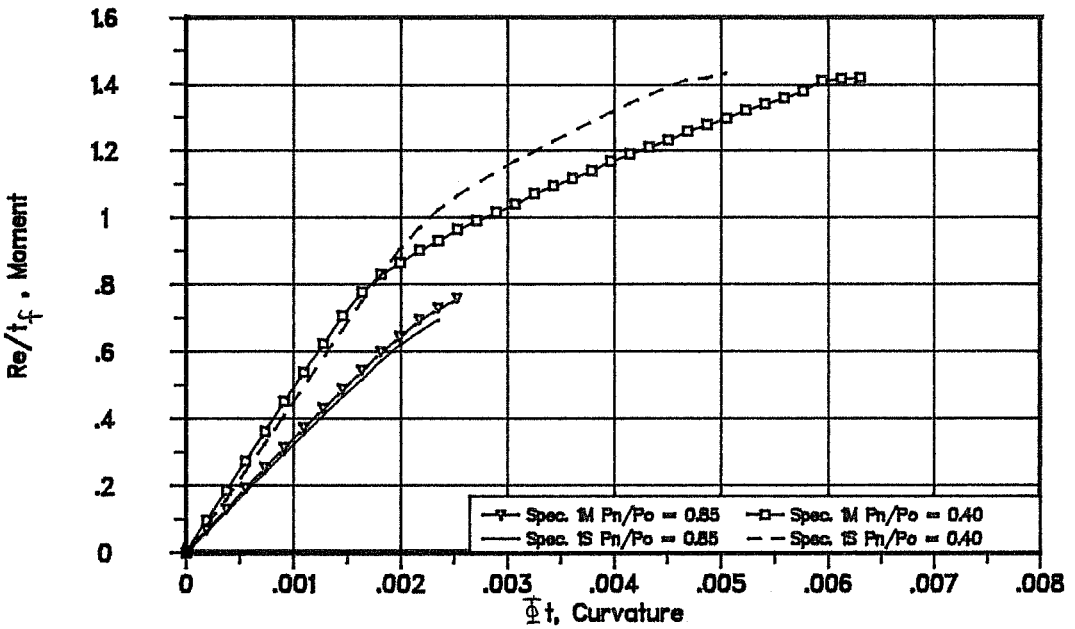

Specimens 1M and 1S Moment-Curvature Relationships

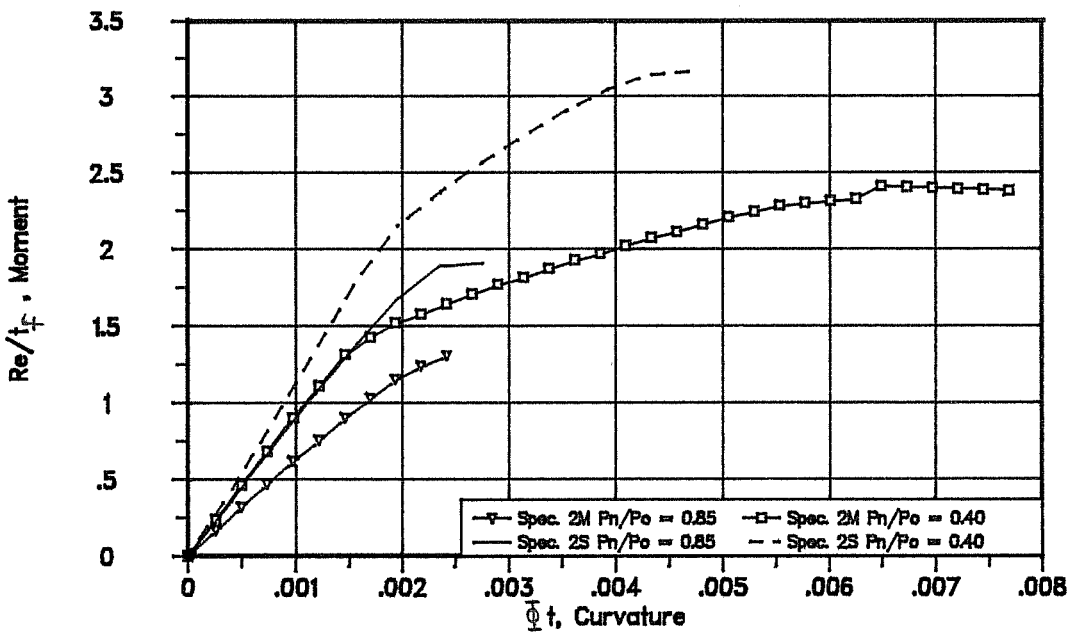

Specimens 2M and 2S Moment-Curvature Relationships

Figure 5.28 Comparison of Moment-Curvature Diagrams

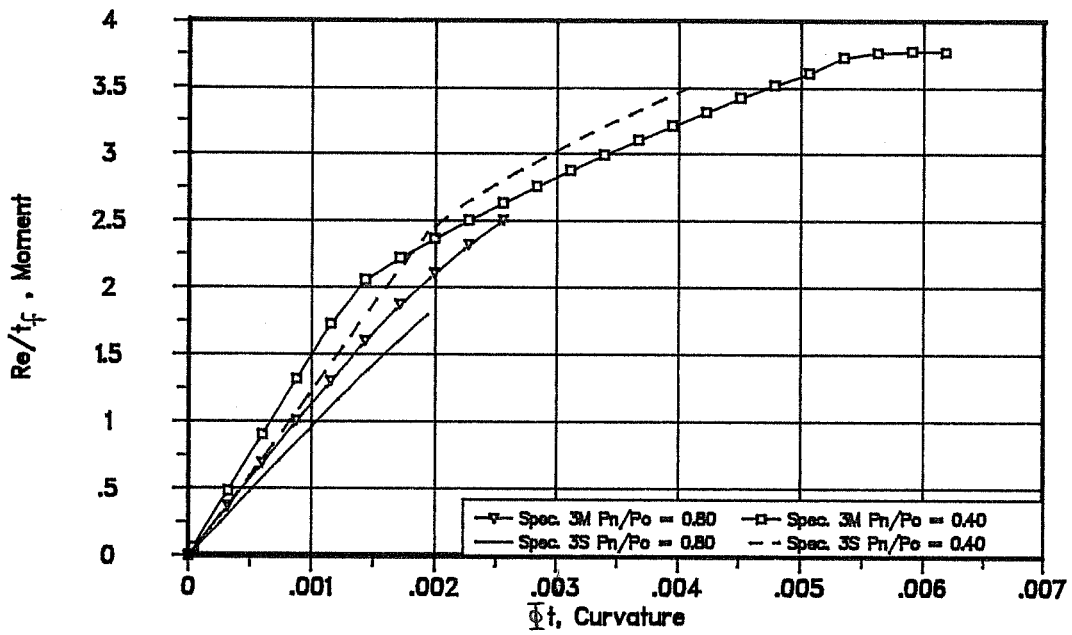

Specimens 3M and 3S Moment-Curvature Relationships

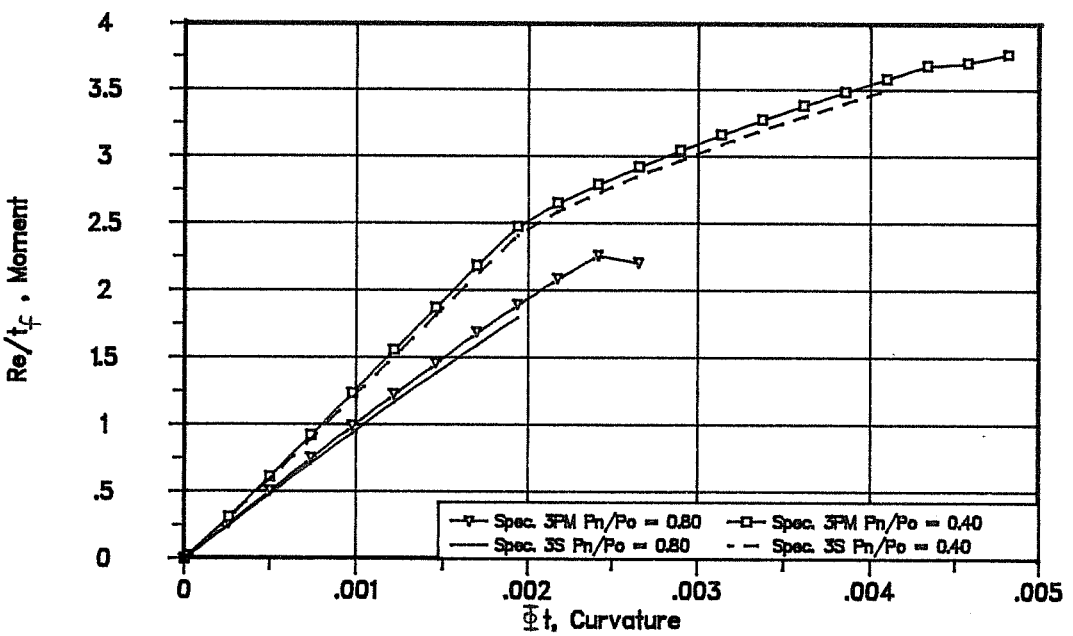

Specimens 3PM and 3S Moment-Curvature Relationships

Figure 5.29 Comparison of Moment-Curvature Diagrams

2M and 2S may be primarily attributed to their widely differing concrete strengths (7705 vs. 4837 psi).

4) Since the only significant difference in the results shown from the analyses of Specimens 3M and 3PM in Figure 5.27 is the addition of the post-tensioning tendons and associated force, it is evident that the post-tensioning force causes a reduction in initial stiffness. However, the addition of the post-tensioning tendons and force causes little difference in the moment-rotation capacity of the section.

5.4 Conclusions

From the analytical results presented, several conclusions can be made.

1) In addition to experimental error, there seems to be a significant strength reduction due to local instability of the compression flange of the test specimens. From the test results of Chapter 4 and the reduction observed in almost all specimens in comparison with the predicted strength shown in Chapter 5, it appears that the failures were significantly influenced by local buckling of the compression flange.

2) Surprisingly, the discontinuous mild reinforcement in the segmental piers exhibits behavior similar to that of the continuous mild reinforcement in each of the monolithic specimens. By comparing the analysis of the segmental piers

which included the mild reinforcement with the analysis excluding the mild reinforcement, it was shown that the discontinuous mild reinforcement provides a significant increase in strength over the capacity predicted when the reinforcement is neglected.

3) There is a substantial reduction (20 to 50%) in the moment capacity of the segmental specimens with the exclusion of the longitudinal mild reinforcement. Since the majority of the piers failed at large levels of axial load and relatively low values of bending moment, the reduction in moment capacity due to the use of discontinuous mild longitudinal reinforcement may not have been evident in the tests. Therefore, the inclusion of the discontinuous mild reinforcement might not be correct for analyses of pier sections subjected to low levels of axial load and large bending moments. However, since the curvature ductility of the section seemed unaffected by the discontinuous mild reinforcement, substantial moment capacity was apparently provided by the continuous post-tensioned reinforcement.

4) The addition of the post-tensioning force and tendons seems to influence the behavior of the cross-section in several ways: (1) The initial stiffness of the section seems to be reduced by the post-tensioning force; (2) There was an apparent reduction in the axial load capacity of the section; (3) There was an apparent increase in the moment capacity of the section;

(4) There was a slight decrease in rotational capacity, but no significant differences were noted in the moment-rotation capacity of the cross-section.

5.5 Design Recommendations

From the comparison of the segmental and monolithic specimens presented in Chapters 4 and 5, several design recommendations can be made for the design of segmentally constructed piers.

1) The design strength of segmentally constructed bridge piers should be calculated in the same manner as that of monolithically constructed piers. Based on the experimental results presented in Chapter 4 and the analytical results presented in Chapter 5, there is no apparent reason for reducing the design strength of piers with low eccentricities because of their segmental construction. The effects of the discontinuous mild reinforcement and epoxied joints do not seem to cause a significant reduction in pier strength. However, the design strength of the segmental piers must be based on the capacity available after post-tensioning.

2) The rotational stiffness of segmentally constructed bridge piers should be considered to be 20 percent less than that of monolithically constructed piers. Based on the test results presented in Chapter 4 and the analysis results

presented in Chapter 5, the addition of a post-tensioning force causes a reduction in the rotational stiffness of the piers. In addition, from the observed behavior reported in Chapter 4, the ductility of the segmental piers seems to be less than that of the monolithic piers. Therefore, caution should be exercised regarding the dependence on ductility of the segmental piers.

3) Reinforcement that is not continuous across the joints between segments should be excluded from the design strength of segmentally constructed piers subjected to eccentricities about the weak axis greater than 5 percent of the overall section depth (t). Tests of segmental piers were not conducted for loads at eccentricities greater than 5 percent of the overall section depth (t). Therefore, contribution of the discontinuous longitudinal reinforcement to the strength of sections loaded at large eccentricities is unknown.

4) Current AASHTO (10) and ACI (11) specifications for piers and walls can provide a basis for detailing the piers but need further clarification for application to hollow sections. Two curtains of steel should be used in the walls and all reinforcement, prestressed and non-prestressed, should be well confined. The two curtains of reinforcement should be tied together with crossties placed on alternate sections of longitudinal steel at the same spacing as the lateral reinforcement (see Fig. 2.3). Lateral reinforcement spacing

should not exceed the least dimension of the compression member or 12 inches, where the least dimension of the member is considered to be the wall thickness, t_f, of the hollow piers. From the test results presented in Chapter 4, it is apparent that the reinforcement details used in the test specimens performed well.

5) Segments should be joined in such a way as to insure strain compatibility between sections. This recommendation is based on the favorable behavior of the segmental specimens with epoxied joints and grouted tendons presented in this study. In addition, the epoxied joint avoids the local stress concentration which might occur in a dry joint. The behavior of segmental specimens with unbonded segments is not known.

6) There should be some continuous bonded reinforcement across the joint between each segment. This continuous reinforcement can be either mild reinforcement or prestressed reinforcement. This recommendation is also based on the behavior of the segmental specimens presented in this study. This requirement insures that there is some large eccentricity moment-capacity across the weakest section of the pier.

7) In addition to the current strength reduction factor used by the codes (10,11,23), there should be a further reduction in design strength to account for possible problems

due to construction difficulties and local wall instability of the thin-walled piers.

The following table illustrates the understrength of the test specimens in regard to their calculated capacities.

Table 5.11 Comparison of Failure Loads and Calculated Capacities

Specimen	X_u/t_f	P_{test}/P_n
1M	10	0.96
1S	8.4	0.91
2M	18	0.72
2S	15.5	0.84
3M	24.7	0.90
3S	22.3	0.95
3PM	22.3	0.98
AVERAGE		0.89
STANDARD DEVIATION		0.08

As previously discussed, the pier specimens presented in this report were subjected to several other factors which may have contributed to their understrength. However, there seems to be a definite amount of strength reduction from the predicted strength of the piers. Therefore, based on these limited test results and the reasoning behind the present strength reduction factor required by the codes (10,11,23), it is recommended that the strength reduction factor, Φ, be reduced by approximately 10 percent. The strength reduction factor for thin-walled piers with X_u/t_f ratios greater than 8 would therefore become 0.65.

It is evident from Table 5.12 that the proposed strength reduction factor causes the ratio of the test failure load to the calculated capacity to fall closer to the value of 1.0/0.7 = 1.43 inferred by present codes (10,11,23).

Table 5.12 Comparison of Failure Loads, Code Capacities, and Recommended Capacities

Specimen	X_u/t_f	$P_{test}/\Phi P_n$ $\Phi = 0.70$	$P_{test}/\Phi P_n$ $\Phi = 0.65$
1M	10	1.37	1.47
1S	8.4	1.30	1.40
2M	18	1.03	1.11
2S	15.5	1.20	1.30
3M	24.7	1.29	1.39
3S	22.3	1.36	1.46
3PM	22.3	1.39	1.50
AVERAGE		1.28	1.38
STANDARD DEVIATION		0.12	0.12

8) The maximum concrete stress should be limited to $0.85f'_c$. Because of the casting position and shape of the piers, Hognestad's proposed stress reduction factor, $k_3 = 0.85$, should be used in calculating the capacity of the piers.

CHAPTER 6

SUMMARY AND CONCLUSIONS

6.1 Summary

The objective of this study was to determine the effects of segmental construction on the behavior of hollow bridge piers. To determine the effects of segmental construction, a series of segmentally constructed, post-tensioned pier specimens was compared to a companion series of monolithically constructed specimens.

A series of seven test specimens were addressed in this study. The design and construction of the specimens was described in Chapter 2. Test procedures and instrumentation for each specimen were detailed in Chapter 3.

A summary of the physical behavior of each specimen was presented in Chapter 4. Differences in the experimental behavior of the companion specimens were thoroughly investigated by comparing their test data. Conclusions based on the experimental behavior of the specimens were made.

An analytical model to predict the behavior of segmental piers was proposed in Chapter 5. An extensive analysis which investigated the behavior of the segmental specimens was performed. By comparing the results of the analysis of the

segmental specimens with the results from the analysis of the monolithic specimens, several conclusions were drawn.

Based on the experimental results from Chapter 4 and the analytical results discussed in Chapter 5, recommendations for the design of segmental piers were proposed. The basis for these recommendations were discussed at the end of Chapter 5.

6.2 Conclusions

6.2.1 Strength and Stiffness

Several factors related to the strength and stiffness of the segmental piers were addressed.

1) The discontinuity of mild reinforcement at the joint appeared to have little effect on the strength of these specimens with low eccentricity ratios. However, there seemed to be some reduction in the moment capacity of the cross-section.

2) The discontinuity in the concrete caused by the joint also appeared to have little effect on the behavior of the specimens. No significant differences were noted in the experimental behavior of the monolithic and segmental test specimens.

3) The addition of post-tensioning tendons and associated post-tensioning force to the segmental specimens caused some differences in behavior. The rotational stiffness of the

segmentally constructed piers was approximately 20 percent less than that of the monolithically constructed piers. However, the segmentally constructed specimens were axially stiffer than the monolithically constructed specimens.

4) There seems to be a significant strength reduction due to local instability of the compression flange of the test specimens. From the test results of Chapter 4 and the reduction observed in the test specimens in comparison with the predicted strength shown in Chapter 5, it appears that the failures were significantly influenced by local buckling of the compression flange.

6.2.2 Analytical Model

Since all of the test specimens failed below their predicted capacities, a recommendation was made to reduce the strength reduction factor, Φ, from 0.70 to 0.65 for thin-walled piers with wall slenderness ratios, X_u/t_f, less than 8.

For additional studies, the analytical model needs to be refined to reflect reductions in stiffness due to the cracking observed in the test specimens.

6.2.3 Design Criteria

Briefly stated, the design recommendations for segmental piers are as follows:

1) The design strength of the segmental piers should not be reduced for discontinuities due to the joints between segments.

2) The rotational stiffness of segmental piers should be considered to be 20 percent less than that of monolithically constructed piers.

3) Reinforcement that is not continuous across the joints between segments should not be included in the design strength of segmentally constructed piers subjected to weak axis eccentricities greater than 5 percent of overall section depth (t).

4) Two curtains of reinforcement should be used in the walls and all reinforcement should be tied together and well confined.

5) Segments should be joined in such a manner as to insure strain compatibility between the concrete in adjacent segments.

6) Continuous bonded reinforcement, either prestressed or nonprestressed, should cross the joint between each segment.

7) The strength reduction factor, Φ, for both monolithically and segmentally constructed piers with a wall slenderness ratio, X_u/t_f, less than 8 should be 0.65.

8) The maximum flexural concrete stress of the piers should be limited to $0.85f'_c$.

APPENDIX A

ADDITIONAL TEST DATA

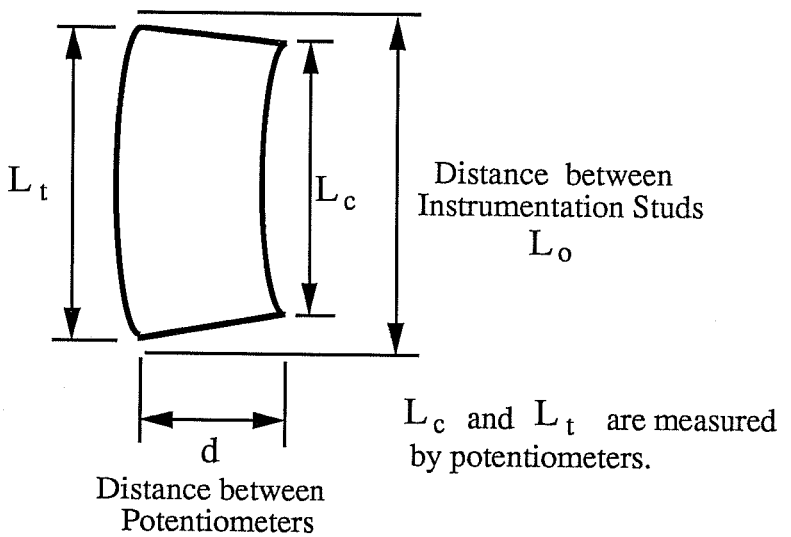

From geometry,

$$\text{Curvature} = \frac{(L_o - L_c) - (L_o - L_t)}{(L_o * d)}$$

Figure A.1 Method of Obtaining Curvature from Potentiometer Setup

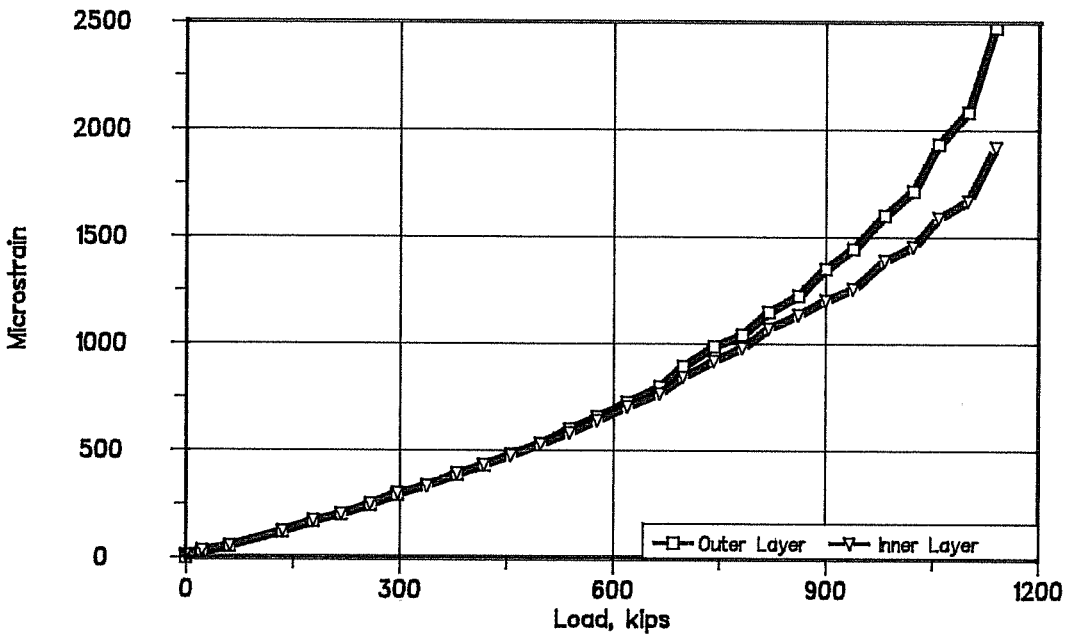

Comparison of Average Strains on Inner and Outer Layers of Steel Specimen 1S

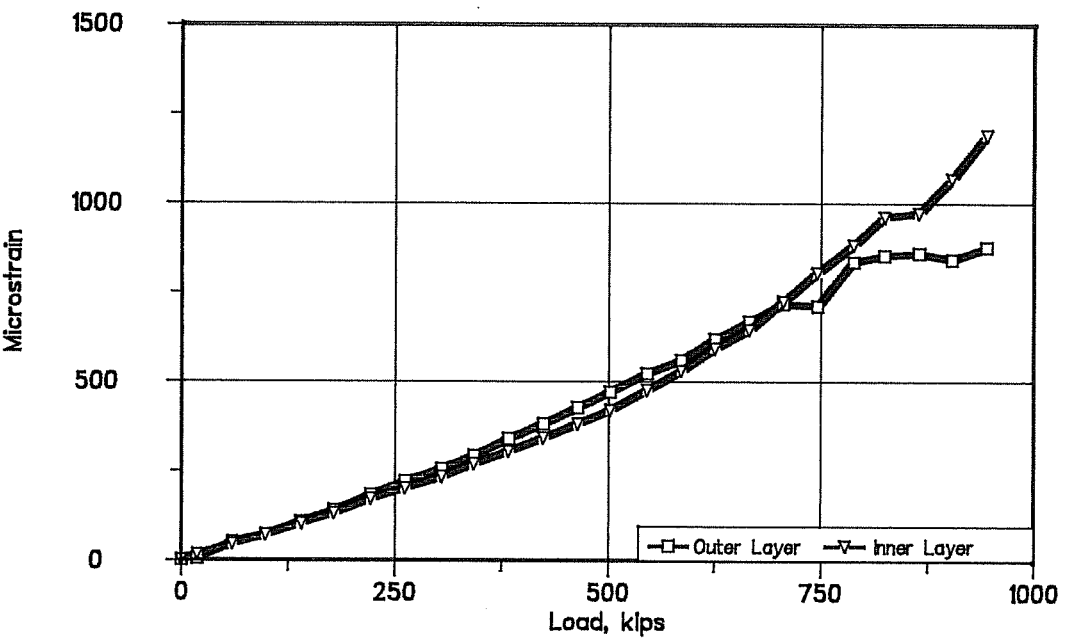

Comparison of Average Strains on Inner and Outer Layers of Steel Specimen 2S

Figure A.2 Specimens 1S and 2S Strain Gage Data

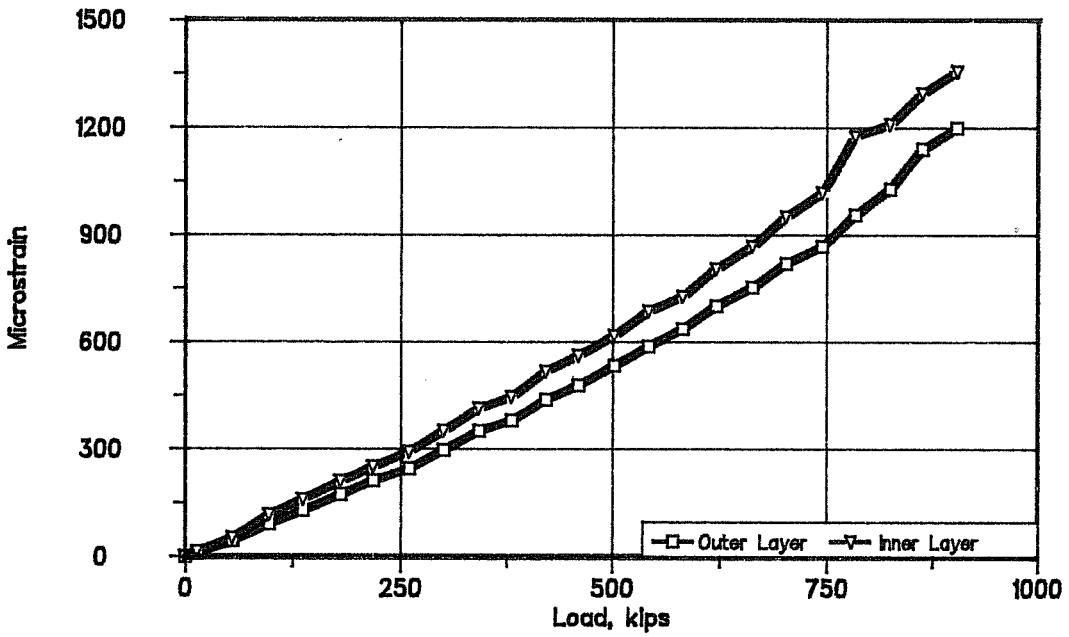

Comparison of Strains on Inner and Outer Layers of Steel Specimen 3M

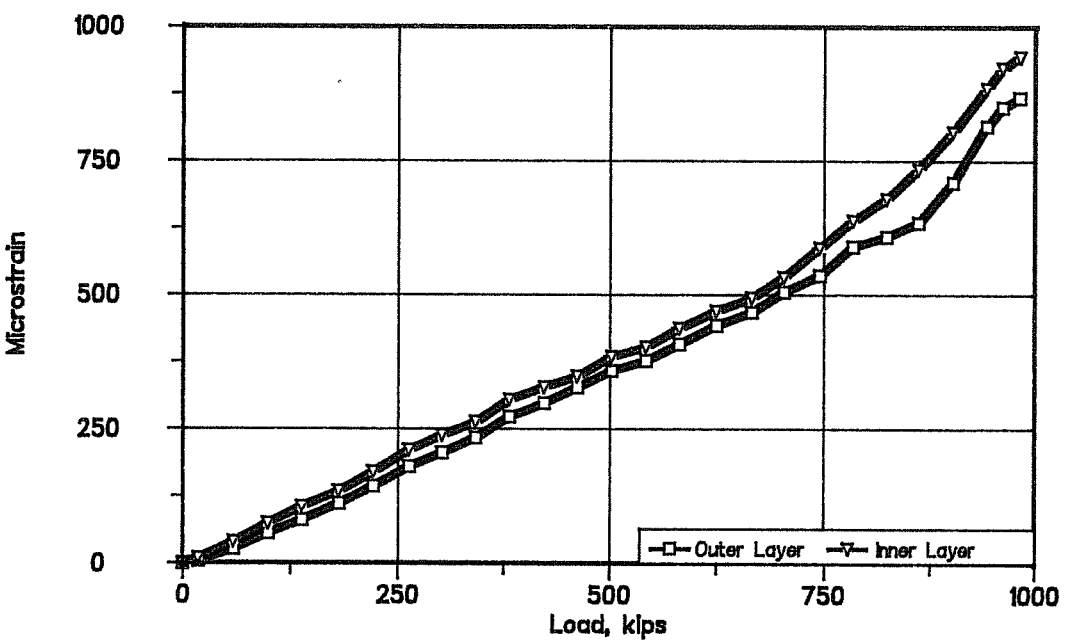

Comparison of Strains on Inner and Outer Layers of Steel Specimen 3S

Figure A.3 Specimens 3M and 3S Strain Gage Data

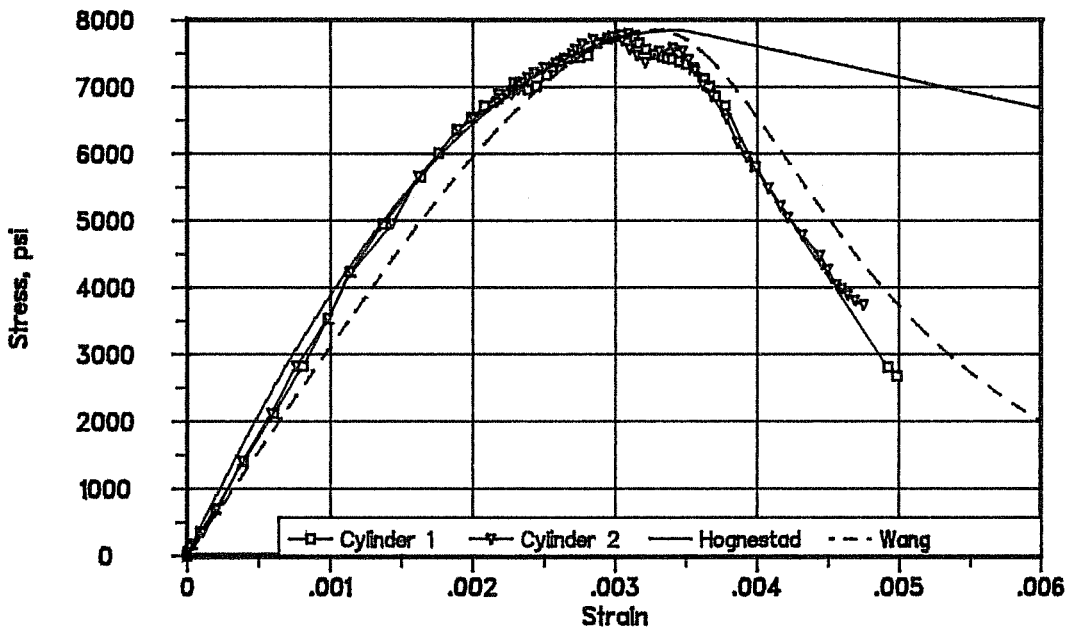

Specimen 1M Concrete Stress-Strain Comparison

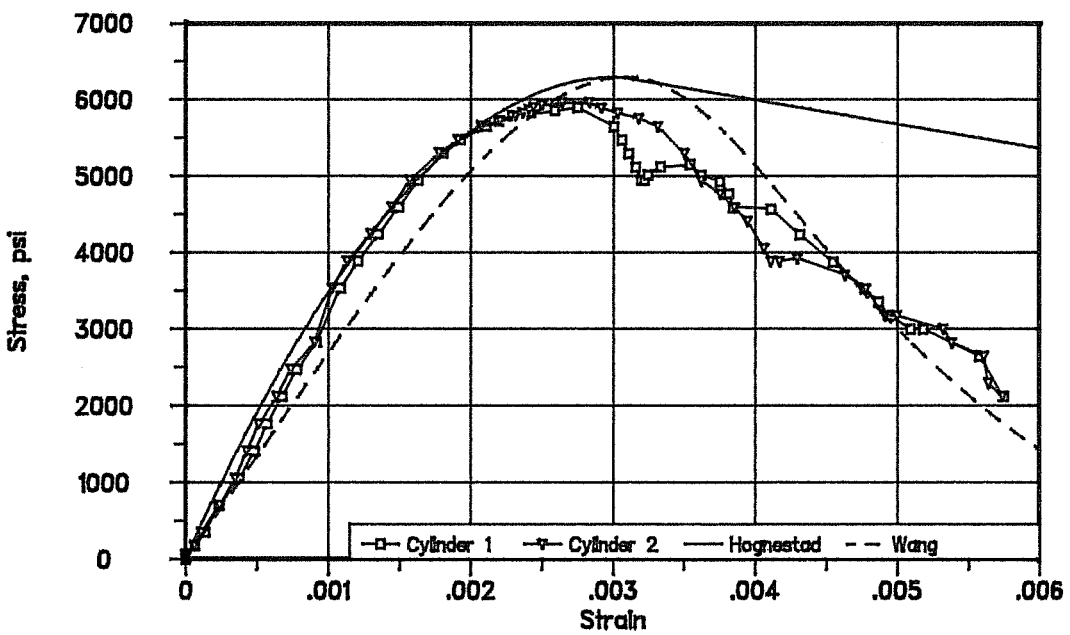

Specimen 3M Concrete Stress-Strain Comparison

Figure A.4 Comparison of Concrete Stress-Strain Relationships

APPENDIX B

PROGRAM PLCRST USER'S GUIDE

B.1 General

The computer program PLCRST discussed in this appendix was written to facilitate the rapid solution of the critical stress of a reinforced concrete plate loaded in-plane with certain geometric and material properties and edge conditions. The program can handle the specific boundary conditions of plates with simply supported loaded edges while the unloaded edges can be:

1. simply supported (case 1),
2. completely restrained (case 2), or
3. partially restrained (case 3).

The program was written so that it can be run in either an interactive mode or a batch-process mode. The input and output procedure for each mode differs a little although the same input information is needed and the same output information will be provided.

The program was written in FORTRAN-77 language on an IBM-compatible personal computer. It was compiled and linked using Microsoft FORTRAN. The entire source code of the program is given in Appendix D.

B.2 Description of Input and Output Data

The input variables and output variables are described in this section. The description of the input data file and

interpretation of the output data file is discussed in Section B.3.

Input data are entered in a free format for both interactive and batch modes.

B.2.1 Input Variables:

A = height (or length) of plate, in

B = width of plate, in

H = thickness of plate, in

FPC = f'_c = concrete compressive strength, ksi

EPSO = ϵ_o = concrete strain at maximum compressive stress, in/in

EPSMAX = ϵ_u = ultimate concrete strain

NU = Poisson's ratio of concrete

K3 = k_3 = Hognestad's stress block factor

FSY = f_y = mild reinforcement yield stress, ksi

ES = E_s = mild reinforcement modulus of elasticity, ksi

RO = total percentage of reinforcement, %

ZBAR = distance from the middle plane of the plate to the center of reinforcement layer, in

ISS = Concrete stress-strain model flag

1 = Hognestad's model

2 = Wang's model

3 = Wang's model with user-defined input variables

NCASE = edge condition,

1 = simply supported unloaded edges,

2 = completely restrained unloaded edges, or

3 = partially restrained unloaded edges.

BF = width of restraining plate, in., (needed only for edge condition 3.)

For the hollow piers discussed in this thesis, the edge condition of the plates corresponded to NCASE = 3, partially restrained unloaded edges.

B.2.2 Output Variables:

A/B = aspect ratio,

B/H = wall slenderness ratio,

M = number of half waves,

RK = coefficient of buckling,

SIGCR = critical stress, ksi,

BMD = code for buckling mode,

1 = crushing of concrete,

2 = buckling of plate with reinforcement yielded,

3 = buckling of plate with reinforcement not yielded,

4 = buckling of plate induced by yielding of reinforcement,

B/BF = ratio of width of main plate to width of restraining plate.

B.3 Description of Input File and Output File for Batch-Process Mode

B.3.1 Preparation of Input File

The description of the input file is as follows. In the description of each line of the input file, the names of input variables are in capital letters followed by the description of any variable that has not been described in the previous section.

Line 1: - NEX, number of records to be processed

Line 2: - NCASE

Line 3: * - K3,NU,FSY,ES,RO,FPC,EPSO,EPSMAX,ISS

* Remarks:

- these values will be assumed to be applicable to all cases to be processed
- EPSO could be left blank. If it is not available, the program will compute it.
- commas are not needed to separate the variables.

Line 4: ** - A,B,H,BF,ZBAR

** Remarks:

- this line of input is required for each of the cases to be processed,
- for boundary conditions 1 and 2, BF is not required, however, it should be assigned a value

different from zero to avoid the error of "dividing by zero".

B.3.2 Output Files

All input data will be printed in the output for examination. For edge condition cases 1 and 2, the column labeled "B/BF" should be ignored.

The output file for stress-strain data from the specified concrete stress-strain model will be created automatically. The names of the file to be created are as follows:

HOG.CSV - for Hognestad's stress-strain model

WANG.CSV - for Wang's stress-strain model

USR.CSV - for the User-Defined stress-strain model

The stress-strain data contained in these files is in comma-separated-value format for ease in importing to spreadsheet applications for plotting.

B.4 Running the Program

As soon as the program starts, the following prompt will appear on the screen after the title lines:

"INTERACTIVE MODE (1) OR BATCH PROCESS MODE (2) >".

To respond, the user enters a "1" for interactive mode or a "2" for the batch-process mode.

In interactive mode, the user enters input data as prompted on the screen. After specifying the concrete stress-

strain relation desired, the program immediately calculates the required input data from the desired model. For the user-defined stress-strain model, the user is prompted for additional input data to define the stress-strain relationship. The additional data is as follows:

EC = E_c = the secant modulus of concrete at $0.45k_3f'_c$, in ksi

EPSO = ϵ_o = concrete strain at maximum compressive strength, in/in

EPSI = ϵ_{ci} = concrete strain for first inflection point

FI = f_i = concrete stress for first inflection point

F2I = f_{2i} = concrete stress for second inflection point

This input data will then echo on the screen and the user will be asked check the data for accuracy before the program proceeds. If an input value has been incorrectly entered, the user will have the choice to correct by re-entering the data listed above. After calculating the required data, the subroutine will return to the main program.

When all input data have been entered, it will be echo printed on the screen and the user will be asked to check the data for accuracy before the program proceeds. If an input value has been incorrectly entered, the user then has a chance to correct it; however, all other data will have to be re-entered as well.

Once the input data are confirmed, the program will proceed with the calculation. The output will then be written to the screen and the output file specified by the user.

In the batch-process mode, the input data has to be prepared in advance and saved in an input file. During execution of the program, the user will be asked to provide the names of the input file and output file in which the output data will be saved. During execution, the program will indicate the number of the record being processed on the screen.

A sample run using the data for Specimen 1S in the batch-process mode is presented in the next section.

B.5 PLCRST Example

The use of the program to calculate the critical buckling stress of the component plates of Specimen 1S is as follows:

Considering the compression flange of Specimen 1S,

the following values were obtained.

RO = 1.81%
A = 72"
B = 21"
H = 2.443" (average measured wall thickness)
BF = 6"
ZBAR = 0.5"

As with the other specimens,

NCASE = 3
K3 = 0.85
NU = 0.2
FSY = 75.1 ksi
ES = 29000 ksi

EPSO = 0.0 (program will calculate)
EPSMAX = 0.003
ISS = 1 (use Hognestad's stress-strain model)

FPC = 6.980 ksi (for Specimen 1S)

The input file created from this data is shown below.

```
   1
   3
0.85    0.2    75.1    29000.   1.81    6.980   0.0     .003   1
 72.    21.    2.443   6.       0.5
```

The output file created after running the program is shown on the following page.

This appendix was slightly modified from the user's guide presented by Tran (20) for the original program.

```
**  PROGRAM PLCRST

**           WRITTEN BY TAN D TRAN
**               SPRING 1989
**      THE UNIVERSITY OF TEXAS AT AUSTIN

***        MODIFIED BY RANDALL B. ROWELL
***               SPRING 1990
***      THE UNIVERSITY OF TEXAS AT AUSTIN


 EDGE CONDITION :         3
   1 = UNLOADED EDGE SIMPLY SUPPORTED
   2 = UNLOADED EDGE FIXED, AND
   3 = UNLOADED EDGE PARTIALLY FIXED.

 MATERIAL PROPERTIES
     CONCRETE STRENGTH (KSI) =              6.9800
     HOGNESTAD FACTOR K3 =                   .8500
     POISSON RATIO =                         .2000
     CONCRETE STRAIN AT FPC =            .2908E-02
     MAXIMUM USABLE CONCRETE STRAIN =    .3000E-02
     MODULUS OF ELASTICITY (PSI) =         4081.04

     STEEL STRENGTH (KSI) =                  75.10
     STEEL MODULUS (KSI) =                29000.00
     TOTAL REINF. RATIO (%) =                 1.81


   A/B     B/H     B/BF    ZBAR    M      K      CRIT. STRESS   CODE

  3.43    8.60     3.50    .50     4     5.52       5.92965       2

 CODE 1 = CRUSHING OF CONCRETE
      2 = BUCKLING WITH STEEL YIELDED
      3 = BUCKLING WITH STEEL NOT YIELDED
      4 = BUCKLING INDUCED BY YIELDING OF STEEL.
```

APPENDIX C

PROGRAM MOMINT USER'S GUIDE

C.1 General

The computer program MOMINT discussed in this appendix was written in order to calculate the capacity of hollow, reinforced concrete sections with or without uniform post-tensioning. By manipulating the data generated by the program, the complete P-M-Φ relationship for the section can be established.

The program was written in FORTRAN-77 language on an IBM-compatible personal computer. It was compiled and linked using Microsoft FORTRAN. The entire source code of the program is given in Appendix E.

C.2 Description of Input and Output Data

The input variables and output variables are described in this section. The description of the input data file and interpretation of the output data file is discussed in Section C.3. All input data is entered in free format.

C.2.1 Input Variables

FPSC = f'_c = concrete compressive strength, ksi

FY = f_y = mild reinforcement yield stress, ksi

EU = ultimate mild longitudinal steel strain

FU = ultimate mild longitudinal steel stress

FYPT = f_{ypt} = ultimate post-tensioning tendon stress

ES = E_s = mild reinforcement modulus of elasticity, ksi

ESP = post-tensioning tendons modulus of elasticity, ksi

EPSMAX = ϵ_u = ultimate concrete strain

EPSO = ϵ_o = concrete strain at maximum compressive stress

FACTOR = k_3 = Hognestad's stress block factor

H = depth of section

TF = flange thickness

N = number of strips into which the section is divided

NOSTEP = number of points that will be calculated for the interaction diagram

IFLAG1 = flag indicating strip thickness;

- 0 = equal
- 1 = unequal

NOCURV = number of curvatures from which moment and axial load are calculated

PHIMAX = the maximum value of curvature to be searched by the program

PHIMIN = the minimum value of curvature to be searched by the program

ERROR = maximum allowable error range for specified axial load

FFLAG = flag which indicates if program is to read axial loads directly from the input file

SIGCR = critical stress calculated from program PLCRST using elastic buckling theory

ISS = concrete stress-strain flag

- 1 = Hognestad's model
- 2 = Wang's model
- 3 = Wang's model with user-defined constants

AC = array of concrete area in each strip

AS = array of mild steel area in each strip

ASP = array of post-tensioning steel area in each strip

YBAR = array of depth of centroid of each strip (optional)

FORC = array that contains desired axial loads for calculating section capacity (optional)

EPSPIS = initial strain in post-tensioning steel (-) (optional)

EPSPIC = initial strain in concrete and mild steel (+) (optional)

C.2.2 Output Variables

APHI = array of curvatures associated with each point on the interaction diagram

AP = array containing axial load capacities of section

AMOM = array containing moment capacity of section for a particular value of axial load

ECCEN = eccentricities associated with specified values of axial load and moment

AEPS = array of strains associated with each point on the interaction diagram

IFLAG2 = flag indicating mode of failure at each point on the interaction diagram

0 = material failure

1 = buckling of flange

BMOMA = array of moments for specified range of curvatures at each level of axial load

BMOMB = similar to BMOMA, but only calculated when failure mode is buckling of flange for comparison

BPHI = array of curvatures calculated for each axial load

BPHIB = similar to BPHI, but only calculated when failure mode is buckling of flange for comparison

CONINI = initial stress in concrete due to post-tensioning force

STLINI = initial mild steel stress due to post-tensioning force

PTSINI = initial stress in post-tensioning tendons due to post-tensioning force

EPSCR = critical strain calculated from critical buckling stress of flange, SIGCR

C.3 Description of Input and Output Files

C.3.1 Preparation of Input File

All input data are entered in free format. In the description of each line of the input file, the names of input variables are in capital letters.

Line 1: FPSC, FY, EU, FU, FYPT, ES, ESP, EPSMAX, EPSO

- EPSO could be left blank. If it is not available, the program will compute it.

Line 2: FACTOR, H, TF, N, NOSTEP, IFLAG1

Line 3: NOCURV, PHIMAX, PHIMIN, ERROR, FFLAG

Line 4 to Line xx: FORC

- these lines are optional and must be omitted if FFLAG = 0

Line 4 to Line xx: YBAR, AC, AS, ASP

- one line is required for each strip specified by N
- YBAR is optional and must be omitted if IFLAG1 = 0

During execution, the program will prompt the user for the remainder of the input data, SIGCR, ISS, and EPSPIC, EPSPIS, or PTF.

Some discretion should be used in the selection of NOCURV, PHIMAX, and PHIMIN in Line 3 of the input file. The program uses a brute-force method to calculate the moments and

curvatures for the specified axial loads. Therefore, a wide range of curvatures must be selected in order to accommodate the spectrum of axial loads required for constructing the interaction diagram. The range of curvatures used in this study was anywhere from 0.000001 to 0.001.

For a wide range of curvatures, the number of curvatures, NOCURV, must be fairly large in order to have small enough intervals to get several points for the moment-curvature diagram. Experience has shown that 50 values is usually sufficient.

C.3.2 Output Files

All input data will be printed in the output file for examination.

The program creates two additional files PMOUT.CSV and MOMCUR.CSV. These two files contain output data in comma-separated-value format for ease in importing to spreadsheet applications for plotting. PMOUT.CSV contains values of axial load and moment for plotting the interaction diagram. MOMCUR.CSV contains values of moment and curvature for plotting the moment-curvature relationship for a particular value of axial load.

If an axial load within the desired error range of a specified axial load is not computed, the program will print the

message "THERE WAS NO CONVERGENCE FOR POINT NUMBER X" where X is the number corresponding to the Xth value of axial load.

In addition to the output files already discussed, the output file for stress-strain data from the specified concrete stress-strain model will be created automatically. The names of the file to be created are as follows:

HOG.CSV - for Hognestad's stress-strain model

WANG.CSV - for Wang's stress-strain model

USR.CSV - for the User-Defined stress-strain model

The stress-strain data contained in these files is in comma-separated-value format for ease in importing to spreadsheet applications for plotting.

C.4 Running the Program

As soon as the program starts, the user is prompted for the names of the input data file and output file to be created. The following prompt will then appear, "ENTER CRITICAL STRESS: " After this prompt, the user should either enter the critical buckling stress previously calculated by program PLCRST or "0", if the user does not desire to include the possible buckling of the pier walls.

The following prompt will appear next, "ENTER 1 FOR HOGNESTAD, 2 FOR WANG, 3 FOR USER-DEFINED: ". The user should enter the number corresponding to the concrete stress-strain

model desired. For the user-defined stress-strain model, the user is prompted for additional input data to define the stress-strain relationship. The additional data is as follows:

EC = E_c = the secant modulus of concrete at $0.45k_3f'_c$, in ksi

EPSO = ϵ_o = concrete strain at maximum compressive strength, in/in

EPSI = ϵ_{ci} = concrete strain for first inflection point

FI = f_i = concrete stress for first inflection point

F2I = f_{2i} = concrete stress for second inflection point

After the following prompt,

"IF YOU WISH TO LET THE PROGRAM COMPUTE THE INITIAL STRAINS DUE TO THE POST-TENSIONING FORCE ENTER "1" ELSE ENTER "0" "

the user has a choice of entering the initial strain in the section due to the post-tensioning force or entering the total post-tensioning force applied to the section. If the post-tensioning force is entered, the program will calculate the initial strains based on the assumption that the post-tensioning force is uniformly distributed across the section.

When all input data have been entered, it will be echo-printed on the screen and the user will have the opportunity to check the data and proceed with the program or exit the program if the input data is unsatisfactory.

During execution, the program will indicate the number of the axial load being currently processed along with the total number of points desired for construction of the interaction diagram. A sample run using the data for Specimen 1S is presented in the next section.

C.5 MOMINT Example

The use of the program to calculate the capacity of Specimen 1S is as follows:

Using the assumptions from the analysis presented in Chapter 5, the following input file was created.

```
6.980   75.1  .099   90.4   138.2    29000.   29000.  .003   0.
0.85    15.       2.440          30        15        0
50     0.0006    0.000001      40.        0
14.64     0.        0.
13.88     0.76      0.
14.64     0.        0.
13.88     0.76      0.
14.64     0.        0.28
2.44      0.        0.28
2.25      0.19      0.
2.44      0.        0.
2.44      0.        0.
2.25      0.19      0.
2.44      0.        0.
2.44      0.        0.
2.25      0.19      0.
2.44      0.        0.
2.345     0.095     0.
2.345     0.095     0.
2.44      0.        0.
2.25      0.19      0.
2.44      0.        0.
2.44      0.        0.
2.25      0.19      0.
2.44      0.        0.
```

2.44	0.	0.
2.25	0.19	0.
2.44	0.	0.28
14.64	0.	0.28
13.88	0.76	0.
14.64	0.	0.
13.88	0.76	0.
14.64	0.	0.

From PLCRST, the critical buckling stress of the compression flange of Specimen 1S is

SIGCR = 5.93 ksi.

The total post-tensioning force applied to the section was

PTF = 126 kips.

The output file created after running the program is shown on the following pages.

THERE WAS NO CONVERGENCE FOR POINT NUMBER 1

CONCRETE STRENGTH, KSI	6.98
HOGNESTAD FACTOR K3	.85
STEEL STRENGTH, KSI	75.10
POST-TENSIONED STEEL STRENGTH, KSI	138.20
CONCRETE E, KSI	4081.04
MILD STEEL ULTIMATE STRAIN	.0990000
MILD STEEL ULTIMATE STRESS, KSI	90.40
MAX. USEABLE CONCRETE STRAIN	.0030000
EPSO (CONC. STRAIN AT FPSC)	.0029076
INITIAL CONC. AND MILD STL. STRAIN	.0001421
INITIAL POST-TENSIONED STL. STRAIN	-.0038793
INITIAL CONC. STRESS	.56588
INITIAL MILD STL. STRESS	4.12192
INITIAL TENDON STRESS	-112.50000
CRITICAL STRESS, KSI	5.93
STRAIN AT CRITICAL STRESS	.0030000
SECTION DEPTH, IN.	15.00
THICKNESS OF FLANGE, IN.	2.44

STRIP	YBAR	CONC IN^2	STEEL IN^2	PSTEEL IN^2
1	.250	14.640	.000	.000
2	.750	13.880	.760	.000
3	1.250	14.640	.000	.000
4	1.750	13.880	.760	.000
5	2.250	14.640	.000	.280
6	2.750	2.440	.000	.280
7	3.250	2.250	.190	.000
8	3.750	2.440	.000	.000
9	4.250	2.440	.000	.000
10	4.750	2.250	.190	.000
11	5.250	2.440	.000	.000
12	5.750	2.440	.000	.000
13	6.250	2.250	.190	.000
14	6.750	2.440	.000	.000
15	7.250	2.345	.095	.000
16	7.750	2.345	.095	.000
17	8.250	2.440	.000	.000
18	8.750	2.250	.190	.000
19	9.250	2.440	.000	.000
20	9.750	2.440	.000	.000

21	10.250	2.250	.190	.000
22	10.750	2.440	.000	.000
23	11.250	2.440	.000	.000
24	11.750	2.250	.190	.000
25	12.250	2.440	.000	.280
26	12.750	14.640	.000	.280
27	13.250	13.880	.760	.000
28	13.750	14.640	.000	.000
29	14.250	13.880	.760	.000
30	14.750	14.640	.000	.000

CURVATURE	AXIAL LOAD	MOMENT	ECCEN	FAIL STRAIN	FAIL MODE
.0000000	.00	.00	.00	.000000	0
.0000609	1332.67	447.89	.34	.002857	0
.0000968	1221.46	988.52	.81	.002829	0
.0001328	1121.01	1543.17	1.38	.002914	0
.0001567	1021.34	2054.73	2.01	.002914	0
.0001807	909.42	2632.66	2.89	.002914	0
.0002047	810.45	3156.70	3.89	.002971	0
.0002286	700.97	3696.17	5.27	.002971	0
.0002765	592.20	4040.75	6.82	.003000	0
.0003364	485.40	4307.52	8.87	.002971	0
.0004083	384.12	4502.66	11.72	.002971	0
.0005641	276.13	4389.92	15.90	.003000	0
.0006000	170.83	3904.58	22.86	.002571	0
.0006000	71.43	3374.28	47.24	.002143	0
.0005880	-32.69	2780.25	-85.04	.001714	0

NOTE: FAILURE MODE CODE: 0 = MATERIAL FAILURE
1 = BUCKLING OF FLANGE.

APPENDIX D

PROGRAM PLCRST SOURCE CODE

```
      PROGRAM PLCRST
      CHARACTER*1 TAB
      CHARACTER*20 FILIN, FILOUT
      DOUBLE PRECISION K,DSIG,RW,SW,SIGMA,PSIGMA,CHECK
      REAL NU, K3
      INTEGER BMD
C
C  FORMAT STATEMENTS
C    GENERAL INPUT AND OUTPUT
 1001 FORMAT('**  PROGRAM PLCRST'//
     *       '**          WRITTEN BY TAN D TRAN'/
     *       '**               SPRING 1989'/
     *       '**      THE UNIVERSITY OF TEXAS AT AUSTIN'//
     *       '***       MODIFIED BY RANDALL B. ROWELL'/
     *       '***               SPRING 1990'/
     *       '***     THE UNIVERSITY OF TEXAS AT AUSTIN'//)
 1002 FORMAT(1X,'INTERACTIVE MODE (1) OR
     +        BATCH PROCESS MODE (2)  > ')
 1003 FORMAT(/1X,'CODE 1 = CRUSHING OF CONCRETE'/
     *        1X,'     2 = BUCKLING WITH STEEL YIELDED'/
     *        1X,'     3 = BUCKLING WITH STEEL NOT YIELDED'/
     *        1X,'     4 = BUCKLING INDUCED BY YIELDING OF '
     *                                  ,'STEEL.'/)
C   FOR INTERACTIVE MODE
 1004 FORMAT(1X,'ENTER PLATE DIMENSIONS IN INCHES ',
     *          '(HEIGHT, WIDTH, THICKNESS)')
 1005 FORMAT(1X,'ENTER EDGE CONDITION CODE: 1, 2 OR 3 > ')
 1006 FORMAT(1X,'ENTER WIDTH OF RESTRAINING PLATE (INCH)> ')
 1007 FORMAT(1X,'ENTER CONCRETE STRENGTH (KSI), CONCRETE STRAIN'
     *        ,'AT FPC')
 1008 FORMAT(1X,'ENTER POISSONS RATIO, HOGNESTAD FACTOR K3 >')
 1009 FORMAT(1X,'ENTER STEEL YIELD STRENGTH (KSI), STEEL ',
     * 'MODULUS OF ELASTICITY (KSI) >')
 1010 FORMAT (1X,'ENTER TOTAL REINFORCEMENT RATIO (PERCENT),',
     *           ' LOCATION OF REINF. LAYER (INCH) >')
 1011 FORMAT(/1X,'PLATE DIMENSION (INCHES)'/
     *       5X,'LENGTH = ',3X,F10.2/5X,'WIDTH = ',4X,F10.2/
     *       5X,'THICKNESS = ',F10.2//
     *       1X,'EDGE CONDITION : ',6X,I3/
     *       1X,'  1 = UNLOADED EDGE SIMPLY SUPPORTED'/
     *       1X,'  2 = UNLOADED EDGE FIXED, AND'/
     *       1X,'  3 = UNLOADED EDGE PARTIALLY FIXED.'//
     *       1X,'MATERIAL PROPERTIES'/
     *       5X,'CONCRETE STRENGTH (KSI) = ',4X,F15.2/
     *       5X,'HOGNESTAD FACTOR K3 = ',13X,F10.2/
     *       5X,'POISSONS RATIO = ',18X,F10.2/
     *       5X,'CONCRETE STRAIN AT FPC = ',10X,E10.4/
     *       5X,'ULTIMATE CONCRETE STRAIN = ',8X,E10.4/
```

```
     *       5X,'MODULUS OF ELASTICITY (KSI) = ',F15.2//
     *       5X,'STEEL STRENGTH (KSI) = ',12X,F10.2/
     *       5X,'STEEL MODULUS OF ELASTICITY(KSI) = ',F10.0/
     *       5X,'TOTAL REINF. RATIO (%) = ',10X,F10.2/
     *       5X,'LOCATION OF REINF. LAYER (INCH) = ',1X,F10.2/)
 1012 FORMAT(1X,'WIDTH OF RESTRAINING PLATE (INCH) = ',
     +         ,3X,F10.2//)
 1013 FORMAT(1X,'IF INPUT INFORMATION IS CORRECT TYPE "1", '
     +       ,' ELSE TYPE "0"')
 1014 FORMAT(8X,'A/B',9X,'B/H',5X,'M',10X,'K',4X,'CRIT. STRESS',
     +        5X,'CODE')
 1015 FORMAT(1X,F10.2,3X,F10.2,2X,I3,2X,F10.2,2X,F10.5,4X,I6//)
 1016 FORMAT(1X,'IF YOU WISH PROGRAM TO CONTINUE TYPE "1",
     +         ELSE TYPE "0" ')
C
C  FOR BATCH PROCESS MODE
 1017 FORMAT(/'     *  ENTER INPUT FILE NAME    *    '/)
 1018 FORMAT(//'    *  ENTER OUTPUT FILE NAME   *    '/)
 1019 FORMAT(I4)
 1020 FORMAT(6F10.2,2E10.4,I4)
 1021 FORMAT(1X,'EDGE CONDITION : ',6X,I3/
     *       1X,'  1 = UNLOADED EDGE SIMPLY SUPPORTED'/
     *       1X,'  2 = UNLOADED EDGE FIXED, AND'/
     *       1X,'  3 = UNLOADED EDGE PARTIALLY FIXED.'//
     *       1X,'MATERIAL PROPERTIES'/
     *       5X,'CONCRETE STRENGTH (KSI) = ',4X,F15.4/
     *       5X,'HOGNESTAD FACTOR K3 = ',13X,F10.4/
     *       5X,'POISSON RATIO = ',19X,F10.4/
     *       5X,'CONCRETE STRAIN AT FPC = ',10X,E10.4/
     *       5X,'ULTIMATE CONCRETE STRAIN = ',8X,E10.4/
     *       5X,'MODULUS OF ELASTICITY (KSI) = ',F15.2//
     *       5X,'STEEL STRENGTH (KSI) = ',13X,F10.2/
     *       5X,'STEEL MODULUS (KSI) = ',14X,F10.2/
     *       5X,'TOTAL REINF. RATIO (%) = ',11X,F10.2//)
 1022 FORMAT(5F10.2)
 1023 FORMAT (F7.2,1X,F7.2,1X,F7.2,1X,F7.2,1X,I3,1X,
     *        F7.2,1X,F10.5,3X,I6)
 1024 FORMAT(3X,'A/B',4X,'B/H',6X,'B/BF',5X,'ZBAR',2X,'M',
     *      6X,'K',3X,'CRIT. STRESS',3X,'CODE'/)
 1025 FORMAT(1X,'CALCULATING COEFFICIENT OF BUCKLING K'/)
 1026 FORMAT(1X,'PROCESSING RECORD NUMBER :',I4/)
 1027 FORMAT(1X,'CALCULATING CRITICAL STRESS'/)
 1028 FORMAT(1X,'ENTER THE MAXIMUM USABLE CONCRETE STRAIN'/)
 1029 FORMAT(/1X,'ENTER "0.0" AT PROMPT FOR THE CONCRETE STRAIN
                 AT FPC',
     + ' UNLESS YOU WANT'/' TO ENTER THE VALUE DIRECTLY FOR ',
     +  'HOGNESTADS STRESS-STRAIN RELATION.'
     +//' FOR THE OTHER TWO STRESS- STRAIN MODELS, '
```

```
     +    'YOU MUST ENTER "0.0"'//)
      WRITE(*,1001)
 10   WRITE(*,1002)
      READ(*,*) MODE
      IF (MODE.EQ.1) THEN
          GOTO 20
      ELSEIF (MODE.EQ.2) THEN
          GOTO 30
      ELSE
          GOTO 10
      ENDIF
C
C  INTERACTIVE MODE
C
C READ PERTINENT INPUT DATA
 20   WRITE(*,1004)
      READ(*,*)A,B,H
      WRITE(*,1029)
      WRITE(*,1007)
      READ(*,*) FPC,EPSO
      WRITE(*,1008)
      READ(*,*)NU,K3
      WRITE(*,1009)
      READ(*,*)FSY,ES
      WRITE(*,1010)
      READ(*,*)RO,ZBAR
      WRITE(*,1005)
      READ(*,*)NCASE
C  FOR CASE OF PARTIALLY RESTRAINED EDGE, GET WIDTH OF
C       RESTRAINING PLATE
      IF (NCASE.EQ.3) THEN
      WRITE(*,1006)
      READ(*,*) BF
      ELSE
      BF = 1.0
      ENDIF
C **NOTE BF ALWAYS NEEDS TO BE GIVEN A VALUE EVEN FOR CASES
C   1 AND 2 TO PREVENT UNNECESSARY ERROR OF DIVIDING BY ZERO
C   WHEN BF = 0
      WRITE (*,1028)
      READ (*,*) EPSMAX
C   ENTER CODE FOR TYPE OF STRESS-STRAIN RELATION DESIRED
 25     WRITE (*,1099)
 1099 FORMAT(1X,'ENTER 1 FOR HOGNESTAD, 2 FOR WANG, 3 FOR ',
     +            'USER DEFINED:  ')
      READ(*,*) ISS
C  CALL APPROPRIATE SUBROUTINE FOR TYPE OF STRESS-STRAIN
C  RELATION DESIRED
```

```
      IF (ISS.EQ.1) THEN
      CALL HOG(FPC,K3,EC,EPSO,EPSMAX)
      ELSEIF (ISS.EQ.2) THEN
      CALL WANG(FPC,K3,EC,EO,EPSO,EPSI,EPS2I,FI,F2I,
     +            AW,BW,CW,DW,A1,B1,C1,D1,EPSMAX)
      ELSEIF (ISS.EQ.3) THEN
      CALL USER(FPC,K3,EC,EO,EPSO,EPSI,EPS2I,FI,F2I,
     +            AW,BW,CW,DW,A1,B1,C1,D1,EPSMAX)
      ELSE
        GOTO 25
      ENDIF
C ECHO PRINT INPUT DATA
      WRITE(*,1011) A,B,H,NCASE,FPC,K3,NU,EPSO,EPSMAX,EC,FSY,
     +                ES,RO,ZBAR
      IF (NCASE.EQ.3) THEN
      WRITE(*,1012) BF
      ENDIF
C  DETERMINE IF INPUT DATA ARE CORRECT, IF SO PROCEED
C  WITH CALCULATIONS
      WRITE(*,1013)
      READ(*,*) INOK
      IF (INOK.EQ.0) GOTO 20
C  FIRST CALCULATE THE COEFFICIENT OF BUCKLING K
      WRITE(*,1025)
      CALL CALK(A/B,NCASE,NU,B/BF,M,K)
      RK = REAL(K)
C  NEXT CALCULATE THE CRITICAL STRESS
      WRITE(*,1027)
      CALL
CALSTCR(RK,B,H,FPC,K3,NU,FSY,ES,RO,ZBAR,EPSO,EC,SIGCR,BMD,
     +   ISS,AW,BW,CW,DW)
C  WRITE OUT RESULTS ON SCREEN
      WRITE(*,1003)
      WRITE(*,1014)
      WRITE(*,1015) A/B,B/H,M,RK,SIGCR,BMD
C DETERMINE IF PROGRAM IS TO CONTINUE
      WRITE(*,1016)
      READ(*,*) IANS
      IF (IANS.EQ.0) GOTO 20
C  OPEN OUTPUT FILE
      WRITE(*,1018)
      READ(*,9999) FILOUT
 9999 FORMAT (A)
      OPEN (2,FILE=FILOUT,STATUS='NEW')
      WRITE(2,1001)
      WRITE(2,1021) NCASE,FPC,K3,NU,EPSO,EPSMAX,EC,FSY,ES,RO
      WRITE(2,1024)
      WRITE(2,1023) A/B,B/H,B/BF,ZBAR,M,RK,SIGCR,BMD
```

```
      WRITE(2,1003)
      GOTO 60
C
C ****BATCH PROCESS MODE
C  FIRST GET INPUT AND OUTPUT FILE NAMES AND OPEN FILES
 30   WRITE(*,1017)
      READ(*,9999) FILIN
      WRITE(*,1018)
      READ(*,9999) FILOUT
      OPEN (1,FILE=FILIN,STATUS='OLD')
      OPEN (2,FILE=FILOUT,STATUS='NEW')
C  READ IN PERTINENT INPUT DATA
      READ(1,*) NEX
      READ(1,*) NCASE
      READ(1,*) K3,NU,FSY,ES,RO,FPC,EPSO,EPSMAX,ISS
C
C  CALCULATE STRESS-STRAIN RELATIONS FROM SPECIFIED MODEL
C  CALL APPROPRIATE SUBROUTINE FOR TYPE OF STRESS-STRAIN
C  RELATION DESIRED
      IF (ISS.EQ.1) THEN
      CALL HOG(FPC,K3,EC,EPSO,EPSMAX)
      ELSEIF (ISS.EQ.2) THEN
      CALL WANG(FPC,K3,EC,EO,EPSO,EPSI,EPS2I,FI,F2I,
     +            AW,BW,CW,DW,A1,B1,C1,D1,EPSMAX)
      ELSEIF (ISS.EQ.3) THEN
      CALL USER(FPC,K3,EC,EO,EPSO,EPSI,EPS2I,FI,F2I,
     +            AW,BW,CW,DW,A1,B1,C1,D1,EPSMAX)
      ELSE
        GOTO 60
      ENDIF
C  ECHO OUTPUT TO OUTPUT FILE
      WRITE(2,1001)
      WRITE(2,1021) NCASE,FPC,K3,NU,EPSO,EPSMAX,EC,FSY,ES,RO
      WRITE(2,1024)
C  LOOP FOR CALCULATION OF SEVERAL SETS OF DATA
      DO 40 I = 1,NEX
      READ(1,*) A,B,H,BF,ZBAR
C  NOTE BF ALWAYS NEEDS TO BE GIVEN A VALUE EVEN FOR
C  CASES 1 AND 2 TO PREVENT UNNECESSARY ERROR OF
C  DIVIDING BY ZERO WHEN BF = 0
C
      WRITE(*,1026) I
C  FIRST CALCULATE THE COEFFICIENT OF BUCKLING K
      WRITE(*,1025)
      CALL CALK(A/B,NCASE,NU,B/BF,M,K)
      RK = REAL(K)
C  NEXT CALCULATE THE CRITICAL STRESS
      WRITE(*,1027)
```

```
      CALL CALSTCR(RK,B,H,FPC,K3,NU,FSY,ES,RO,ZBAR,
     +               EPSO,EC,SIGCR,BMD,ISS,AW,BW,CW,DW)
C  WRITE RESULTS TO OUTPUT FILE
      WRITE(2,1023) A/B,B/H,B/BF,ZBAR,M,RK,SIGCR,BMD
 40   CONTINUE
 50   WRITE(2,1003)
 60   STOP
      END
C ************************************************************
      SUBROUTINE CALK(RATIO,NCASE,NU,BRATIO,M,AK)
C
C  THIS SUBROUTINE SOLVES FOR K VALUES FOR THE CASE OF
C  RECTANGULAR PLATES UNDER UNIFORM COMPRESSION, SIMPLY
C  SUPPORTED ALONG LOADED EDGES,
C  BOTH UNLOADED EDGES ARE 1) simply supported (Case 1)
C                          2) fixed (Case 2)
C                          3) elastically built-in (Case 3)
C  SOLUTION IS BASED ON TRIAL AND ERROR METHOD
C
      DOUBLE PRECISION PK,AK
      REAL NU,KMNXT
C
      M = 1
      MP = M
C  CALCULATE K FOR M=1 (M IS NUMBER OF HALFWAVES)
      GOTO (10,20,30) NCASE
 10   CALL CASE1(M,RATIO,PK)
      GOTO 40
 20   DRB = 1.
C  DRB IS A DUMMY VALUE OF RB SINCE IT IS NOT NEEDED FOR
C  CASE 2
      CALL CASE23(M,RATIO,NU,DRB,NCASE,PK)
      GOTO 40
 30   CALL CASE3(M,RATIO,NU,BRATIO,PK)
      GOTO 40
C
C  CALCULATE K FOR NEXT HIGHER M
 40   M = M + 1
      GOTO (50,60,70) NCASE
 50   CALL CASE1(M,RATIO,AK)
      GOTO 80
 60   DRB = 1.
C  DRB IS A DUMMY VALUE OF RB SINCE IT IS NOT NEEDED FOR
C  CASE 2
      CALL CASE23(M,RATIO,NU,DRB,NCASE,AK)
      GOTO 80
 70   CALL CASE3(M,RATIO,NU,BRATIO,AK)
      GOTO 80
```

```
C  IF K CALCULATED FOR THIS M IS HIGHER THAN FOR THE
C  PREVIOUS M, THEN A MINIMUM VALUE OF K FOR APPROPRIATE
C  M IS FOUND WHICH IS THE PREVIOUSLY FOUND VALUE; IF K
C  CALCULATED FOR THIS M IS SMALLER THAN THE ONE FOR THE
C  PREVIOUS M BUT LESS THAN THE MIN K OF THE NEXT M THEN K
C  IS ALSO FOUND WHICH IS THE CURRENT VALUE OF K; OTHERWISE
C  CONTINUE FOR THE NEXT HIGHER VALUE OF M
C
 80    KMNXT = ((M+1)/RATIO)**2
       IF (AK.GT.PK) THEN
       AK = PK
       M = MP
       GOTO 90
           ELSE
           IF(AK.LT.KMNXT) GOTO 90
           PK = AK
           MP = M
           GOTO 40
       ENDIF
 90    RETURN
       END
C ***************************************************************
       SUBROUTINE CASE1(M,R,AK)
C
C  THIS SUBROUTINE CALCULATES A "K" VALUE FOR THE CASE WHEN
C  THE UNLOADED EDGES ARE SIMPLY SUPPORTED
C
       DOUBLE PRECISION AK
       AK = (M/R + R/M)**2
       RETURN
       END
C ***************************************************************
       SUBROUTINE CASE23(M,R,NU,RB,NCASE,AK)
C
C  THIS SUBROUTINE CALCULATES A "K" VALUE FOR THE CASE WHEN
C  THE UNLOADED EDGES ARE BOTH FIXED OR PARTIALLY FIXED
C
       DOUBLE PRECISION AK,PK,DELK
       REAL NU
       DATA PI/3.141592654/
       NCHG = 0
       DELK = 1.0
       PHI = (PI*M/R)**2
C  ASSUME A STARTING TRIAL VALUE OF K
       CALL INITK(M,R,AK)
       PK = AK
C  GET THE INITIAL DIFFERENCE
       IF (NCASE.EQ.2) THEN
```

```
      CALL CALEQ2(AK,PHI,PI,PDEL)
          ELSEIF (NCASE.EQ.3) THEN
          CALL CALEQ3(AK,PHI,PI,RB,PDEL)
      ENDIF
 200  AK = AK+DELK
C  GET THE DIFFERENCE
      IF (NCASE.EQ.2) THEN
      CALL CALEQ2(AK,PHI,PI,DEL)
          ELSEIF (NCASE.EQ.3) THEN
          CALL CALEQ3(AK,PHI,PI,RB,DEL)
      ENDIF
C
C  IF THE DIFFERENCE CHANGES SIGN FROM THE PREVIOUS K TO
C  CURRENT K THEN INCREMENT OF K IS REDUCED.  ITERATION IS
C  RESUMED STARTING FROM THE LAST VALUE OF K UNTIL K IS
C  ACCURATE TO THE 7TH PLACE
C
      IF (((PDEL.GT.0.0) .AND. (DEL.LE.0.0)) .OR.
     *    ((PDEL.LT.0.0) .AND. (DEL.GE.0.0))) THEN
      DELK = DELK/10.0
      AK = PK
      NCHG = NCHG + 1
      GOTO 200
      ENDIF
      PDEL = DEL
      PK = AK
      IF (NCHG.GE.7) GOTO 300
      GOTO 200
 300  RETURN
      END
C ***************************************************************
      SUBROUTINE CASE3(MW,ABW,NU,BBFR,RKW)
C
C  THIS SUBROUTINE SOLVES FOR K VALUES GIVEN ANY HALF WAVE
C  NUMBER FOR THE CASE OF RECTANGULAR PLATES UNDER UNIFORM
C  COMPRESSION, SIMPLY SUPPORTED ALONG LOADED EDGES.  BOTH
C  UNLOADED EDGES ARE ELASTICALLY BUILT-IN (Case 3).
C  SOLUTION IS BASED ON TRIAL AND ERROR METHOD
C
      DOUBLE PRECISION KW1,KW2,RKW
      REAL NU
      DATA PI/3.141592654/
      RANGE = 0.0001
C  THIS RANGE CORRESPONDS TO 0.01%
      ABF = ABW*BBFR
      MF = MW
      CALL INITK(MW,ABW,KW1)
      RKW1 = REAL(KW1)
```

```
      RINC = 1.
      PRKW1 = RKW1
C  A VALUE OF KW IS ASSUMED (RKW1)
 100  RKW1 = RKW1 + RINC
      RKF = RKW1/BBFR**2
C  A CORRESPONDING STIFFNESS OF RESTRAINING PLATE, THUS THE
C  COEFFICIENT OF FIXITY IS CALCULATED.
C  A VALUE OF KW RELATING TO THIS FIXITY IS FOUND (RKW22)
      CALL COFIX(ABF,MF,BBFR,RKF,PI,RB)
      IF (RB.LE.0.0) THEN
        IF (ABS(RB).LT.0.0001) THEN
        RB = 0.0001
        GOTO 300
        ENDIF
      RINC = RINC/10.0
      RKW1 = PRKW1
      GOTO 100
      ENDIF
      IF (RB.LT.0.0001) RB = 0.0001
 300  CALL CASE23(MW,ABW,NU,RB,3,KW2)
      RKW2 = REAL(KW2)
C  COMPARISON BETWEEN THE ASSUMED AND CALCULATED VALUES OF
C  RKW'S WHEN THEY ARE APPROXIMATELY EQUAL (WITHIN 0.01% OF
C  ONE ANOTHER), A TRUE VALUE OF KW IS FOUND.
      DIF = ABS((RKW2-RKW1)/RKW1)
      IF (DIF.LT. RANGE) GOTO 200
      IF (RKW2.GT.RKW1) THEN
      PRKW1 = RKW1
      GOTO 100
          ELSE
          RINC = RINC/10.0
          RKW1 = PRKW1
          GOTO 100
      ENDIF
 200  RKW = RKW2
      RETURN
      END
C ***************************************************************
      SUBROUTINE CALEQ2(AK,PHI,PI,DEL)
C  THIS SUBROUTINE CALCULATES THE DIFFERENCE BETWEEN TWO
C  SIDES OF THE TRANSCENDENTAL EQUATION FOR CASE 22
      DOUBLE PRECISION AK
C  FIRST CALCULATE LEFT-HAND SIDE AND RIGHT-HAND SIDES OF
C  THE EQUATION
      BALPHA = (PHI+(PI**2*AK*PHI)**0.5)**0.5
      BBETA = (-PHI+(PI**2*AK*PHI)**0.5)**0.5
      SINBB = SIN(BBETA)
      COSBB = COS(BBETA)
```

```
      SINHBA = SINH(BALPHA)
      COSHBA = COSH(BALPHA)
      ALHS = 2*BALPHA*BBETA*(1-COSBB*COSHBA)
      RHS = -(BALPHA**2-BBETA**2)*SINBB*SINHBA
C  GET THE DIFFERENCE
      DEL = ALHS - RHS
      RETURN
      END
C ************************************************************
      SUBROUTINE CALEQ3(AK,PHI,PI,RB,DEL)
C  THIS SUBROUTINE CALCULATES THE DIFFERNCE BETWEEN TWO
C  SIDES OF THE TRANSCENDENTAL EQUATION FOR CASE 3.
      DOUBLE PRECISION AK
C  FIRST CALCULATE LEFT-HAND SIDE AND RIGHT-HAND SIDE OF
C  THE EQUATION
      BALPHA = (PHI+(PI**2*AK*PHI)**0.5)**0.5
      BBETA =  (-PHI+(PI**2*AK*PHI)**0.5)**0.5
      SINBB = SIN(BBETA)
      COSBB = COS(BBETA)
      SINHBA = SINH(BALPHA)
      COSHBA = COSH(BALPHA)
      ALHS = (BALPHA**2-BBETA**2)*SINBB*SINHBA
     *        +2*BALPHA*BBETA*(1-COSBB*COSHBA)
      RHS = -((BALPHA**2+BBETA**2)**2/RB**2)*SINBB*SINHBA
     *      +2*BBETA/RB*(BALPHA**2+BBETA**2)*COSBB*SINHBA
     *      -2*BALPHA/RB*(BALPHA**2+BBETA**2)*SINBB*COSHBA
C  GET THE DIFFERENCE
      DEL = ALHS - RHS
      RETURN
      END
C ************************************************************
      SUBROUTINE INITK(M,R,AK)
C  THIS SUBROUTINE FINDS A FIRST TRIAL VALUE OF K.
C  K SHOULD BE > (M/RATIO)**2 DUE TO SOME CONSTRAINTS ON THE
C  TRANSCENDENTAL EQUATION (I.E. TO HAVE BBETA REAL).
      DOUBLE PRECISION AK,D
C  K IS FIRST ASSUMED TO BE THE SMALLEST INTEGER
C  > (M/RATIO)**2
      K = 4
      IF (K.LT.(M/R)**2) THEN
      K = (M/R)**2 + 1
      ENDIF
      AK = K
      IF (AK.EQ.4.0) AK = AK + 0.00001
      RETURN
      END
C ************************************************************
      SUBROUTINE COFIX(AB,M,BBFR,RK,PI,RB)
```

```
C  THIS SUBROUTINE CALCULATES COEFFICIENT OF FIXITY FOR
C  A GIVEN STRESS LEVEL APPLIED ON THE RESTRAINING PLATE.
      ALPHA2 = PI*((M/AB)**2+(M/AB)*RK**0.5)**0.5/2
      BETA2 = PI*(-(M/AB)**2+(M/AB)*RK**0.5)**0.5/2
      TANHA2 = TANH(ALPHA2)
      COTHA2 = 1/TANH(ALPHA2)
      TANB2 = TAN(BETA2)
      COTB2 = 1/TAN(BETA2)
      C = (ALPHA2*TANHA2+BETA2*TANB2-ALPHA2*COTHA2+BETA2
     *    *COTB2)/(ALPHA2*TANHA2+BETA2*TANB2+ALPHA2*COTHA2
     *    -BETA2*COTB2)
      S2 = (ALPHA2**2+BETA2**2)/(ALPHA2*TANHA2+BETA2*TANB2+
     *     ALPHA2*COTHA2-BETA2*COTB2)
      FK = S2/(1+C)
      RB = 4.0*FK*BBFR
      RETURN
      END
C ***********************************************************
      SUBROUTINE CALSTCR(AK,B,H,SIGC,K3,NU,FSY,ES,RO,ZBAR,
     *              EPSO,EC,SIGCR,MB,ISS,AW,BW,CW,DW)
C  THIS SUBROUTINE CALCULATES THE CRITICAL BUCKLING STRESS
C  OF A PLATE WHICH HAS CERTAIN GEOMETRY, MATERIAL PROPERTIES
C  AND EDGE CONDITIONS.  ONLY THE ASCENDING BRANCH OF THE
C  STRESS-STRAIN CURVE FOR CONCRETE IS USED.
      DOUBLE PRECISION SIGMA,PSIGMA,DSIG,RW,SW,CHECK
      REAL K3,NU
      DATA PI/3.141592654/
C  OTHER CONSTANTS
      EPSY = FSY/ES
      RANGE = 0.0005
C  RANGE IS 0.05%
      DSIG = 100.0
      CAK = AK*(PI**2/(B**2*H))
C  FOR THE CASE OF BUCKLING INDUCED BY YIELDING OF STEEL
C  RANGE OF B/H IS CALCULATED.  IF ACTUAL B/H FALLS WITHIN
C  THIS RANGE. CRITICAL STRESS IS ASSUMED TO BE CONCRETE
C  STRESS AT STRAIN COMPATIBLE WITH STEEL YIELD STRAIN
      IF (EPSO.GT.EPSY) THEN
      IF (ISS.EQ.1) THEN
      ETY = EC*(1-EPSY/EPSO)
      SIGCRY = K3*SIGC*(2.*(EPSY/EPSO)-(EPSY/EPSO)**2)
      ELSE
      ETY = K3*SIGC*(((1+CW*(EPSY/EPSO)+DW*(EPSY/EPSO)**2)*
     +        (AW/EPSO+2*BW*EPSY/EPSO**2))-((AW*EPSY/EPSO+
     +        BW*(EPSY/EPSO)**2)*(CW/EPSO+2*DW*EPSY/EPSO**2)))
     +     /(1+CW*EPSY/EPSO+DW*(EPSY/EPSO)**2)**2
      SIGCRY = K3*SIGC*(AW*EPSY/EPSO+BW*(EPSY/EPSO)**2)/
     +           (1+CW*EPSY/EPSO+DW*(EPSY/EPSO)**2)
```

```
      ENDIF
      BH1 = SQRT(AK*PI**2*ETY/(SIGCRY*12.*(1-NU**2)))
      BH2 = SQRT(AK*PI**2/SIGCRY*(ETY/(12.*(1-NU**2))
     +          + (ES*1000.)*(RO/100.)*(ZBAR/H)**2))
          IF ((B/H.GE.BH1).AND.(B/H.LE.BH2)) THEN
          SIGCR = SIGCRY
          MB = 4
          GOTO 500
          ENDIF
      ENDIF
      SIGMA = 0.0
      PSIGMA = 0.0
      DIF1 = 0.0
      DIF2 = 0.0
C  ITERATION LOOP WITH INCREMENTAL VALUES OF ACTUAL STRESS
 100  SIGMA = SIGMA + DSIG
      IF (SIGMA.GT.K3*SIGC) SIGMA = K3*SIGC
C  CALCULATE A CRITICAL STRESS
      IF (ISS.EQ.1) THEN
         EPS = EPSO*(1-(1-SIGMA/(K3*SIGC))**0.5)
         ET = EC*(1-EPS/EPSO)
      ELSE
         RW = DW - BW*K3*SIGC/SIGMA
         SW = CW - AW*K3*SIGC/SIGMA
         CHECK = SW**2 - 4.0*RW
       IF (CHECK .LT. 0.000001) CHECK = 0.0
         EPS = EPSO*(-SW-SQRT(CHECK))/(2.0*RW)
         ET = K3*SIGC*(((1+CW*(EPS/EPSO)+DW*(EPS/EPSO)**2)*
     +         (AW/EPSO+2*BW*EPS/EPSO**2))-((AW*EPS/EPSO+
     +         BW*(EPS/EPSO)**2)*(CW/EPSO+2*DW*EPS/EPSO**2)))
     +      /(1+CW*EPS/EPSO+DW*(EPS/EPSO)**2)**2
      ENDIF
      IF (EPS.GT.EPSY) THEN
      ESI = 0.0
      ELSE
      ESI = ES
      ENDIF
      DCONC = ET*H**3/(12.*(1-NU**2))
      DSTE = (ESI*1000.0)*H*(RO/100.0)*ZBAR**2
      SIGCR = CAK*(DCONC+DSTE)
C  IF THIS CRITICAL STRESS IS GREATER THAN ACTUAL STRESS AND
C  IT IS NOT NEAR COMPRESSIVE STRENGTH OF CONCRETE, THEN
C  CONTINUE TO MOVE UP THE STRESS-STRAIN CURVE; OTHERWISE
C  IF IT IS NEAR THE COMPRESSIVE STRENGTH OF CONCRETE THEN
C  A CRITICAL STRESS IS NOT AVAILABLE
      IF (SIGCR.GT.SIGMA) THEN
      DIF1 = (K3*SIGC-SIGMA)/(K3*SIGC)
      IF (DIF1.GT.RANGE) THEN
```

```
          PSIGMA = SIGMA
          GOTO 100
          ENDIF
        SIGCR = K3*SIGC
        MB = 1
        GOTO 500
        ELSE
C   IF THIS CRITICAL STRESS IS SMALLER THAN ACTUAL STRESS
C   AND NOT CLOSE TO THE ACTUAL STRESS THEN REDUCE THE STRESS
C   INCREMENT AND CONTINUE TO ITERATE UNTIL THE TWO VALUES
C   ARE WITHIN RANGE(0.01% OF ONE ANOTHER), THEN THE CRITICAL
C   STRESS IS FOUND.
        DIF2 = (SIGMA-SIGCR)/SIGMA
          IF (DIF2.GT.RANGE) THEN
          DSIG = DSIG/10.0
          SIGMA = PSIGMA
          GOTO 100
          ENDIF
          IF (ESI.EQ.0.0) THEN
          MB = 2
          ELSE
          MB = 3
          ENDIF
        GOTO 500
        ENDIF
C   BUCKLING STRESS IS FOUND, RETURN TO MAIN PROGRAM
 500   RETURN
       END
C*****************************************************************
C   THIS SUBROUTINE CALCULATES AND RETURNS TO THE
C   MAIN PROGRAM THE NECESSARY PARAMATERS FOR
C   HOGNESTAD'S STRESS-STRAIN RELATION
C   THE SUBROUTINE ALSO COMPUTES THE STRESS-STRAIN DIAGRAM
       SUBROUTINE  HOG(FPSC,FACTOR,EC,EPSO,EPSMAX)
       DIMENSION STRAIN(100),STRESS(100)
C   COMPUTE E-CONCRETE AND EPSO USING CORNELL EXPRESSION
       IF (EPSO .EQ. 0.0) THEN
       EC = 1000. + 40.0*SQRT(FACTOR*FPSC*1000.)
       EPSO = 2.0*FACTOR*FPSC/EC
       ELSE
       EC = 2.0*FACTOR*FPSC/EPSO
       ENDIF
C   COMPUTE STRESS-STRAIN CURVE
       STRAIN(1) = 0.0
       STRESS(1) = 0.0
       STRINC = EPSMAX/50.
       DO 1500 K = 2,51
       STRAIN(K) = STRAIN(K-1) + STRINC
```

```
      X = STRAIN(K)/EPSO
      IF(STRAIN(K).LE.EPSO) THEN
        STRESS(K) = FACTOR*FPSC*(2.0*X-X**2)
      ELSEIF(STRAIN(K).GT.EPSO) THEN
      STRESS(K)=FACTOR*FPSC-(STRAIN(K)-EPSO)*(0.15*FACTOR*FPSC)/
     +           (EPSMAX-EPSO)
      ENDIF
 1500 CONTINUE
      OPEN(4,FILE='HOG.CSV',STATUS='NEW')
      WRITE(4,89) FPSC,EC,EPSMAX,EPSO,FACTOR
  89  FORMAT(10X,'CONCRETE STRENGTH, KSI      ',F10.2,
     +     /,10X,'CONCRETE E, KSI              ',F10.2,
     +    //,10X,'MAX. USEABLE STRAIN          ',F10.7,
     +     /,10X,'EPSO (CONC. STRAIN AT FPSC) ',F10.7,
     +     /,10X,'HOGNESTAD FACTOR K3         ',F10.2,
     +   ///,3X,'STRAIN        STRESS ',/,5('-----'),//)
      DO 1550 L = 1,51
       WRITE(4,91) STRAIN(L),STRESS(L)
  91    FORMAT(F10.8,',',5X,F10.3)
 1550 CONTINUE
      CLOSE(UNIT=4)
      RETURN
      END
C*****************************************************************
C  THIS SUBROUTINE CALCULATES AND RETURNS TO
C  THE MAIN PROGRAM THE NECESSARY PARAMATERS FOR
C  WANG'S STRESS-STRAIN RELATION
C  THE SUBROUTINE ALSO COMPUTES THE STRESS-STRAIN DIAGRAM
      SUBROUTINE WANG(FPSC,FACTOR,EC,EO,EPSO,EPSI,EPS2I,FI,F2I,
     +          A,B,C,D,A1,B1,C1,D1,EPSMAX)
      DIMENSION STRAIN(100), STRESS(100)
      AKFPSC = FACTOR*FPSC
C  EC = SECANT MODULUS OF CONCRETE AT 0.45*FACTOR*F'C
      EC = 271. * AKFPSC + 978.
      IF (EPSO .EQ. 0.0) EPSO = .000125 * AKFPSC + .00230
      EO = AKFPSC/EPSO
      EPSI = .00005 * AKFPSC + .00401
      FI = .580 * AKFPSC + .774
      EPS2I = EPSI + (EPSI - EPSO)
      IF (AKFPSC .LT. 6.5) THEN
      F2I = .085 * AKFPSC + 1.5
      ELSE
      F2I = .085 * AKFPSC + 2.024
      ENDIF
C  CALCULATE CONSTANTS FOR ASCENDING BRANCH OF
C  STRESS-STRAIN CURVE
      A = EC/EO
      D = (A**3 -2.45 * A**2 + 1.9 * A - 0.45)/(.55*A - 0.2475)
```

```
      C = -1. - (0.55 * D)/(1. - A)
      B = C + D + 1. - A
C  CALCULATE CONSTANTS FOR DESCENDING BRANCH OF
C  STRESS-STRAIN CURVE
      XA = EPSI/EPSO
      XB = FI/(AKFPSC)
      XC = EPS2I/EPSO
      XD = F2I/(AKFPSC)
      XM = XC*(XB/XA - XD/XC - XB*XC/(XA*(1.0-XA))+(XB+XC-
     +        XA)/(1.0-XA))
      XN = XC*(XA*XB - (XC-XA)*(XA*XB-1.0)/(1.0-XA) - XC*XD)
      XQ = XC*(XD - XB + (XC-XA)*(XB-1.0)/(1.0-XA))
      XE = -XA + XB/XA + XM*(XB-XA)/XQ
      XK = XA*XB - XA + XN*(XB-XA)/XQ
      XG = (2.0 + XM/XQ)*(XB/XA + (XB-1.0) * XM/XQ - 1.0)
      XH = XN/XQ * (3.0 - 2.0*XB - XB/XA)+(XM/XQ + 2.0)*(1.0-
     +       XA*XB) + 2.0 * XM*XN*(1.0 - XB)/XQ**2
      XL = -XN/XQ*(XA*XB - 1.0 + XN/XQ*(XB-1.0))
      D1 = (-XH - XK + XE - SQRT((XH+XK-XE)**2 - 4.0*(XE-XG)
     +       *(XL-XK)))/(2.0*(XL-XK))
      C1 = (XM + XN * D1)/XQ
      B1 = -1.0/(1.0-XA) * (XB/XA + (XB-1.0)*C1 +
C     +      (XA*XB-1.0)*D1 - 1.0)
      A1 = XB*(1.0/XA + C1) + XA*(XB*D1-B1)
C  COMPUTE STRESS-STRAIN CURVE
      STRAIN(1) = 0.0
      STRESS(1) = 0.0
      STRINC = EPSMAX/50.
      DO 1600 K = 2,51
      STRAIN(K) = STRAIN(K-1) + STRINC
      X = STRAIN(K)/EPSO
      IF(STRAIN(K).LE.EPSO) THEN
       STRESS(K) = AKFPSC*((A*X+B*X**2)/(1+C*X+D*X**2))
      ELSEIF(STRAIN(K).GT.EPSO) THEN
       STRESS(K) = AKFPSC*((A1*X+B1*X**2)/(1+C1*X+D1*X**2))
      ENDIF
 1600 CONTINUE
      OPEN(5,FILE='WANG.CSV',STATUS='NEW')
      WRITE(5,94) FPSC,EC,EO,EPSMAX,EPSO,EPSI,FI,
     +            EPS2I,F2I,FACTOR
 94   FORMAT(5X,'CONCRETE STRENGTH, KSI',F10.2,
     +     /,5X,'SECANT MODULUS AT .45*K3*FPSC, KSI',F10.2,
     +     /,5X,'SECANT MODULUS AT PEAK STRESS, KSI',F10.2,
     +     /,5X,'MAX. USEABLE STRAIN',F10.7,
     +     /,5X,'STRAIN AT PEAK STRESS (EPSO)',F10.7,
     +     /,5X,'STRAIN AT INFLECTION POINT (EPSI)',F10.7,
     +     /,5X,'STRESS AT INFLECTION POINT (FI)',F10.2,
     +     /,5X,'STRAIN AT SECOND POINT (EPS2I)',F10.7,
```

```
     +     /,5X,'STRESS AT SECOND POINT (F2I)',F10.2,
     +     /,5X,'STRESS BLOCK FACTOR (K3)            ',F5.3,
     +   ///,3X,'STRAIN        STRESS ',/,5('-----'),//)
      DO 1650 L = 1,51
      WRITE(5,95) STRAIN(L),STRESS(L)
  95    FORMAT(F10.8,',',5X,F10.3)
 1650 CONTINUE
      CLOSE(UNIT=5)
      RETURN
      END
C*****************************************************************
C THIS SUBROUTINE CALCULATES AND RETURNS TO THE MAIN PROGRAM THE
C NECESSARY PARAMATERS FOR USER-DEFINED STRESS-STRAIN RELATIONS
C BASED ON WANG'S FITTED EQUATIONS
C THE SUBROUTINE ALSO COMPUTES THE STRESS-STRAIN DIAGRAM
      SUBROUTINE USER(FPSC,FACTOR,EC,EO,EPSO,EPSI,EPS2I,FI,F2I,
     +          A,B,C,D,A1,B1,C1,D1,EPSMAX)
      DIMENSION STRAIN(100),STRESS(100)
 1659     WRITE(*,1660)
 1660 FORMAT(1X,'ENTER THE SECANT MODULUS OF CONCRETE IN KSI')
      READ(*,*) EC
      WRITE(*,1665)
 1665 FORMAT(1X,'ENTER CONCRETE STRAIN COINCIDING WITH
     +        PEAK STRESS')
      READ(*,*) EPSO
      WRITE(*,1670)
 1670 FORMAT(1X,'ENTER CONCRETE STRAIN FOR
     +       FIRST INFLECTION POINT')
      READ(*,*) EPSI
      WRITE(*,1675)
 1675 FORMAT(1X,'ENTER CONC. STRESS FOR
     +       1st INFLECTION POINT, IN KSI')
      READ(*,*) FI
      WRITE(*,1680)
 1680 FORMAT(1X,'ENTER CONC. STRESS FOR 2nd Pt.
     +         ON DESC. BRANCH (KSI)')
      READ(*,*) F2I
      WRITE(*,1690) FPSC,FACTOR,EC,EPSMAX,EPSO,EPSI,FI,F2I
 1690 FORMAT(5X,'CONCRETE STRENGTH, KSI              ',F10.2,
     +     /,5X,'STRESS BLOCK FACTOR (K3)            ',F5.3,
     +     /,5X,'SECANT MODULUS AT .45*K3*FPSC, KSI  ',F10.2,
     +     /,5X,'MAX. USEABLE STRAIN                 ',F10.7,
     +     /,5X,'STRAIN AT PEAK STRESS (EPSO)        ',F10.7,
     +     /,5X,'STRAIN AT INFLECTION POINT (EPSI)   ',F10.7,
     +     /,5X,'STRESS AT INFLECTION POINT (FI)     ',F10.2,
     +     /,5X,'STRESS AT SECOND POINT (F2I)        ',F10.2,//)
      WRITE(*,1695)
 1695 FORMAT(1X,'IF THE PRECEDING INFORMATION
```

```
     +   IS INCORRECT ENTER "1" ', ' ELSE ENTER "0" ')
      READ(*,*) IUSR
      IF (IUSR.EQ.1) GOTO 1659
      EO = FACTOR*FPSC/EPSO
      EPS2I = EPSI + (EPSI - EPSO)
C  CALCULATE CONSTANTS FOR ASCENDING BRANCH OF
C  STRESS-STRAIN CURVE
      A = EC/EO
      D = (A**3 -2.45 * A**2 + 1.9 * A - 0.45)/(.55*A-0.2475)
      C = -1. - (0.55 * D)/(1. - A)
      B = C + D + 1. - A
C  CALCULATE CONSTANTS FOR DESCENDING BRANCH OF
C  STRESS-STRAIN CURVE
      XA = EPSI/EPSO
      XB = FI/(FACTOR*FPSC)
      XC = EPS2I/EPSO
      XD = F2I/(FACTOR*FPSC)
      XM = XC*(XB/XA - XD/XC - XB*XC/(XA*(1.0-XA))+
     +       (XB+XC-XA)/(1.0-XA))
      XN = XC*(XA*XB - (XC-XA)*(XA*XB-1.0)/(1.0-XA) - XC*XD)
      XQ = XC*(XD - XB + (XC-XA)*(XB-1.0)/(1.0-XA))
      XE = -XA + XB/XA + XM*(XB-XA)/XQ
      XK = XA*XB - XA + XN*(XB-XA)/XQ
      XG = (2.0 + XM/XQ)*(XB/XA + (XB-1.0) * XM/XQ - 1.0)
      XH = XN/XQ * (3.0 - 2.0*XB - XB/XA)+(XM/XQ + 2.0)*
     +       (1.0- XA*XB)+ 2.0 * XM*XN*(1.0 - XB)/XQ**2
      XL = -XN/XQ*(XA*XB - 1.0 + XN/XQ*(XB-1.0))
      D1 = (-XH - XK + XE - SQRT((XH+XK-XE)**2 - 4.0*(XE-XG)
     +       *(XL-XK)))/(2.0*(XL-XK))
      C1 = (XM + XN * D1)/XQ
      B1 = -1.0/(1.0-XA) * (XB/XA + (XB-1.0)*C1 +
     +       (XA*XB-1.0)*D1 - 1.0)
      A1 = XB*(1.0/XA + C1) + XA*(XB*D1-B1)
C  COMPUTE STRESS-STRAIN CURVE
      STRAIN(1) = 0.0
      STRESS(1) = 0.0
      STRINC = EPSMAX/50.
      DO 1700 K = 2,51
      STRAIN(K) = STRAIN(K-1) + STRINC
      X = STRAIN(K)/EPSO
      IF(STRAIN(K).LE.EPSO) THEN
       STRESS(K) = FACTOR*FPSC*((A*X+B*X**2)/(1+C*X+D*X**2))
      ELSEIF(STRAIN(K).GT.EPSO) THEN
       STRESS(K) = FACTOR*FPSC*((A1*X+B1*X**2)/(1+C1*X+D1*X**2))
      ENDIF
 1700 CONTINUE
      OPEN(7,FILE='USR.CSV',STATUS='NEW')
      WRITE(7,101)  FPSC,EC,EO,EPSMAX,EPSO,EPSI,FI,
```

```
     +              EPS2I,F2I,FACTOR
101   FORMAT(5X,'CONCRETE STRENGTH, KSI',F10.2,
     +     /,5X,'SECANT MODULUS AT .45*K3*FPSC, KSI',F10.2,
     +     /,5X,'SECANT MODULUS AT PEAK STRESS, KSI',F10.2,
     +     /,5X,'MAX. USEABLE STRAIN',F10.7,
     +     /,5X,'STRAIN AT PEAK STRESS (EPSO)',F10.7,
     +     /,5X,'STRAIN AT INFLECTION POINT (EPSI)',F10.7,
     +     /,5X,'STRESS AT INFLECTION POINT (FI)',F10.2,
     +     /,5X,'STRAIN AT SECOND POINT (EPS2I)',F10.7,
     +     /,5X,'STRESS AT SECOND POINT (F2I)',F10.2,
     +     /,5X,'STRESS BLOCK FACTOR (K3)            ',F5.3,
     +   ///,3X,'STRAIN        STRESS ',/,5('-----'),//)
      DO 1750 L = 1,51
      WRITE(7,105) STRAIN(L),STRESS(L)
105     FORMAT(F10.8,',',5X,F10.3)
1750  CONTINUE
      CLOSE(UNIT=7)
      RETURN
      END
```

APPENDIX E

PROGRAM MOMINT SOURCE CODE

```
      PROGRAM MOMINT
      CHARACTER*15 FILIN,FILOUT
      DOUBLE PRECISION PHI,PHIMAX,PHIMIN,PHIINC,
     +      CDIF,CSTRES,CTEMP
      DIMENSION  AP(200),AMOM(200),AP2(200),
     +        AMOM2(200),DEPNA(200)
      DIMENSION AEPS(200),AEPS2(200),APHI(200),
     +        FORC(100)
      INTEGER IFLAG2(200),FFLAG
      COMMON /BLOCK1/ YBAR(200),AC(200),AS(200),ASP(200),
     + EPSPIS,EPSPIC,ES,ESP,FY,EU,FU,FYPT,EPSO,FACTOR,
     + FPSC,H,N,EPSMAX,A,B,C,D,A1,B1,C1,D1
      COMMON /BLOCK2/ FORCEA(200),BMOMA(60,60),EPSA(200),
     2        BPHI(60,60),IERR(200),BMOMB(60,60),BPHIB(60,60)
C*****************************************************************
C SIGN CONVENTION:
C   COMPRESSIVE FORCES, STRESSES AND STRAINS ARE POSTIVE
C   TENSILE FORCES, STRESSES AND STRAINS ARE NEGATIVE
C *****************************************************************
C LIST OF PRINCIPAL PROGRAM VARIABLES:
C     AC: ARRAY OF AREA OF CONCRETE IN EACH STRIP
C    ACT: TOTAL AREA OF CONCRETE IN CROSS-SECTION
C     AS: ARRAY OF AREA OF MILD STEEL IN EACH STRIP
C    AST: TOTAL AREA OF MILD STEEL IN CROSS-SECTION
C    ASP: ARRAY OF AREA OF POST-TENSIONED STEEL IN EACH STRIP
C   ASPT: TOTAL AREA OF POST-TENSIONED STEEL IN CROSS-SECTION
C   AEPS: ARRAY OF FAILURE STRAINS
C  AEPS2: SIMILAR TO AEPS, BUT ONLY CALCULATED WHEN FAILURE MODE
C         IS BUCKLING OF FLANGE FOR COMPARISON
C     AP: ARRAY OF FAILURE FORCES
C    AP2: SIMILAR TO AP BUT ONLY CALCULATED WHEN FAILURE
C         MODE IS BUCKLING OF FLANGE FOR COMPARISON
C   AMOM: ARRAY OF MOMENT IN EACH STRIP
C  AMOM2: SIMILAR TO AMOM BUT ONLY CALCULATED WHEN FAILURE
C         MODE IS BUCKLING OF FLANGE FOR COMPARISON
C   APHI: ARRAY OF CURVATURES ASSOCIATED WITH EACH POINT
C         ON THE INTERACTION DIAGRAM
C   APNO: MAXIMUM THEORETICAL STRENGTH FOR A CONCENTRICALLY
C         LOADED SHORT COLUMN
C   BMOM: MOMENT, CALCULATED & RETURNED FORM SUBROUTINE
C         CALPM, OF THE SECTION WITH A CERTAIN N.A. DEPTH
C  BMOMA: ARRAY OF MOMENTS CALCULATED FOR SPECIFIED RANGE OF
C         CURVATURES AT EACH LEVEL OF AXIAL LOAD
C  BMOMB: SIMILAR TO BMOMA, BUT ONLY CALCULATED WHEN FAILURE
C         MODE IS BUCKLING OF FLANGE FOR COMPARISON
C   BPHI: ARRAY OF CURVATURES CALCULATED FOR EACH AXIAL LOAD
C         SO THAT MOMENT-CURVATURE RELATIONSHIP CAN BE PLOTTED
C  BPHIB: SIMILAR TO BPHI, BUT ONLY CALCULATED WHEN FAILURE MODE
```

```
C          IS BUCKLING OF FLANGE FOR COMPARISON
C  BUKLE: FLAG USED TO INDICATE IF BUCKLING OF FLANGE
C          HAS OCCURRED
C  CINIT: INITIAL DEPTH OF NEUTRAL AXIS, SPECIFIED IN INPUT
C    CNA: NEUTRAL AXIS DEPTH
C CONINI: STRESS IN CONCRETE DUE TO POST-TENSIONING FORCE
C  DEPNA: ARRAY OF DEPTH OF NEUTRAL AXIS OF EACH DATA POINT
C  ECCEN: ECCENTRICITIES CORRESPONDING TO SPECIFIED VALUES OF
C          AXIAL LOAD AND MOMENT
C  ERROR: MAXIMUM ALLOWABLE ERROR RANGE FOR FINDING AXIAL LOAD
C     ES: STEEL MODULUS OF ELASTICITY, ksi
C    ESP: POST-TENSIONED STEEL MODULUS OF ELASTICITY, ksi
C     EC: CONCRETE MODULUS OF ELASTICITY, ksi
C   EPSA: CONCRETE EXTREME FIBER STRAIN AT FAILURE
C EPSMAX: MAXIMUM USABLE STRAIN OF CONCRETE
C EPSLIM: MAXIMUM DEVELOPED STRAIN OF CONCRETE IN THE
C          SECTION, i.e. MAX. USABLE STRAIN OR CRITICAL STRAIN
C  EPSCR: CRITICAL STRAIN CALCULATED FROM GIVEN CRITICAL
C          BUCKLING STRESS OF FLANGE
C   EPSO: STRAIN AT MAX. CONCRETE STRESS. IF INPUT AS 0.0,
C          PROGRAM WILL CALCULATE BASED ON MODEL USED
C    EPS: CONCRETE STRAIN AT CENTER OF EACH STRIP DUE TO
C          EXTERNAL LOADS (+)
C   EPST: CONCRETE STRAIN AT CENTER OF EACH STRIP DUE TO
C          COMBINATION OF EXTERNAL LOAD AND INITIAL STRAIN (+)
C EPSPIC: INITIAL STRAIN IN CONCRETE AND MILD STEEL (+)
C EPSPIS: INITIAL STRAIN IN POST-TENSIONED STEEL (-)
C     EU: ULTIMATE MILD STEEL STRAIN
C     EY: MILD STEEL YIELD STRAIN
C FACTOR: HOGNESTAD FACTOR K3
C  FFLAG: FLAG READ FROM DATA FILE WHICH INDICATES IF PROGRAM
C          IS TO COMPUTE THE DESIRED NUMBER OF AXIAL LOADS
C          OR IF THE LOADS ARE INPUT DIRECTLY FROM THE FILE
C             0  - COMPUTED FROM PROGRAM
C             1  - INPUT FROM DATA FILE
C   FORC: ARRAY THAT CONTAINS AXIAL LOADS READ INTO PROGRAM
C          FROM THE DATA FILE, NULL IF FFLAG = 0
C  FORCE: FORCE, CALCULATED & RETURNED FORM SUBROUTINE
C        CALPM, OF THE SECTION WITH A CERTAIN N.A. DEPTH
C FORCEA: ARRAY FOR TEMPORARY STORAGE OF FORCES
C   FPSC: CONCRETE STRENGTH
C     FU: ULTIMATE MILD STEEL STRESS
C     FY: MILD STEEL YIELD STRESS
C   FYPT: POST-TENSIONED STEEL YIELD STRESS
C      H: SECTION OVERALL DEPTH
C   IERR: FLAG WHICH INDICATES IF A POINT ON THE INTERACTION
C          DIAGRAM CORRESPONDING TO A CERTAIN LEVEL OF AXIAL
C          LOAD WAS FOUND
```

```
C            - NOT FOUND = 0
C            - FOUND = 1
C IFLAG1: FLAG INDICATING STRIP THICKNESS;
C            - EQUAL = 0
C            - UNEQUAL = 1
C IFLAG2: FLAG INDICATING MODE OF FAILURE AT EACH DATA POINT
C            - MATERIAL FAILURE = 0
C            - BUCKLING OF FLANGE = 1
C    ISS: CONCRETE STRESS-STRAIN MODEL FLAG
C            - 1 FOR HOGNESTAD'S MODEL
C            - 2 FOR WANG'S MODEL
C            - 3 FOR WANG'S MODEL WITH USER-DEFINED CONSTANTS
C      N: NUMBER OF STRIPS INTO WHICH THE SECTION IS DIVIDED
C NOCURV: NUMBER OF POINTS THAT WILL MAKE UP THE MOMENT-
C         CURVATURE DIAGRAM
C NOSTEP: NUMBER OF DATA POINTS THAT WILL BE CALCULATED
C         FOR THE DIAGRAM
C    PHI: VARIABLE FOR TEMPORARY STORAGE OF CURVATURE
C PHIMIN: INPUT TO THE PROGRAM, THIS VARIABLE CONTAINS THE
C       MINIMUM VALUE OF CURVATURE TO BE SEARCHED BY THE PROGRAM
C PHIMAX: INPUT TO THE PROGRAM, THIS VARIABLE CONTAINS THE
C      MAXIMUM VALUE OF CURVATURE TO BE SEARCHED BY THE PROGRAM
C    PTF: TOTAL FORCE DUE TO POST-TENSIONING TENDONS
C PTSINI: STRESS IN POST-TENSIONED TENDON DUE POST-TENSIONING
C         FORCE
C     SH: STRAIN HARDENING COEFFICIENT
C SIGSTL: AVERAGE STEEL STRESS IN EACH STRIP DUE TO EXT. LOADS
C TSGSTL: AVG. STEEL STRESS IN EACH STRIP DUE TO COMBINATION OF
C         EXTERNAL LOAD AND INITIAL STRAIN
C  SIGPT: AVG. POST-TENSIONED STEEL STRESS IN STRIP DUE TO
C         EXTERNAL LOADS
C SIGCON: AVERAGE CONCRETE STRESS IN EACH STRIP DUE TO EXT.
C         LOADS
C  SIGCR: CRITICAL STRESS CALCULATED USING ELASTIC
C         BUCKLING THEORY
C STLINI: MILD STEEL STRESS DUE TO POST-TENSIONING FORCE
C     TF: FLANGE THICKNESS
C   YBAR: ARRAY OF DEPTH OF CENTROID OF EACH STRIP
C*************************************************************
C  READ NAMES OF INPUT AND OUTPUT FILES
      WRITE (*,1998)
 1998 FORMAT(1X,'         THIS PROGRAM WAS WRITTEN BY      ',//,
     +          '     ANDREW W. TAYLOR AND RANDY B. ROWELL ',//,
     +          '     AT THE UNIVERSITY OF TEXAS AT AUSTIN ',/,
     +          '                SPRING 1990               ',//)
      WRITE (*,1999)
 1999 FORMAT(1X,'**************** NOTICE*****************',/,
     +   ,'  THIS PROGRAM IS NOT INTENDED FOR DISTRIBUTION',/,
```

```
     +    ,'              OR FOR USE IN DESIGN          ',//)
      WRITE (*,2001)
 2001 FORMAT (/'   *  ENTER INPUT FILE  *   '/)
      READ (*,1000) FILIN
 1000 FORMAT (A)
      WRITE (*,2002)
 2002 FORMAT (//'   *  ENTER OUTPUT FILE  *   '/)
      READ (*,1000) FILOUT
C  OPEN INPUT AND OUTPUT FILES
      OPEN (1,FILE=FILIN,STATUS='OLD')
      OPEN (2,FILE=FILOUT,STATUS='NEW')
C  READ MATERIAL PROPERTIES
      READ(1,*) FPSC,FY,EU,FU,FYPT,ES,ESP,EPSMAX,EPSO
C  READ HOGNESTAD K3 FACTOR,SECTION DEPTH, FLANGE THICKNESS,
C  NO. OF STRIPS, NO. OF STEPS, STRIP THICKNESS FLAG
      READ(1,*) FACTOR,H,TF,N,NOSTEP,IFLAG1
C  READ NUMBER OF CURVATURES DESIRED FOR MOMENT-CURVATURE
C  RELATIONSHIP,MAXIMUM VALUE OF CURVATURE,MINIMUM VALUE
C  OF CURVATURE, ERROR RANGE DESIRED FOR DESIRED AXIAL LOAD,
C  AND FLAG WHICH INDICATES DESIRED AXIAL LOAD INPUT
      READ(1,*) NOCURV,PHIMAX,PHIMIN,ERROR,FFLAG
      IF (FFLAG .EQ. 1) THEN
         DO 5 I = 1,NOSTEP
         READ(1,*) FORC(I)
  5      CONTINUE
      ENDIF
C  ENTER CRITICAL STRESS FROM PLCRST PROGRAM
      WRITE(*,2003)
 2003 FORMAT(1X,'ENTER CRITICAL STRESS:  ')
      READ(*,*) SIGCR
      IF (SIGCR .LE. 0.1) SIGCR = FACTOR * FPSC
C     ENTER CODE FOR TYPE OF STRESS-STRAIN RELATION DESIRED
  25  WRITE(*,2010)
 2010 FORMAT(1X,'ENTER 1 FOR HOGNESTAD, 2 FOR WANG, 3 FOR ',
     +        'USER DEFINED: ')
      READ(*,*) ISS
C  CALL APPROPRIATE SUBROUTINE FOR TYPE OF STRESS-STRAIN
C     RELATION DESIRED
      IF(ISS.EQ.1) THEN
      CALL HOG(FPSC,FACTOR,EC,EPSO,EPSMAX)
      ELSEIF(ISS.EQ.2) THEN
      CALL WANG(FPSC,FACTOR,EC,EO,EPSO,EPSI,EPS2I,FI,F2I,
     +          A,B,C,D,A1,B1,C1,D1,EPSMAX)
      ELSEIF(ISS.EQ.3) THEN
      CALL USER(FPSC,FACTOR,EC,EO,EPSO,EPSI,EPS2I,FI,F2I,
     +          A,B,C,D,A1,B1,C1,D1,EPSMAX)
      ELSE
      GOTO 25
```

```
      ENDIF
C  COMPUTE STRIP THICKNESS
      AN = N
      YINC = H/AN
C  INITIALIZE TOTAL AREAS OF CONC., MILD STEEL,
C  AND POST-TENS. STEEL
      ACT = 0.0
      AST = 0.0
      ASPT = 0.0
C  IF ALL STRIP DEPTHS ARE EQUAL, READ CONC. AND STEEL AREAS
      IF(IFLAG1.EQ.0) THEN
      DO 100 I = 1,N
      READ(1,*) AC(I),AS(I),ASP(I)
      ACT = ACT + AC(I)
      AST = AST + AS(I)
      ASPT = ASPT + ASP(I)
 100  CONTINUE
C  COMPUTE DEPTHS OF CENTROIDS OF STRIPS
      DO 200 J = 1,N
      AJ = J
 200  YBAR(J) = YINC*(AJ-0.50)
      ELSE
C  IF STRIP DEPTHS ARE UNEQUAL READ DEPTH, CONC. AREAS,
C  AND STEEL AREAS
      DO 250 I = 1,N
      READ(1,*) YBAR(I),AC(I),AS(I),ASP(I)
        ACT = ACT + AC(I)
        AST = AST + AS(I)
        ASPT = ASPT + ASP(I)
 250  CONTINUE
      ENDIF
C  THE FOLLOWING ROUTINE ALLOWS THE USER TO ONLY INPUT THE
C  TOTAL POST-TENSIONING FORCE AND LET THE PROGRAM CALCULATE
C  INITIAL STRAINS
      WRITE(*,2050)
 2050 FORMAT(1X,'IF YOU WISH TO LET THE PROGRAM COMPUTE THE',
     +  /,'   INITIAL STRAINS DUE TO THE POST-TENSIONING FORCE',
     +  /,'   ENTER "1", ELSE ENTER "0" ')
      READ(*,*) AYN
      IF (AYN .EQ. 1)  THEN
      CALL ISTRN(EPSO,ES,ESP,FACTOR,FPSC,ISS,A,B,C,D,EPSPIC,
     +           EPSPIS,ACT,AST,ASPT,CONINI,STLINI,PTSINI)
      ELSE
C  ENTER INITIAL STRAINS DUE TO POST-TENSIONING
 28   WRITE(*,2100)
 2100 FORMAT(1X,'ENTER THE INITIAL STRAIN IN THE CONCRETE',/,
     +     ' AND MILD STEEL DUE TO THE POST-TENSIONING FORCE')
      READ(*,*) EPSPIC
```

```
      WRITE(*,2150)
 2150 FORMAT(1X,'ENTER THE STRAIN IN THE POST-TENSIONING ',/,
     +'STEEL DUE TO THE POST-TENSIONING FORCE (NEGATIVE VALUE)')
      READ(*,*) EPSPIS
      X = EPSPIC/EPSO
      CONINI = FACTOR*FPSC*(2.0*X-X**2)
      STLINI = ES*EPSPIC
      PTSINI = ESP*EPSPIS
      ENDIF
C  SET VALUE OF CRITICAL STRAIN
      IF (SIGCR .GE. .99*(FACTOR*FPSC)) THEN
         EPSCR = EPSMAX
         EPSLIM = EPSMAX
C  CALCULATE CRITICAL STRAIN FROM CRITICAL STRESS BASED ON
C  HOGNESTAD'S MODEL
      ELSEIF (SIGCR.LT.(FACTOR*FPSC) .AND. ISS.EQ.1) THEN
      EPSCR = EPSO*(1-SQRT(1-(SIGCR/(FACTOR*FPSC))))
        EPSLIM = EPSCR
      ELSE
C  CALCULATE CRITICAL STRAIN FROM CRITICAL STRESS BASED ON
C  WANG'S MODEL
      R = D - B*FACTOR*FPSC/SIGCR
      S = C - A*FACTOR*FPSC/SIGCR
      EPSCR = EPSO*(-S-SQRT(S**2-4.0*R))/(2.0*R)
      EPSLIM = EPSCR
      ENDIF
C  ECHO-PRINT INPUT DATA
      WRITE(*,40) FPSC,FACTOR,FY,FYPT,EC,EU,FU,EPSMAX,EPSO,
     +     EPSPIC,EPSPIS,CONINI,STLINI,PTSINI,SIGCR,EPSCR,H,TF
      WRITE(*,42)
      ISTOP = 0
  42  FORMAT(1X,'IF YOU WISH TO CONTINUE TYPE "0"',
     +           ' ELSE TYPE "1" ')
      READ(*,*) ISTOP
      IF (ISTOP .EQ. 1)  GOTO 9999
C
C  CALCULATE STARTING POINT FOR INTERACTION DIAGRAM
C
      TFY = (EPSO-EPSPIC)*ES
      IF (TFY.GT.FY)  TFY = FY
      APNO = (0.85*FPSC-CONINI)*ACT + TFY*AST +
     +           (EPSO-EPSPIC)*ESP*ASPT
      ANOST = NOSTEP-1
      PINC = 1.02*APNO/ANOST
      TFORCE = 1.02*APNO + PINC
      BUKLE = 0.0
C  BEGIN OUTER LOOP FOR REQUIRED NUMBER OF POINTS
 258  DO 500 I = 1,NOSTEP
```

```
      FORCE = TFORCE - PINC*I
      IF (FFLAG.EQ.1) FORCE = FORC(I)
      WRITE(*,29) I,NOSTEP
 29   FORMAT(1H+,'COMPUTING POINT ',I3,' OUT OF ',I3)
C  CALCULATE DESIRED P AND ASSOCIATED M FOR VARIOUS
C  VALUES OF CURVATURE
      IERR(I) = 0
 260  CALL CALMC(EPSLIM,PHI,FORCE,BMOM,EPSFAL,ISS,EPSPIC
     2           ,NOCURV,ERROR,I,EPSO,PHIMAX,PHIMIN,APNO,BUKLE)
      IF (IERR(I).EQ.0) THEN
      WRITE(2,43) I
  43  FORMAT(1X,'THERE WAS NO CONVERGENCE FOR POINT NUMBER ',I3)
      ENDIF
      AP(I) = FORCE
      AMOM(I) = BMOM
      AEPS(I) = EPSFAL
      APHI(I) = PHI
C  DETERMINE FAILURE MODE
      IF (SIGCR .GE. .99*(FACTOR*FPSC)) THEN
      IFLAG2(I) = 0
      ELSEIF (EPSFAL .LE. .99*EPSLIM) THEN
      IFLAG2(I) = 0
      ELSE
      IFLAG2(I) = 1
      ENDIF
C  IF FAILURE MODE IS BUCKLING OF FLANGE, GO BACK TO
C  CALCULATE FORCE AND MOMENT FOR THE CASE OF MATERIAL
C  FAILURE AS WELL FOR COMPARISON.
      IF (IFLAG2(I) .EQ. 1) THEN
      BUKLE = 1.0
      CALL CALMC(EPSMAX,PHI,FORCE,BMOM,EPSFAL,ISS,EPSPIC
     2          ,NOCURV,ERROR,I,EPSO,PHIMAX,PHIMIN,APNO,BUKLE)
      AP2(I) = FORCE
      AMOM2(I) = BMOM
      AEPS2(I) = EPSFAL
      ELSE
      AP2(I) = AP(I)
      AMOM2(I) = AMOM(I)
      AEPS2(I) = AEPS(I)
      ENDIF
 500  CONTINUE
C   PRINT INPUT VALUES AND PRINT OUT RESULTS TO A FILE
      WRITE(2,40) FPSC,FACTOR,FY,FYPT,EC,EU,FU,EPSMAX,EPSO,
     +    EPSPIC,EPSPIS,CONINI,STLINI,PTSINI,SIGCR,EPSCR,H,TF
 40   FORMAT(10X,'CONCRETE STRENGTH, KSI              ',F10.2,
     +     /,10X,'HOGNESTAD FACTOR K3                ',F10.2,
     +     /,10X,'STEEL STRENGTH, KSI                ',F10.2,
     +     /,10X,'POST-TENSIONED STEEL STRENGTH, KSI ',F10.2,
```

```
     +     /,10X,'CONCRETE E, KSI                    ',F10.2,
     +     /,10X,'MILD STEEL ULTIMATE STRAIN         ',F10.7,
     +     /,10X,'MILD STEEL ULTIMATE STRESS, KSI    ',F10.2,
     +    //,10X,'MAX. USEABLE CONCRETE STRAIN       ',F10.7,
     +     /,10X,'EPSO (CONC. STRAIN AT FPSC)        ',F10.7,
     +    //,10X,'INITIAL CONC. AND MILD STL. STRAIN ',F10.7,
     +     /,10X,'INITIAL POST-TENSIONED STL. STRAIN ',F10.7,
     +    //,10X,'INITIAL CONC. STRESS                ',F10.5,
     +     /,10X,'INITIAL MILD STL. STRESS           ',F10.5,
     +     /,10X,'INITIAL TENDON STRESS              ',F10.5,
     +    //,10X,'CRITICAL STRESS, KSI                ',F10.2,
     +     /,10X,'STRAIN AT CRITICAL STRESS          ',F10.7,
     +    //,10X,'SECTION DEPTH, IN.                  ',F10.2,
     +     /,10X,'THICKNESS OF FLANGE, IN.           ',F10.2)
      WRITE(2,50)
 50   FORMAT(//,5X,'STRIP',5X,'YBAR        CONC IN^2     ',
     +       'STEEL IN^2       PSTEEL IN^2',/,14('-----'))
      DO 600 I = 1,N
      WRITE(2,60) I,YBAR(I),AC(I),AS(I),ASP(I)
 60   FORMAT(6X,I3,4X,F8.3,6X,F8.3,7X,F8.3,9X,F8.3)
 600  CONTINUE
      WRITE(*,70)
      WRITE(2,70)
  70  FORMAT(///,' CURVATURE     AXIAL LOAD',5X,
     +'MOMENT    ECCEN   FAIL STRAIN  FAIL MODE',/,
     + 14('-----'))
      DO 650 I = 1,NOSTEP
      IF (AP(I) .EQ. 0.0) GOTO 9997
      ECCEN = AMOM(I)/AP(I)
 9997 WRITE(2,80) APHI(I),AP(I),AMOM(I),ECCEN,AEPS(I),IFLAG2(I)
      WRITE(*,80) APHI(I),AP(I),AMOM(I),ECCEN,AEPS(I),IFLAG2(I)
  80  FORMAT(F10.7,3X,F10.2,3X,F10.2,2X,F6.2,5X,F8.6,8X,I1)
 650  CONTINUE
      WRITE(2,81)
  81  FORMAT(/5X,'NOTE: FAILURE MODE CODE: 0 = MATERIAL '
     +  ,'FAILURE',/,5X,
     +  '                          1 = BUCKLING OF FLANGE.')
C  WRITE AXIAL LOADS AND MOMENTS TO SEPARATE FILES FOR PLOTTING
      CLOSE(UNIT=1)
      CLOSE(UNIT=2)
      OPEN(3,FILE='PMOUT.CSV',STATUS='NEW')
      OPEN (9,FILE='MOMCUR.CSV',STATUS='NEW')
      DO 700 I = 1,NOSTEP
      WRITE(3,85) AP(I),AMOM(I),AP2(I),AMOM2(I)
  85  FORMAT(3(F12.2,',',3X),F12.2)
      WRITE(9,91) AP2(I)
  91  FORMAT(1X,'AXIAL LOAD = ',F12.2,1X,'KIPS')
         DO 720 J = NOCURV+1,1,-1
```

```
          WRITE(9,89) BMOMB(I,J),BPHIB(I,J),BMOMA(I,J),BPHI(I,J)
  89      FORMAT(F12.2,',',3X,F12.8,',',3X,F12.2,',',3X,F12.8)
 720     CONTINUE
 700   CONTINUE
 9999  STOP
       END
C*************************************************************
C  SUBROUTINE TO FIND THE MAXIMUM MOMENT FOR VARIOUS
C  VALUES OF AXIAL LOAD AND TO CONSTRUCT M-CURV DIAGRAM
       SUBROUTINE CALMC(EPSLIM,PHI,FORCE,BMOM,EPSFAL,ISS,EPSPIC
      2         ,NOCURV,ERROR,L,EPSO,PHIMAX,PHIMIN,APNO,BUKLE)
       COMMON /BLOCK2/ FORCEA(200),BMOMA(60,60),EPSA(200),
      2           BPHI(60,60),IERR(200),BMOMB(60,60),BPHIB(60,60)
       DOUBLE PRECISION PHI,PHIMAX,PHIMIN,PHIINC
       ACURV = NOCURV
       IF(FORCE .GT. 0.98*APNO) THEN
          PHIINC = (PHIMAX/10. - PHIMIN)/ACURV
          PHI = PHIMAX/10. + PHIINC
        ELSE
          PHIINC = (PHIMAX - PHIMIN)/ACURV
          PHI = PHIMAX + PHIINC
       ENDIF
       DO 750 K = 1,NOCURV+1
         PHI = PHI - PHIINC
             IF((EPSO+EPSPIC) .GE. EPSLIM) THEN
                  EPSTRY = EPSPIC
                  EPSINC = (EPSLIM-EPSPIC)/100.
                  GOTO 1111
             ENDIF
         E1 = EPSO+EPSPIC
         CNA = E1/PHI
         CALL CALPM(E1,CNA,FTRY1,BMTRY,ISS)
         E2 = .0005 + EPSPIC
         CNA = E2/PHI
         CALL CALPM(E2,CNA,FTRY2,BMTRY,ISS)
         IF(FORCE.GT.FTRY1) THEN
         EPSINC = (EPSLIM-E1)/100.
         EPSTRY = E1
         GOTO 1111
         ELSEIF(FORCE.LT.FTRY1 .AND. FORCE.GT.FTRY2) THEN
         EPSINC = (EPSO-.0005)/100.
         EPSTRY = E2
         GOTO 1111
         ELSE
         EPSINC = .0005/100.
         EPSTRY = EPSPIC
         ENDIF
       CNA = 0.0
```

```
 1111 DO 1000 I = 1,100
         EPSTRY = EPSTRY + EPSINC
         CNA = EPSTRY/PHI
C       WRITE(2,3002) EPSTRY,CNA,PHI
C 3002 FORMAT(1X,'EPSTRY = ',F10.7,'CNA = ',
     +         F10.5,'PHI = ',F10.7)
       CALL CALPM(EPSTRY,CNA,FTRY,BMTRY,ISS)
C  STORE VALUES OF LOAD, MOMENT, AND PHI FOR DESIRED P
         IF (ABS(FORCE-FTRY).LT.ERROR) THEN
           IERR(L) = 1
           FORCEA(K) = FTRY
               IF (BUKLE .EQ. 1.0) THEN
                   BMOMB(L,K) = BMOMA(L,K)
                   BPHIB(L,K) = BPHI(L,K)
               ENDIF
           BMOMA(L,K) = BMTRY
           EPSA(K) = EPSTRY
           BPHI(L,K) = PHI
           GOTO 750
         ENDIF
 1000 CONTINUE
  750 CONTINUE
C  PERFORM SORT TO DETERMINE THE MAXIMUM MOMENT CAPACITY
C  OF THE SECTION FOR THE DESIRED AXIAL LOAD
       BMOM = -1.0E12
       DO 1120 J = 1,NOCURV+1
       IF (BMOMA(L,J).GT.BMOM) THEN
         IF(BMOM .EQ. 0.0) BMOM = -1.0E12
         FORCE = FORCEA(J)
         BMOM = BMOMA(L,J)
         EPSFAL = EPSA(J)
         PHI = BPHI(L,J)
       ENDIF
 1120 CONTINUE
  400  RETURN
       END
C*************************************************************
C  SUBROUTINE TO CALCULATE FORCE AND MOMENT OF THE SECTION
C  FOR A CERTAIN NEUTRAL AXIS DEPTH
       SUBROUTINE CALPM(EPSLIM,CNA,FORCE,BMOM,ISS)
       COMMON /BLOCK1/ YBAR(200),AC(200),AS(200),ASP(200),EPSPIS,
      +  EPSPIC,ES,ESP,FY,EU,FU,FYPT,EPSO,FACTOR,
      +  FPSC,H,N,EPSMAX,A,B,C,D,A1,B1,C1,D1
       SUMF = 0.0
       SUMMOM = 0.0
C  INCREMENT STRIPS IN SECTION
  301  DO 300 J = 1,N
         EPS = (EPSLIM-EPSPIC)*(1.0-YBAR(J)/CNA)
```

```
      EPST = EPS + EPSPIC
      X = EPST/EPSO
      X2 = EPSPIC/EPSO
C   FIND AVG. STEEL STRESS IN STRIP DUE TO TOTAL LOADS
      SIGSTL = ES * EPST
      EY = FY/ES
      SH = (FU-FY)/(EU-EY)
      IF(SIGSTL.GT.FY) SIGSTL=FY + (EPST-EY)*SH
      IF(SIGSTL.LT.-FY) SIGSTL=-FY + (EPST-EY)*SH
C   FIND AVG. STEEL STRESS IN STRIP DUE TO EXTERNAL LOAD
      SIGSTL = SIGSTL - ES*EPSPIC
C   FIND AVG. POST-TENSIONED STEEL STRESS IN STRIP
C   DUE TO EXT. LOADS
C   REMEMBER THAT EPSPIS IS TENSILE (-) STRAIN
      SIGPT = ESP*EPS + ESP*EPSPIS
      IF (SIGPT .GT. FYPT) SIGPT = FYPT
      IF (SIGPT .LT. -FYPT) SIGPT =  -FYPT
      SIGPT = SIGPT - ESP*EPSPIS
C   ---NOTE: SIGPT SHOULD NEVER YIELD
C   FIND AVG. CONCRETE STRESS IN STRIP DUE TO EXTERNAL LOAD
C   HOGNESTAD'S STRESS-STRAIN MODEL  ISS = 1
C   WANG'S MODEL  ISS = 2   USER DEFINED  ISS = 3
C
C   ASSUME THAT THE INITIAL STRAIN DUE TO POST-TENSIONING
C   IS ON THE ASCENDING BRANCH OF THE
C   CONCRETE STRESS-STRAIN CURVE
      IF(EPST.LE.0.0) THEN
      SIGCON = -FACTOR*FPSC*(2.0*X2-X2**2)
      ELSEIF(EPST.LE.EPSO) THEN
      IF(ISS.EQ.1) SIGCON=FACTOR*FPSC*((2.0*X-X**2)-
     +         (2.0*X2-X2**2))
      IF(ISS.NE.1) SIGCON=FACTOR*FPSC*((A*X+B*X**2)/(1+C*X+
     2   D*X**2))- FACTOR*FPSC*((A*X2+B*X2**2)/(1+C*X2+D*X2**2))
      ELSEIF(EPST.GT.EPSO) THEN
      IF(ISS.EQ.1) SIGCON=FACTOR*FPSC-(EPST-EPSO)*(0.15*FACTOR*
     +      FPSC)/(EPSMAX-EPSO) - FACTOR*FPSC*(2.0*X2-X2**2)
      IF(ISS.NE.1) SIGCON=FACTOR*FPSC*((A1*X+B1*X**2)/(1+C1*X+
     2  D1*X**2)) -FACTOR*FPSC*((A*X2+B*X2**2)/(1+C*X2+D*X2**2))
      ENDIF
C  COMPUTE RESULTANT AVG. STEEL AND CONC. FORCES ON STRIP
      CFORCE = AC(J)*SIGCON
      SFORCE = AS(J)*SIGSTL + ASP(J)*SIGPT
C  ADD STRIP FORCE AND MOMENT TO TOTAL FORCE AND MOMENT
      SUMF = SUMF+CFORCE+SFORCE
      SUMMOM = SUMMOM+(CFORCE+SFORCE)*(H/2.0-YBAR(J))
 300  CONTINUE
      FORCE = SUMF
      BMOM = SUMMOM
```

```
      RETURN
      END
C  ***************************************************************
C THIS SUBROUTINE CALCULATES AND RETURNS TO THE MAIN PROGRAM THE
C NECESSARY PARAMATERS FOR HOGNESTAD'S STRESS-STRAIN RELATION
C   THE SUBROUTINE ALSO COMPUTES THE STRESS-STRAIN DIAGRAM
      SUBROUTINE  HOG(FPSC,FACTOR,EC,EPSO,EPSMAX)
      DIMENSION STRAIN(100),STRESS(100)
C  COMPUTE E-CONCRETE AND EPSO USING CORNELL EXPRESSION
      IF (EPSO .EQ. 0.0) THEN
      EC = 1000. + 40.0*SQRT(FACTOR*FPSC*1000.)
      EPSO = 2.0*FACTOR*FPSC/EC
      ELSE
      EC = 2.0*FACTOR*FPSC/EPSO
      ENDIF
C  COMPUTE STRESS-STRAIN CURVE
      STRAIN(1) = 0.0
      STRESS(1) = 0.0
      STRINC = EPSMAX/50.
      DO 1500 K = 2,51
        STRAIN(K) = STRAIN(K-1) + STRINC
        X = STRAIN(K)/EPSO
        IF(STRAIN(K).LE.EPSO) THEN
        STRESS(K) = FACTOR*FPSC*(2.0*X-X**2)
        ELSEIF(STRAIN(K).GT.EPSO) THEN
        STRESS(K)=FACTOR*FPSC-(STRAIN(K)-EPSO)*
     +        (0.15*FACTOR*FPSC)/(EPSMAX-EPSO)
        ENDIF
 1500 CONTINUE
      OPEN(4,FILE='HOG.CSV',STATUS='NEW')
      WRITE(4,89) FPSC,EC,EPSMAX,EPSO,FACTOR
  89  FORMAT(10X,'CONCRETE STRENGTH, KSI      ',F10.2,
     +     /,10X,'CONCRETE E, KSI              ',F10.2,
     +    //,10X,'MAX. USEABLE STRAIN          ',F10.7,
     +     /,10X,'EPSO (CONC. STRAIN AT FPSC) ',F10.7,
     +     /,10X,'HOGNESTAD FACTOR K3         ',F10.2,
     +   ///,3X,'STRAIN        STRESS ',/,5('-----'),//)
      DO 1550 L = 1,51
        WRITE(4,90) STRAIN(L),STRESS(L)
  90    FORMAT(F10.8,',',5X,F10.3)
 1550 CONTINUE
      CLOSE(UNIT=4)
      RETURN
      END
C ***************************************************************
C THIS SUBROUTINE CALCULATES AND RETURNS TO THE MAIN PROGRAM THE
C NECESSARY PARAMATERS FOR WANG'S STRESS-STRAIN RELATION
C   THE SUBROUTINE ALSO COMPUTES THE STRESS-STRAIN DIAGRAM
```

```
      SUBROUTINE WANG(FPSC,FACTOR,EC,EO,EPSO,EPSI,EPS2I,FI,F2I,
     +          A,B,C,D,A1,B1,C1,D1,EPSMAX)
      DIMENSION STRAIN(100), STRESS(100)
      AKFPSC = FACTOR*FPSC
C  EC = SECANT MODULUS OF CONCRETE AT 0.45*FACTOR*F'C
      EC = 271. * AKFPSC + 978.
      IF (EPSO .EQ. 0.0) EPSO = .000125 * AKFPSC + .00230
      EO = AKFPSC/EPSO
      EPSI = .00005 * AKFPSC + .00401
      FI = .580 * AKFPSC + .774
      EPS2I = EPSI + (EPSI - EPSO)
      IF (AKFPSC .LT. 6.5) THEN
        F2I = .085 * AKFPSC + 1.5
        ELSE
        F2I = .085 * AKFPSC + 2.024
      ENDIF
C  CALCULATE CONSTANTS FOR ASCENDING BRANCH
C  OF STRESS-STRAIN CURVE
      A = EC/EO
      D = (A**3 -2.45 * A**2 + 1.9 * A - 0.45)/(.55*A - 0.2475)
      C = -1. - (0.55 * D)/(1. - A)
      B = C + D + 1. - A
C  CALCULATE CONSTANTS FOR DESCENDING BRANCH
C  OF STRESS-STRAIN CURVE
      XA = EPSI/EPSO
      XB = FI/(AKFPSC)
      XC = EPS2I/EPSO
      XD = F2I/(AKFPSC)
      XM = XC*(XB/XA - XD/XC - XB*XC/(XA*(1.0-XA))+
     2       (XB+XC-XA)/(1.0-XA))
      XN = XC*(XA*XB - (XC-XA)*(XA*XB-1.0)/(1.0-XA) - XC*XD)
      XQ = XC*(XD - XB + (XC-XA)*(XB-1.0)/(1.0-XA))
      XE = -XA + XB/XA + XM*(XB-XA)/XQ
      XK = XA*XB - XA + XN*(XB-XA)/XQ
      XG = (2.0 + XM/XQ)*(XB/XA + (XB-1.0) * XM/XQ - 1.0)
      XH = XN/XQ * (3.0 - 2.0*XB - XB/XA)+(XM/XQ + 2.0)*
     2      (1.0 - XA*XB) + 2.0 * XM*XN*(1.0 - XB)/XQ**2
      XL = -XN/XQ*(XA*XB - 1.0 + XN/XQ*(XB-1.0))
      D1 = (-XH - XK + XE - SQRT((XH+XK-XE)**2 - 4.0*(XE-XG)
     +       *(XL-XK)))/(2.0*(XL-XK))
      C1 = (XM + XN * D1)/XQ
      B1 = -1.0/(1.0-XA)*(XB/XA+(XB-1.0)*C1+(XA*XB-1.0)*D1-1.0)
      A1 = XB*(1.0/XA + C1) + XA*(XB*D1-B1)
C  COMPUTE STRESS-STRAIN CURVE
      STRAIN(1) = 0.0
      STRESS(1) = 0.0
      STRINC = EPSMAX/50.
      DO 1600 K = 2,51
```

```
        STRAIN(K) = STRAIN(K-1) + STRINC
        X = STRAIN(K)/EPSO
        IF(STRAIN(K).LE.EPSO) THEN
         STRESS(K) = AKFPSC*((A*X+B*X**2)/(1+C*X+D*X**2))
         ELSEIF(STRAIN(K).GT.EPSO) THEN
         STRESS(K) = AKFPSC*((A1*X+B1*X**2)/(1+C1*X+D1*X**2))
        ENDIF
 1600 CONTINUE
      OPEN(5,FILE='WANG.CSV',STATUS='NEW')
      WRITE(5,94) FPSC,EC,EO,EPSMAX,EPSO,EPSI,FI,EPS2I,
     +             F2I,FACTOR
 94    FORMAT(5X,'CONCRETE STRENGTH, KSI              ',F10.2,
     +     /,5X,'SECANT MODULUS AT .45*K3*FPSC, KSI  ',F10.2,
     +     /,5X,'SECANT MODULUS AT PEAK STRESS, KSI  ',F10.2,
     +     /,5X,'MAX. USEABLE STRAIN                 ',F10.7,
     +     /,5X,'STRAIN AT PEAK STRESS (EPSO)        ',F10.7,
     +     /,5X,'STRAIN AT INFLECTION POINT (EPSI)   ',F10.7,
     +     /,5X,'STRESS AT INFLECTION POINT (FI)     ',F10.2,
     +     /,5X,'STRAIN AT SECOND POINT (EPS2I)      ',F10.7,
     +     /,5X,'STRESS AT SECOND POINT (F2I)        ',F10.2,
     +     /,5X,'STRESS BLOCK FACTOR (K3)            ',F5.3,
     +   ///,3X,'STRAIN        STRESS ',/,5('-----'),//)
       DO 1650 L = 1,51
         WRITE(5,95) STRAIN(L),STRESS(L)
  95     FORMAT(F10.8,',',5X,F10.3)
 1650 CONTINUE
      CLOSE(UNIT=5)
      RETURN
      END
C ************************************************************
C THIS SUBROUTINE CALCULATES AND RETURNS TO THE MAIN PROGRAM THE
C NECESSARY PARAMATERS FOR USER-DEFINED STRESS-STRAIN RELATIONS
C BASED ON WANG'S FITTED EQUATIONS
C   THE SUBROUTINE ALSO COMPUTES THE STRESS-STRAIN DIAGRAM
      SUBROUTINE USER(FPSC,FACTOR,EC,EO,EPSO,EPSI,EPS2I,FI,F2I,
     +          A,B,C,D,A1,B1,C1,D1,EPSMAX)
      DIMENSION STRAIN(100),STRESS(100)
 1659 WRITE(*,1660)
 1660 FORMAT(1X,'ENTER THE SECANT MODULUS OF CONCRETE IN KSI')
      READ(*,*) EC
      WRITE(*,1665)
 1665 FORMAT(1X,'ENTER CONCRETE STRAIN COINCIDING ',
     +         'WITH PEAK STRESS')
      READ(*,*) EPSO
      WRITE(*,1670)
 1670 FORMAT(1X,'ENTER CONCRETE STRAIN FOR ',
     +           'FIRST INFLECTION POINT')
      READ(*,*) EPSI
```

```
      WRITE(*,1675)
 1675 FORMAT(1X,'ENTER CONC. STRESS FOR ',
     +          '1st INFLECTION POINT, IN KSI')
      READ(*,*) FI
      WRITE(*,1680)
 1680 FORMAT(1X,'ENTER CONC. STRESS FOR 2nd Pt. ',
     +        'ON DESC. BRANCH(KSI)')
      READ(*,*) F2I
      WRITE(*,1690) FPSC,FACTOR,EC,EPSMAX,EPSO,EPSI,FI,F2I
 1690 FORMAT(5X,'CONCRETE STRENGTH, KSI               ',F10.2,
     +     /,5X,'STRESS BLOCK FACTOR (K3)             ',F5.3,
     +     /,5X,'SECANT MODULUS AT .45*K3*FPSC, KSI   ',F10.2,
     +     /,5X,'MAX. USEABLE STRAIN                  ',F10.7,
     +     /,5X,'STRAIN AT PEAK STRESS (EPSO)         ',F10.7,
     +     /,5X,'STRAIN AT INFLECTION POINT (EPSI)    ',F10.7,
     +     /,5X,'STRESS AT INFLECTION POINT (FI)      ',F10.2,
     +     /,5X,'STRESS AT SECOND POINT (F2I)         ',F10.2,//)
      WRITE(*,1695)
 1695 FORMAT(1X,'IF THE PRECEDING INFORMATION IS ',
     + 'INCORRECT ENTER "1", ELSE ENTER "0" ')
      READ(*,*) IUSR
      IF (IUSR.EQ.1) GOTO 1659
      EO = FACTOR*FPSC/EPSO
      EPS2I = EPSI + (EPSI - EPSO)
C  CALCULATE CONSTANTS FOR ASCENDING BRANCH
C  OF STRESS-STRAIN CURVE
      A = EC/EO
      D = (A**3 -2.45 * A**2 + 1.9 * A - 0.45)/(.55*A - 0.2475)
      C = -1. - (0.55 * D)/(1. - A)
      B = C + D + 1. - A
C  CALCULATE CONSTANTS FOR DESCENDING BRANCH
C  OF STRESS-STRAIN CURVE
      XA = EPSI/EPSO
      XB = FI/(FACTOR*FPSC)
      XC = EPS2I/EPSO
      XD = F2I/(FACTOR*FPSC)
      XM = XC*(XB/XA - XD/XC - XB*XC/(XA*(1.0-XA))+
     2       (XB+XC-XA)/(1.0-XA))
      XN = XC*(XA*XB - (XC-XA)*(XA*XB-1.0)/(1.0-XA) - XC*XD)
      XQ = XC*(XD - XB + (XC-XA)*(XB-1.0)/(1.0-XA))
      XE = -XA + XB/XA + XM*(XB-XA)/XQ
      XK = XA*XB - XA + XN*(XB-XA)/XQ
      XG = (2.0 + XM/XQ)*(XB/XA + (XB-1.0) * XM/XQ - 1.0)
      XH = XN/XQ * (3.0 - 2.0*XB - XB/XA)+(XM/XQ + 2.0)*
     +        (1.0 - XA*XB) + 2.0 * XM*XN*(1.0 - XB)/XQ**2
      XL = -XN/XQ*(XA*XB - 1.0 + XN/XQ*(XB-1.0))
      D1 = (-XH - XK + XE - SQRT((XH+XK-XE)**2 - 4.0*(XE-XG)
     +       *(XL-XK)))/(2.0*(XL-XK))
```

```
      C1 = (XM + XN * D1)/XQ
      B1 = -1.0/(1.0-XA) * (XB/XA + (XB-1.0)*C1 +
     +       (XA*XB-1.0)*D1 - 1.0)
      A1 = XB*(1.0/XA + C1) + XA*(XB*D1-B1)
C  COMPUTE STRESS-STRAIN CURVE
      STRAIN(1) = 0.0
      STRESS(1) = 0.0
      STRINC = EPSMAX/50.
      DO 1700 K = 2,51
       STRAIN(K) = STRAIN(K-1) + STRINC
       X = STRAIN(K)/EPSO
       IF(STRAIN(K).LE.EPSO) THEN
       STRESS(K) = FACTOR*FPSC*((A*X+B*X**2)/(1+C*X+D*X**2))
       ELSEIF(STRAIN(K).GT.EPSO) THEN
       STRESS(K) = FACTOR*FPSC*((A1*X+B1*X**2)/(1+C1*X+D1*X**2))
      ENDIF
 1700 CONTINUE
      OPEN(7,FILE='USR.CSV',STATUS='NEW')
      WRITE(7,100) FPSC,EC,EO,EPSMAX,EPSO,EPSI,FI,EPS2I,
     +                F2I,FACTOR
 100  FORMAT(5X,'CONCRETE STRENGTH, KSI              ',F10.2,
     +     /,5X,'SECANT MODULUS AT .45*K3*FPSC, KSI  ',F10.2,
     +     /,5X,'SECANT MODULUS AT PEAK STRESS, KSI  ',F10.2,
     +     /,5X,'MAX. USEABLE STRAIN                 ',F10.7,
     +     /,5X,'STRAIN AT PEAK STRESS (EPSO)        ',F10.7,
     +     /,5X,'STRAIN AT INFLECTION POINT (EPSI)   ',F10.7,
     +     /,5X,'STRESS AT INFLECTION POINT (FI)     ',F10.2,
     +     /,5X,'STRAIN AT SECOND POINT (EPS2I)      ',F10.7,
     +     /,5X,'STRESS AT SECOND POINT (F2I)        ',F10.2,
     +     /,5X,'STRESS BLOCK FACTOR (K3)            ',F5.3,
     +   ///,3X,'STRAIN        STRESS ',/,5('-----'),//)
      DO 1750 L = 1,51
      WRITE(7,105) STRAIN(L),STRESS(L)
 105    FORMAT(F10.8,',',5X,F10.3)
 1750 CONTINUE
      CLOSE(UNIT=7)
      RETURN
      END
C ***************************************************************
C  THE FOLLOWING SUBROUTINE ALLOWS THE USER TO ONLY INPUT THE
C  TOTAL POST-TENSIONING FORCE AND LET THE PROGRAM CALCULATE
C  INITIAL STRAINS ASSUMING FORCE IS DISTRIBUTED UNIFORMLY
C  ACROSS THE SECTION
      SUBROUTINE ISTRN(EPSO,ES,ESP,FACTOR,FPSC,ISS,A,B,C,D,
     +       EPSPIC,EPSPIS,ACT,AST,ASPT,CONINI,STLINI,PTSINI)
      DOUBLE PRECISION CDIF,CSTRES,CTEMP
 1800 WRITE(*,1830)
 1830 FORMAT(1X,'ENTER THE TOTL FORCE DUE TO ',
```

```
     +            'POST-TENSIONING, (+)kips')
      READ(*,*) PTF
      WRITE(*,1840) PTF
 1840 FORMAT(1X,'FORCE DUE TO POST-TENSIONING, kips  ',F10.3,//)
      WRITE(*,1845)
 1845 FORMAT(1X,'ENTER "1" IF PRECEDING VALUE IS INCORRECT ',
     +       /,'      "0" IF PRECEDING VALUE IS CORRECT ')
      READ(*,*) ISERR
      IF (ISERR.EQ.1) GOTO 1800
      CSTRES = 0.001
      CTEMP = 0.0
      DO 1890  I = 1,100
       IF (ISS .EQ. 1) THEN
       CSTRES=(PTF-EPSO*AST*ES*(1-SQRT(1-CSTRES/
     +           (FACTOR*FPSC))))/ACT
       ELSE
       R = D - B*FACTOR*FPSC/CSTRES
       S = C - A*FACTOR*FPSC/CSTRES
       CSTRES=(PTF-EPSO*AST*ES*(-S-SQRT(S**2-4.0*R))
      +           /(2.0*R))/ACT
       ENDIF
      CDIF = ABS(CSTRES - CTEMP)
      IF (CDIF .LT. 0.000001) GOTO 1895
      CTEMP = CSTRES
 1890 CONTINUE
 1895 IF (ISS .EQ. 1) THEN
      EPSPIC = EPSO*(1-SQRT(1-CSTRES/(FACTOR*FPSC)))
      ELSE
      EPSPIC = EPSO*(-S-SQRT(S**2-4.0*R))/(2.0*R)
      ENDIF
      EPSPIS = -PTF/(ASPT*ESP)
C  CALCULATE INITIAL STRESSES DUE TO POST-TENSIONING FROM
C  INITIAL STRAINS
      CONINI = CSTRES
      STLINI = ES*EPSPIC
      PTSINI = ESP*EPSPIS
      RETURN
      END
```

References

1. Poston, R.W., Diaz, M., and Breen, J.E., "Design Trends for Concrete Bridge Piers," ACI Journal, Vol. 83, No. 1, January/February 1986, pp. 14-20.

2. Poston, R.W., Gilliam, T.E., Yamamoto, Y., and Breen, J.E., "Hollow Concrete Bridge Pier Behavior," ACI Journal, Vol. 82, No. 6, November/December 1985, pp. 779-787.

3. Jobse, H.J. and Moustafa, S.E., "Applications of High Strength Concrete for Highway Bridges," PCI Journal, Vol. 29, No. 3, May/June 1984, pp. 44-73.

4. Proctor, A.N., "Hollow Rectangular Reinforced Concrete Columns," Civil Engineering (London), September 1977, pp. 45-49.

5. Proctor, A.N., "Hollow Concrete Columns," Civil Engineering (London), September 1976, pp. 53-55.

6. Nathan, N.D., "Rational Analysis and Design of Prestressed Concrete Beam Columns and Wall Panels," PCI Journal, Vol. 30, No. 3, May/June 1985, pp. 82-133.

7. Chaudwani, R. and Nathan, N.D., "Precast Prestressed Sections Under Axial Load and Bending," PCI Journal, Vol. 16, No. 3, May/June 1971, pp. 10-32.

8. Nathan, N.D., "Slenderness of Prestressed Concrete Beam-Columns," PCI Journal, Vol. 17, No. 6, November/December 1972, pp. 45-57.

9. Zia, P. and Moreadith, F.L., "Ultimate Load Capacity of Prestressed Concrete Columns," ACI Journal, Vol. 63, No. 7, July 1966, pp. 767-786.

10. American Association of State Highway and Transportation Officials, Standard Specification for Highway Bridges, Thirteenth Edition, Washington, D.C., 1983.

11. American Concrete Institute, Building Code Requirements for Reinforced Concrete (ACI 318-83), Detroit, 1983.

12. American Society for Testing and Materials, "Standard Test Method for Compressive Properties of Rigid Plastics (ASTM D 695-88)," Philadelphia, 1988.

13. Post-Tensioning Institute, Post-Tensioning Manual, Fourth Edition, 1985.

14. Hognestad, E., "A Study of Combined Bending and Axial Load in Reinforced Concrete Members," University of Illinois Engineering Experiment Station Bulletin, Series No. 399, 1951.

15. Wang, P.T., Shah, S.P., and Naaman, A.E., "Stress-Strain Curves of Normal and Lightweight Concrete in Compression," ACI Journal, Vol. 75, No. 11, November 1978, pp. 603-611.

16. Carriera, D.J. and Chu, K.H., "Stress-Strain Relationship for Plain Concrete in Compression," ACI Journal, Vol. 82, No. 6, November/December 1985, pp. 797-804.

17. Desayi, P. and Krishnan, S., "Equation for the Stress-Strain Curve of Concrete," ACI Journal, Vol. 61, No. 3, March 1964, pp. 345-350.

18. Fowler, T.J., "Reinforced Concrete Columns Governed by Concrete Compression," unpublished Ph. D. dissertation, The University of Texas at Austin, January 1966.

19. Carrasquillo, R.L., Nilson, A.H., and Slate, F.O., "Properties of High Strength Concrete Subject to Short-Term Loads," ACI Journal, Vol. 78, No.3, May/June 1981, pp. 171-178.

20. Tran, T.D., "Local Buckling of Thin, In-Plane Loaded Reinforced Concrete Plates," unpublished Masters thesis, The University of Texas at Austin, August 1989.

21. Pfrang, E.O., Siess, C.P., and Sozen, M.A., "Load-Moment-Curvature Characteristics of Reinforced Concrete Cross Sections," ACI Journal, Vol. 61, No. 7, July 1964.

22. Breen, J.E., "The Restrained Long Concrete Column as a Part of a Rectangular Frame," unpublished Ph. D. dissertation, The University of Texas at Austin, June 1962.

23. Prestressed Concrete Institute, PCI Design Handbook, Third Edition, Chicago, 1985.

VITA

Randall Brent Rowell was born in Jackson, Mississippi, on November 7, 1966, the son of Brenda Bracey Rowell and H.B. Rowell. After graduating from Columbia Academy High School, Columbia, Mississippi, in 1984, he entered The University of Mississippi in University, Mississippi. He received the degree of Bachelor of Science in Civil Engineering from The University of Mississippi in May, 1988. In September, 1988, he entered The Graduate School of The University of Texas at Austin.

Permanent address: Route 1, Box 91-A
Kokomo, Mississippi 39643

This thesis was typed by the author.